

**The pathogenic part of the *Photorhabdus* and  
*Xenorhabdus* lifecycle with regard to the  
development of novel drugs**

**Dissertation**

Zur Erlangung des Doktorgrades  
der Naturwissenschaften

(Dr. rer. nat.)

der Fakultät für Biologie

der Ludwig-Maximilians-Universität München

vorgelegt von

**Jannis Cornelius Brehm**

München, 11.02.2021

1. Gutachter: Prof. Dr. Ralf Heermann, JGU Mainz

2. Gutachter: Prof Dr. Heinrich Jung, LMU München

Datum der Abgabe: 11.02.2021

Datum der mündlichen Prüfung: 29.04.2021

## **Eidesstattliche Erklärung**

Ich versichere hiermit an Eides statt, dass die vorgelegte Dissertation von mir selbstständig und ohne unerlaubte Hilfe angefertigt wurde. Des Weiteren erkläre ich, dass ich nicht anderweitig ohne Erfolg versucht habe, eine Dissertation einzureichen oder mich der Doktorprüfung zu unterziehen. Die folgende Dissertation liegt weder ganz, noch in wesentlichen Teilen einer anderen Prüfungskommission vor.

München, den 02.06.2021

Jannis Brehm

## **Statutory Declaration**

I declare that I have authored this thesis independently, that I have not used other than the declared sources/resources. As well I declare that I have not submitted a dissertation without success and not passed the oral exam. The present dissertation (neither the entire dissertation nor parts) has not been presented to another examination board.

Munich, 02.06.2021

Jannis Brehm

# **Table of content**

Eidesstattliche Erklärung .....	III
Statutory Declaration .....	III
Table of content.....	IV
Nomenclature .....	VIII
Abbreviations.....	IX
Summary .....	XI
Zusammenfassung .....	XIV
1 Introduction .....	1
1.1 Bacterial secondary metabolites as drugs .....	1
1.2 Life cycle of the entomopathogens <i>Photorhabdus</i> and <i>Xenorhabdus</i> .....	2
1.2.1 <i>Photorhabdus</i> species.....	4
1.3 Bacterial communication .....	5
1.3.1 Quorum sensing.....	5
1.3.2 PPYs and DARs as QS molecules in <i>Photorhabdus</i> species.....	8
1.3.3 LuxR solos in <i>Photorhabdus</i> .....	9
1.3.4 The PAS domain and PAS4-LuxR solos in <i>Photorhabdus</i> .....	11
1.3.5 Inter-kingdom signaling .....	14
1.4 FadD and FadL .....	15
1.5 <i>Galleria mellonella</i> as a model organism for studying insect pathogenicity.....	17
1.6 Secondary metabolites.....	19
1.6.1 Secondary metabolites in <i>Photorhabdus</i> and <i>Xenorhabdus</i> .....	19
1.6.2 Cytotoxic secondary metabolites .....	22
Aim of the thesis .....	24
2 Material and Methods.....	26
2.1 Media used for cultivation.....	26
2.2 Buffers used in this work .....	26
2.3 Bacterial strains used in this work .....	29
2.4 Cell lines used in this work .....	32
2.5 Plasmids used in this work .....	33
2.6 Oligonucleotides used in this work .....	35
2.7 Microbiological Methods.....	38
2.7.1 Bacteria cultivation .....	38

2.7.2	Overproduction of secondary metabolites and generation of cell free culture fluids .....	38
2.8	Molecular biological Methods .....	39
2.8.1	DNA amplification via PCR.....	39
2.8.2	Generation of plasmids .....	40
2.8.3	Generation of gene deletions in the <i>Photorhabdus</i> genome .....	43
2.9	Transformation .....	44
2.10	Extraction Methods.....	46
2.10.1	Extraction of <i>Xenorhabdus</i> and <i>Photorhabdus</i> secondary metabolites .....	46
2.10.2	Extraction and analysis of PPYD from <i>Photorhabdus</i> cultures.....	46
2.11	Analytical Methods .....	47
2.11.1	HPLC analysis.....	47
2.11.2	LC-MS analysis .....	48
2.11.3	Reporter based fluorescence assay to quantify promoter activity .....	48
2.11.4	Reporter-based luminescence assays to quantify promoter activity.....	49
2.11.5	Fluorescence microscopy.....	49
2.12	Protein chemical methods .....	50
2.12.1	Protein overproduction .....	50
2.12.2	Cell disruption .....	50
2.12.3	Protein purification .....	50
2.12.4	SDS-PAGE .....	51
2.12.5	Coomassie staining.....	51
2.12.6	Western blot.....	52
2.13	Protein analytical Methods .....	52
2.13.1	Thermal shift assay (nanoDSF).....	52
2.13.2	Surface plasmon resonance (SPR) spectroscopy .....	53
2.14	Entomological methods performed with <i>G. mellonella</i> .....	54
2.14.1	Larvae rearing.....	54
2.14.2	Generation of insect homogenate.....	54
2.14.3	Pathogenicity assay .....	55
2.15	Cell biological methods .....	55
2.15.1	Cell cultures .....	55
2.15.2	Cell viability assay.....	56
2.15.3	Life Cell imaging.....	56
2.16	Bioinformatical Methods .....	57
2.16.1	Structure prediction and modelling of proteins.....	57

2.16.2	Amino acid sequence comparison.....	57
3	Results.....	58
3.1	Inter-kingdom signaling by <i>P. luminescens</i> - PikR1 / PikR2 sense <i>G. mellonella</i> originated compounds.....	58
3.1.1	PAS4-LuxR solo PikR1 / PikR2 regulate pathogenicity towards <i>G. mellonella</i> larvae .....	58
3.1.2	PikR1 / PikR2 sense a signaling molecule derived from <i>G. mellonella</i> .....	60
3.1.3	Purification of signaling molecule from <i>G. mellonella</i> sensed by PikR1 / PikR2 ..	63
3.1.4	PikR1 / PikR2 sense palmitic acid and stearic acid .....	67
3.1.5	Buffer optimization and purification of PikR2 .....	70
3.1.6	Pikr1/Pikr2 regulate genes for insect pathogenicity .....	72
3.2	Transport of QS signaling molecules of <i>Photorhabdus</i> spec. by FadL.....	79
3.2.1	FadD and FadL homologs in <i>Photorhabdus</i> .....	79
3.2.2	<i>P. luminescens</i> $\Delta fadL$ and $\Delta fadD$ mutants shows altered pigmentation but wild-type like pathogenicity .....	81
3.2.3	<i>P. luminescens</i> $\Delta fadL$ and <i>P. asymbiotica</i> $\Delta fadL$ show decreased $P_{pcfA}$ activity	85
3.2.4	PPYD import is facilitated by FadL in <i>P. luminescens</i> .....	87
3.2.5	Deletion of <i>fadL</i> and <i>fadD</i> reduces relative activity of $P_{plu0258}$ in <i>P. luminescens</i>	89
3.3	Identification of cytotoxic secondary metabolites from <i>Xenorhabdus</i> and <i>Photorhabdus</i> .....	91
3.3.1	Cytotoxic effects of cell free culture supernatants of <i>Xenorhabdus</i> and <i>Photorhabdus</i> wild type cultures.....	93
3.3.2	Secondary metabolites from <i>Xenorhabdus</i> and <i>Photorhabdus</i> show cytotoxic activity .....	95
3.3.3	Xenorhabdin induces apoptosis in HeLa cells .....	101
3.3.4	Xenocoumacin induces apoptosis in HCT116 cells .....	102
3.3.5	Xenocoumacin 2 is a cytotoxic bacterial secondary metabolite .....	105
4	Discussion.....	108
4.1	Inter-kingdom signaling via the PAS4-LuxR solos PikR1 / PikR2 by sensing of fatty acids from <i>G. mellonella</i> .....	108
4.2	Transport of QS signaling molecules in <i>Photorhabdus</i> species .....	112
4.3	Secondary metabolites xenocoumacin 2 and xenorhabdin from <i>Xenorhabdus</i> induce apoptosis .....	119
4.4	Conclusion .....	125
5	Outlook.....	129
6	References.....	133

Supplements.....	155
Acknowledgement .....	159
Curriculum vitae.....	161

## **Nomenclature**

Deletions of genes are marked by the symbol “ $\Delta$ ”. Integrations of genes or resistance cassettes into the genome were marked with “::”. Resistance against an antibiotic is labeled with “R” (e.g. Km<sup>R</sup>).

## **Abbreviations**

aa	Amino acids
AHL	Acyl homoserine lactone
ALA	Aminolevulinic acid
AQ	Anthraquinone
BCIP	5-Bromo-4-chloro-3-indolylphosphat
bps	Base pairs
Carb	Carbenicillin
CASO	Casein-Soja-Pepton
Cm	Chloramphenicol
CFU	Colony forming units
CFCS	Cell free culture supernatant
DMEM	Dulbecco's Modified Eagle Medium
DNA	Deoxyribonucleic acid
DNase	Deoxyribonuclease
DTT	1,4-Dithiothreitol
(NH <sub>4</sub> ) <sub>2</sub> SO <sub>4</sub>	Diammonium sulfate
EA	Ethanolamine
EtOH	Ethanol
FCS	Fetal calve serum
FeSO <sub>4</sub> x 7H <sub>2</sub> O	Iron (II) sulfate heptahydrate
Gent	Gentamycin
n-His tag	Affinity tag composed of n histidine residues
HEHEAA	<i>N</i> -(2-hydroxyethyl)-2-(2-hydroxyethylamino) acetamide
HTH	Helix-turn-helix
Km	Kanamycin
KH <sub>2</sub> PO <sub>4</sub>	Potassium dihydrogen phosphate

LB	Lysogeny broth
NaCl	Sodium chloride
MgSO <sub>4</sub>	Magnesium sulfate
MeOH	Methanol
PAGE	Polyacrylamide gel electrophoresis
PCR	Polymerase chain reaction
Pcf	<i>Photorhabdus</i> clumping factor
PpyS	Photopyrone synthase
QS	Quorum sensing
QQ	Quorum quenching
RNA	<sup>15.</sup> Ribonucleic acid
RNA-P	RNA polymerase
RT	Room temperature
SDS	Sodium dodecyl sulphate
Suc	Sucrose
SPR	Surface plasmon resonance
preXcn1	Prexenocoumacin 1
Xcn1	Xenocoumacin 1
Xcn2	Xenocoumacin 2

## Summary

The Gram-negative entomopathogenic bacteria of the genus *Photorhabdus* and *Xenorhabdus* have a versatile and complex lifecycle, which requires the recurring switch between symbiosis and pathogenicity. The bacteria are mutually associated with *Heterorhabditis* and *Steinernema* nematodes, respectively, which are able to invade insect larvae and release the bacteria into the hemolymph where the bacteria then enter their pathogenic life cycle. The larvae are killed by various bacterial virulence factors and the insect cadaver is used as nutrient source by the bacteria and the nematodes. Since entomopathogenic bacteria are well accessible for molecular tools and they share mechanisms with human pathogens to regulate and mediate pathogenicity, they represent excellent model organisms to investigate molecular mechanisms of pathogenicity and to exploit them for the development of novel drugs. However, many aspects of the pathogenic part of the lifecycle of these entomopathogens are yet unclear. For that reason, this work focusses on the investigation of the pathogenic part of the lifecycle with respect to the future development of novel drugs. In particular the sensing of the insect host to adapt to the new host environment referred to as inter-kingdom signaling as well as the transport of quorum sensing molecules was elucidated, which might serve as drug targets for novel antimicrobials. Furthermore, the cytotoxicity of several secondary metabolites from *Photorhabdus* and *Xenorhabdus* was determined, which might serve as novel drugs in cancer therapy.

*P. luminescens* harbor a vast amount of PAS4-LuxR solo receptors, which have been assumed to be involved in inter-kingdom signaling between the insect host and the bacteria. For the PAS4-LuxR solos PikR1 / PikR2 it was demonstrated that they influence the pathogenicity against *G. mellonella* larvae since a *P. luminescens*

$\Delta pikR1/pikR2$  mutant was reduced in pathogenicity towards the insects. Several genes are regulated by PikR1 / PikR2 in *P. luminescens* in presence of the insect homogenate, which might contribute to the overall pathogenicity of the bacteria. Using reporter strain analyses it could be shown that the signal sensed by PikR1 / PikR2 is derived from *G. mellonella*. To identify the chemical nature of the molecule sensed by PikR1 / PikR2, *G. mellonella* larvae homogenate was fractionated using HPLC and analyzed via LC-MS, and the chemical nature of the signaling molecules sensed by the PAS4-LuxR solos PikR1 / PikR2 were identified as the fatty acids stearic acid and palmitic acid. Thereby, this thesis identifies novel inter-kingdom signaling molecules for the first time, which are sensed by bacterial PAS4-LuxR solo receptors. Since PAS4-LuxR solos are widespread in pathogenic bacteria, these systems might serve as specific novel drug targets in infection therapy.

To coordinate group-coordinated behavior and to regulate the overall pathogenicity during the pathogenic part of the lifecycle *P. luminescens*, *P. temperata* and the human pathogen *P. asymbiotica* are known to communicate via the quorum sensing signaling molecules photopyrones and dialkylresorcinols, respectively. Here it was shown for the first time that the fatty acid transporter FadL facilitates the import of the signaling molecules through the cell membrane as well as that FadD and FadL mediate the transport of the PikR1 / PikR2 sensed signaling molecules. Furthermore, it could be demonstrated that FadD and FadL influence the production of secondary metabolites in *Photorhabdus* species. However, gene deletions of *fadD* and *fadL* did not affect the pathogenicity of the bacteria against insects.

Moreover, *Xenorhabdus* and *Photorhabdus* produce a high number of secondary metabolites in the pathogenic part of the lifecycle to kill the new host and to defend the cadaver from other microorganisms like antibiotics and fungicides. As it was not clear whether *Photorhabdus* and *Xenorhabdus* secondary metabolites also have a

cytotoxic potential, a viability assay with selected secondary metabolites from these entomopathogenic bacteria was performed on human and mouse cell cultures. Cell free culture fluids of *Xenorhabdus* and *Photorhabdus* cultures, producing only one class of secondary metabolites, were analyzed on cytotoxicity. Thereby, fabclavin, xenorhabdin and xenocoumacin 2, were identified to have a high cytotoxic potential, whereas xenorhabdin and xenocoumacin 2 emerged to mediate cytotoxicity via induction of apoptosis. Therefore, cytotoxic compounds that are produced by entomopathogenic bacteria have been identified, which might have potential as novel drugs used for cancer therapy.

In summary this work identified new molecular mechanisms of regulation and mediation of pathogenicity in entomopathogenic bacteria. The investigations of several aspects in the pathogenic part of the lifecycle of *Xenorhabdus* and *Photorhabdus* add novel target proteins and molecules to the portfolio in future development of specific antimicrobial drugs and the identification of secondary metabolites as cytotoxic compounds for cancer therapy in the future.

## Zusammenfassung

Die Gram-negativen und entomopathogenen Bakterien der Gattung *Photorhabdus* und *Xenorhabdus* haben einen komplexen Lebenszyklus, welcher einen immer wiederkehrenden Wechsel zwischen Pathogenität und Symbiose umfasst. Die Bakterien leben in enger Symbiose mit Nematoden der Gattung *Heterorhabditis* bzw. *Steinernema*, welche Insektenlarven befallen. Die Nematoden dringen in die Insekten ein und setzen die Bakterien in die Hämolymphe frei, womit der pathogene Teil des bakteriellen Lebenszyklus beginnt. Die Bakterien produzieren eine große Bandbreite unterschiedlicher Virulenzfaktoren, was die Larve effektiv und schnell tötet. Der Insektenkadaver wird anschließend von den Bakterien und den Nematoden als Nährstoffquelle genutzt. Entomopathogene Bakterien sind ausgezeichnete Modellorganismen für die Erforschung molekularer Mechanismen der Pathogenität, da sie viele dieser Mechanismen mit humanpathogenen Bakterien teilen und molekular sehr gut zugänglich sind. Daher bieten sie auch vielversprechendes Potential für die Entwicklung von neuen Wirkstoffen. Viele molekulare Mechanismen im pathogenen Teil des Lebenszyklus von *Photorhabdus* und *Xenorhabdus* sind bisher unbekannt. Daher liegt der Fokus dieser Arbeit in der Untersuchung spezifischer molekularer Mechanismen der Pathogenität in diesem Teils des Lebenszyklus der entomopathogenen Bakterien im Hinblick auf die Entwicklung neuer Wirkstoffe.

Ein besonderes Augenmerk wurde dabei auf das Erkennen des Insektenwirtes durch die Bakterien, dem sogenannten „inter-kingdom signaling“, sowie auf die bakterielle Kommunikation untereinander, dem sogenannten „quorum sensing“, gelegt. Diese Kommunikationswege könnten zukünftig als Angriffspunkte neuer Anti-Infektiva dienen. Außerdem wurden verschiedene Sekundärmetabolite von *Xenorhabdus* und

*Photorhabdus* auf zytotoxische Eigenschaften untersucht, welche zukünftig zur Entwicklung von neuen Krebswirkstoffen dienen könnten.

*P. luminescens* besitzt eine hohe Anzahl an PAS4-LuxR-Solo Rezeptoren, welche bereits mit dem „inter-kingdom signaling“ in Verbindung gebracht wurden. Für die PAS4-LuxR-Solo Rezeptoren PikR1 / PikR2 konnte hier gezeigt werden, dass diese die Pathogenität von *P. luminescens* gegenüber *G. mellonella* Insektenlarven regulieren, da eine  $\Delta pikR1/pikR2$  Mutante eine verringerte Pathogenität im Vergleich zum Wild-typ zeigte. PikR1 / PikR2 regulieren so in Gegenwart von Insektenlarven-Homogenisat eine Vielzahl von Genen in *P. luminescens*, denen ein Beitrag an der hohen Pathogenität der Bakterien zugeschrieben wird. Durch ein fluoreszenz-basiertes Reportersystem konnte gezeigt werden, dass das Signalmolekül, welches von PikR1 / PikR2 wahrgenommen wird, aus *G. mellonella* stammt. Um die chemische Natur dieses Signalmoleküls aufzuklären, wurde *G. mellonella* Larvenhomogenisat zunächst mittels HPLC fraktioniert und dann durch LC-MS auf die Bestandteile analysiert und diese dadurch identifiziert. Hier zeigte sich, dass die PAS4-LuxR Solos PikR1 / PikR2 die beiden Fettsäuren Stearinsäure und Palmitinsäure als Signale wahrnehmen. Damit konnten erstmalig zwei „inter-kingdom signaling“ Moleküle beschrieben werden, welche von bakteriellen PAS4-LuxR Solos wahrgenommen werden. Da PAS4-LuxR Solos unter pathogenen Bakterien weitverbreitet sind, könnten diese Systeme als neue Zielstrukturen in der Entwicklung von antimikrobiellen Wirkstoffen dienen.

*P. temperata*, *P. luminescens* und humanpathogene *P. asymbiotica* nutzen Photopyrone bzw. Dialkylresorcinole als „quorum sensing“ Signalmoleküle, um die Pathogenität während des pathogenen Teils des Lebenszyklus zu regulieren und Gruppen-abhängig zu koordinieren, wobei der Transport dieser Moleküle über die Zellhülle bisher nicht bekannt war. Im Rahmen dieser Arbeit konnte erstmalig gezeigt

werden, dass der Transporter FadL beim Import dieser Moleküle durch die äußere Membran eine entscheidende Rolle spielt. Weiterhin sind FadL und der cytoplasmatische Transporter FadD auch am Transport der „inter-kingdom“ Signalmoleküle, die von PikR1 / PikR2 wahrgenommen werden, beteiligt. Allerdings scheint der Transport der Signalmoleküle keinen Einfluss auf die Pathogenität der Bakterien zu haben, da die Gendeletion von *fadD* und *fadL* die Pathogenität der Bakterien gegenüber Insektenlarven nicht beeinflusste.

Im pathogenen Teil ihres Lebenszyklus produzieren *Xenorhabdus* und *Photorhabdus* eine Vielzahl von Sekundärmetaboliten, um den neuen Wirt zu töten und andere Mikroorganismen aus dem Kadaver zu verdrängen. Über zytotoxischen Eigenschaften dieser Sekundärmetabolite war bisher wenig bekannt. Deshalb wurden ausgewählte Sekundärmetabolite dieser entomopathogenen Bakterien auf ihre Zytotoxizität untersucht. Dazu wurden Viabilitätstests mit zellfreien *Xenorhabdus* und *Photorhabdus* Kulturüberständen, welche nur eine Klasse von Sekundärmetaboliten produzieren, an menschlichen und murinen Zelllinien durchgeführt. Dabei konnten Fabclavin, Xenorhabdin und Xenocoumacin 2 als Substanzen mit hoher zytotoxischer Aktivität identifiziert werden. Für Xenorhabdin und Xenocoumacin 2 konnte durch Immunfluoreszenzmarkierungen der behandelten Zellen nachgewiesen werden, dass diese Apoptose auslösen. Diese Sekundärmetabolite könnten daher als Basis für die Entwicklung neuer Wirkstoffe dienen, welche in der Tumorthherapie Anwendung finden.

Zusammenfassend wurden in dieser Arbeit neue molekulare Mechanismen der bakteriellen Pathogenität aufgeklärt, und damit eine weitere Basis für die Entwicklung neuer antimikrobieller Wirkstoffe und Krebstherapeutika geschaffen.

# 1 Introduction

## 1.1 Bacterial secondary metabolites as drugs

In general, the need for novel drugs to treat diseases better and more efficient is omnipresent. Resistant pathogenic bacteria are an emerging issue worldwide (Ventola 2015), which demands for the development of novel antimicrobial drugs.

In the development and discovery of drugs always natural products were the main source (Newman und Cragg 2020). Penicillin was one of the first antibiotics discovered by Sir Alexander Fleming in 1928 (Fleming 1929). In the following decades more and more antibiotics were discovered with a broad range of drug targets (Silver 2011, 2016). In a very fast correlation resistant bacteria were discovered shortly after the introduction of novel antimicrobial drugs (Ventola 2015). Several of the introduced antibiotics such as streptomycin (Schatz et al. 1944) and kanamycin (Umezawa 1958) are secondary metabolites produced by *Streptomyces* (Procópio et al. 2012). Over 70% of all antibacterial substances that are in the preclinical pipeline have novel targets (Theuretzbacher et al. 2020). This underlines the need to find new targets for antimicrobial drugs.

Not only antimicrobial substances are required urgently, but also cytotoxic compounds to develop new drugs for cancer treatment.

Secondary metabolites from bacteria also have potential as drugs for cancer therapy. Actinomycin D from *Streptomyces parvulus* (Cibi und Nair 2016) is an example of a bacterial secondary metabolite used in cancer therapy (Merkel et al. 2012).

Promising candidates for novel drug targets for the development of antimicrobial substances might be found in the inter-kingdom signaling and quorum sensing pathways of the entomopathogenic *Photorhabdus* bacteria. Furthermore, candidates for novel drugs in the field of cancer research might be found among the broad

spectrum of secondary metabolites produced by *Photorhabdus* and the closely related entomopathogenic *Xenorhabdus*.

## **1.2 Life cycle of the entomopathogens *Photorhabdus* and *Xenorhabdus***

The entomopathogens *Photorhabdus* and *Xenorhabdus* are very similar in many properties and have a similar lifecycle (**Fig 1.1A**). *Photorhabdus* species are mutually associated with *Heterorhabditis* nematodes, whereas *Xenorhabdus* species live in symbiosis with *Steinernema* nematodes (Maneesakorn et al. 2011; Tailliez et al. 2006). These nematodes carry the bacteria in their intestines (Goodrich-Blair und Clarke 2007) and are able to enter insect larvae through natural openings or directly through the intersegmental areas such as leg and maxilla joints (Gaugler 2002; Wang und Gaugler 1998), where the bacteria are released by the nematode into the haemocoel either via defecation (Martens et al. 2003) or through the mouth (Ciche und Ensign 2003). This is the moment when the bacteria have to switch from symbiotic to pathogenic lifestyle and sense the host by so far unknown signals. While multiplying and colonizing the host, the bacteria release toxins and exoenzymes that kill the larvae within 48h and bioconvert the cadaver to a rich nutrient soup (Forst und Clarke 2002). This goes along with coordinated group behavior through quorum sensing signaling molecules that are released into the surrounding and sensed at a certain threshold (**Fig. 1.1B**). Once the nutrients are used up the primary cells re-associate with the nematodes and the nematodes emerge from the cadaver to search for new prey. In the case of *P. asymbiotica* the bacteria are also able to infect human wounds (Peel et al. 1999; Gerrard et al. 2003b; Gerrard et al. 2006). Recently, it was shed light on the association and interaction of secondary *Photorhabdus* cells with plant roots (Regaiolo et al. 2020).

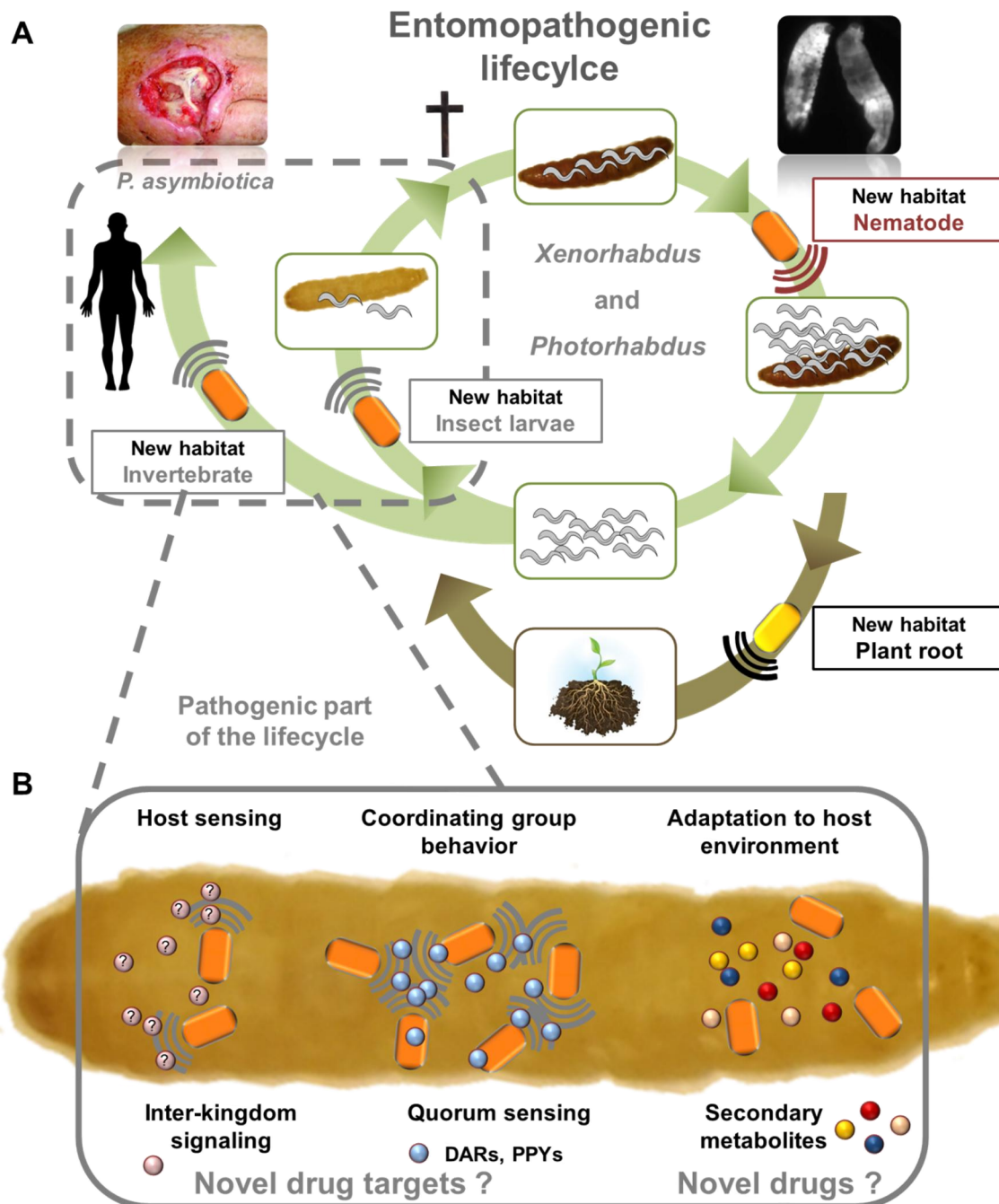


**Figure 1.1: Life cycle of entomopathogenic *Xenorhabdus* and *Photorhabdus* bacteria.** **A)** During the symbiotic part of the lifecycle *Photorhabdus* spec. are mutually associated with *Heterorhabditis* nematodes in the infective juvenile (IJ) stage and *Xenorhabdus* spec. with *Steinernema* nematodes, respectively. The entomopathogens are colonizing the gut of the IJs and are directly released into the insect's hemolymph after the nematodes invaded the insect larvae. In case of *P. asymbiotica* the bacteria are also able to infect human wounds (Gerrard et al. 2006). The bacteria then switch to a pathogenic life style by starting rapid proliferation, production of toxins, antibiotics, lipases, exoenzymes and bioluminescence. Within 48h the insect larvae is dead and serves as a rich food source for the bacteria and nematodes. After the nutrients are used up the bacteria re-associate with the nematodes, which search for new prey (Gerrard et al. 2006; Waterfield et al. 2009).

In the cadaver also primary cells switch to the secondary form, which is not able to live in symbiosis with the nematodes, but interact with plants roots in the soil (Regaiolo et al. 2020). Each time the bacteria switch the host or environment, they need to sense and to adapt to the new conditions. **B)** In the pathogenic part of the lifecycle the bacteria sense the insect host via inter-kingdom signaling and the QS system coordinates group behavior for appropriate response at a certain cell density. Photopyrones are the QS signaling molecules in *P. luminescens* and *P. temperata* and DARs are the corresponding molecules in *P. asymbiotica*. To kill the host, when switching to a pathogenic lifestyle and to adapt to the hostile environment, several secondary metabolites are produced. The receptors and the proteins involved in the communication systems harbor many opportunities for putative drug targets as well as the potential use of the secondary metabolites as drugs produced during this part of the lifecycle.

In summary *Photorhabdus* and *Xenorhabdus* species have a complex and versatile life cycle with several different hosts, environmental changes and have to switch the lifestyle from pathogenic to symbiotic and vice versa. Thus *Photorhabdus* and *Xenorhabdus* are perfect organisms to study communication and potential use of the broad range of secondary metabolites. The exploration of the receptors and the proteins involved in the transport of the quorum sensing molecules harbors many opportunities for putative drug targets as well as the potential use of the secondary metabolites as drugs produced during the pathogenic part of the lifecycle.

### **1.2.1 *Photorhabdus* species**

In 1979 a bioluminescent bacterium from the family Enterobacteriaceae was isolated (Thomas and Poinar 1979). The Gram-negative, rod shaped entomopathogen and lives as symbiont with *Heterorhabditis* nematodes in their infective juvenile (IJ) stage and was first named *Xenorhabdus luminescens*. However, due to strong differences in DNA–DNA comparison the novel bacteria was classified to the genus of *Photorhabdus* and renamed to *Photorhabdus luminescens* (*P. luminescens*) (Boemare et al. 1993). Later, biomolecular analyses revealed two other species of the genus *Photorhabdus* named *Photorhabdus temperata* (*P. temperata*) and

*Photorhabdus asymbiotica* (*P. asymbiotica*) (Fischer-Le Saux et al. 1999). Lately several more species were described and identified as subspecies of *Photorhabdus* (Machado et al. 2018). *Photorhabdus* species were characterized due to their bioluminescence and their symbiotic association with entomopathogenic *Heterorhabditis* nematodes of the family Heterorhabditidae. Furthermore, *Photorhabdus* species are able to infect a broad range of insect larvae such as *Galleria mellonella* and *Manduca sexta* (Forst et al. 1997). *P. asymbiotica* is additionally a human pathogen infecting wounds (Gerrard et al. 2003a). *Photorhabdus* species appear in two different phenotypical forms, called primary and secondary. Although both are pathogenic towards insect larvae, the primary variant is able to associate with nematodes, whereas the secondary variant lacks of that ability. Furthermore, among many other differences the production of secondary metabolites such as anthraquinones, responsible for the pigmentation, is decreased (Eckstein und Heermann 2019). Moreover, *Heterorhabditis* nematodes and their symbionts are distributed in almost every region and habitat on the planet including eukaryotes as well as human tissue. This broad range of hosts and the diversity of living environments results in a complex lifecycle.

## **1.3 Bacterial communication**

### **1.3.1 Quorum sensing**

In 1970 bioluminescence was observed to only occur at a specific cell density in *Photobacterium fischeri* (Nealson et al. 1970). Later this phenomenon was described as quorum sensing (QS) and the cell-density dependent bacterial gene expression was shown in *Vibrio fischeri* and *Vibrio harveyi* (Nealson und Hastings 1979; Eberhard 1972). The common QS system in Gram-negative bacteria relies on N-acyl-L-homoserine lactones (AHLs) for communication, which are sensed by a LuxR-type

receptor and are produced by a cognate LuxI-like synthase (**Fig. 1.2**) (Waters und Bassler 2005). This leads to cell density dependent gene expression, resulting in changes in phenotypical behavior, like bioluminescence, biofilm formation, motility or sporulation (Waters und Bassler 2005). AHLs are composed of a homoserine lactone ring (**Fig. 1.2**) and differ in length of the acyl chain from 4 up to 20 carbon atoms (Marketon et al. 2002; Rajput et al. 2016), level of unsaturated carbon bonds and whether it is substituted at C3 (Whitehead et al. 2001). This determines the hydrophobicity and other characteristics of the molecules besides from the structural specificity, which is necessary for the particular sensing by the specific LuxR receptor although some receptors are able to detect several different AHLs (Hawver et al. 2016). LuxR-type receptors contain a N-terminal signal binding domain (SBD) (Zhang et al. 2002; Vannini 2002; Hanzelka und Greenberg 1995) and a C-terminal helix-turn-helix (HTH) DNA binding domain (DBD) (Choi und Greenberg 1991). When the SBD binds the specific signaling molecule the receptor undergoes a conformational change and binds to target promoters thereby regulating gene expression (Kiratisin et al. 2002). Considering TraR as a model LuxR-type receptor, there are six conserved amino acids in the SBD (W57, Y61, D70, P71, W85 and G113) responsible for binding AHLs (Brameyer et al. 2014; Patankar und González 2009), whereas three amino acids (E178, L182 and G188) are conserved in the HTH DBD with respect to TraR (Patankar und González 2009). Respective their signal binding and folding, LuxR-type receptors can be divided in three groups (Liu et al. 2011). In the case of LasR, an example for class I, the LuxR-type receptor incorporates the signaling molecule irreversibly (Schuster et al. 2004). QscR of *P. aeruginosa*, a protein of class II, requires AHL for solubility and activity form, but the AHL binds reversibly to the receptor (Liu et al. 2010). Proteins of the class III, like RhIR and EsaR, bind the signaling molecule reversibly AHL and correctly fold without it (Medina et al. 2003; Minogue 2005).

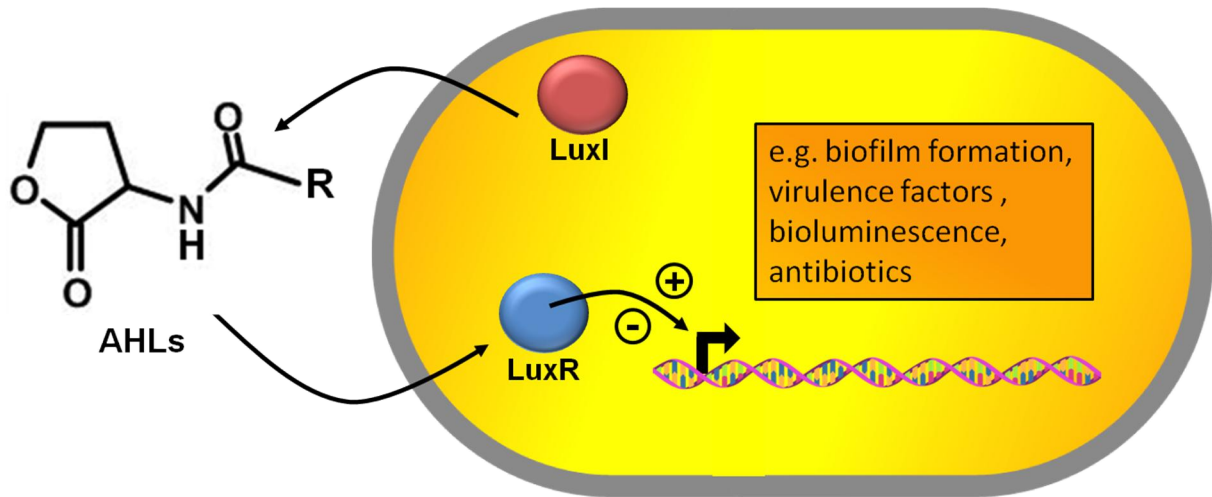


**Figure 1.2: Prototypical quorum sensing system of Gram-negative bacteria.** The LuxI synthase produces AHLs, which are released from the cell and are sensed by neighboring cells when reaching at a certain threshold concentration by the LuxR-type receptor, which then regulates expression of genes responsible for virulence, stress response, metabolism and many other functions. On the left side is the structure of an N-acyl-homoserine lactone ring with an “R”, where the acyl substituents are bound.

In Gram-negative bacteria also other QS systems have been identified besides from AHLs sensed by LuxR receptor proteins. In addition to AHLs, a new family of LuxI independent autoinducer, named AI-2, was subsequently described in *V. harveyi* and *V. fischeri* (Gilson et al. 1995; Surette et al. 1999). AI-2 is a furanosyl borate diester, synthesized by LuxS (Schauder et al. 2001), with a structure that differs significantly from that of AHL. *P. luminescens* and *Y. enterocolitica* also harbor *luxS* homologs (*plu1253*, *ye0839*). The *luxS* pathway was also shown to negatively control the expression of genes for carbapenem antibiotic biosynthesis in *P. luminescens* (Derzelle et al. 2002). In *P. luminescens* over 300 genes are affected by AI-2, including genes for metabolism, stress response and pathogenicity (Krin et al. 2006). *Ralstonia solanacearum* and *Ralstonia pseudosolanacearum* use (R)-methyl 3-hydroxymyristic acid methyl ester (3-OH MAME) and (R)-methyl 3-hydroxypalmitic acid methyl ester (3-OH PAME) (Kai et al. 2015; Flavier et al. 1997; Kimatu 2018) as signaling molecules different to AHLs. Also in contrast to AHL signaling by Proteobacteria, examples of peptides, as QS molecules via two component systems,

are widespread among those that are Gram-positive. Peptides play a role in competence in *Bacillus subtilis* (Magnuson et al. 1994) antibiotic production (Maldonado et al. 2004) and transfer of conjugative plasmids in *Streptococcus faecalis* (M. Mori et al. 1988). Besides these QS signaling systems some more are known so far (Tobias et al. 2020), but the bacterial communication still has large scope for further research on the mechanism and the variety of QS molecules rather than AHLs.

### **1.3.2 PPYs and DARs as QS molecules in *Photorhabdus* species**

As described above the AHL SBDs have a six conserved amino acid motif (WYDPWG) that is different in PluR of *P. luminesces* and *P. temperata*. PluR contains a TYDQCS motif (Brameyer et al. 2014) at these positions showing that AHLs are not sensed by this LuxR solo. Photopyrones (PPYs) were described to be synthesized by PpyS, a photopyrones synthase, and sensed by PluR. The transcriptional regulator then activates the expression of *pcfABCDE* operon, leading to the production of the *Photorhabdus* clumping factor (PCF) (**Fig. 1.4A**) (Brachmann et al. 2013). The production of PCF results in cell clumping and was shown to be a virulence factor contributing to the overall pathogenicity of the bacteria (Brachmann et al. 2013). A similar clumping was shown for the human pathogen *P. asymbiotica*. The corresponding LuxR solo activating the expression of *pcfABCDE* operon is PauR. When comparing the six conserved aa motif of the ligand binding pocket, there is a difference in the last two amino acids compared to PluR. PauR has a TYDQYI motif not sensing PPYs, but dialkylresorcinols (DARs). Those are produced by the DarABC complex and the sensing by PauR also results also in binding and activating of the promoter of *pcfA* (**Fig. 4B**) (Brameyer et al. 2015c).

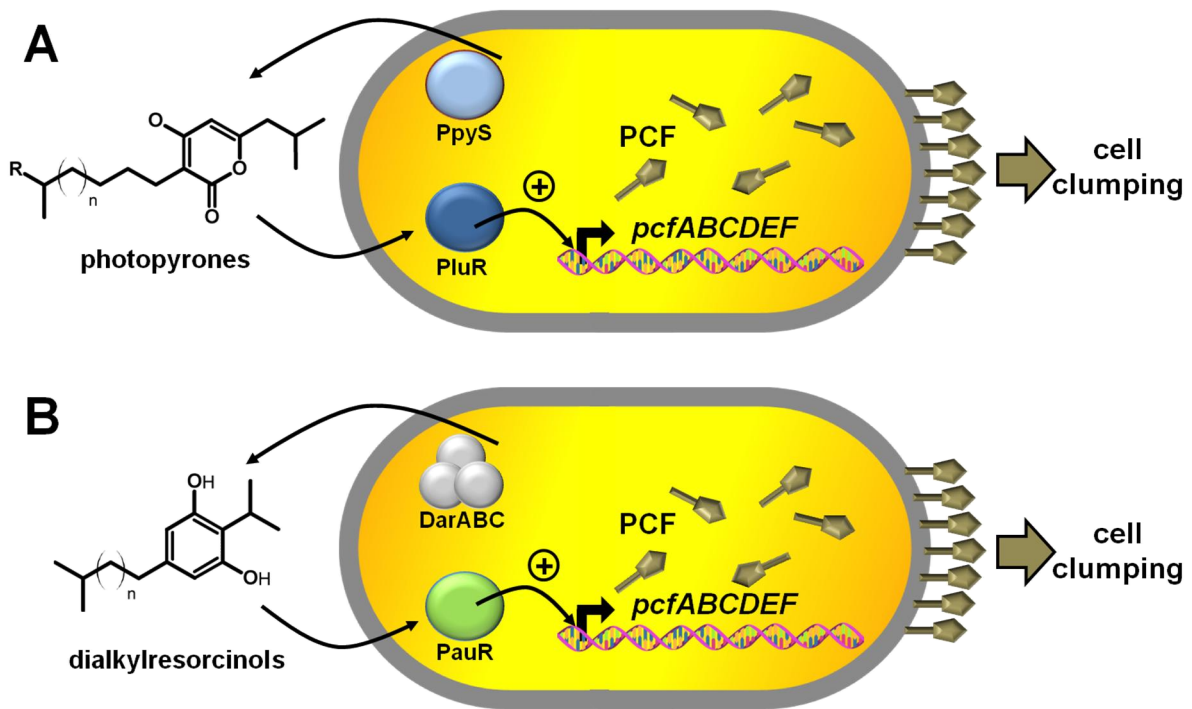


**Figure 1.4: Quorum sensing systems in *Photorhabdus* spec.** **A)** The QS system of *P. luminescens* and *P. temperata* with the signaling molecule PPY, which is produced by PpyS. PluR senses photopyrones and activates  $P_{pcfA}$ , resulting in cell clumping via production of PCF. **B)** The QS system of *P. asymbiotica* with the signaling molecule DAR, which is produced by DarABC. PauR senses the DARs and activates  $P_{pcfA}$ , resulting in cell clumping by production of the PCF (Brachmann et al. 2013).

This shows that the LuxR solos PluR of *P. luminescens* and *PauR* of *P. asymbiotica* are part of the unique QS systems or might sense AHLs produced by other organisms. Nevertheless, there is a high number of PAS4-LuxR solos in *Photorhabdus* species, which might hold a vast communication capacity allowing the potential sensing of internal as well as external signals.

### 1.3.3 LuxR solos in *Photorhabdus*

The genus of *Photorhabdus* is one genus of those bacteria not using AHLs as QS molecules. All *Photorhabdus* species have many LuxR-type regulators (Brameyer et al. 2014), but do not contain *luxI* homologous genes. LuxR-type receptors in organisms without cognate LuxI-like synthases are referred to as LuxR solos

(Subramoni und Venturi 2009). An extremely high number of these LuxR-type solos were identified via bioinformatics analyses in *P. luminescens* (Heermann and Fuchs, 2008). They all share the typical domain modularity of QS LuxR-type regulators containing an N-terminal SBD and a C-terminal DBD including the conserved "HTH LuxR" motif. *P. temperata* possesses 38 and *P. asymbiotica* 22 LuxR solos. *P. luminescens* harbors so far known the highest number with 40 LuxR solos, which were classified into four different types regarding the characteristics of the SBD (**Fig. 1.3**). 35 of the N-terminal SBDs contain a PAS4 domain (P fam08448), with unknown signaling molecules in *Photorhabdus*. In *Vibrio cholerae* the signaling molecule sensed by the PAS4-SBD of VqmA was identified as 3,5-dimethylpyrazin-2-one (DPO) (Papenfort et al. 2017).

Another kind of SBD has the LuxR solo Plu0320 from *P. luminescens* as it contains a predicted SdiA-like SBD, with similarities to SdiA from *E. coli*. SdiA senses AHLs (Sperandio 2010). Therefore this LuxR solo is potentially sensing externally produced AHLs as *P. luminescens* does not have an LuxI synthases (Heermann und Fuchs 2008). Two LuxR solos have a yet undefined SBD domain.

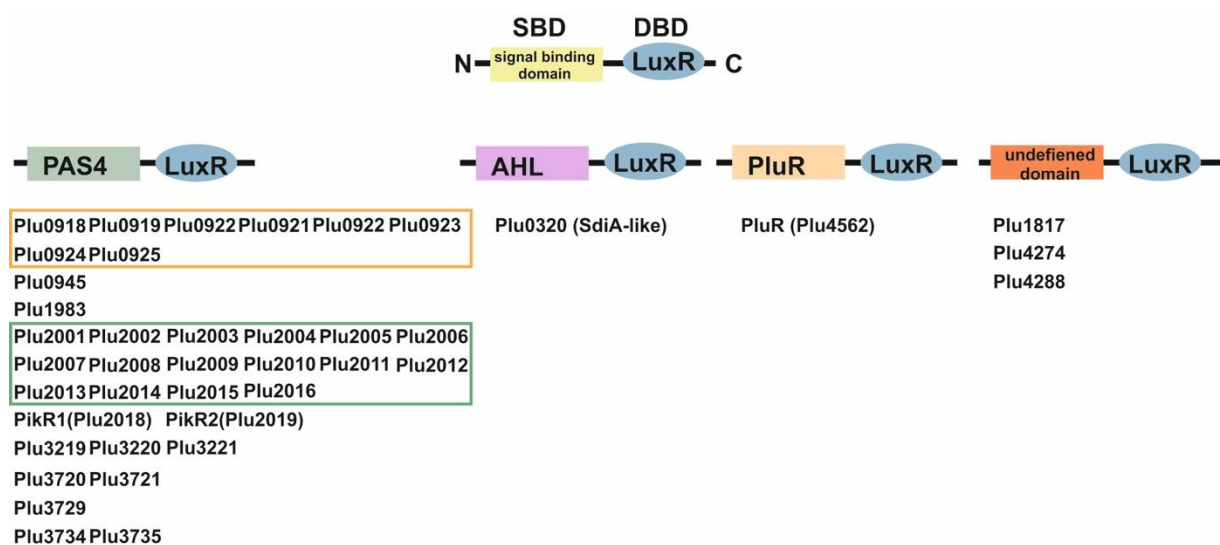


**Figure 1.3: The 40 LuxR solos in *P. luminescens*.** The LuxR solos of *P. luminescens* are classified into four different groups regarding their SBDs. PluR is the receptors for the QS signaling molecules of *P. luminescens*. Plu0320 has an SdiA-

like SBD and two LuxR solos have a yet undefined SBD. The 35 receptors with a PAS4 SBD represent the largest group among the LuxR solos of which 24 are organized in two large clusters of highly homologue genes. Figure adapted from (Brameyer et al. 2014)

#### **1.3.4 The PAS domain and PAS4-LuxR solos in *Photorhabdus***

Per-ARNT-Sim (PAS) domains were identified by sequence homology in the *Drosophila* proteins period (Per) and single-minded (Sim), and the vertebrate aryl hydrocarbon receptor nuclear transporter (ARNT) (Nambu et al. 1991; Hoffman et al. 1991). PAS domains are widely spread and are present in all kingdoms of life (Henry und Crosson 2011), which is shown in the Pfam database (*PAS\_Fold* (CL0183), version 33.1, Nov. 2020) including 222716 entries of proteins distributed in 17 families from over 7300 species, bacteria, archaea and eukaryotes (Finn et al. 2006). Usually, the domain consists of about 100-120 residues, which are able to detect a wide range of chemical and physical stimuli and regulate the activity of functionally diverse effector domains (Hefti et al. 2004). In contrast to this chemical, physical and functional diversity, the structure of the core of PAS domains is broadly conserved and comprises a five-stranded antiparallel  $\beta$ -sheet and several  $\alpha$ -helices. Signals originate within the conserved core and generate structural and dynamic changes predominantly within the  $\beta$ -sheet, from which they propagate via amphipathic  $\alpha$ -helical and coiled-coil linkers at the N- or C-termini of the core to the covalently-attached effector domain (Möglich et al. 2009). In the case of PAS4-LuxR solos from *Photorhabdus* the effector domain is a C-terminally attached HTH LuxR-type DNA binding domain. PAS domains occur often in two-component systems (Rickman et al. 2004; Ji et al. 2016; Zhou et al. 2018) as well as in one-component systems where the N-terminal PAS domain binds a ligand and the C-terminal helix-turn-helix domain binds DNA (Brameyer et al. 2014). One example is the PAS-LuxR receptor TraR, regulating responding to N-(3-oxo-octanoyl)-L-homoserine lactone N-terminally and

then is able to bind its corresponding DNA (Vannini 2002). However, most LuxR homologs with the more variable PAS4 signal-binding domain still lack a known binding molecule.

In the Pfam database (*PAS\_4* (Pfam08448), version 33.1, Nov. 2020) there are over 45.000 entries for sequences with a PAS4 fold occurring in 5288 species. Over 80% of these originate from bacteria but are also present in eukaryotes and archaea. 80 LuxR solos in *Photorhabdus* have a PAS4 (Pfam08448) SBD and represent the majority of the 99 identified LuxR receptors (Heermann und Fuchs 2008). In contrast according to a BLAST analysis (Altschul et al. 1990) *Xenorhabdus nematophila* only harbors three PAS4-luxR receptors. *P. luminescens* contains 35 LuxR solos with an N-terminal PAS4 domain and a C-terminal HTH LuxR-type DBD. The signaling molecules of any of those transcriptional regulators are still unknown. In the genome many of them are arranged in two large clusters (**Fig. 1.5**) with high homology among the genes. The related PAS3 domain in the Met protein from *Drosophila melanogaster* plays a role insect development by sensing a juvenile hormone (Ashok et al. 1998; Charles et al. 2011; Dubrovsky 2005).

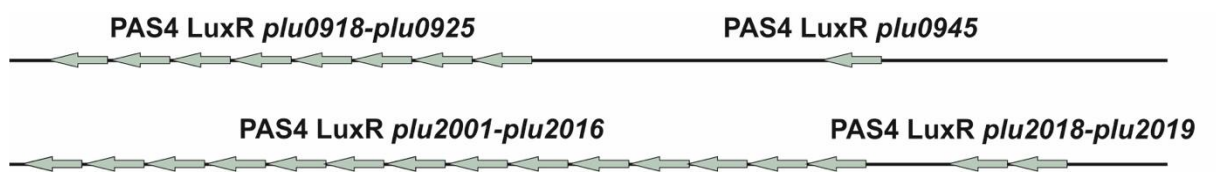


**Figure 1.5: Most LuxR solos of *P. luminescens* are organized in gene clusters.** The 24 PAS4-LuxR solos of *P. luminescens*, *plu0918-plu0925*, *plu2001-plu2016* and *plu2018-plu2019* (*pikR1-pikR2*), are arranged in large clusters of high sequence identity among each other.

Previous investigation into the function of PAS4-LuxR solos showed recognition of molecules from nematodes and insect larvae by several PAS4-LuxR solos, which affected the expression of several genes in *P. luminescens* (Rothmeier 2010) (**Fig. 1.6**). Knockout mutants of the two large gene clusters *plu0918-plu0925*, *plu2001-plu2016* and a third cluster of *plu2018-plu2019* (*pikR1-pikR2*) showed altered

response in presence of nematode homogenate or insect larvae homogenate, compared to the wild type. Plu2001-Plu2016 were shown to respond to nematode homogenate, leading to the assumption that at least one of those LuxR solos binds a molecule originating from the *H. bacteriophora*, whereas Plu2018-Plu2019 showed response towards homogenate from *G. mellonella* larvae (Rothmeier 2010). The response to the homogenate still occurred after heat treatment and alkalization, is smaller than 30kDa and is hydrophobic (Rothmeier 2010). This specific host sensing by different PAS4-LuxR solos was demonstrated as the  $\Delta plu2018-plu2019$  ( $\Delta pikR1 / pikR2$ ) deletion mutant had reduced pathogenicity against *G. mellonella*, but wild type like pathogenicity against *Manduca sexta* (*M. sexta*) larvae. The opposite was shown for a deletion mutant lacking the PAS4-LuxR solo gene cluster *plu2001-plu2016*. *P. luminescens*  $\Delta plu2001-plu2016$  killed *G. mellonella* larvae within 48 h but had highly reduced pathogenicity when injected into *M. sexta* larvae (Manske 2011).

It was revealed in a proteomic analysis via 2D-SDS PAGE that several genes are regulated by Plu2018 / Plu2019 (**Fig 1.6**). The genes *plu2095*, *plu4211*, *ahpC* are down-regulated and *plu0258*, *plu1561*, *plu1962*, *wrbA*, *plu3012*, *plu3795* are up-regulated in presence of a yet unknown molecule present in larvae homogenate from *G. mellonella*. (Rothmeier 2010). Most of these genes are involved in stress response, metabolism and virulence. Three of these genes encode proteins with high similarities to toxins. Plu4211 was found to be similar to XaxA subunit A (Vigneux et al. 2007), Plu1962 shows similarities to an Hcp family type VI secretion system effector and Plu0258 shows similarities to a cornworm toxin from *Pseudomonas chlororaphis* (Schellenberger et al. 2016) (**Supplementary Tab S 3.1.2**)

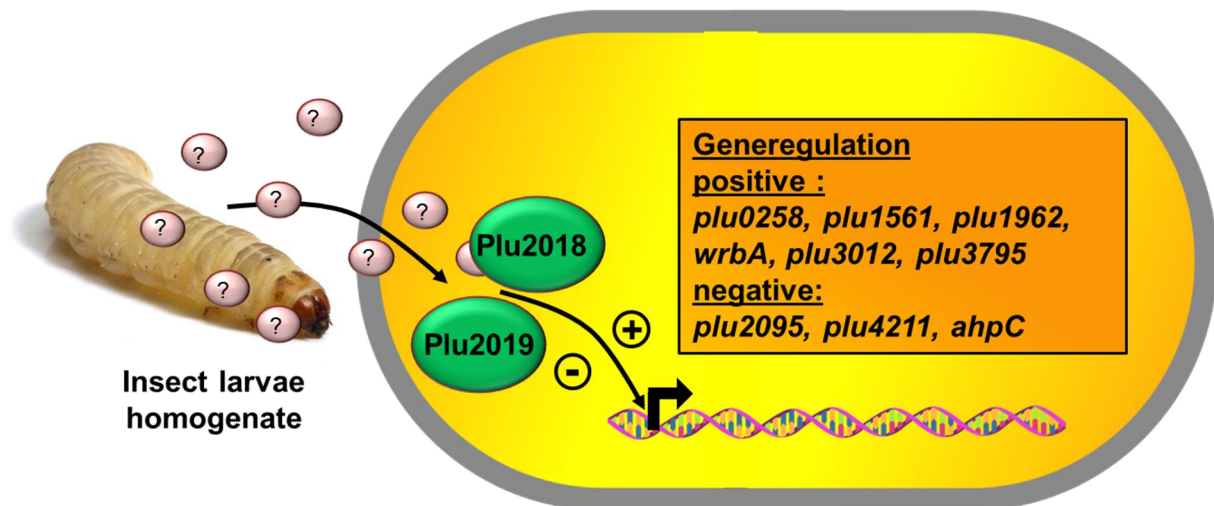


**Figure 1.6: Genes regulated by the PAS4-LuxR solos Plu2018 / Plu2019 in presence of larvae homogenate.** Plu2018 and / or Plu2019 of *P. luminescens* regulate several genes. The genes *plu2095, plu4211, ahpC* are down-regulated and *plu0258, plu1561, plu1962, wrbA, plu3012, plu3795* are up-regulated in presence of a yet unknown molecule present in larvae homogenate from *G. mellonella* (Rothmeier 2010).

As *plu2018-plu2019* showed strong evidence on sensing a molecule originating from an eukaryotic host they were renamed in *pikR1-pikR2* as “**Photorhabdus inter-kingdom receptor”.**

However, the signaling molecule(s) PikR1 / PikR2 are not identified and will be investigated in this thesis as especially the PAS4-LuxR solos harbor high potential as putative future targets for drugs interfering with the communication of Gram-negative bacteria.

### 1.3.5 Inter-kingdom signaling

Inter-kingdom signaling describes the communication between kingdoms of life such as prokaryotes and eukaryotes (Hughes und Sperandio 2008). The sensing of the environment is beneficial and is believed to be essential for survival for bacteria, as they are then able to adapt to the specific eukaryotic host by producing virulence factors as well as activating stress response and metabolic related genes. One of the

first bacterial inter-kingdom signaling systems was described in enterohaemorrhagic *E. coli* (EHEC), which senses the eukaryotic hormone epinephrine and norepinephrine as well as autoinducer AI-3. These signals activate expression of a pathogenicity island, the Shiga toxin, and the flagella regulon (Pacheco und Sperandio 2009). Another inter-kingdom signaling system has recently been identified in plant-associated bacteria. The LuxR solo PipR from the *Populous* root endophyte *Pseudomonas* sp. GM79 senses *N*-(2-hydroxyethyl)-2-(2-hydroxyethylamino) acetamide (HEHEAA), which is formed spontaneously from plant-derived ethanolamine (EA) (Coutinho et al. 2018). The majority of the LuxR solos in *Photorhabdus* spp. contains a PAS4 domain which is homologous to the juvenile hormone binding PAS3 domain of the fruit fly *Drosophila melanogaster* (Dubrovsky 2005). In summary, this large number of versatile PAS4-LuxR solos are predestinated to be major players in inter-kingdom signaling through the detection of hormone specific signals from their eukaryotic hosts like nematodes, insect larvae and plants (Heermann und Fuchs 2008; Brameyer et al. 2014; Regaiolo et al. 2020). However, the chemical nature of these eukaryotic signals has yet to be elucidated.

#### **1.4 FadD and FadL**

All the above described signaling molecules and external signals are mostly hydrophobic and need to cross the cell membrane(s) of the bacteria. Bacteria synthesize and release QS-signaling molecules into the environment, which accumulate in a cell number-dependent manner. These signaling molecules have to cross the cell envelope in order to be recognized by the corresponding receptor. Short-chain acyl-HSLs are assumed to enter the cells via diffusion (Krol und Becker 2014). However, through the presence of the polar lipopolysaccharide layer on the outside of the cell, the outer membrane is an efficient barrier for diffusion of hydrophobic substrates, like long-chain acyl-HSLs (Hearn et al. 2009). One option is

the facilitation of the transport by FadD and FadL. For *E. coli* it was shown that the FadL protein family members transport hydrophobic compounds across the bacterial outer membrane (OM). The OM integrated transporter FadL of *E. coli* transports long-chain fatty acids (LCFAs) (Black 1988). Furthermore, FadL homologs are widespread in Gram-negative bacteria and this suggests a general function in other organisms. LCFAs enter the inner membrane (IM) subsequently and “flip-flop” to the inner leaflet, which occurs quick and spontaneously (Kamp et al. 1995). Via the IM-associated fatty acyl-CoA synthetase FadD the LCFAs are then removed from the IM and activated (van den Berg et al. 2004). Moreover, expression of *fadD* and *fadL* as well as fatty acid degradative genes is activated by FadR, the long-chain acyl-CoA, at high intracellular long-chain acyl-CoA concentrations. This allows the cell to adapt the metabolism rapidly to different conditions of LCFA levels (Dirusso und Black 2004). Indeed the transport of long-chain AHLs is facilitated by FadL in *Sinorhizobium meliloti* (*S. meliloti*) (Krol und Becker 2014). whereas some systems for long-chain acyl-HSLs transport have been identified in *Pseudomonas aeruginosa* (*P. aeruginosa*) (Pearson et al. 1999), and *Burkholderia pseudomallei* (Chan et al. 2007), which use an active efflux system. PPYs and CHDs/DARs show structural differences to acyl-HSLs albeit sharing their hydrophobic properties (Brameyer et al. 2015b). RNA-Sequencing analysis revealed that, among several other genes, *fadD* and *fadL* are significantly higher expressed in *P. luminescens* TT01  $\Delta$ *pluR*. Furthermore, in a heterologous reporter assay it was demonstrated that in *E. coli*  $\Delta$ *fadD* and *E. coli*  $\Delta$ *fadL* the QS signaling molecule import was decreased (Brameyer 2015a). A structure prediction of FadL homolog proteins of *E. coli*, *P. asymbiotica*, *P. luminescens* DJC and *S. meliloti* (**Fig. 1.7**) showed the common  $\beta$ -barrel structure occurring in the FadL family members (Fairman et al. 2011). A bioinformatics comparison of the FadL protein sequences revealed high identity between *P. luminescens* DJC and *P. asymbiotica* (63% and 61%, respectively) and *E. coli* but

only 21% and 22%, respectively, with the long-chain AHL facilitating FadL from *S. meliloti*. Therefore FadL and FadD are not very likely to be involved in AHL transport, but in the transport of the *Photorhabdus* QS molecules and inter-kingdom signaling molecules in *Photorhabdus* species and other bacteria. However, this has not been demonstrated yet.

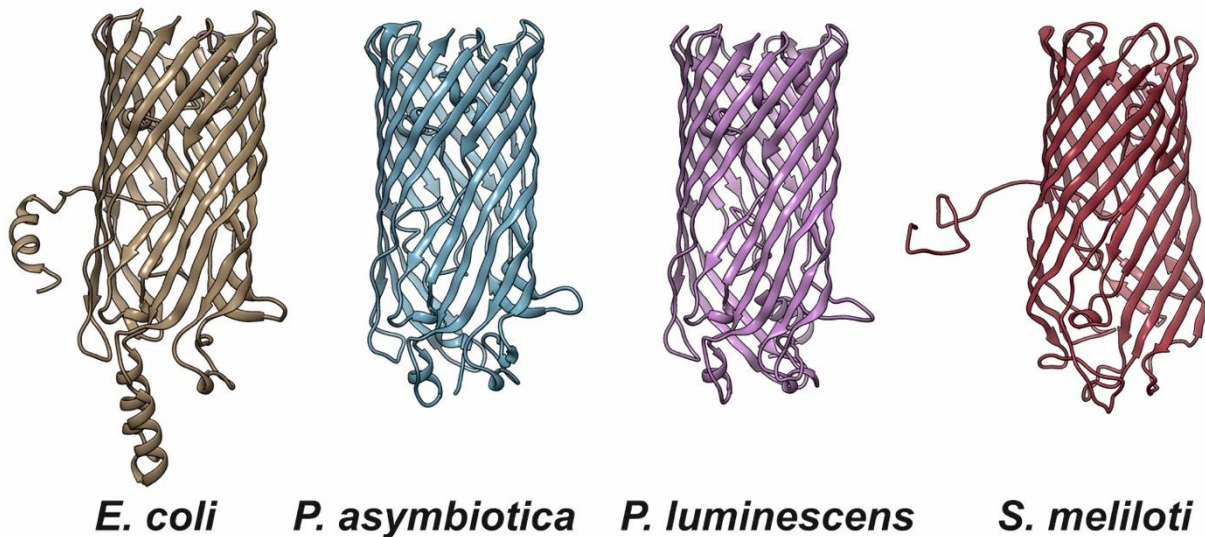


**Figure 1.7: Structure prediction of FadL homologs.** The FadL homologs of *E. coli*, *P. asymbiotica*, *P. luminescens* DJC and *S. meliloti* show a  $\beta$ -barrel structure. Figure adapted from (Brameyer 2015a; Brehm et al. 2021).

### 1.5 *Galleria mellonella* as a model organism for studying insect pathogenicity

An example of a host that is recognized and identified as prey for entomopathogenic nematodes is the larva of the greater wax moth (*Galleria mellonella*). *G. mellonella* is a typical holometabolous insect from the order Lepidoptera and develops through the four distinct life stages egg, larva, pupa, and adult within about 4-7 weeks (**Fig. 1.8**). Before pupation, in the last instar, the larvae are about 25-30 mm in length and 5-7 mm in diameter (Kwadha et al. 2017). *G. mellonella* is a great pest for honeybees as the larvae are crawling into the bee combs and can lead to colony absconding (Kwadha et al. 2017). The larvae of *G. mellonella* have been shown to be a useful tool to analyze the pathogenesis of a wide range of microbial infections such as

mammalian fungal and bacterial pathogens (Harding et al. 2013; Ramarao et al. 2012; Mowlds et al. 2008; Brachmann et al. 2013). An insect model has also the advantages of not being a subject to the ethical limitations of mammalian models. In addition, the larvae can be easily maintained, can be injected without anesthesia and sustain incubation at 37 °C (Mowlds und Kavanagh 2008).

These insect larvae produce insect hormones used for the development such as juvenile hormone I (JH I), JH II and JH III (Rembold und Sehna 1987) and are rich in nutrients like proteins and fatty acids (Kouřimská und Adámková 2016; Mlcek et al. 2014). *Photorhabdus* specifically sense the host and adapt the toxin and secondary metabolite production, metabolism and other functional genes to kill the eukaryotic host and turn the cadaver into an accessible nutrient soup. This might be orchestrated by the PAS4-LuxR solos PikR1 / PikR2 that detect one of the several insect hormones or another molecule present in the larvae tissue and regulates the pathogenicity and adaptation.

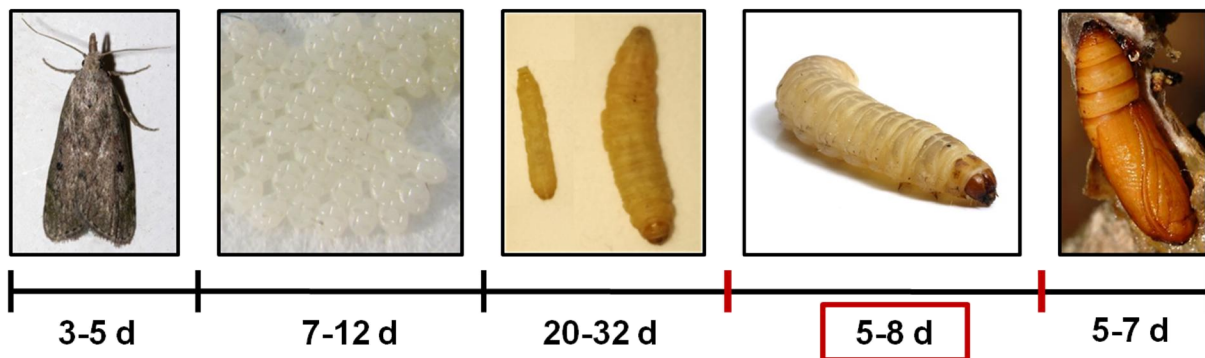


**Figure 1.8: The development of *G. mellonella*:** The fully developed wax moth lays eggs after 3-5 days. The larvae will hatch from the eggs after 1-2 weeks and will grow from first to last instar within 20-32 days. The last instar will pupate within 5-8 days, which will result in the next moth generation after another 5-7 days. Figure is adapted from (Lady 2021; McCann 2007).

## 1.6 Secondary metabolites

### 1.6.1 Secondary metabolites in *Photorhabdus* and *Xenorhabdus*

Secondary metabolites are ubiquitous in almost all bacteria, archaea and fungi but are not essential for growth in normal conditions. They are known for fulfilling numerous functions in all aspects of inter-actions between the microbes and their environment, for example as antibiotics, siderophores, and toxins or signaling molecules (Molloy und Hertweck 2017; Schmidt et al. 2019). Adapting to changing habitats is often going along with changes in secondary metabolite production to improve the adaptation to the environment. However, subsequent studies of microbial ecology have revealed that typical secondary metabolites (also referred to as specialized metabolites) may indeed have an “essential” role but only under specific conditions of growth and or competition (Sharon et al. 2014). *Photorhabdus* and *Xenorhabdus* have a complex life cycle with different hosts and produce a large range of toxins, antibiotics, stilbenes, siderophores, QS molecules and anthraquinones. (Heermann und Fuchs 2008; Orozco et al. 2016; Brachmann et al. 2007; Brameyer et al. 2014; Ciche et al. 2003; Hu et al. 2006; Hu 2000). The mutualistic relationship of *Photorhabdus* and the nematodes also relies on secondary metabolites that assist the development and replication of *H. bacteriophora* (Tobias et al. 2017). With at least 23 biosynthesis clusters, over 6.5% of the genes of *P. luminescens* are involved in secondary metabolite production (Bode 2009). The *Xenorhabdus nematophila* ATCC19061 (*X. nematophila*) genome harbors at least as many genes for the synthesis of small molecules as *Streptomyces* or myxobacteria (Crawford et al. 2010; Shi und Bode 2018). Both *Xenorhabdus* and *Photorhabdus* produce a large variety of small molecules, toxins and other secondary metabolites (Reimer et al. 2013; Vizcaino et al. 2014). The RNA chaperone Hfq, which is relevant for the expression of the biosynthesis gene clusters through sRNA/mRNA

interactions, plays a major role in the secondary metabolite production (Tobias et al. 2017). *hfq* deficient mutants of *Photorhabdus* and *Xenorhabdus* lack of most of the secondary metabolites such as the pigment anthraquinone. This allows to individually produce one secondary metabolite by introducing an inducible promoter into the genome to express one specific biosynthesis gene cluster and brings huge advantages for the isolation and characterization of only one metabolite (Bode et al. 2019). In *P. luminescens*  $\Delta hfq$ , the known secondary metabolites GameXPepptideA, glidobactin, and ririwpeptide (Vizcaino et al. 2014; Shi und Bode 2018) and in *X. szentirmaii*  $\Delta hfq$  GameXPepptides, rhabdopeptides, pyrrolizixenamides and xenocoumacin were individually produced and shown to be bioactive. Especially xenocoumacin from *X. nematophila* showed a broad spectrum of bioactivity including antibiotic activity (Bode et al. 2019; Reimer et al. 2011; McInerney et al. 1991; Vizcaino et al. 2014; Dreyer et al. 2018; Schimming et al. 2015). Xenocoumacin has two preliminary forms (prexenocoumacin 1 and xenocoumacin 1) before being converted to xenocoumacin 2. The preliminary molecules in the synthesis pathway (Reimer et al. 2011) (**Fig. 1.9**) have different antibiotic activities (Park et al. 2009). Due to this broad variety of bioactivity (Bode et al. 2019), including antibiotic activity and inhibition of NO and prostaglandin E<sub>2</sub> production, the full spectrum of bioactivity seems to hold more attributes of xenocoumacin and has to be discovered.

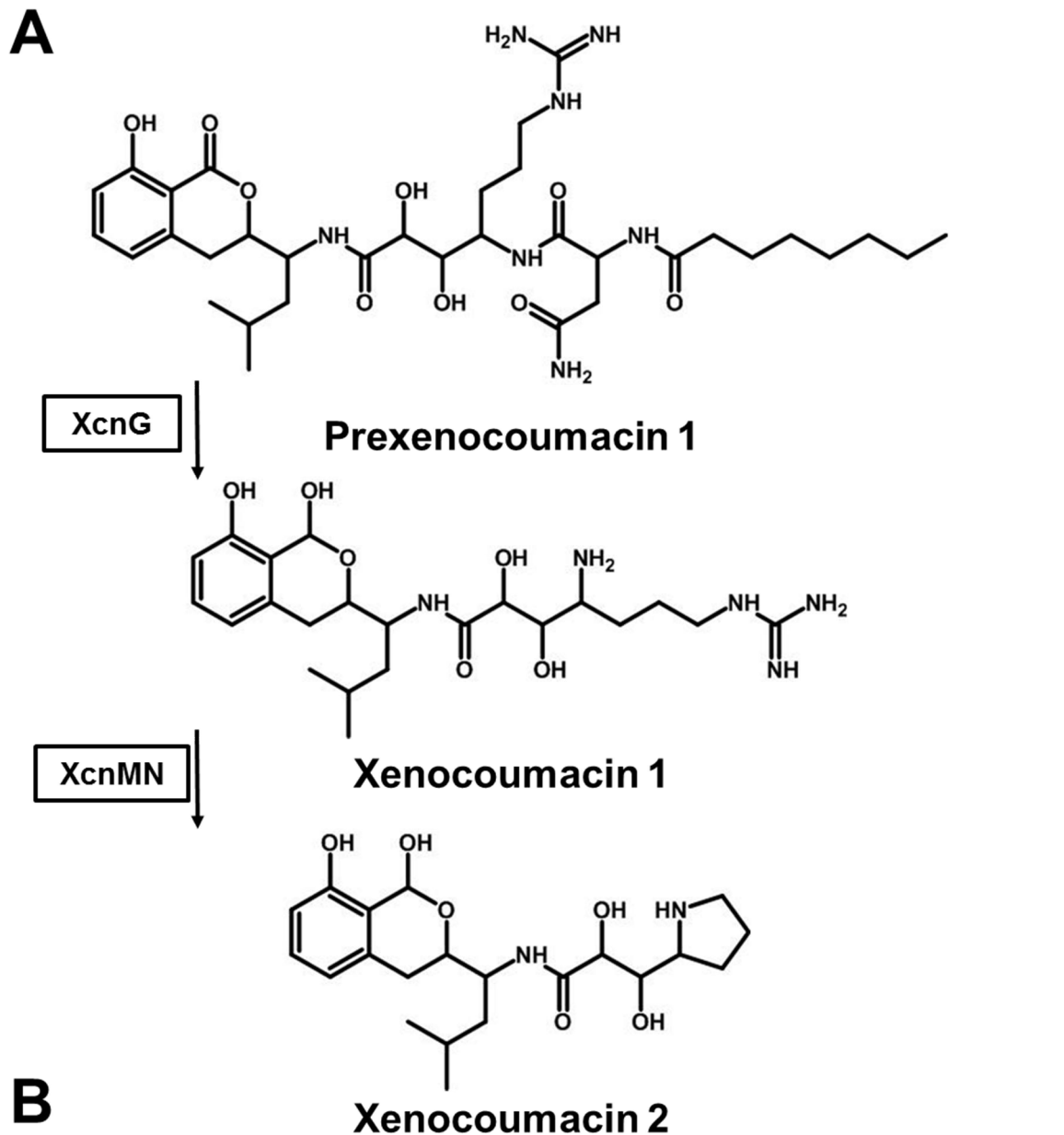


**Figure 1.9: Part of the xenocoumacin biosynthesis pathway** **A)** Showing the last steps in the synthesis of xenocoumacin 2. XcnG converts prexenocoumacin 1 to xenocoumacin 1 and in the final step XcnMN form the pyrrolidine ring to produce xenocoumacin 2. **B)** The biosynthesis gene cluster of xenocoumacin contains 14 genes. In darker grey are the non-ribosomal peptide synthetases and the polyketide synthetases. Figure adapted from (Park et al. 2009)

## 1.6.2 Cytotoxic secondary metabolites

Specialized metabolites have properties, so that bacteria, plants or fungi often use to create advantages over competitors and defend predators. Often molecules with antibacterial and antifungal activities also show cytotoxic effects on human cells (Arivudainambi 2014; Oka et al. 1988). *Photorhabdus* and *Xenorhabdus* both are known to produce a high number of small molecules with antibiotic and or antifungal activity (Bode 2009). Epoxystilbene (Joyce et al. 2008; Hu et al. 2006; Wesche et al. 2017) and Fabclavine (Fuchs et al. 2014) are either produced by *Photorhabdus* or *Xenorhabdus*, respectively. Phenethylamides are produced in *X. nematophila* and are known to be cytotoxic (Bode 2009). Glidobactin A is another omnipotent molecule produced by *Photorhabdus* showing antifungal, antibacterial and cytotoxic activities (Wesche et al. 2017; Dudnik et al. 2013; Theodore et al. 2012) and was shown to be lethal towards pancreatic cells (Theodore et al. 2012). As both, *Photorhabdus* species as well as *Xenorhabdus* species produce more specialized molecules, they hold also the capability to produce substances, which are cytotoxic and potentially are active against human cancer cell lines.

Cancer was the second most abundant cause of death in 2018 in Germany (Statistisches Bundesamt 2020), therefore the discovery of new potent cytotoxic substances is urgent. Cancer is an example, where the normal mechanisms of cell cycle regulation are dysfunctional, with either an over proliferation of cells and/or decreased removal of cells (King und Cidlowski 1998). Paclitaxel is a cytotoxic secondary metabolite from *Taxus brevifolia* (Parness & Horwitz 1981) and inhibits the depletion of the microtubule in eukaryotic cells, thus is inducing apoptosis (Di Yu-Wei et al. 2020; Pan et al. 2014). Therefore paclitaxel it is a potent anti-tumor drug and I use against several cancer types in human (Hou et al. 2017; Abu Samaan et al. 2019). A similar mechanism is known for epothilone A and B, which are microtubule-

stabilizing agents (Höfle et al. 1996) from the myxobacterium *Sorangium cellulosum* (Epothilone 2008; Bollag et al. 1995). Apoptosis was described first 1972 and includes cell shrinkage, nuclear condensation and fragmentation, membrane blebbing and formation of apoptotic bodies (Kerr et al. 1972; Elmore 2007). In contrast to necrosis, apoptosis is a highly regulated process, and the cell compartments and cell material is not released into the surrounding tissue. Apoptotic bodies are formed and carry the cell material until phagocytes engulf them. Research on cytotoxic compounds is often executed on human cancer cell lines such as HCT116, a colon cancer cell line (Rajput et al. 2008) to find new potential apoptosis inducing drugs.

During the pathogenic part of the lifecycle of *Photorhabdus* and *Xenorhabdus* the transport of QS signaling molecules of *Photorhabdus* is still unclear as well as the communication of *Photorhabdus* species with the environment and in particular with its insect host. The sensing of the environment determines the adaption to the new surroundings, including the production of secondary metabolites, which still hide large potential for a broad range of beneficial applications, to counteract pathogenic bacteria as well as treatment for human disease.

## **Aim of the thesis**

The pathogenic part of the lifecycle of the entomopathogenic bacteria *Xenorhabdus* and *Photorhabdus* still has many puzzling aspects. During the pathogenic part in the lifecycle sensing the insect host is important to adapt to the new host to regulate pathogenicity. Therefore, one objective of this thesis is to identify the chemical nature of the signaling molecule(s) originating from *G. mellonella* sensed by PAS4-LuxR solos. For that purpose, HPLC fractionation and LC-MS analysis should be used to purify and chemically identify the signaling molecule(s) sensed by the LuxR solos PikR1 /PikR2. Thereby, the response of PikR1 / PikR2 in presence of the signaling molecule(s) should be determined by analyzing the relative activity of a promotor regulated by the PAS4-LuxR solos. Identification of the signaling molecule(s) and expanded knowledge about the molecular mechanism of inter-kingdom signaling mediated by PikR1 / PikR2 could support the future development of specific inhibitors of PAS4-LuxR receptors.

Furthermore, the transport of the unique QS signaling molecules of *Photorhabdus*, PPYD and DARs, is not identified until now. For that reason, this thesis should contribute to the better understand of the transport mechanism of the QS signaling molecules of *P. luminescens* and *P. asymbiotica*. Therefore, the effect of FadD and FadL on the transport of the QS signaling molecules should be analyzed by extraction of the intracellular as well as extracellular QS signaling molecules and by LC-MS analysis of the extracts.

Moreover, several secondary metabolites from *Xenorhabdus* and *Photorhabdus* should be examined for cytotoxicity via viability assays with human and mouse cell lines to identify potential drug candidates for implementation in cancer therapy research. Furthermore, a first analysis of the molecular mechanism of the putative identified cytotoxins should be performed using specific antibodies on treated cell cultures.

The pathogenic part of the lifecycle of the entomopathogenic bacteria of *Photorhabdus* and *Xenorhabdus* is supposed to harbor high potential for the future development of novel drugs. Therefore, the investigation of the inter-kingdom signaling molecule(s) sensed by the PAS4-LuxR solo PikR1 / PikR2 and identification of transport mechanisms for the QS signaling molecules should be set in context as putative drug targets for the future development of novel antimicrobials. The putative cytotoxic potential of the identified secondary metabolites produced by *Xenorhabdus* and *Photorhabdus* should be set in context for their application as drugs in cancer therapy.

## 2 Material and Methods

### 2.1 Media used for cultivation

**Table 2.1: List of the media used for the cultivation of bacteria.** CASO and LB are the nutrient rich media for cultivation, whereas the minimal media M63 was used for cultivation under nutrient limiting conditions.

CASO	0.5% (W/V) NaCl, 1.5% (W/V) Tryptone, 0.5% (W/V) Soy peptone
LB	1% (W/V) NaCl, 1% (W/V) Tryptone, 0.5% (W/V) Yeast extract
M63	0.1 M $\text{KH}_2\text{PO}_4$ , 15 mM $(\text{NH}_4)_2\text{SO}_4$ , after autoclaving: 1.8 $\mu\text{l}$ 1M $\text{FeSO}_4 \times 7 \text{H}_2\text{O}$ , 1 ml 1 M $\text{MgSO}_4 \times 7 \text{H}_2\text{O}$ , 1 $\mu\text{g/ml}$ Thiamin [1 mg/ml], 0.2 % Caseinhydrolysat, 0.2 % Glycerol (just before Usage), pH 7.0

### 2.2 Buffers used in this work

**Table 2.2: List of the buffers used in this work.**

Lysis-buffer	50 mM TRIS, 5% (V/V) Glycerin, 100 mM Sucrose, 400 mM NaCl, 20 mM Imidazol, pH depending on pI the protein, before usage: 1 mM $\beta$ -mercapotethanol, tip of a spatula DNase, 1 mM PMSF
Wash-buffer	50 mM TRIS, 5% (V/V) Glycerin, 100 mM Sucrose, 400 mM NaCl, 40 mM Imidazol, pH depending on pI the protein, 1 mM $\beta$ -mercapotethanol (before usage)
Elution-buffer	50 mM TRIS, 5% (V/V) Glycerin, 100 mM Sucrose, 400 mM NaCl, 250 mM Imidazol, pH depending on pI the protein, 1 mM $\beta$ -mercapotethanol (before usage)
Laemmli-buffer	25 mM TRIS, 192 mM Glycin 0.1 % (W/V) SDS, pH 8.3
Buffer A	153 mM NaCl, 50 mM TRIS, pH 7.4

Blotting buffer	25 mM TRIS, 192 mM Glycin, 20% Methanol
Coomassie-colouring solution	1.75% (W/V) Serva Blue G, 30% (V/V) Methanol, 5% (V/V) Acetic acid, 10% (V/V) Trichloroacetic acid
SDS loading buffer 2x	4% (W/V) SDS, 2.5% (V/V) Glycerol, 2% (V/V) Bromphenol blue [0.1%], 10% (V/V) Stacking buffer
De-staining-solution	5% (V/V) Methanol, 7.5% (V/V) Acetic acid
Substrate buffer BCIP	41 mM Na-Carbonate, pH 9.5, 0.01% Nitro-Blue-Tetrazolium, 5mg/ml BCIP
Running-buffer	1.5 M TRIS, 0.4% (W/V) SDS, pH 8.8
Stacking-buffer	0.5 M TRIS, 0.4% (W/V) SDS, pH 6.76
Running gel mixture for 12.5% gels	24.176 ml contain: 6 ml Running buffer, 8 ml H <sub>2</sub> O, 10 ml Acrylamide / Bisacrylamide, 160 µl (10% (V/V)) Ammoniumpersulfate (APS), 16 µl TEMED
Stacking gel mixture for 12.5% gels	10.05 ml contain: 2.5 ml Stacking buffer, 5.86 ml H <sub>2</sub> O, 1.64 ml Acrylamide / Bisacrylamide, 45 µl (10% (V/V)) Ammoniumpersulfate (APS), 15 µl TEMED
TAE-buffer	1 mM EDTA, 50mM Na-acetate, 50 mM TRIS, pH 8.0
DNA loading Dye	10 mM TRIS-HCl, 0.03% bromophenol blue, 0.03% (V/V) xylene cyanol FF, 60% (V/V) Glycerol, 60 mM EDTA, pH 7.6
HBS-EP+	0.01 M HEPES pH 7.4, 0.15 M NaCl, 3 mM EDTA, 0.05% v/v Surfactant P20

PBS	140.0 mM NaCl, 2.7 mM KCl, 10.0 mM Na <sub>2</sub> HPO <sub>4</sub> , 1.8 mM KH <sub>2</sub> PO <sub>4</sub> , pH 7.4
Inoue-transformation buffer	10 mM PIPES, 15 mM CaCl <sub>2</sub> , 250 mM KCl, 55 mM MgCl <sub>2</sub> , pH 6.7

All chemicals used in this work had analytical standard and were ordered from Carl Roth GmbH & Co. KG (Karlsruhe) New England Biolabs (USA) or Merck KGaA (Darmstadt).

## 2.3 Bacterial strains used in this work

**Table 2.3: List of the cultivated and modified bacteria strains in this work.**

<i>P. luminescens</i> subsp. <i>laumondii</i> TT01	Wild type	(Duchaud et al. 2003)
<i>P. luminescens</i> subsp. <i>laumondii</i> DJC	Wild type	(Zamora-Lagos et al. 2018)
<i>P. luminescens</i> subsp. <i>laumondii</i> TT01 $\Delta plu2018-plu2019$	Km <sup>R</sup> , $\Delta plu2018-plu2019$	R. Heermann (2009)
<i>P. luminescens</i> ssp. <i>laumondii</i> TT01 $\Delta plu0918-plu0925$	Km <sup>R</sup> , $\Delta plu0918-0925$	(Rothmeier 2010)
<i>P. luminescens</i> ssp. <i>laumondii</i> TT01 $\Delta plu2001-plu2016$	Km <sup>R</sup> , $\Delta plu2001-2016$	R. Heermann (2009)
<i>E. coli</i> ST18	S17 $\lambda pir\Delta hemA$	(Thoma und Schobert 2009)
<i>E. coli</i> BL21 (DE3) <i>pLysS</i>	F <sup>-</sup> , <i>ompT</i> , <i>hsdS<sub>B</sub></i> ( <i>r<sub>B</sub></i> <sup>-</sup> , <i>m<sub>B</sub></i> <sup>-</sup> ), <i>dcm</i> , <i>gal</i> , $\lambda$ (DE3), <i>pLysS</i> , Cm <sup>r</sup>	Promega GmbH, Walldorf
<i>E. coli</i> LMG194	F- $\Delta lacX74$ <i>galE thi rpsL</i> $\Delta phoA$ ( <i>Pvull</i> ) $\Delta ara714$ <i>leu:Tn10</i>	(Invitrogen, California, USA)
<i>E. coli</i> MG1655	F <sup>-</sup> , $\lambda$ -, <i>rph-1</i>	(Jensen 1993)
<i>P. luminescens</i> DJC $\Delta fadD$	$\Delta fadD$	This work
<i>P. luminescens</i> DJC $\Delta fadL$	$\Delta fadL$	This work
<i>P. luminescens</i> DJC $\Delta fadD \Delta fadL$	Km <sup>R</sup> , $\Delta fadD \Delta fadL:: Km$	This work
<i>P. asymbiotica</i> PB68.1 $\Delta fadD$	Km <sup>R</sup> , $\Delta fadD:: Km$	This work
<i>P. asymbiotica</i> PB68.1 $\Delta fadL$	Km <sup>R</sup> , $\Delta fadL:: Km$	This work

<i>P. asymbiotica</i> PB68.1	Wild-type isolate	(Thanwisai et al. 2012; Tobias et al. 2016)
<i>Photorhabdus luminescens</i> DJC $\Delta hfq$ pCEP- <i>plu1881</i>	$\Delta hfq$ ; ::pCEP upstream of the glidobactin biosynthesis gene cluster	H. Bode (Goethe-Universität Frankfurt am Main)
<i>Photorhabdus luminescens</i> DJC $\Delta hfq$ pCEP- <i>plu3263</i>	$\Delta hfq$ ; ::pCEP upstream of the GameXpeptide biosynthesis gene cluster	H. Bode (Goethe-Universität Frankfurt am Main)
<i>Xenorhabdus doucetiae</i> DSM17909	Wild type	(Tailliez et al. 2006)
<i>Xenorhabdus doucetiae</i> DSM17909 $\Delta hfq$ pBAD decarboxylase	$\Delta hfq$ ; ::pBAD upstream of the phenethylamid/tryptamide biosynthesis gene cluster	H. Bode (Goethe-Universität Frankfurt am Main)
<i>Xenorhabdus doucetiae</i> DSM17909 $\Delta hfq$ pBAD <i>gxpsA</i>	$\Delta hfq$ ; ::pBAD upstream of the GameXpeptide biosynthesis gene cluster	H. Bode (Goethe-Universität Frankfurt am Main)
<i>Xenorhabdus doucetiae</i> DSM17909 $\Delta hfq$ pBAD <i>xcnA</i>	$\Delta hfq$ ; ::pBAD upstream of the xenocoumacin biosynthesis gene cluster	H. Bode (Goethe-Universität Frankfurt am Main)
<i>Xenorhabdus doucetiae</i> DSM17909 $\Delta hfq$ pBAD <i>xrdA</i>	$\Delta hfq$ ; ::pBAD upstream of the xenorhabdin biosynthesis gene cluster	H. Bode (Goethe-Universität Frankfurt am Main)
<i>Xenorhabdus szentirmaii</i>	Wild type	(Lengyel et al. 2005)
<i>Xenorhabdus szentirmaii</i> $\Delta hfq$ pCEP-KM-3397	$\Delta hfq$ ; ::pCEP upstream of the rhabdopeptide biosynthesis gene cluster Rhabdopeptide	H. Bode (Goethe-Universität Frankfurt am Main)
<i>Xenorhabdus szentirmaii</i> $\Delta hfq$ pCEP-KM- <i>fcIC</i>	$\Delta hfq$ ; ::pCEP upstream of the fabclavin biosynthesis gene cluster	H. Bode (Goethe-Universität Frankfurt am Main)
<i>Xenorhabdus szentirmaii</i> $\Delta hfq$ pCEP-KM- <i>xfSA</i>	$\Delta hfq$ ; ::pCEP upstream of the xenofuranone biosynthesis gene cluster	H. Bode (Goethe-Universität Frankfurt am Main)

<i>Xenorhabdus nematophila</i> ATCC 19061 $\Delta hfq$ pBAD <i>xcnA</i>	$\Delta hfq$ , ::pBAD upstream of the xenocoumacin biosynthesis gene cluster	H. Bode (Goethe- Universität Frankfurt am Main)
<i>Xenorhabdus nematophila</i> ATCC 19061 $\Delta hfq$ $\Delta xcnNM$ pBAD <i>xcnA</i>	$\Delta hfq$ , $\Delta xcnNM$ , ::pBAD upstream of the xenocoumacin biosynthesis gene cluster	H. Bode (Goethe- Universität Frankfurt am Main)
<i>Xenorhabdus nematophila</i> ATCC 19061 $\Delta hfq$ $\Delta xcnG$ pBAD <i>xcnA</i>	$\Delta hfq$ , $\Delta xcnG$ , ::pBAD upstream of the xenocoumacin biosynthesis gene cluster	H. Bode (Goethe- Universität Frankfurt am Main)

## 2.4 Cell lines used in this work

**Table: 2.4: List of cell lines used in this work for viability assays.**

HeLa Kyoto	Cervical cancer cells	(Gey et al. 1952)
NIH3T3	Murine embryonic fibroblasts	(Todaro und Green 1963)
HCT116	Colon cancer cells	(Rajput et al. 2008)

## 2.5 Plasmids used in this work

**Table 2.5: List of plasmids used in this work**

pBAD33- $P_{pcfA.P.a.}$ -mCherry	<i>mCherry</i> under the control of $P_{pcfA}$ of <i>P. asymbiotica</i> , Cm <sup>R</sup>	(Brameyer et al. 2015c)
pBR- $P_{pcfA.P.l.}$ -mCherry	<i>mCherry</i> under the control of $P_{pcfA}$ of <i>P. luminescens</i> , Carb <sup>R</sup>	(Brachmann et al. 2013)
pNPTS138-R6KT	Km <sup>R</sup>	(Lassak et al. 2010)
pNPTS-fadDpluAB	Plasmid with 600 bps upstream and 600bp downstream region of <i>fadD</i> in <i>P. luminescens</i> , Km <sup>R</sup>	This work
pNPTS-fadDpauA	Plasmid with 600 bps region of <i>fadD</i> in <i>P. asymbiotica</i> PB68.1, Km <sup>R</sup>	This work
pNPTS-fadLpluAB	Plasmid with 600 bps upstream and 600bp downstream region of <i>fadL</i> in <i>P. luminescens</i> , Km <sup>R</sup>	This work
pNPTS-fadLpauA	Plasmid with 600 bps region of <i>fadL</i> in <i>P. asymbiotica</i> PB68.1, Km <sup>R</sup>	This work
pNPTS-fadLinKmplu	Plasmid with 600 bps region of <i>fadL</i> in <i>P. luminescens</i> , Km <sup>R</sup>	This work
pBR- $P_{plu0258}$ -mCherry	<i>mCherry</i> under the control of $P_{plu0258}$ of <i>P. luminescens</i> , Carb <sup>R</sup>	(Rothmeier 2010)

pBBR1-MSC5- <i>P<sub>plu0258</sub>-lux</i>	<i>lux-CDABE</i> operon under the control of <i>P<sub>plu0258</sub></i> of <i>P. luminesces</i> , Gent <sup>R</sup>	This work
pET16b- <i>pikR2</i> -6His	<i>pikR2</i> with an N-terminal 6x His tag, IPTG inducible, Carb <sup>R</sup>	This work
pBAD24- <i>pikR2</i>	<i>pikR2</i> , arabinose inducible, Carb <sup>R</sup>	(Kuzlik 2016)
pBAD24- <i>pas3-pikR2</i>	<i>pas3-pikR2</i> , arabinose inducible, Carb <sup>R</sup>	(Kuzlik 2016)
pBAD24- <i>traR-pikR2</i>	<i>traR-pikR2</i> , arabinose inducible, Carb <sup>R</sup>	(Kuzlik 2016)
pBAD24- <i>pluR-pikR2</i>	<i>pluR-pikR2</i> , arabinose inducible, Carb <sup>R</sup>	(Kuzlik 2016)
pBAD24	arabinose inducible, Carb <sup>R</sup>	(Guzman et al. 1995)
pET16b	IPTG inducible, Carb <sup>R</sup>	Merck, Darmstadt
pET16bPikR2	<i>pikR2</i> -His, IPTG inducible, Carb <sup>R</sup>	This work

## 2.6 Oligonucleotides used in this work

**Table 2.6: List of the oligonucleotides used in this work for amplification of DNA fragments**

Check_fadDplurv	5'-AGTCTGCAGTTGCAGTCATCAAGATAT-3'
Check_fadDplufw	5'-GTGGAATTCAAAGTGTGGTTTCCTTGT-3'
Check_fadLplurv	5'-AGTCTGCAGGATGTTGCAACGATGGCAA-3'
Check_fadLplufw	5'-GTGGAATTCATCACCTTGCTGTGTCACT-3'
Check_fadDpaurv	5'-GGCGAATTCCCTCGCAGTTCCCTTCGAAG-3'
Check_fadDpaufw	5'-GATGTGTATCTCAACCTGAGC-3'
Check_fadLpaurv	5'-CAGTTTCTTGCGTGGTAACCCATAT-3'
Check_fadLpaufw	5'-GTCATGAAGACAAACCGACTC-3'
fadDpluArv	5'-CAGCTGCACGCACTCCTGCAATTTCTCCAAGGTAGTACT-3'
fadDpluAfw	5'-GTGGAATTCAAAGTGTGGTTTCCTTGT-3'
fadDpluBrv	5'-AGTCTGCAGTTGCAGTCATCAAGATAT-3'
fadDpluBfw	5'-TTGCAGGAGTGCGTGCAGCTGGTAGCATAGCCTGAGATC- 3'
fadLpluArv	5'-CAGCTGCACGCACTCCTGCAACATAACCAAACCTCTTG- 3'
fadLpluAfw	5'-GTGGAATTCATCACCTTGCTGTGTCACT-3'
fadLpluBrv	5'-AGTCTGCAGGATGTTGCAACGATGGCAA-3'
fadLpluBfw	5'TTGCAGGAGTGCGTGCAGCTGCGCATTCTAATAATATCCA C3'
fadLinKm_fw	5'-GCGCTGCAGCACCCGTTTCAGCATTAGCGG-3'
fadLinKm_rv	5'-GGCGAATTCCAGCAGGGATCGGGCTGTCATC-3'
fadDpauKmArv	5'-GGCGAATTCCCTCGCAGTTCCCTTCGAAG-3'
fadDpauKmAfw	5'-GCGCTGCAGTGGTGGTGGCATGCCAGTTC-3'

fadLpauKmArv	5'-GGCGAATTCCAAAGGCGATACCGGTACGG-3'
fadLpauKmAfw	5'-GCGCTGCAGCGACTAAACGATAACTTCAG-3'
2019HTHXbalrv	TTCGGCTCTAGATTAATAATAGTAAAAATTTTTTCGG-3'
2019HTHEcoRIfw	TTCGGCGAATTCCCCACATCTATTATATTTC-3'
2019HTHXholfw	5'-TTCGGCCTCGAGCCCACATCTATTATATTTC-3'
PAS_3Xmalfw	5'-GCGAATCCCGGGATGAATCC-3'
PAS_3Xholrv	5'-TTCGGCCTCGAGGTGCTGCT-3'
PluRSBDXholrv	5'-GCGAATCCCGGGTATATGATGAGGAAAATCTT-3'
PluRSBDXmalfw	5'-GGCCTCGAGAAATGTTTTTATGCATTC-3'
TraRSBDXmalfw	5'-TTCGGCGAATTCGGTAGGGGTGGTGCGAAGGA-3'
TraRSBDEcoRIrv	5'-GCGAATCCCGGGCACCGCATAGGAGGTATGGA-3'
plu2019BamHIfw	5'-GATAGGATCCATGAAAAAATTAATGGAACATAC-3'
plu2019Pstlrv	5'-GCCTGCAGTTAAAATAGTAAAAATTTTTTCGGGTAC-3'
Pplu0258_fwd	5'-AGCGGGATCCGGCATAAATCATATTAATTCTC-3'
Pplu0258_rev	5'-AGCGTCTAGAGTGTACGGTATTAGCGCAACA-3'
pBAD24_seq_sense	5'-ATGCCATAGCATTTTTATCC-3'
pBAD24_seq_anti	5'-GATTTAATCTGTATCAGG-3'
pBR_cherry_Seq_fwd	5'-GTAAGGCAACCCCGCCAGCC-3'
pBR_cherry_Seq_rev	5'-CCTTCCATGTGAACTTTG-3'
pNTPS_Seq_fwd	5'-GTCATATTTGCCCTCCTGG-3'
pNTPS_Seq_rev	5'-GGAGCTTGCGGCCCGGACG-3'
Plu2019pETHindIIIrv	5'-GCGAAGCTTTTAAAATAGTAAAAATTT-3'
Plu2019pETXholfw	5'-GCGCTCGAGCACTATAATAGGCATTAATCATGAAA-3'
pET16b_up	5'-ACCCTGGATGCTGTAGGCATAG-3'
pET16b_down	5'-ACCTGTGGCGCCGGTGATGCCG-3'

PAS3_SBD	5'- GCGAATCCCGGGATGAATCCCAGTCTGCATCTAACGGACACTCT AATGCAACTGCTGGACTGCTGCTTCCTCACCCCTAACCTGCAGTG GCCAAATCGTTTTGGTATCCACCAGCGTGGAGCAGCTATTGGGT CACTGTCAGTCCGATTTGTATGGCCAGAATCTACTGCAGATCAC GCATCCCGATGATCAGGATCTGTTAAGACAGCAGCTAATACCCA GGGATATAGAGACCCTGTTCTATCAGCATCAGCACCACCAGCAG CAGGGGCACAATCCCCAGCAGCACCTCGAGGCCGAA-3'
----------	---

All oligonucleotides were ordered from Merck KGaA (Darmstadt) except from "PAS3\_SBD", which was ordered from Eurofins NDSC Food Testing Germany GmbH (Hamburg).

## 2.7 Microbiological Methods

### 2.7.1 Bacteria cultivation

*E. coli* ST18 (Thoma und Schobert 2009) strains were grown at 37°C in LB medium after addition of aminolevulinic acid and antibiotics if necessary. *E. coli* LMG194 (Invitrogen, California, USA) and *E. coli* MG1655 (Jensen 1993) strains were grown at 37°C in LB or M63 medium with antibiotics if necessary. *Photorhabdus luminescens* DJC (Zamora-Lagos et al. 2018), *Photorhabdus luminescens* TT01 (Duchaud et al. 2003), *Photorhabdus asymbiotica* PB68.1 (Thanwisai et al. 2012) and *Xenorhabdus nematophila* (Akhurst und Boemare 1988) strains were cultivated at 26°C or 30°C in LB or CASO medium. When carrying a plasmid or any integrated resistance gene the corresponding antibiotic was added to the culture. (Carbenicillin (Carb) 100 µg/ml, Kanamycin (Km) 50 µg/ml, Chloramphenicol (Cm) 100 µg/ml, Gentamycin (Gent))

### 2.7.2 Overproduction of secondary metabolites and generation of cell free culture fluids

For the overproduction of secondary metabolites wild type strains of *P. luminescens*, *X. szentirmaii*, *X. doucetiae* and *X. nematophila* and the corresponding  $\Delta hfq$  mutants were used (**Tab. 2.3**). The biosynthesis gene clusters of the corresponding synthesis proteins of a specific secondary metabolite are under the control of the  $P_{ara}$  promotor and are inducible by arabinose. 100 ml of CASO medium, containing 0.1% (W/V) arabinose, were inoculated with 200 µl of an overnight culture of the corresponding strain. The culture was aerobically cultivated at 30°C for 72 h. Then the culture was centrifuged (2352 rcf, 25 min, RT) and the supernatant was sterile filtrated (0.22 µm). The supernatant then was freeze dried and resuspended in 10 ml deionized water. Further, Proteinase K (400 µg/ml) was added and incubated over night at 55°C with a

following inactivation at 95°C for 10 min. After sterile filtration the extract was stored at 4°C.

## **2.8 Molecular biological Methods**

### **2.8.1 DNA amplification via PCR**

The polymerase chain reaction (PCR) was performed to amplify specific DNA strands from a DNA template. For that purpose, an upstream and a downstream primer pair was designed with at least 18 homolog base pairs (bps) at the beginning and the end of the sequence, respectively. 25 µl of PCR master mix contained 17 µl H<sub>2</sub>O, 5 µl 5x reaction buffer (New England Biolabs, USA) (corresponding to the polymerase), 1 µl dNTPs (10 mM), 1 µl of each primer 10 mM), 0.5 µl DNA template (<1000 ng) and 0.25 µl polymerase (2 U/µl). 25 µl of the master-mix were transferred into PCR tubes and placed into the PCR cycler (Eppendorf™ Mastercycler™ Nexus Thermal Cycler, Eppendorf). A PCR cycle started with a denaturation step followed by an annealing step and ended with an elongation step. The time of each step was individually changed according to the primer and the length of the amplified sequence. The temperature of the denaturation and elongation steps depended on the polymerase used (94°C, 68°C for OneTaq, 98°C, 72°C for Q5 (both from New England Biolabs, USA)). For an overlap PCR, 12 PCR cycles were performed without primers, which were added afterwards for another following 30 cycles.

For a colony PCR, instead of DNA template, a bacterial colony was picked from an agar plate, streaked on another agar plate and then resuspended in 10 µl of water with a sterile toothpick. The master-mix was then arranged with less water and without DNA template. The PCR started with 10min of heat treatment (94°C - 98°C) to disrupt the cells (temperature corresponding to the polymerase) before the PCR cycles started.

For the determination of the size of a linear DNA fragment a gel electrophoresis was performed. Therefore 1% of agarose was solved in TAE buffer and mixed with an appropriate amount of Midori green (NIPPON genetics Europe, Düren) and purred into a chamber with a ridge to build chambers into the gel. The hardened gel was transferred into a gel electrophoresis chamber filled with TAE buffer and the DNA was mixed with DNA loading buffer (New England Biolabs, USA). 30 µl of DNA was loaded into each chamber and electrophoresis was performed with 110V for 25 min. The DNA was visualized under UV light.

### **2.8.2 Generation of plasmids**

Plasmids (**Tab. 2.5**) were generated via ligation of a PCR product and a restricted plasmid backbone. There for the empty plasmid and the PCR product were incubated with two different restriction enzymes at 37°C for 1 h without shaking (4 µl Cutsmart buffer (New England Biolabs, USA), 30 µl DNA, 4µl H<sub>2</sub>O, 1 µl of each restriction enzyme 2 U/µl)). For dephosphorization, 1 µl shrimp alkaline phosphates (rSAP) was added to the plasmid and incubated for 15 min. The rSAP was then deactivated at 65°C for 10 min. Both DNA strands were purified via a PCR clean up Kit (HiYield PCR Clean-up / Gel Extraction Kit, SLG). The ligation of the DNA fragment and the plasmid was performed via incubation for 90 min at RT. (15 µl of the DNA fragment, 3 µl of restricted plasmid, 2.5 µl T4 ligation buffer (New England Biolabs, USA), 1 µl T4 ligase (New England Biolabs, USA), 3.5 µl H<sub>2</sub>O). Competent *E. coli* DH5α cells were then transformed with the constructed plasmid via heat shock and plated on LB-agar plates containing the corresponding antibiotic.

The generation of the plasmids for gene deletion in *P. luminescens* (pNPTS-fadDpluAB and pNPTSfadLpluAB) the DNA fragments 600 bps downstream and upstream of *fadD* and *fadL* were amplified with the corresponding primers (**Tab. 2.6**).

The DNA fragments were purified (HiYield PCR Clean-up / Gel Extraction Kit, SLG) and an overlap PCR was performed with the primers *fadDpluAfw* and *fadDpluBrv* or *fadLpluBrv* and *fadLpluAfw*, respectively. The generation of the plasmids for the destruction of *fadD* and *fadL* in *P. luminesces* and *P. asymbiotica* (pNPTS-*fadDpauA*, pNPTS-*fadLpauA* and pNPTS-*fadLinKmplu*) was performed by integration of a kanamycin resistance cassette in the plasmid backbone into the gene of interest. To amplify the 600 bps DNA fragments within the genes of interest, the corresponding primers were used (**Tab. 2.6**). As DNA template for all amplifications the genomic DNA of *P. luminesces* or *P. asymbiotica* was used. These 600 bps DNA fragments and the DNA fragments from the overlap PCR were purified (HiYield PCR Clean-up / Gel Extraction Kit, SLG) and restricted with *EcoRI* and *PstI*. The same was done with the plasmid pNPTS138-R6KT. After inactivation of the restriction enzymes the plasmid and the DNA fragments were ligated and *E. coli* DH5 $\alpha$  cells were then transformed with the constructed plasmid via heat shock and plated on LB-agar plates containing the corresponding antibiotic and X-Gal.

The generation of the plasmids pET16b-*pikr2*-6His and pBBR1-*MSC5-Pplu0258-lux* followed the same scheme. The DNA fragments were amplified with the primers *Plu2019pETHindIIIrv* and *Plu2019pETXholfwor* *Pplu0258\_fwd* and *Pplu0258\_rev* (**Tab 2.5**). As template the genomic DNA of *P. luminescens* was used. The DNA fragment was purified (HiYield PCR Clean-up / Gel Extraction Kit, SLG) and restricted with *HindIII* and *XhoI* or *BamHI* and *XbaI*, respectively. The restriction enzymes were inactivated and ligated with the restricted plasmids (pET16b, pBBR1-*MSC5-lux*). After the ligation procedure *E. coli* DH5 $\alpha$  cells were then transformed with the constructed plasmid via heat shock and plated on LB-agar plates containing the corresponding antibiotic.

When a pNPTS138-R6KT plasmid was used as vector a blue-white screening was performed to see whether the *lacZα* gene is functional. This was used to scan ligation performance of plasmids containing the *lacZα*. For the screening, 150μl of culture was plated on agar plates, containing X-Gal and the corresponding antibiotic, after transformation of the ligation approach. The plates were incubated at 37°C. After 12h colonies with an integration and therefore disruption of the *lacZα* gene show no coloring. Colonies, which have re-ligated plasmid without the insert of interest show blue color as the *lacZα* gene is still functional. The white colonies were then picked, and a colony PCR was performed to verify generation of the correct plasmid.

For the generation of the plasmids (**Tab. 2.5**) containing genes encoding the hybrid proteins TraR-PikR2, PluR-PikR2 and PAS3-PikR2 the procedure was similar. Only the DNA fragment that was inserted into the vector was a combination of two PCR fragments, which were connected before ligation with the plasmid. One fragment contained the DNA fragment of the DBD of *plu2019* (*pikR2*) and the other one the corresponding DNA fragment of the SBD of *traR*, *PAS3* and *pluR*. Therefore, the DNA fragment of the DBD encoding part of *pikR2* was amplified with the primers 2019HTHXbalrv and 2019HTHXholfw (2019HTHEcoRIfw for the combination with the *traR* fragment)). Similarly, the DNA fragments of the SBD encoding region of *traR*, and *pluR* were amplified with the corresponding primers (**Tab. 2.6**). As template the genomic DNA of *P. luminesces* TT01 was used. The DNA fragment of the PAS3 region from *met* was ordered from Eurofins (Hamburg). The amplified DNA fragments were purified (HiYield PCR Clean-up / Gel Extraction Kit, SLG) and restricted at one end with XhoI (EcoRI in the case of the *traR* DNA fragment). After inactivation of the restriction enzyme and another purification step (HiYield PCR Clean-up / Gel Extraction Kit, SLG) the two corresponding fragments *pas3* (SBD) and *pikr2* (DBD), *traR* (SBD) and *pikr2* (DBD), and *pluR* (SBD) and *pikr2* (DBD) were ligated. This

combined DNA fragment was amplified with the primer 2019HTHXbalrv and the corresponding forward primer (**Tab. 2.6**). The amplified fragment was purified (HiYield PCR Clean-up / Gel Extraction Kit, SLG) and restricted (37°C, 1 h) with XbaI and XmaI (4 µl Cutsmart buffer (New England Biolabs, USA), 30 µl DNA, 4µl H<sub>2</sub>O, 1 µl of each restriction enzyme 2 U/µl). The same restriction was performed with the pBAD24 vector. After that the DNA fragments (*pas3* (SBD) and *pikr2* (DBD), *traR* (SBD) and *pikr2* (DBD), and *pluR* (SBD) and *pikr2* (DBD)) were ligated (90 min, RT) with the restricted vector pBAD24. Competent *E. coli* DH5α cells were then transformed with the constructed plasmid via heat shock and plated on LB-agar plates containing the corresponding antibiotic.

To prove that the generated plasmid was correct a colony PCR was performed with the corresponding primers (**Tab. 2.5**) as well as sequence analysis (Starseq, Mainz).

All restriction enzymes and polymerases were obtained from New England Biolabs (USA).

### **2.8.3 Generation of gene deletions in the *Photorhabdus* genome**

For the investigation of the role and influence of specific genes in *Photorhabdus*, these genes were deleted from the genome by double homologue recombination or disrupted by integration of a resistance cassette within the corresponding gene.

Briefly, deletion of genes in the *Photorhabdus* genome was conducted via double homologue recombination. For that purpose, two homolog 600 bps regions surrounding the gene of interest were fused via overlap PCR. These fragments were cloned into the plasmid pNPTS136-R6KT. *E. coli* ST18 cells were transformed with the generated plasmid (**Tab. 2.5**) via heat shock. The cells were plated on LB-Kanamycin (Km) agar plates containing 0.5 mM aminolevulinic acid (ALA). By conjugation the plasmid was brought into *Photorhabdus*. For that reason, 5 ml of

*Photorhabdus* overnight culture was centrifuged. 2 ml of an *E. coli* ST18 culture carrying the plasmid of interest was centrifuged (1505 rcf, RT, 2 min), when an optical density of 1 was reached. The cell pellet was washed with LB medium without ALA and mixed with the cell pellet of the *Photorhabdus* culture. The combined cell pellet was resuspended in 100 µl LB medium, spotted on an LB agar plate and incubated over night at 30°C. Due to the missing ALA the *E. coli* ST18 cells were not viable and after 12h the cells were scratched from the agar plate and resuspended in 500 µl LB medium. Cells then were placed on LB- Km agar plates to screen for Km resistance. 10 colonies were picked and plated on LB-Km and LB-sucrose agar plates to screen for the *sacB* gene in the pNPTS136-R6KT plasmid. Then, the sucrose sensitive but Km resistant colonies were incubated for two days in LB medium without Km and plated on LB- sucrose agar. After 48 h, Km sensitive, but sucrose resistant colonies were picked. Only cells with a second homologue recombination would grow on these agar plates. Mutants were confirmed via PCR and sequencing (Starseq, Mainz). The second gene deletion in the double mutant was performed by introducing a kanamycin cassette into the gene via pNPTS136-R6KT with only one 600 bps DNA fragment homologue to a DNA sequence within the gene of interest. Deletion mutants in *P. asymbiotica* were performed via single homologue recombination by introducing a kanamycin cassette into *fadD* and *fadL* via pNPTS136-R6KT with only one homologue sequence within the plasmid.

## 2.9 Transformation

To achieve competent *E. coli* cells for transformation via heat shock, 125 ml of LB-medium were inoculated with an *E. coli* overnight culture to an  $OD_{600} = 0.05$ . The culture was incubated at 27°C. When the cell density reached  $OD_{600} = 0.2-0.5$  the culture was centrifuged (1505 rcf, 4°C, 10 min). The cell pellet was resuspended in Inoue-transformation buffer (**Tab. 2.2**) and centrifuged 1505 rcf, 4°C, 10 min). The

cell pellet was resuspended in 5 ml Inoue-transformation buffer (**Tab. 2.2**) and 0.5 ml of DMSO was added and incubated on ice for 10 min. 150 µl of the competent cells were then aliquoted in tubes and shock frozen with liquid nitrogen and stored at -80°C before usage.

To transform *E. coli* cells with a plasmid the competent *E. coli* cells were defrosted on ice for 10 minutes before the addition of 1 µl of plasmid (retransformation) or 25 µl of a ligation composition. The mixture was incubated on ice for 20 minutes until the heat shock was performed at 42 °C for 90 s. After the heat shock the cells were incubated on ice for 5 minutes. 1 ml LB medium was added and the cells were incubated at 37°C for 40 minutes. The cells were then centrifuged (2352 rcf, 2 min, RT), resuspended in 150 µl LB medium and plated on LB agar plates containing the corresponding antibiotic.

To transform *P. luminescens* and *P. asymbiotica* strains (**Tab. 2.3**) with a plasmid an electroporation was performed. Therefore 100 ml LB medium was inoculated with 2 ml of an overnight culture of *Photobacterium* and were cultivated at 30°C until OD<sub>600</sub>=1. The culture was centrifuged (15 min, 1505 rcf, RT) and the cells were resuspended in (10% (V/V)) glycerol. This was repeated three times with decreasing amounts of (10% (V/V)) glycerol (50 ml, 15 ml and 5 ml). The final cell pellet was resuspended in 300 µl of (10% (V/V)) glycerol. 2 µl of plasmid were added to 90 µl of resuspended cells and were incubated for 10 minutes. These 92 µl were then transferred into a sterile electroporation cuvette and pulsed with 1.8 KV for 5 ms. The cells were resuspended in 1 ml of LB medium and incubated for >90 min at 30 °C. The cells were then centrifuged (2352 rcf, 2 min, RT), resuspended in 150 µl LB medium and plated on LB agar plates containing the corresponding antibiotic.

## 2.10 Extraction Methods

### 2.10.1 Extraction of *Xenorhabdus* and *Photorhabdus* secondary metabolites

For the production and extraction of secondary metabolites from *Photorhabdus* and *Xenorhabdus* (the corresponding strains (**Tab. 2.3**) were incubated for 72 h at 30°C in 100 ml CASO medium. 3 h after inoculation 0.1% arabinose was added to induce the gene expression for specific secondary metabolite production. Afterwards the culture was centrifuged (1905 rcf, 4°C 25 min) and the cell pellet was discarded. If no continuative extraction was needed the cell free culture was frozen with liquid nitrogen and lyophilized. For further usage the lyophilisate was re-suspended in the appropriate volume of water.

In case of extraction of specifically the hydrophobic part of the cell free supernatant 10% (W/V) Amberlite XAD-16 resin (Sigma-Aldrich, USA) was added and shaken for 8h at room temperature. The resin then was filtrated and bound molecules were extracted with methanol (MeOH) by incubation for 3 h at RT. The methanol was filtrated (0.22 µm) to separate unsolved particles and evaporated in a rotary evaporator to concentrate the extracted substances. The evaporated residue was stored at -20°C before further usage.

### 2.10.2 Extraction and analysis of PPYD from *Photorhabdus* cultures

For the extraction of PPYD and DARs cultures of *P. luminescens* DJC strains, *P. luminescens* WT, *P. luminescens*  $\Delta$ fadD, *P. luminescens*  $\Delta$ fadL, *P. luminescens*  $\Delta$ fadL  $\Delta$ fadD, were grown at 26°C for 4 days (5 L LB medium). The culture was centrifuged (1905 rcf, 4°C, 20min) to separate cells from culture supernatant. The cells were disrupted by via French press (Glen Mills, USA). The hydrophobic contents of the culture supernatant and the cell lysate were extracted with pure

cyclohexane three times to extract the hydrophobic molecules. The cyclohexane extract was dried via vacuum evaporation. The weight of the residue was determined and resuspended in pure acetonitrile (ACN). The concentration was adjusted to 5 mg/ml.

## 2.11 Analytical Methods

### 2.11.1 HPLC analysis

Substances from the cell free culture supernatants and from the cell pellets of *P. luminescens* DJC wild type (WT), *P. luminescens* DJC  $\Delta fadD$ , *P. luminescens* DJC  $\Delta fadL$  and *P. luminescens* DJC  $\Delta fadD \Delta fadL$  were resuspended in MeOH (5  $\mu$ g/ml) and analyzed via HPLC UV-Vis (Shimadzu LC20). For the analysis a C18 column (Waters, Sunfire, C18, 5  $\mu$ m, 250 x 4.6 mm) was used at a temperature of 20°C and a linear gradient of 1% of acetonitrile (ACN) and 99% water (with 0,1% trifluoroacetic acid) to 100% ACN within 20 min, followed by 3 min of 100% ACN.

For fractionation of the larvae homogenate extract the samples were resuspended in ACN and sampled by time. For the separation in 15 fractions a C18 column (hypersilGOLD, Thermo Fischer, USA, 5  $\mu$ m, 250 x 4.6 mm) was used at a temperature of 30°C and a linear gradient starting with 1% of ACN (with 0.1% of formic acid) and 99% water (with 0.1% of formic acid) to 99% ACN within 25 min followed by 5 min of 99% ACN.

For the fractionation in a 96-well plate a C18 column (Waters, Sunfire, C18, 5  $\mu$ m, 250 x 4.6 mm) was used at a temperature of 20°C and a linear gradient starting with 1% of ACN and 99% water (with 0,1% trifluoroacetic acid) to 100% ACN within 20 min, followed by 3 min of 100% ACN. This was repeated three times and the fractions (F1-F92) were pooled in the same plate.

### 2.11.2 LC-MS analysis

For mass spectroscopy measurement the samples from the cell free culture supernatants and from the cell pellets of *P. luminescens* DJC wild type (WT), *P. luminescens* DJC  $\Delta fadD$ , *P. luminescens* DJC  $\Delta fadL$  and *P. luminescens* DJC  $\Delta fadD \Delta fadL$  were re-suspended in ACN and set to a concentration of 1 g/ml to 20 g/ml. The samples were analyzed by LC-MS (IBWF, Kaiserslautern) with a RP18 Supersper column (4  $\mu$ m particle size, L  $\times$  I.D. 25 cm  $\times$  4 mm) (Merck, Darmstadt) and run with a gradient starting with 0.1% acetonitrile to 100% within 20 minutes at a flowrate of 0.45 ml/min. As ionization method an atmospheric pressure chemical ionization was performed.

### 2.11.3 Reporter based fluorescence assay to quantify promoter activity

Electro-competent *P. luminescens* and *P. asymbiotica* cells were transformed via electroporation (1800V, 0.5 ms) with a plasmid carrying a gene encoding the mCherry under the control of the promoter of interest, e.g. pBR  $P_{plu0258}$ -mCherry. If an *E. coli* strain was used for the reporter assay, the transformation of the plasmid was performed via heat shock. An overnight culture of these strains was grown to OD  $\sim$ 1 at 30°C (37°C for *E. coli*) and diluted to an OD of 0.02 and 150  $\mu$ l were distributed into each well of a 96-well plate (TECAN microplates), where 1.5  $\mu$ l of the required supplement was added. If higher volumes were analyzed 1% (v/v) of supplement was added. The fluorescence assay was taken out in a TECAN Spark 20M (TECAN, Zürich) with measurements (560 nm excitation / 612 nm emission) every 30 min for 48 h. In-between the measurements the plate was shaken in a double orbital matter at 30°C (*E. coli* at 37°C). Furthermore, the absorbance (OD<sub>600</sub>) was measured to quantify growth, as well as the luminescence, if the assay was performed with a *P.*

*luminescens* strain. Fluorescence signal intensity was set in perspective with the optical density of the culture.

#### **2.11.4 Reporter-based luminescence assays to quantify promoter activity**

For the reporter assay, *E. coli* LMG 194 was transformed with the particular plasmid harboring the *lux-CDABE* operon (e.g. pBBR1-*P<sub>plu0258</sub>-lux*), under the control of the promoter of interest, via a heat shock. This strain also was transformed with the plasmid pBAD24 containing an inducible promoter upstream of a gene for the production the regulator of interest (e.g. pBAD24-*pluR-pikR2*, **Tab 2.5**). An overnight culture of the reporter strain was grown to  $OD_{600} = 1$  at 37°C and diluted to an  $OD = 0.02$ . 150 µl of this culture was then distributed into a 96-well plate (TEACN microplates) where 1.5 µl of the required supplement was added. The luminescence was measured in a TEACN Spark 20M (TECAN, Zürich) with recordings every 30 minutes for 48h. In-between the plate was shaken in a double orbital matter at 37°C. Furthermore the absorbance ( $OD_{600}$ ) was measured to quantify growth. Luminescence intensity was set in perspective with the optical density of the culture.

#### **2.11.5 Fluorescence microscopy**

Overnight cultures of *P. luminescens* reporter strains (**2.11.3**) were inoculated in LB medium to an  $OD_{600}$  of 0.1 and supplemented with 10 nM (or 1% (v/v)) of the corresponding signaling molecule. At an  $OD_{600}$  of 1 5 µl were placed on an agar strip and visualized under fluorescence microscope (Leica DMI8, Leica, Wetzlar). For mCherry an excitation at 560 nm and emission at 612 nm was used. The mean fluorescence of the cells was calculated determined via ImageJ (ImageJ 1.53a, National Institute of Mental Health; <http://rsb.info.nih.gov/ij/>).

## 2.12 Protein chemical methods

### 2.12.1 Protein overproduction

*E. coli* BL21 (DE3) pLysS (Merck, Darmstadt) was transformed via heat shock with the plasmid containing the gene encoding the His-tagged PikR2. 1 liter of LB medium with the corresponding antibiotic was inoculated to an  $OD_{600} = 0.1$  with an overnight culture of *E. coli* BL21 (DE3) pLysS and incubated at 37°C until the optical density reached  $OD_{600} = 0.5$ . Then the incubation temperature was set to 30°C and the gene expression was induced by the addition of 0.5 mM IPTG. After 2-3 h the culture was centrifuged (1505 rcf, 25 min, 4°C) and the cell pellet was shock frozen with liquid nitrogen and stored at -80°C before use.

### 2.12.2 Cell disruption

The cell pellet of a culture, in which a protein was overproduced, was slowly defrosted on ice and then resuspended in lysis buffer (0.2 g/ml) (**Tab. 2.2**). The resuspended cells were treated with a sonifier (Branson Analog Sonifier 450 Ultrasonic Processor, Branson, USA) two times (1 min, 70% amplitude, 0.5 s pulsation) and finally disrupted with a French Press (G-M High Pressure Cell Disruptor, Glen Mills Inc., USA). The procedure was repeated three times with a pressure of 20.000 psi. To separate cell debris and membrane material the bulk was centrifuged (45.000 rpm, 4°C, 80 min). The cytosolic fraction was stored on ice at 4°C for further procedure.

### 2.12.3 Protein purification

For the purification of the His-tagged PikR2 1 ml Nickel NTA agarose (Qiagen) was washed twice with deionized water (10ml) and equilibrated with lyses buffer (**Tab. 2.2**). The Nickel NTA agarose was then added to the cytosol containing the His-

tagged PikR2 and was equilibrated for 1 h at 4°C. The Nickel NTA and cytosolic fraction was then loaded on a column and the flow through was collected. Two times the Nickel NTA was washed with 15 ml washing buffer (**Tab. 2.2**) before the elution was performed with 1 ml of elution buffer (**Tab. 2.2**). The elution was repeated 6 times. All fractions were collected in tubes on ice and stored at 4°C for further usage. For determination of protein concentration, a NanoDrop device (NanoDrop™ One, Thermo Fischer, USA) was used.

#### **2.12.4 SDS-PAGE**

For the SDS-PAGE 30 µl of each fraction from the protein purification was mixed with 5µl of SDS loading buffer (6x) (**Tab. 2.2**), heated for 15 min (99°C) and let cool down to RT. SDS gels with 12.5% (V/V) acrylamide were prepared by filling up about 80% of a glass chamber with running gel components. After this part of the gel was hardened, the chamber was filled up with the stacking gel mixture and a comb was inserted to create pockets in the upper part of the SDS gel. After about 25 min the gel was hardened and stored at 4°C until use. The SDS gels were placed into an electrophoresis chamber (Mini-PROTEAN® Tetra Vertical Electrophoresis Cell, BIO-RAD) and 30 µl of the fractions were loaded into each pocket. 200V were applied until the blue loading dye was run to the bottom of the gel. The gel then was removed from the chamber for further staining or blotting.

#### **2.12.5 Coomassie staining**

To visualize proteins on an SDS gel, the gel was transferred into a flat container and treated with 20 ml coomassie coloring solution (**Tab. 2.2**) for 30 min. The elimination of non-bound coomassie was contained by washing with 15 ml of de-staining solution (**Tab 2.2**) which was applied 3 times for 1 h or overnight.

## **2.12.6 Western blot**

His-tagged proteins separated via SDS-gels were detected via Western-blot analysis. For that purpose, the proteins, separated on an SDS gel, were transferred onto a nitrocellulose membrane (Amersham™ Protran® Western blotting membranes, Cytiva, Freiburg) with a Trans-Blot Turbo Transfer System (BIO-RAD Laboratories, California, USA) using blotting buffer (**Tab. 2.2**). The membrane was then equilibrated for 1h with buffer A (**Tab 2.2**) in a falcon tube. Afterwards the buffer was exchanged with buffer A, containing 3% BSA and 1µl of a rabbit anti-His-antibody (0.5 mg/ml), and incubated for 1h. This was followed by 3 washing steps with buffer A (15 ml, 5 min). Then the membrane was equilibrated for 1h with buffer A, containing 3% BSA and 3 µl anti rabbit antibody with conjugated horseradish peroxidase (0.5 mg/ml). After 3 washing steps (15 ml, 10 min) with buffer A, the membrane was placed in a flat bowl containing 10 ml substrate buffer with BCIP and incubated at 37°C. Dark blue marks visualized the spots where His-tagged protein was detected. The enzymatic process was stopped as soon as the spots were visible by washing with H<sub>2</sub>O.

## **2.13 Protein analytical Methods**

### **2.13.1 Thermal shift assay (nanoDSF)**

To analyze thermal stability shift of proteins in different buffer conditions and in presence of different compounds or homogenate a Prometheus NT.48 (NanoTemper, Munich) was used. Purified protein was set to a defined concentration (at least 0.1mg/ml end concentration) and mixed with the compound or buffer in a ratio of 1:3. For this experiment the additives from the Solubility & Stability Screen Kit (Hampton Research, USA) was used. A capillary (Prometheus NT.48 Series nanoDSF Grade Standard Capillaries, NanoTemper, Munich) was filled with the suspension and

measured in the nanoDSF. The temperature gradient was set to 1.5°C / min from 25°C to 80°C. The results were analyzed with PR.ChemControl (NanoTemper, Munich). For the analysis the ration of the signal intensity at 350 nm was divided by the signal intensity at 330 nm. The results were shown by applying the first derivative to the chromatogram of the ration (350nm / 330nm) (shown as “First Derivative”).

### **2.13.2 Surface plasmon resonance (SPR) spectroscopy**

SPR analysis was performed in a Biacore T200 (Cytiva, Freiburg) using carboxymethyl dextran sensor chips that were pre-coated with streptavidin (Sensor Chip SA, Biacore, Uppsala). DNA fragments containing the promoter regions were 5'-biotinylated via PCR using the primers Btn-Pplu0258fwd and Pplu0258rev for genomic Btn-*P<sub>plu0258</sub>* amplification. Btn-*P<sub>plu1561</sub>* was achieved using the primer pair Btn-plu1561fwd + plu1561rev. Last, Btn-*P<sub>plu1692</sub>* was amplified using Btn-Pplu1692fwd and Pplu1692rev.

Before immobilization of the DNA fragment, the chip was equilibrated by three injections using 90µl of 1 M NaCl/50 mM NaOH at a flow rate of 10 µl/min. 10 nM of the respective biotinylated DNA was injected using a contact time of 420 seconds and a flow rate of 10 µl/min. Approximately 600 RU of *P<sub>plu0258</sub>* was captured onto flow cell 2, *P<sub>plu1561</sub>* onto flow cell 3 and *P<sub>plu1962</sub>* onto flow cell 4, respectively, of the chip. Plu2019 was diluted in flow buffer and passed over flow cells 1 to 4 in different concentrations (0 nM, 7,8125 nM, 15,625 nM, 15,625 nM, 62,5 nM, 125 nM, 250 nM, 500nM, 1000 nM and 2000 nM) using a contact time of 120 sec followed by a 600 sec dissociation time before the next cycle started. The experiments were carried out at 25°C at a flow rate of 30 µl/min. After each cycle, regeneration of the surface was achieved by injection of 2.5 M NaCl for 60 sec followed by 0.5% SDS for 60 sec at 30 µ/min flow rate. Sensograms were recorded using the Biacore T200 Control software and analyzed with the Biacore T200 Evaluation Software 3.2.0.5 (Cytiva, Freiburg).

The surface of flow cell 1 was used to obtain blank sensograms for subtraction of bulk refractive index background. The referenced sensograms were normalized to a baseline of 0. The 1:1 binding algorithm was used for calculation of the binding affinity.

## **2.14 Entomological methods performed with *G. mellonella***

### **2.14.1 Larvae rearing**

*G. mellonella* were reared in jars (J. Weck GmbH u. Co. KG, Wehr-Öflingen) at 34°C and fed with a variation of the Haydak medium (Chippendale 1970) (500 g honey, 500 g wheat bran, 400 g glycerol (86%), 300 g wheat flour, 200g semolina, 100 g milk powder, 100 ml water, 84 g bakery yeast). The moths laid on filter paper on top of the jar, which were collected and replaced with fresh filter paper 2-3 times over 1 week. The eggs were placed with the filter paper in jars containing about 100g of medium. After 2-3 weeks the hatched larvae were divided into other jars, containing about 200 larvae and 150 g medium, and let grow for another 2 weeks. When reaching the last instar (2-3 cm in length) 20 Larvae were left in a jar for metamorphosis at 34°C without medium. The moths then were able to lay eggs on filter paper, which were used for the next rearing cycle. The other larvae were collected and frozen with liquid nitrogen or used alive for pathogenicity assays.

### **2.14.2 Generation of insect homogenate**

To generate insect larvae homogenate fifty frozen larvae or 20 g of nematodes, and 12 ceramic beads (6,35mm, MP Biomedicals, USA) were mixed with 20ml PBS buffer (**Tab. 2.2**) in a 50ml falcon tube and homogenated in a FastPrep Homogenizer (MP Biomedicals, USA). The larvae debris was removed by centrifugation (1905 rcf, 15 min). For long term storage the homogenate was freeze-dried and stored at -20°C.

### **2.14.3 Pathogenicity assay**

To perform a pathogenicity assay ten *G. mellonella* larvae in their last instar, were surface sterilized with 70% EtOH and injected with a syringe (Hamilton Company, USA) in the rear leg with 10 µl of culture containing about 1000 cells from an overnight culture of *Photorhabdus* strains (**Tab. 2.3**). The larvae were kept at 30°C and observed for 72 hours. As control the same volume of the related medium was injected into the larvae. This was repeated three times with fresh larvae for each trail. When a larva was turned on the back and was not moving back on the legs it was determined as dead. After 72 h images were taken by a luminescence camera (7 min of integration time, PEQLAB Fusion, Erlangen) to verify that the larvae were killed by the bioluminescent *Photorhabdus* bacteria.

## **2.15 Cell biological methods**

### **2.15.1 Cell cultures**

Cultivation of HeLa Kyoto (Gey et al. 1952), NIH 3T3 cells (Todaro und Green 1963), and HCT116 colon cancer cells (Rajput et al. 2008) were carried out in Dulbecco's Modified Eagle's medium (DMEM) at 37°C and a CO<sub>2</sub> concentration of 5%. The medium was substituted with 10% fetal bovine serum (FBS) and 0.1% gentamycin. For propagation the cells were split in a ratio of 1:10 every two days. The media were removed, and the cells were washed with PBS buffer to remove dead cells before the cells were stripped from the surface with trypsin and incubated for 3-5 min before DMEM was added. The cells were counted using a Fast-Read 102 cell count chamber (Kova international) and an appropriate volume of this cell suspension was transferred into a fresh cell culture plate and diluted with DMEM Cell cultures were cultivated in collaboration with Jeannette Koch and Daniela Meilinger, LMU München

### **2.15.2 Cell viability assay**

500 µl of freshly prepared cells (100.000 cells / ml) for live cell imaging were placed in 24 well plates and let settle overnight. These cells were treated with 100µl bacterial supernatant (2.7.2) or a solution of purified secondary metabolite of *Xenorhabdus* or *Photorhabdus* using the designated concentration. All dilutions of purified metabolites were prepared in DMEM media substituted with 10% (V/V) FBS and gentamycin. Before imaging the cells were washed with PBS to remove dead cells. Determination of viability was performed with an EVOS Cell Imaging System (Thermo Fischer, USA). Quantification of the cytotoxic effectiveness was determined by counting the cells in the visualized area. These cell numbers were compared between treated samples to the negative control, treated with the medium control. An effect was determined to be strong when the number of live cells were decreased by >90% in the visualized area. Images were acquired in collaboration with Jeannette Koch and Daniela Meilinger, LMU München

### **2.15.3 Life Cell imaging**

The DNA dye SiR-DNA was used for live cells for visualizing morphological effects during treatment with purified secondary metabolites from *Xenorhabdus*, *Photorhabdus* or the corresponding culture supernatant extracts. For that 25.000 cells were seeded in 300µl of DMEM in an 8 well plate (ibidi, Gräfelfing) and incubated overnight. Before microscopy the media was removed and replaced with fresh DMEM and 0.1% SiR-DNA dye, followed by 1h of incubation at 37°C. Then the plate was placed under the microscope (Nikon, CSU Spinning Disk, WL: λABS / EM: 652/674 nm) and images were taken every 15 min over a timescale of 25 h using the “time-lapse” function. Images were acquired in collaboration with Anna Lena Weber and Hartmann Harz, LMU München

## 2.16 Bioinformatical Methods

### 2.16.1 Structure prediction and modelling of proteins

The structures of FadL was modelled based on crystal structure of FadL of *E. coli* (van den Berg et al. 2004) using the HHpred tool (Homology detection & structure prediction by HMM-HMM comparison) (Söding et al. 2005) and Phyre2 (Kelley et al. 2015). Visualization of the structure was done with UCSF Chimera (Pettersen et al. 2004). The PDB identifier 1T1L was used for the crystal structure of FadL of *E. coli* (van den Berg et al. 2004). For FadD the structure was predicted with Phyre2 (Kelley et al. 2015) and visualized using UCSF Chimera (Pettersen et al. 2004).

### 2.16.2 Amino acid sequence comparison

The amino acid sequences of FadD and FadL were compared with BLAST [blastp protein-protein BLAST (Altschul et al. 1990)]. The NCBI Reference Sequence: NP\_416319.1 was used as FadD sequence of *Escherichia coli str. K-12* substr. MG1655. The genome sequences of *P. luminescens* subsp. *laumondii* TT01 (GenBank: BX470251.1), *P. luminescens* subsp. *laumondii* DJC (GenBank: CP024900.1) (Zamora-Lagos et al. 2018) and *Photorhabdus asymbiotica* PB68.1 (NZ\_LOMY00000000.1) (Tobias et al. 2016) were used for comparison of FadD and FadL of *Photorhabdus* with the corresponding proteins from *E. coli* MG1655, *P. asymbiotica* *S. meliloti* and *P. aeruginosa*. The translation of the specific genes from nucleotide to amino acid sequence was performed with CLC Workbench 7.

### **3 Results**

The pathogenic part of the lifecycle of *Photorhabdus* and *Xenorhabdus* requires further investigation to specific aspects regarding the communication between the bacteria and the host. It was shown that PikR1 / PikR2 regulated several genes in presence of larvae homogenate via inter-kingdom signaling, but the recognized molecule is not identified yet. When sensing the host, QS coordinates group behavior via PPYD and DARs in *Photorhabdus*. The synthesis of the molecules is revealed, but the transport of the signaling molecules is still unclear. Furthermore, as response to the host a broad range of secondary metabolites are produced by the entomopathogenic bacteria with a wide spectrum of characteristics. The cytotoxic potential of many of the secondary metabolites have not been studied yet.

All of these aspects in the pathogenic part of the lifecycle require deeper investigation for the future development of novel drugs.

#### **3.1 Inter-kingdom signaling by *P. luminescens* - PikR1 / PikR2 sense *G. mellonella* originated compounds**

The identification of the insect host for regulation of the pathogenic lifestyle is a very important step in the beginning of the pathogenic part of *P. luminescens* for adaptation of the changing environment. The high number of PAS4-LuxR solos might play a role in this sensing of the insect host and was investigated in this thesis.

##### **3.1.1 PAS4-LuxR solo PikR1 / PikR2 regulate pathogenicity towards *G. mellonella* larvae**

To investigate the influence of the gene clusters *plu0918-plu0925*, *plu20016-plu2016* and *pikR1-pikR2* on the pathogenicity against *G. mellonella* larvae, a pathogenicity assay was performed with knockout mutants lacking each one of these gene clusters. Approximately 1000 cells of *Photorhabdus* were injected with a syringe in a rear leg

(Hamilton Company, USA) and larvae mortality was monitored for 72h. After 48 hours all *G. mellonella* larvae were killed when injected with the *P. luminescens* wild type. *P. luminescens*  $\Delta plu2001-plu2016$  and *P. luminescens*  $\Delta plu0918-plu0925$  showed wild type like pathogenicity, whereas *P. luminescens*  $\Delta pikR1-pikR2$  was reduced and delayed pathogenic towards the *G. mellonella* larvae. After 48h still about 60% of the larvae were alive and about 30% were not killed within 72h. Larvae injected with the medium control survived until the end of the experiment and did show no change in pigmentation or bioluminescence. All dead larvae injected with *Photorhabdus* culture showed intense bioluminescence and red / brownish pigmentation (Fig. 3.1.1B).

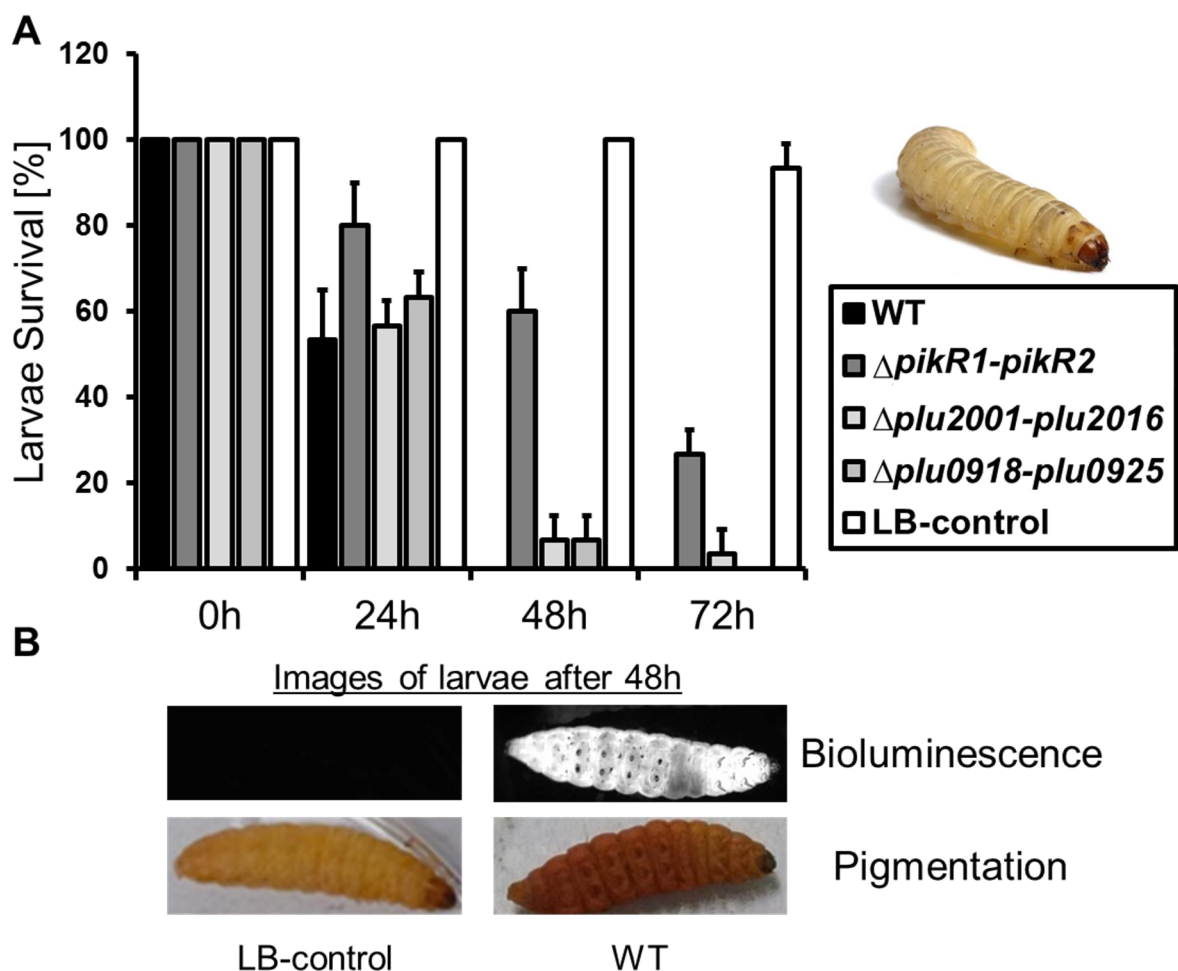


**Figure 3.1.1: Pathogenicity assay in *G. mellonella*.** A) 10 larvae were injected with approximately 1000 cells of *Photorhabdus* of each strain and pathogenicity was observed for 72h. Whereas *P. luminescens*  $\Delta plu0918-plu0925$  and *P. luminescens*  $\Delta plu2001-plu2016$  show wild type-like pathogenicity and died within 48h, the *P.*

*luminescens* mutant lacking *pikR1-pikR2* shows delayed and reduced pathogenicity within 72h. Error bars show standard deviation of three independent experiments. **B)** Exemplary images of live *G. mellonella* larvae after 48h injected with 10 $\mu$ l LB medium and 10 $\mu$ l of *P. luminescens* wild type. Larvae injected with LB survived, showed no bioluminescence and kept the yellow pigmentation. Dead larvae injected with *Photorhabdus* culture showed red pigmentation and intense bioluminescence within 48h.

### **3.1.2 PikR1 / PikR2 sense a signaling molecule derived from *G. mellonella***

With the results from the pathogenicity assay (**Fig 3.1.1**) and previous results showing first characteristics of the signaling molecule sensed by PikR1 / PikR2 (Rothmeier 2010), it is known that the inter-kingdom signaling molecule originates from *G. mellonella* and is supposed to be a small molecule

For the identification and for detection, whether the signaling molecule sensed by PikR1 / PikR2 is present, a fluorescence based reporter system was established. As *plu1561* occurred to be differentially regulated only in the absence of larvae homogenate (Rothmeier 2010) and PikR2 bound to  $P_{plu1962}$  only at relatively high concentrations in the SPR analysis, a reporter assay system under the control of  $P_{plu0258}$  was chosen. A *P. luminescens* reporter strain, containing the plasmid pBBR1  $P_{plu0258}$ -mCherry, was used to visualize the presence of the ligand of PikR1 / PikR2 by measuring the fluorescence intensity of mCherry under the control of the promotor of *plu0258*, which is activated by PikR1 / PikR2 when the ligand is present.

To determine whether PikR1 or PikR2 is essential for sensing a eukaryotic signal from *G. mellonella*, several trials for single deletion of either PikR1 or PikR2 were performed. Unfortunately, neither the *P. luminescens* TT01  $\Delta pikR1$  nor the *P. luminescens* TT01  $\Delta pikR2$  single deletion mutant was achieved due to high DNA sequence similarities. Therefore, all of the following experiments were performed with the *P. luminescens* TT01  $\Delta pikR1 / pikR2$  deletion mutant.

To demonstrate that PikR1 / PikR2 activate  $P_{plu0258}$  in presence of *G. mellonella* larvae homogenate, fluorescence microscopy images were taken from *P. luminescens* TT01 pBR- $P_{plu0258}$ -mCherry and *P. luminescens* TT01  $\Delta pikR1 / pikR2$  pBR- $P_{plu0258}$ -mCherry. The culture of *P. luminescens* TT01 pBR- $P_{plu0258}$ -mCherry showed high fluorescence intensity when supplemented with larvae homogenate, whereas in the non-supplemented culture only a basal fluorescence was visible. In the cultures of *P. luminescens* TT01  $\Delta pikR1 / pikR2$  pBR- $P_{plu0258}$ -mCherry no fluorescence was visible, with or without *G. mellonella* larvae homogenate (**Fig 3.1.2A**).

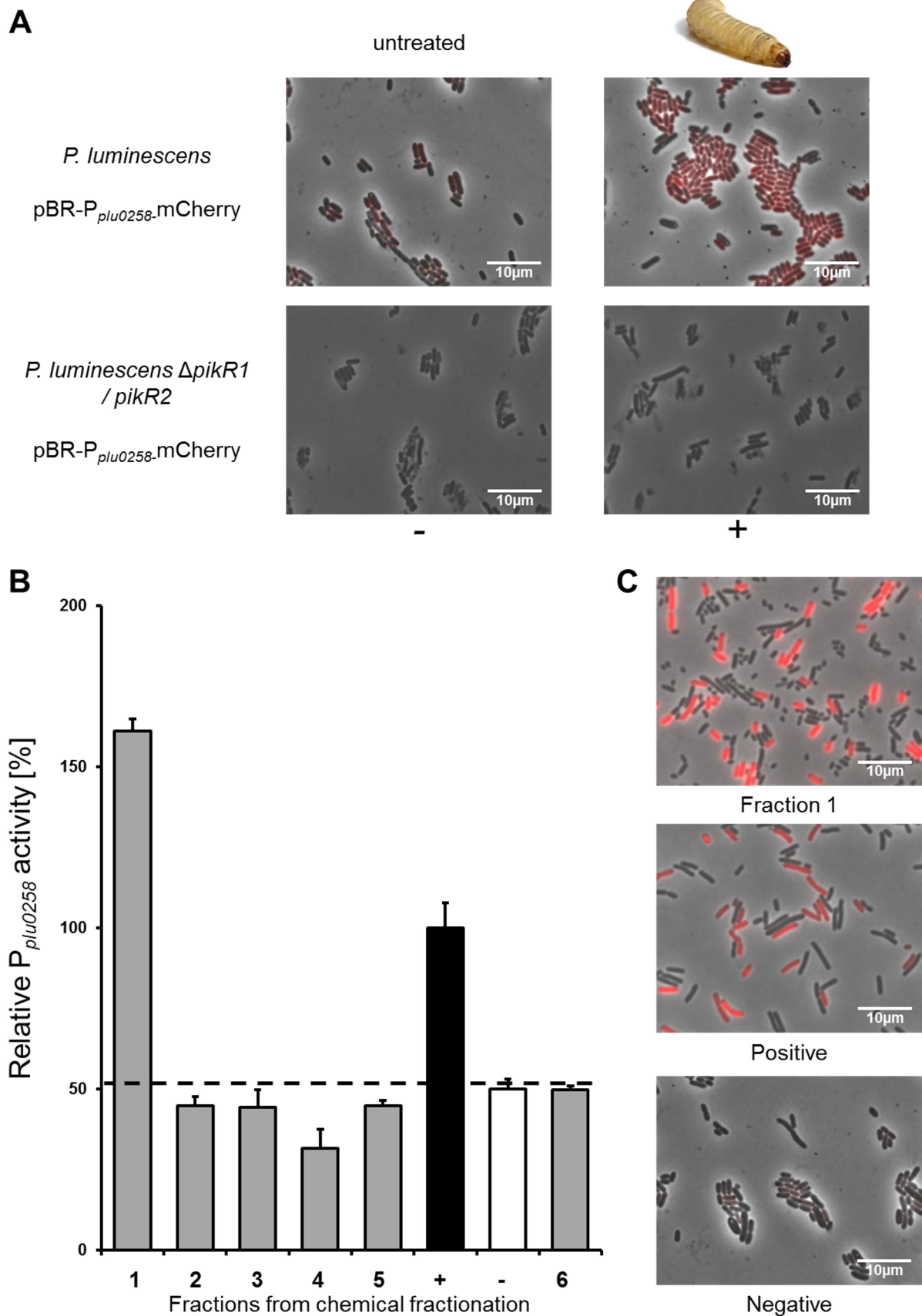


**Figure 3.1.2: Effect of *G. mellonella* homogenate on relative activity of  $P_{plu0258}$**   
**A)** Untreated cultures of *P. luminescens* TT01 pBR- $P_{plu0258}$ -mCherry show only basal levels of fluorescence (top left), whereas the addition of *G. mellonella* homogenate results in high fluorescence levels (top right). Cultures of *P. luminescens* TT01

$\Delta pikR1 / pikR2$  pBR- $P_{plu0258}$ -mCherry did not show fluorescence with nor without *G. mellonella* larvae homogenate (bottom left and right). **B)** Relative activity of  $P_{plu0258}$  in the reporter strain *P. luminescens* TT01 pBR- $P_{plu0258}$ -mCherry supplemented with the different fractions after manual separation. As positive control (black) crude *G. mellonella* larvae homogenate was supplemented. As negative control (white) the reporter strain culture remained untreated but handled as the others. Fractions 1-6 are the extracted from homogenate adjusted to following pH: fraction 1: neutral, fraction 2: pH 1, fraction 3: pH 4-5, fraction 4: pH >10, fraction 5: pH 9 and fraction 6: remaining aqueous phase. Fluorescence signal intensity of cultures treated with fraction 2-6 is similar to the negative control. The culture treated with extract from fraction 1 showed high fluorescence signal intensity. **C)** Fluorescence microscopy images of the culture treated with extract of fraction 1 showed a strong fluorescence signal as the positive control, whereas the negative control only shows low to no fluorescence signal.

### **3.1.3 Purification of signaling molecule from *G. mellonella* sensed by PikR1 / PikR2**

To gain first insights of the chemical characteristics of the signaling molecule the larvae homogenate was fractionated by application of different pH conditions and separation of the hydrophobic parts in each condition. Therefore, the homogenate was adjusted consecutively from neutral pH to pH 1, pH 4-5, pH >10 and pH 9. In each step the hydrophobic molecules were extracted by solvent extraction with ethyl acetate (EAc). In fractions with high fluorescence signal intensity the signaling molecule of PikR1 / PikR2 is present as  $P_{plu0258}$  is activated and mCherry is produced. The reporter strain cultures were analyzed by fluorescence microscopy. The fractions 1-6 (neutral pH, pH 1, pH 4-5, pH 10, pH 9 and the remaining aqueous fraction) were added to the reporter strain *P. luminescens* TT01 pBR- $P_{plu0258}$ -mCherry and fluorescence was analyzed via fluorescence microscopy and quantified using a plate reader. The analysis revealed that the signaling molecule was extracted in the first step in the extract of fraction 1 with neutral pH (**Fig. 3.1.2B**). As positive control pure larvae homogenate was supplemented. As negative control an untreated reporter strain was analyzed for fluorescence signal intensity.

For fractionation of the extract of fraction 1 (In the following as “fraction 1”) an HPLC separation was performed to further reduce the numbers of possible signaling molecules per fraction. These 15 fractions were applied on the fluorescence based reporter assay with the reporter strain *P. luminescens* TT01 pBR-P<sub>plu0258</sub>-mCherry (**Fig. 3.1.3A**). With ascending fraction number the hydrophobicity of the eluent in the HPLC increased, thus the more hydrophobic molecules were eluted in the fractions with higher numbers. *P. luminescens* TT01 pBR-P<sub>plu0258</sub>-mCherry showed high fluorescence signal intensity when supplemented with HPLC fractions 14 and especially HPLC fraction 15.

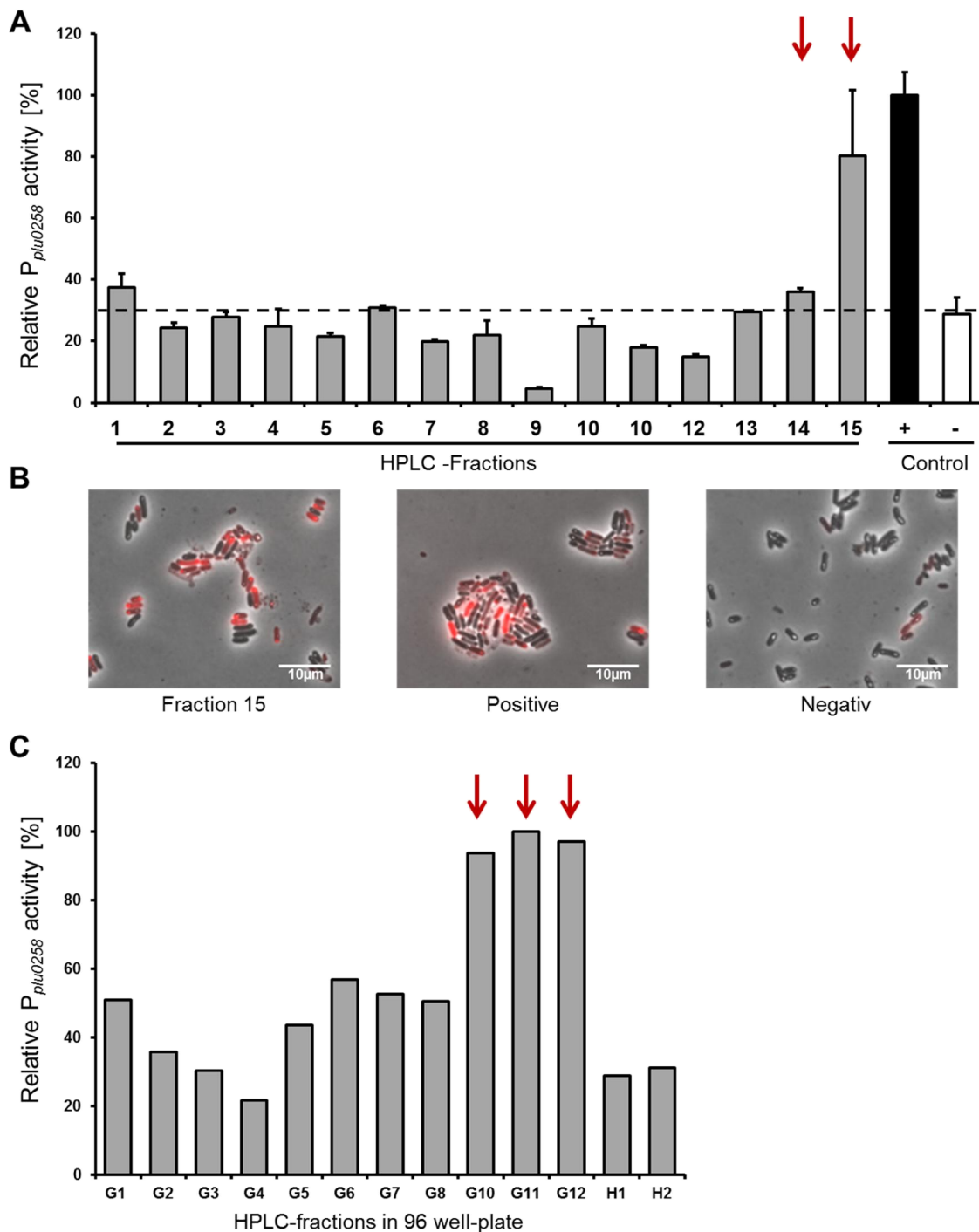


**Figure 3.1.3: Effect of fractions of the separation via HPLC on relative activity of  $P_{plu0258}$  in the *P. luminescens* pBR- $P_{plu0258}$ -mCherry reporter strain. A)** Reporter strain *P. luminescens* TT01 pBR- $P_{plu0258}$ -mCherry was supplemented with 15 different HPLC fractions of the hydrophobic extract of the *G. mellonella* larvae homogenate. With ascending number of the fractions, the eluent became more hydrophobic. As positive control (black) crude *G. mellonella* larvae homogenate was supplemented. As negative control (white) the reporter strain culture remained untreated but handled as the others. In cultures treated with HPLC fraction 14 and 15 (red arrows) high fluorescence signal was measured. **B)** Fluorescence microscopy images of the culture treated with the extract of HPLC fraction 15 show a strong fluorescence signal as the positive control, whereas the negative control only shows

low to no fluorescence signal. **C)** The reporter assay showed high signal intensity in wells G10-G12 (red arrows), demonstrating the presence of the signaling molecule of PikR1 / PikR2 in these fractions. Signal intensity in wells A1-F12 and H3-H8 was similar to the presented wells with lower signal intensity than in G10-G12. With ascending number of the fractions, the eluent became more hydrophobic.

To get further information about the content of HPLC fraction 14 and 15 an LC-MS analysis was performed with “fraction 1”. In this analysis “fraction 1” was fractionated in 92 fractions and collected in a 96-well plate. The eluent was evaporated and 150µl of the reporter strain *P. luminescens* TT01 pBR-P<sub>plu0258</sub>-mCherry were distributed in each well. The 96-well plate with the reporter strain was analyzed for the fluorescence signal intensity. Wells G10-G12 showed high fluorescence signal intensity demonstration the presence of the signaling molecule of PikR1 / PikR2 (**Fig. 3.1.3C**). Therefore, the corresponding MS data from the time frame covering these fractions was analyzed and the detected masses were matched to known compounds in *G. mellonella* larvae (Statistisches Bundesamt 2020) (**Tab 3.1.1**). Many of these identified substances are fatty acids and also known to be present in sunflower oil, which is easily available (Bundesministerium für Lebensmittel und Landwirtschaft 2020) (**Tab. 3.1.1**).

**Table 3.1.1: Masses detected in HPLC fraction G10-G12 during LC-MS analysis of “fraction 1” and the corresponding substances.** This table shows putative signaling molecules sensed by PikR1 / PikR2 as they were detected in an LC-MS analysis of “fraction 1”. A comparison of the masses found in the HPLC fraction G10-G12 with known substances in *G. mellonella* (Statistisches Bundesamt 2020) revealed the fatty acids listed in the table. Also the mass similar to JHIII was detected as it is present in insect larvae. A comparison of substances present in sunflower oil revealed, which fatty acids are present in both: HPLC fractions G10-G12 from “fraction 1” of the *G. mellonella* larvae homogenate and sunflower oil.

<b>Substance, MW</b>	<b>Masses detected via LC-MS</b>	<b>In <i>G. mellonella</i> and sunflower oil</b>
Linolenic acid, 278.43 g/mol	279.0 m/z	<b>yes</b>
Linoleic acid, 280.4472 g/mol	280.1 m/z	<b>yes</b>
Erucic acid, 338.6g/mol	338.0 m/z	<b>no</b>
Juvenile hormone III, 266.38 g/mol	265.0 m/z	<b>no</b>
Behenic acid, 340.58 g/mol	340.0 m/z	<b>no</b>
Stearic acid, 284.4 g/mol	283.0 m/z	<b>yes</b>
Palmitic acid, 256.43 g/mol	255.1 m/z	<b>yes</b>
Oleic acid, 282.47 g/mol	281.1 m/z	<b>yes</b>

### **3.1.4 PikR1 / PikR2 sense palmitic acid and stearic acid**

With these insights the reporter assay was performed with the matching substances, present in sunflower oil and *G. mellonella* larvae, (Tab. 3.1.1) to identify the signaling molecule sensed by PikR1 / PikR2. As the mass peaks 279.0 m/z and 280.1 m/z were identified as linolenic acid and linoleic acid, sunflower oil was chosen as another control for the reporter assay. Sunflower oil contains both fatty acids in a sufficient amount (Bundesministerium für Lebensmittel und Landwirtschaft 2020). As a first luminescence signal analysis of the reporter strain supplemented with sunflower oil showed high luminescence signal intensity (data not shown) we compared all detected peaks, whether they are known to be present in sunflower oil as well as in *G. mellonella* larvae. Erucic acid and behenic acid have similar masses to substances detected in the LC-MS analysis, but are not known to be included in

sunflower oil and *G. mellonella*. Therefore, the reporter assay was performed without the substances detected via LC-MS in the HPLC fractions G10-G12.

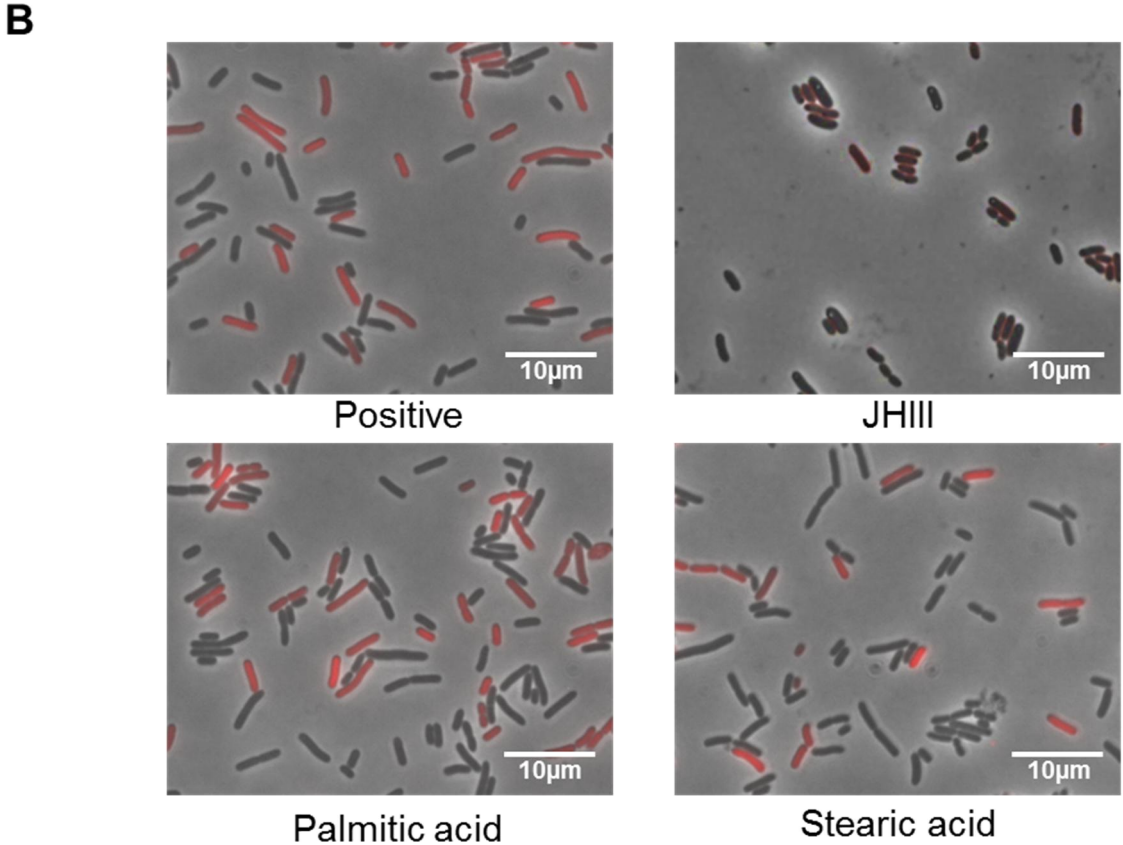
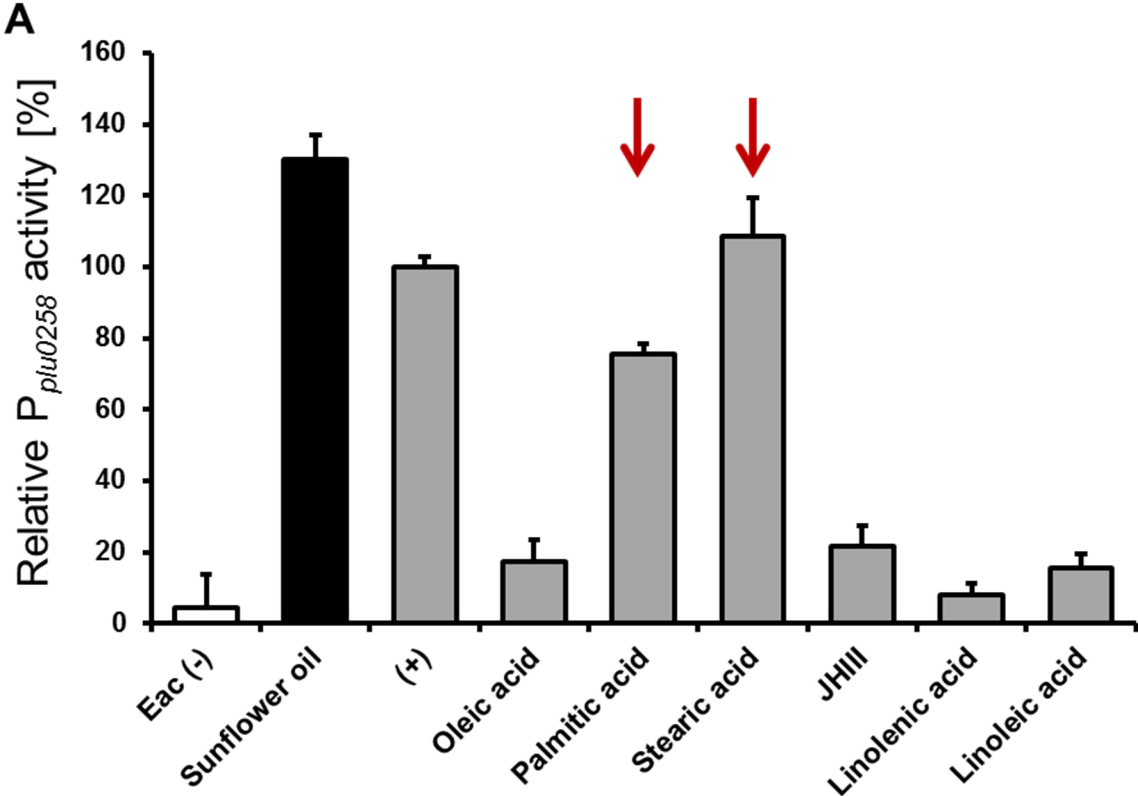


**Figure 3.1.4: Effect of specific substances on relative activity of  $P_{plu0258}$  in the *P. luminescens* pBR- $P_{plu0258}$ -mCherry reporter strain. A)** Reporter strain *P. luminescens* TT01 pBR- $P_{plu0258}$ -mCherry was supplemented with 100  $\mu$ M of different fatty acids and juvenile hormone III (JHIII). As control “fraction 1” and ethyl acetate (EAc) were used. The cultures treated with oleic acid, linolenic acid, linoleic acid and JHIII showed low fluorescence signal intensity, whereas cultures supplemented with sunflower oil, palmitic acid (red arrow) and stearic acid (red arrow) showed high fluorescence signal intensity. **B)** Fluorescence microscopy images of the culture treated with sunflower oil (black), stearic acid, palmitic acid and “fraction 1” (+) show a strong fluorescence signal, whereas cultures treated with oleic acid, JHIII linolenic acid, linoleic acid and the negative control (white) only show low to no fluorescence signal.

As high fluorescence signal intensities were measured in reporter strains supplemented with palmitic acid and stearic acid these two fatty acids were found to be the signaling molecules sensed by PikR1 / PikR2. For investigation of the binding sensitivity of PikR1 / PikR2 sensing stearic acid and palmitic acid a reporter assay was performed with decreasing concentrations of both fatty acids (**Fig. 3.1.5**). When the reporter strain *P. luminescens* TT01 pBR- $P_{plu0258}$ -mCherry was supplemented with concentrations lower than 10 nM of the fatty acids the fluorescence signal intensity of the reporter strain decreased. With these results it was shown that the PAS4-LuxR solos PikR1 / PikR2 sense the palmitic acid and stearic acid in *G. mellonella* at low nM concentrations.

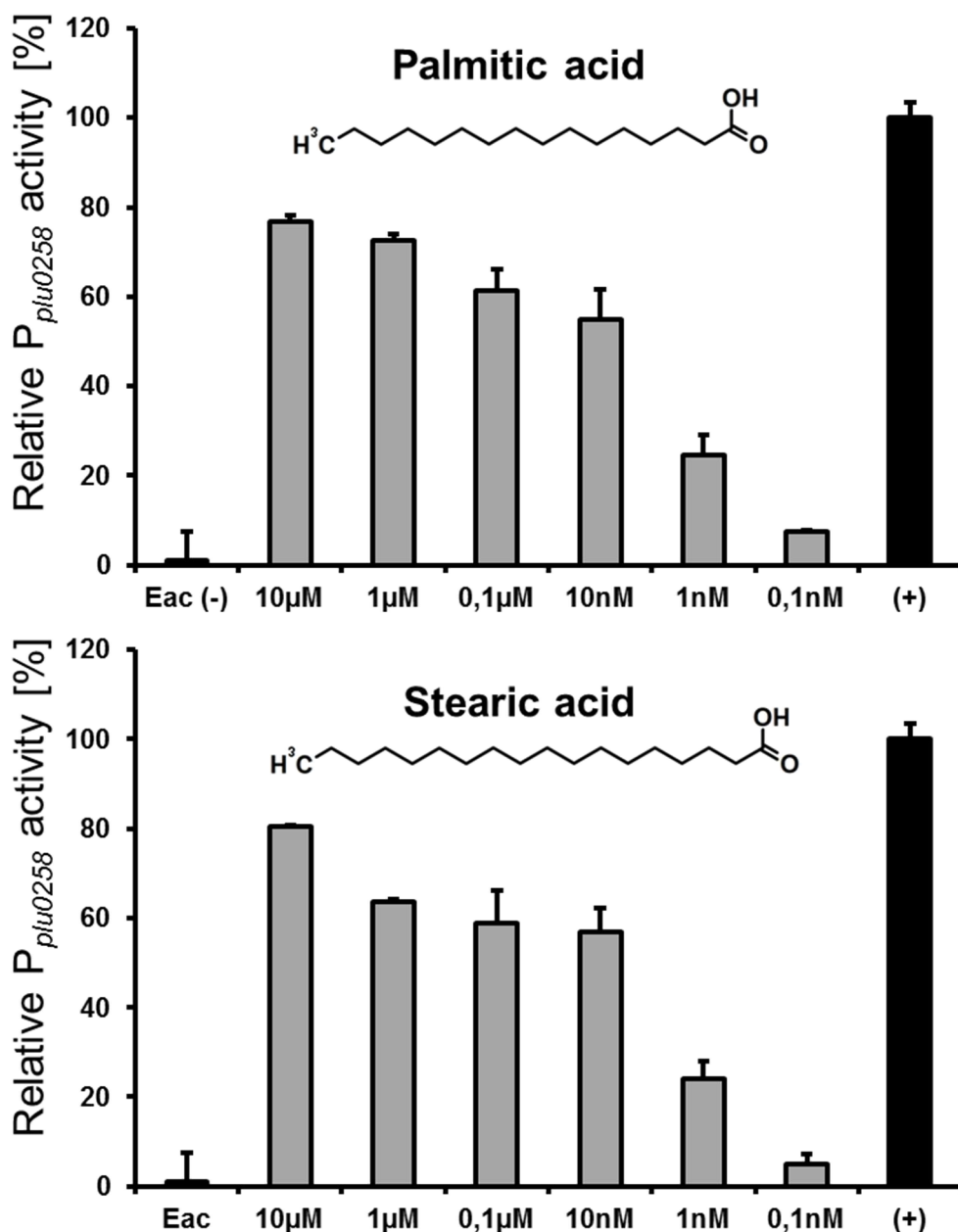


**Figure 3.1.5: Fluorescence signal analysis of the reporter strain supplemented with different concentrations of the signal molecules.** Reporter strain *P. luminescens* TT01 pBR- $P_{plu0258}$ -mCherry was supplemented with different concentrations of stearic acid and palmitic acid. When supplemented with concentrations lower than 10 nM the fluorescence signal intensity of the reporter strain decreased considerably.

### 3.1.5 Buffer optimization and purification of PikR2

Besides from the identification of the signaling molecule sensed by PikR1 / PikR2 also the binding kinetics between PAS4-LuxR solo and promoter region might be relevant for the development for novel drugs.

To better understand the binding kinetics of PikR2 the His-tagged PAS4-LuxR solo was overproduced and purified via Nickel affinity chromatography. LuxR-type proteins are difficult to produce and only very few are crystalized (Wu et al. 2019; Vannini 2002). For better solubility and to enhance protein concentration thermal shift assay was performed to optimize buffer conditions. The thermal shift assay revealed that the addition of osmotic active molecules enhanced protein stability (**Fig. 3.1.6**). Addition of sucrose increased the inflection point of PikR2 by 6.7°C (from 46.8°C to 53.5°C) showing an increased thermal stability, whereas the addition of 1.25% (V/V) of polyethylene glycol monomethyl ether 550 did not change the protein stability. Guanidine hydrochloride even destabilized the protein. Therefore the buffer was optimized by the addition of 100 mM sucrose (end concentration).

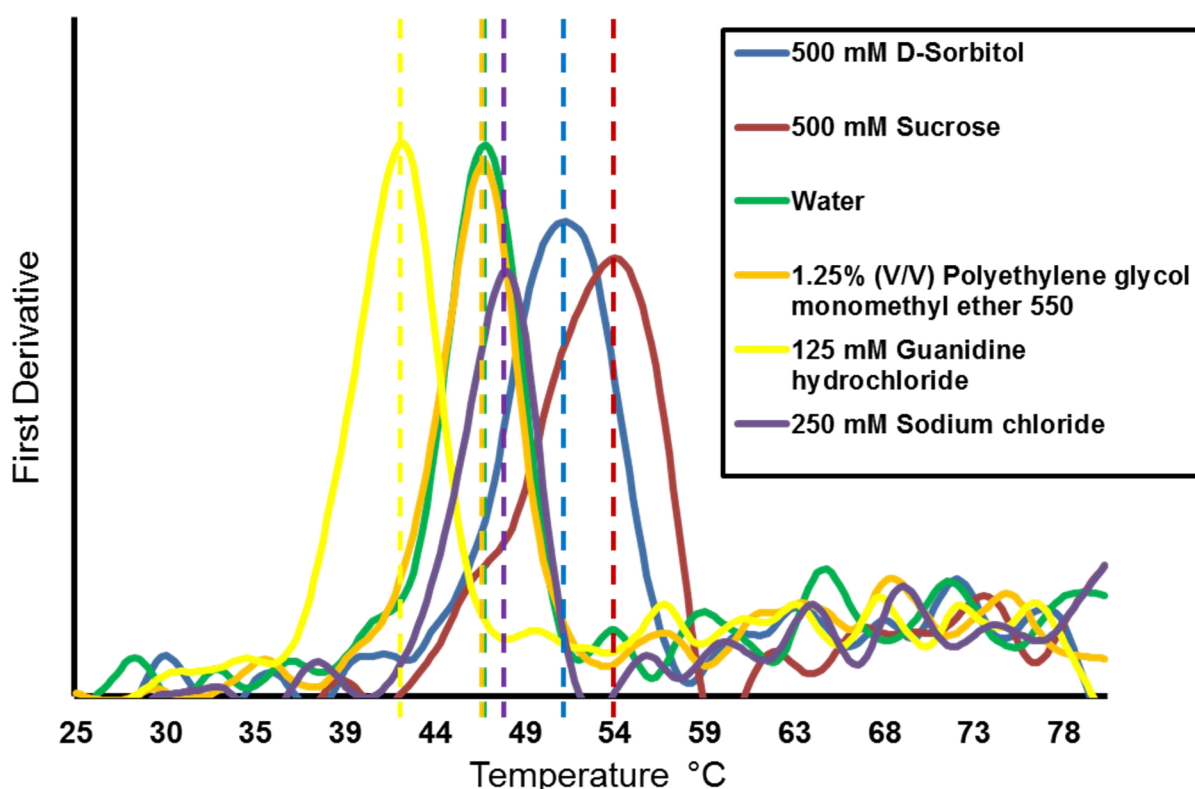


**Figure 3.1.6: Effects on PikR2 stability by the substitution of different additives to the buffer.** Selected additives showed different effects on the protein stability of PikR2. Guanidine hydrochloride (in yellow) destabilized the protein in the thermal shift assay, whereas polyethylene glycol monomethyl ether 550 (in orange) did not affect the stability. Sodium chloride (in purple) enhanced the stability of PikR2 slightly

and D-sorbitol (in blue) and sucrose (in red) increased the inflection point of the first derivative by more than 4°C. The striped line marks the temperature of the inflection points of the first derivative of the 350 nm / 330 nm ratio derived from the thermal shift assay.

With this optimization of the buffers the purification of His tagged PikR2 was efficient enough to analyze binding kinetics between PikR2 and the promoters of *plu0258*, *plu1561* and *plu1692* via SPR.

### 3.1.6 Pikr1/Pikr2 regulate genes for insect pathogenicity

PikR1 / PikR2 regulate several genes with various functions within *P. luminescens*.  
**(Supplementary Tab. S 3.1.2)**

The promoters of *plu0258*, *plu1561* and *plu1692* were chosen for further binding analysis with surface plasmon resonance spectroscopy (SPR). PikR2 showed strong and stable binding to the promoters of *plu0258* and *plu1561*, whereas the binding with  $P_{plu1962}$  occurred only at concentration of 62.5 nM and higher (**Fig. 3.1.7**). All interactions showed very low dissociation rates; thus the overall binding to the DNA was extremely stable. This showed that PikR2 interacts with all of the tested promoters, even without substitution of the signaling molecule. The shape of the sensograms support the idea, that supplemented ligand would increase the association rate as even with higher concentrations of PikR2 the saturation is not reached during the association phase. Due to the very high hydrophobicity of stearic acid and palmitic acid probably too less amount of the fatty acids were dissolved in the buffer used for SPR analysis. Therefore, SPR sensograms carried out with buffers supposed to contain the signaling molecule showed similar curve shapes. The  $K_D$  could not be calculated as the  $k_d$  value was out of the limits (**Supplementary Fig. S 3.1.2**).

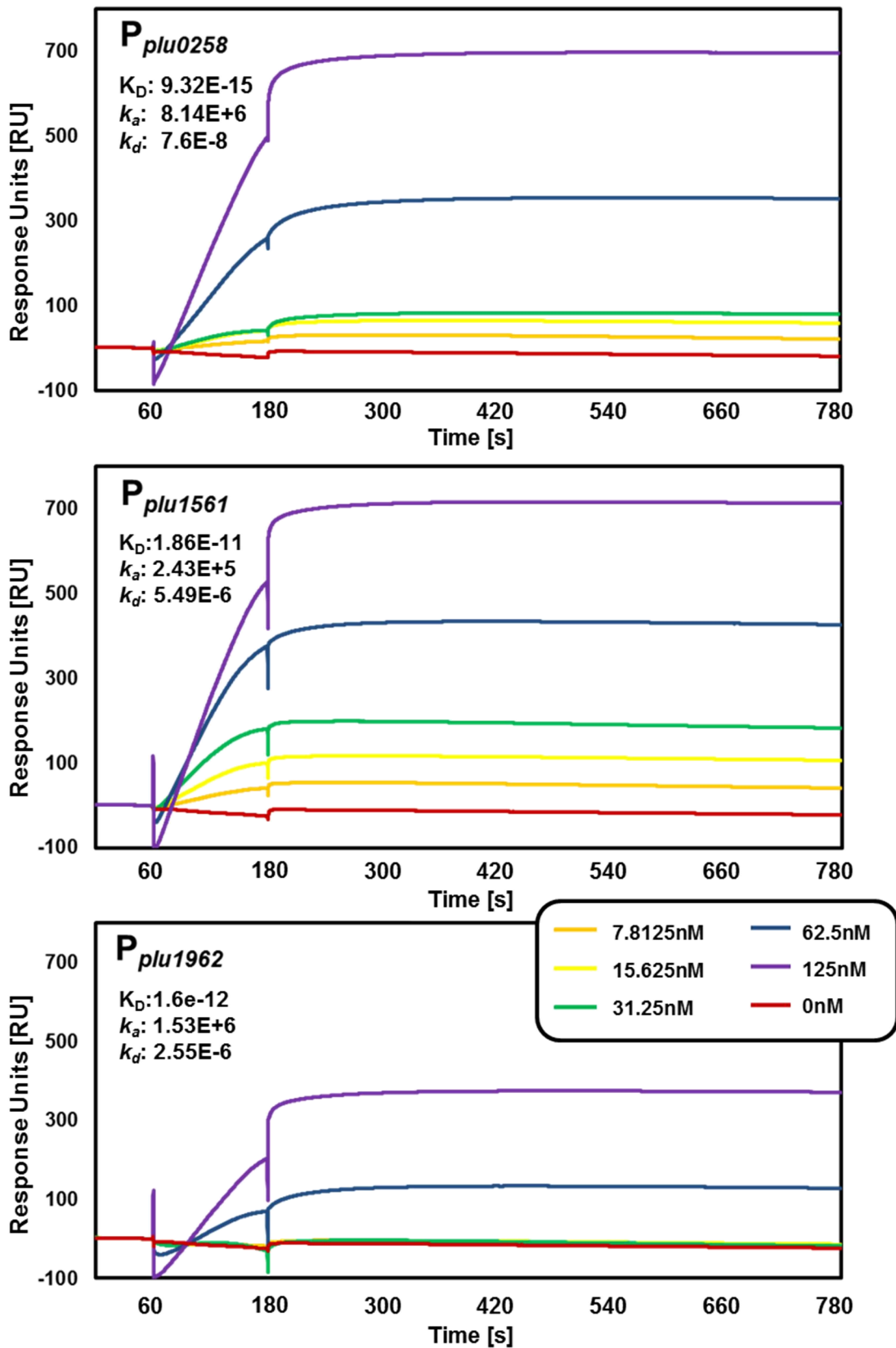


**Figure 3.1.7 SPR binding kinetics of PikR2 to P<sub>plu0258</sub>, P<sub>plu1561</sub> and P<sub>plu1962</sub>.** The three promoters P<sub>plu0258</sub>, P<sub>plu1561</sub> and P<sub>plu1962</sub> were immobilized to a SA sensor chip. Binding affinity kinetics of different concentrations (7.8125 nM (orange)), 15.625 nM (yellow), 31.25 nM (green), 62.5 nM (blue), 125 nM (violet) and 0nM (red)) of PikR2 were measured with 120 seconds of contact time followed by 600 seconds of

dissociation. PikR2 showed binding with all surface bound promoters. Stable binding to  $P_{plu1962}$  was measured at concentrations of 62.5 nM and higher, whereas stable binding occurred with  $P_{plu0258}$  and  $P_{plu1561}$  in all tested concentrations of PikR2. Due to very slow dissociation and bulk effects the  $k_d$  values were outside measurable limits, therefore the calculated  $K_D$  values are vague.

To get more information about the structural characteristics of the binding pocket of PikR2 a structure prediction of the signal binding domain (SBD) was performed, which was compared to other SBDs with known signal molecules. The predicted structure of the PAS4 SBD of PikR2 shows a highly similar structure to the PAS3 SBD of the Met from *Drosophila melanogaster* (*D. melanogaster*) (**Fig. 3.1.8A**), whereas the predicted structures of the SBD of TraR and PluR did not match in an alignment with the PAS4 domain of PikR2 (Chimera).

As the Met receptor from *D. melanogaster* is involved in larvae development and senses juvenile hormone III this was a first hint of similar structure of PikR1 / PikR2. To investigate, whether this structural similarity goes along with functional similarity hybrid proteins were created. These receptors contained the PikR2-DNA binding domain (DBD) and the SBD from PluR, the SBD from TraR and the PAS3 SBD from Met. In a luminescence-based reporter assay with the *lux-CDABE* operon under the control of  $P_{plu0258}$ , the activity of these hybrid proteins was measured in presence of the corresponding signaling molecule heterologously in *E. coli* LMG194. For comparison PikR2 was used as full protein and induced with larvae homogenate. All cultures were supplemented with 0.1% (V/V) arabinose for the induction of the gene expression of *traR-pikR2*, *pikR2*, *pas3-pikR2* and *pluR-pikR2* and with 10nM of the corresponding signaling molecule or 1% of larvae homogenate, respectively. After addition of juvenile hormone III the culture with PAS3-PikR2 activated  $P_{plu0258}$  resulting in an increased luminescence signal by factor 6. Cultures with the hybrid proteins TarR-PikR2 and PluR-PikR2 did not show significant differences in luminescence levels after induction with the corresponding signaling molecule. The

culture with full length PikR2, which was supplemented with *G. mellonella* larvae homogenate, showed an increased induction of luminescence by the factor 12 (**Fig. 3.1.8B**).

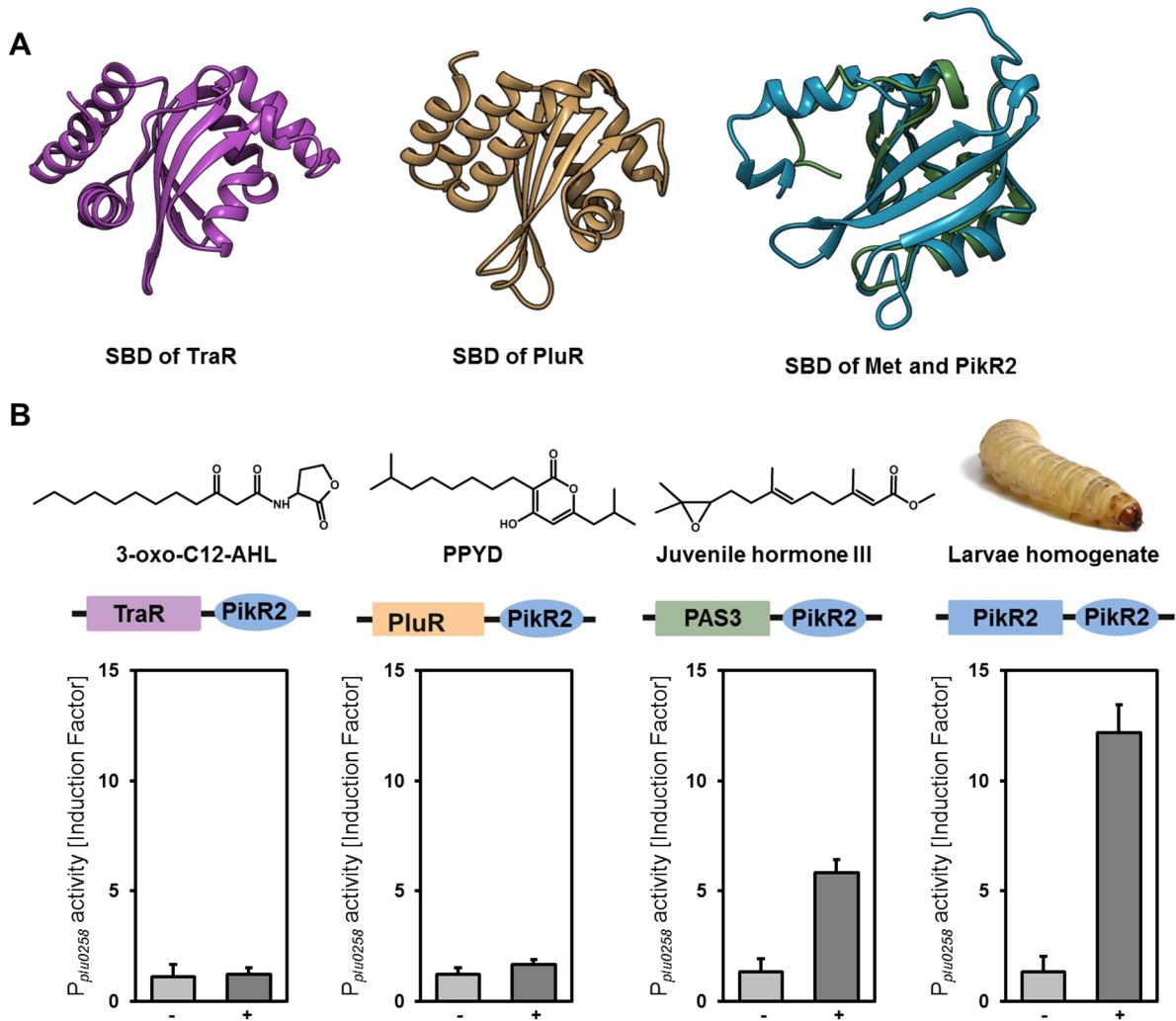


**Figure 3.1.8: Structural and functional analysis of hybrid proteins containing the DBD of PikR2 and the SBD domain of TraR, PluR and Met (PAS3).** **A)** Predicted structures of the SBD of TraR (violet) and PluR (beige) show 6  $\alpha$ -helices and 5  $\beta$ -sheets each. The predicted structures of the PAS4 domain from PikR2 (blue) align structurally with most of the  $\beta$ -sheets and  $\alpha$ -helices of the PAS3 domain from Met (green). Furthermore the predicted structures show less  $\alpha$ -helices surrounding the 5  $\beta$ -sheets in the center. **B)** Addition of 10 nM of the corresponding ligand or 1% (W/V) larvae homogenate, respectively, the culture with PAS3-PikR2 activated  $P_{plu0258}$  resulting in an increased luminescence signal by factor 6. Cultures producing the hybrid proteins TarR-PikR2 and PluR-PikR2 did not show significant differences in luminescence levels after addition of the corresponding signaling molecule. The culture producing PikR2, which was supplemented with *G. mellonella* larvae homogenate, showed an increased activation of  $P_{plu0258}$  by the factor 12. PPYD: photopyrone D, (-): no signaling molecule supplemented, (+) signaling molecule

supplemented, DBD of PikR2 in blue, SBD of TraR in violet, SBD of PluR in orange, SBD of Met in green, SBD of PikR2 in blue

These results demonstrated that the hybrid proteins with SBDs of an AHL receptor (TraR-PikR2) and the QS receptor of *P. luminescens* (PluR-PikR2) do not function when combined with the LuxR DBD of PikR2, whereas the PAS3-PikR2 hybrid protein results in a functioning receptor sensing juvenile hormone III (JHIII). This indicated that the PAS4 domain of PikR2 and the PAS3 of Met are very similar and that putative inhibitors of PikR2 might be structurally similar to inhibitors of the Met receptor in *D. melanogaster*.

Moreover, the corresponding amino acids in the SBD of PikR1 and PikR2 were compared to the conserved amino acid motif in the binding pocket of TraR, LasR, QscR and SdiA. (**Fig. 3.1.9A**). TraR has six conserved amino acids in the SBD (W57, Y61, D70, P71, W85 and G113) responsible for binding AHLs (Patankar und González 2009; Brameyer et al. 2014), which is similar in LasR, QscR and SdiA. When aligning the amino acids (aa) in the same positions of the sequence from PikR1 (WKDKFG) and from PikR2 (WADKYG) four of them are similar. In comparison with the amino acid motif of the AHL receptors still three aa (W57, D70 and G113) are identical.

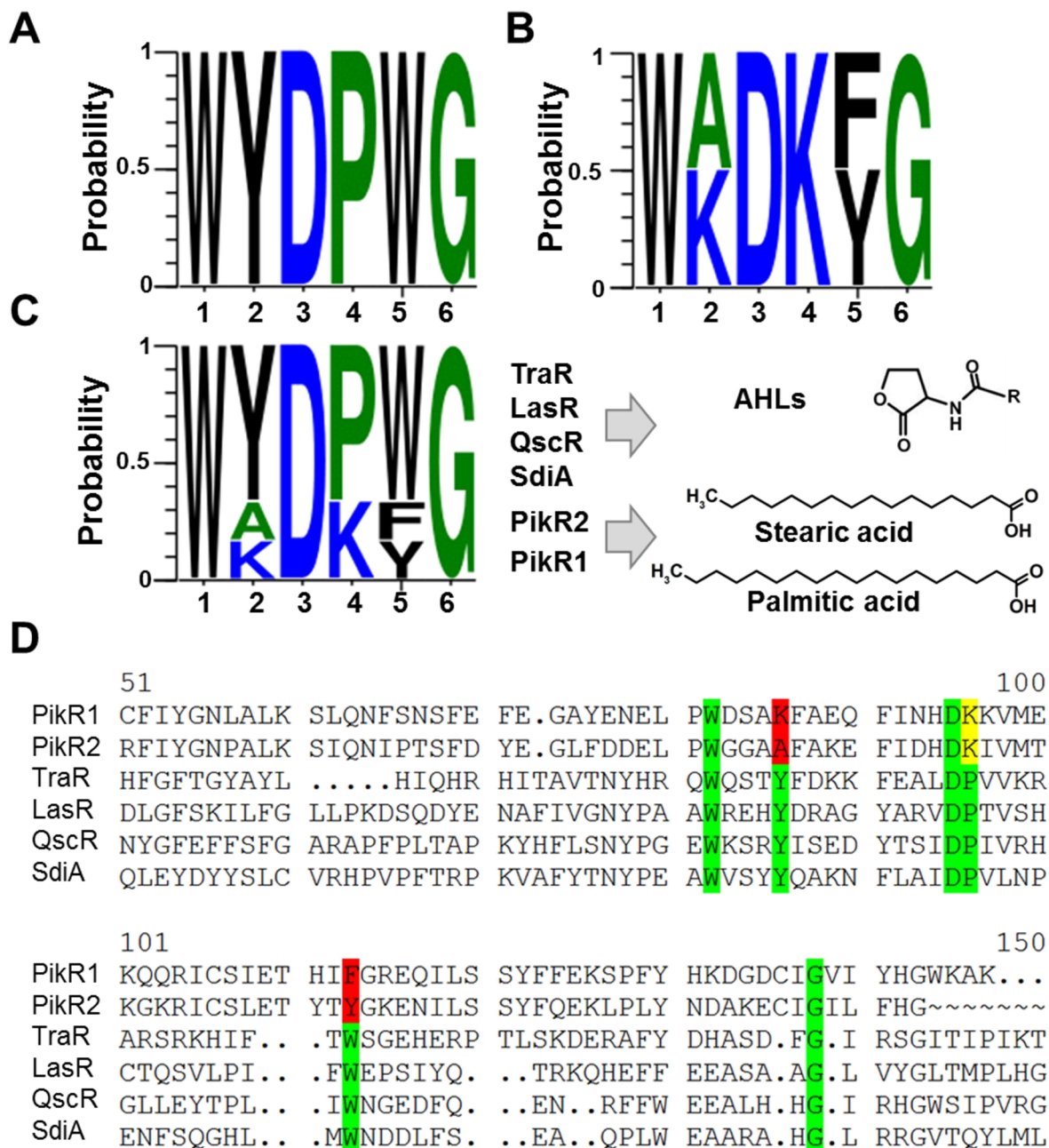


**Figure 3.1.9: Conserved amino acid motifs of LuxR-type proteins. A)** Motif of the six conserved amino acid positions in typical AHL-sensors in the protein sequences of LuxR proteins from *Vibrio fischeri*, TraR from *Agrobacterium tumefaciens*, SdiA from *Escherichia coli*, QscR and LasR from *Pseudomonas aeruginosa* (WYDPWG). **B)** Motif of the six conserved amino acid positions in typical AHL-sensors of PikR1 and PikR2 from *P. luminescens* were used to generate the alignment. **C)** Motif of the six conserved amino acid positions in typical AHL-sensors of protein sequences from LuxR from *Vibrio fischeri*, TraR from *Agrobacterium tumefaciens*, SdiA from *Escherichia coli*, QscR, LasR from *Pseudomonas aeruginosa* and PikR1 and PikR2 from *P. luminescens* were used to generate the alignment. **D)** Section of the amino acid sequence alignment of sequences from PikR1, PikR2, TraR, LasR, QscR and SdiA. The typical positions of the conserved amino acids (aa) responsible for the binding of AHLs in TraR are labeled in green. In red are labeled the aa of PikR1 and

PikR2 that are not matching with each other and with the motif of TraR. The aa of PikR1 and PikR2 that are matching with each other, but not with the motif of TraR are labeled in yellow. The sequence logo was made with WebLogo3.7.4 (Crooks et al. 2004).

These results demonstrate that PikR1 / PikR2 sense the stearic acid and palmitic acid and regulate several genes upon binding the corresponding promotor. PikR1 / PikR2 seem to have high binding sensitivity as concentration of 10nM of stearic acid and palmitic acid show regular signal recognition. Furthermore, the structural analysis of the PAS4 SBD of PikR2 shows high structural similarities to the PAS3 SBD of Met. For the development of drugs targeting PikR1 /PikR2 the structure of the ligands of the PAS4-LuxR solos might be helpful as well as analogs of Met inhibitors.

This sensing of the specific host during the pathogenic part of the lifecycle is important for particular adaptation through production of specialized molecules to respond to competitors and the hostile environment. For this adaptation is important to coordinate the group behavior via quorum sensing.

## 3.2 Transport of QS signaling molecules of *Photorhabdus spec.* by FadL

In the pathogenic part of the lifecycle not only the sensing of stearic acid and palmitic acid is important for *Photorhabdus* but also the transport of the unique quorum sensing (QS) molecules. The QS signaling molecule receptors of PPYD (*P. luminescens*, *P. temperata*) and DARs (*P. asymbiotica*) are identified as well as the proteins involved in the biosynthesis. But the transport of these molecules is so far unknown and might unveil novel targets for interaction with the Qs system in *Photorhabdus*. As described, a RNA-Seq of *P. luminescens* subsp. *laumondii* TT01 and the corresponding  $\Delta pluR$  strain revealed that *fadD* (*PluTT01m\_11030*) and *fadL* (*PluTT01m\_16485*) expression is affected by PluR, the QS receptor of *P. luminescens*. Furthermore a heterologous reporter assay, analyzing the intracellular availability of PPYD and DARs, showed a decrease in signal intensity in the strains *E. coli*  $\Delta fadD$  and *E. coli*  $\Delta fadL$ . A bioinformatics approach showed high sequence identity between FadL homologues from *Photorhabdus* and *E. coli*, which goes along with structural similarity (Brameyer 2015a; Brehm et al. 2021). These were indications that FadD and FadL might play a major role in the transport of PPYD and DARs in *Photorhabdus*.

### 3.2.1 FadD and FadL homologs in *Photorhabdus*

*P. luminescens* subsp. *laumondii* TT01 (*P. luminescens* TT01) and *P. luminescens* subsp. *laumondii* DJC (*P. luminescens* DJC) share very high identity in the amino acid sequence of PluR (100%), FadD (*PluDJC\_11395*) (99.82%) and FadL (91.78%). For further procedure *P. luminescens* DJC was used, as this strain is resistant to rifampicin (Zamora-Lagos et al. 2018) and therefore a more selective work flow is possible.

In the genome of *P. luminescens* (TT01 and DJC) and *Photorhabdus asymbiotica* PB68.1 two genes are annotated as *fadD* homologues. Therefore as the first step a protein sequence comparison was performed for FadD homologs of *P. luminescens* TT01 (PluTT01m\_11030, PluTT01m\_18855) *P. luminescens* DJC (PluDJC\_11395, PluDJC\_18030), *P. asymbiotica* (Pb6\_01559, Pb6\_04001) and *E. coli* to identify the equivalent genes in *P. luminescens* DJC and *P. asymbiotica* to the FadD (PluTT01m\_11030) from *P. luminescens* TT01 that showed altered expression in the RNA-Seq (Brameyer 2015a). High sequence identity was detected for one of the FadD proteins each (**Tab. 3.2.1**).

**Table 3.2.1: Protein sequence identity between the FadD proteins of *P. luminescens* TT01, *P. luminescens* DJC, *P. asymbiotica* and *E.coli*.** In yellow the FadD sequences of *Photorhabdus* that share the higher identity with FadD from *E. coli* compared to the second FadD in the same *Photorhabdus* strain. In light blue are the two FadD homologs from *P. asymbiotica* and *P. luminescens* DJC with high identity to PluTT01m\_11030. (NCBI Reference Sequence: NP\_416319.1)

FadD homologs	Protein Sequence Identity [%]						
	1	2	3	4	5	6	7
PluTT01m_11030 (1)	100	27.63	99.82	27.63	23.66	93.91	76.65
PluTT01m_18855 (2)		100	27.63	100.0	88.18	25.84	22.14
PluDJC_11395 (3)			100	27.63	23.66	94.09	76.83
PluDJC_18030 (4)				100	88.18	25.84	22.14
Pb6_01559 (5)					100	25.42	35.82
Pb6_04001 (6)						100	77.17
FadD <i>E. coli</i> (7)							100

PluDJC\_11395 and Pb6\_04001 showed an identity of 77% with FadD from *E. coli*, whereas PluDJC\_18030 and Pb6\_01559 and were only 22% and 35%, respectively, identical compared to FadD from *E. coli*. Among each other PluDJC\_11395 and Pb6\_04001 show 94% sequence identity, but are only about 28% identical compared to the second FadD homolog within the same genome of each strain (**Tab. 3.2.1**).

With these results it was clarified that *PluDJC\_11395 (fadD)* and *Pb6\_04001 (fadD)* are the genes encoding the FadD, that is similar to *PluTT01m\_11030*. Therefore, the following procedure (structure prediction and gene deletion) was performed with these *fadD* homologs in *P. luminescens* DJC and *P. asymbiotica*. For FadL the typical  $\beta$ -barrel structure of FadL family members was found in the FadL homologs of *P. luminescens* DJC and *P. asymbiotica* PB68.1 (**Fig. 3.2.1**).

The same structure prediction was done for FadD homologs of *E. coli* MG1655, *P. asymbiotica* PB68.1, *P. luminescens* DJC and *P. aeruginosa* and also revealed structural similarity (**Fig. 3.2.1**).

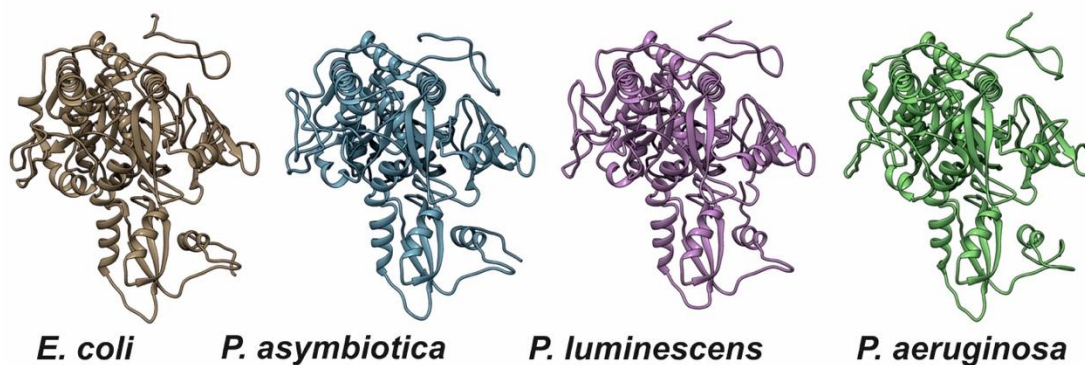


**Figure 3.2.1: Structure predictions of FadD homologs** Structure predictions of FadD homologs of *E.coli* MG1655, *P. asymbiotica* PB68.1, *P. luminescens* (DJC) and *P. aeruginosa* (PAO1). For *P. aeruginosa* (PAO1) the structure of FadD1 was predicted and displayed (Kang et al. 2010). Figure from (Brehm et al. 2021).

For FadL the typical  $\beta$ -barrel structure of FadL family members was found in the FadL homologs of *P. luminescens* DJC and *P. asymbiotica* PB68.1 (**Fig. 1.7**).

### **3.2.2 *P. luminescens* $\Delta$ *fadL* and $\Delta$ *fadD* mutants shows altered pigmentation but wild-type like pathogenicity**

For further investigation of the role of FadD and FadL in *Photorhabdus* the genes of *fadD* and *fadL* in *P. luminescens* strain DJC and *P. asymbiotica* strain PB68.1 were knocked out. In particular the *P. luminescens* DJC strain produces several anthraquinone molecules (Brachmann et al. 2007), which are red-brown pigments,

as well as many other secondary metabolites such as cinnamic acid (Chalabaev et al. 2008). As the pigmentation was altered in cultures of the knockout strains (**Fig. 3.2.2A**), an HPLC analysis was performed to compare the presence of secondary metabolites in *P. luminescens* DJC  $\Delta fadD$ , *P. luminescens* DJC  $\Delta fadL$  and *P. luminescens* DJC  $\Delta fadD \Delta fadL$  mutants and was compared to the wild type. The chromatograms at 300nm showed a reduced diversity of peaks in the mutants. *P. luminescens*  $\Delta fadD$  shows an increased cinnamic acid peak. In all mutants of *P. luminescens* DJC many peaks are lowered or absent in the chromatograms showing the absorption at 300nm (**Fig. 3.2.2B**). The main peak in the part of the chromatogram was identified as cinnamic acid by comparison of the UV spectrum (**Fig. 3.2.2C**). Also at other wavelengths (430nm) an alteration of peak diversity was detected in *P. luminescens* DJC  $\Delta fadD$ , *P. luminescens* DJC  $\Delta fadL$  and *P. luminescens* DJC  $\Delta fadD \Delta fadL$ . Besides from the cinnamic acid peak in *P. luminescens* DJC  $\Delta fadL$  some other, not identified, peaks were observed to be more prominent than the comparable peak in *P. luminescens* DJC wild type, hence also other secondary metabolites were produced or accumulated in *P. luminescens* DJC  $\Delta fadD$ , *P. luminescens* DJC  $\Delta fadL$  and *P. luminescens* DJC  $\Delta fadD \Delta fadL$  (**Supplementary Fig. S 3.1.1**).

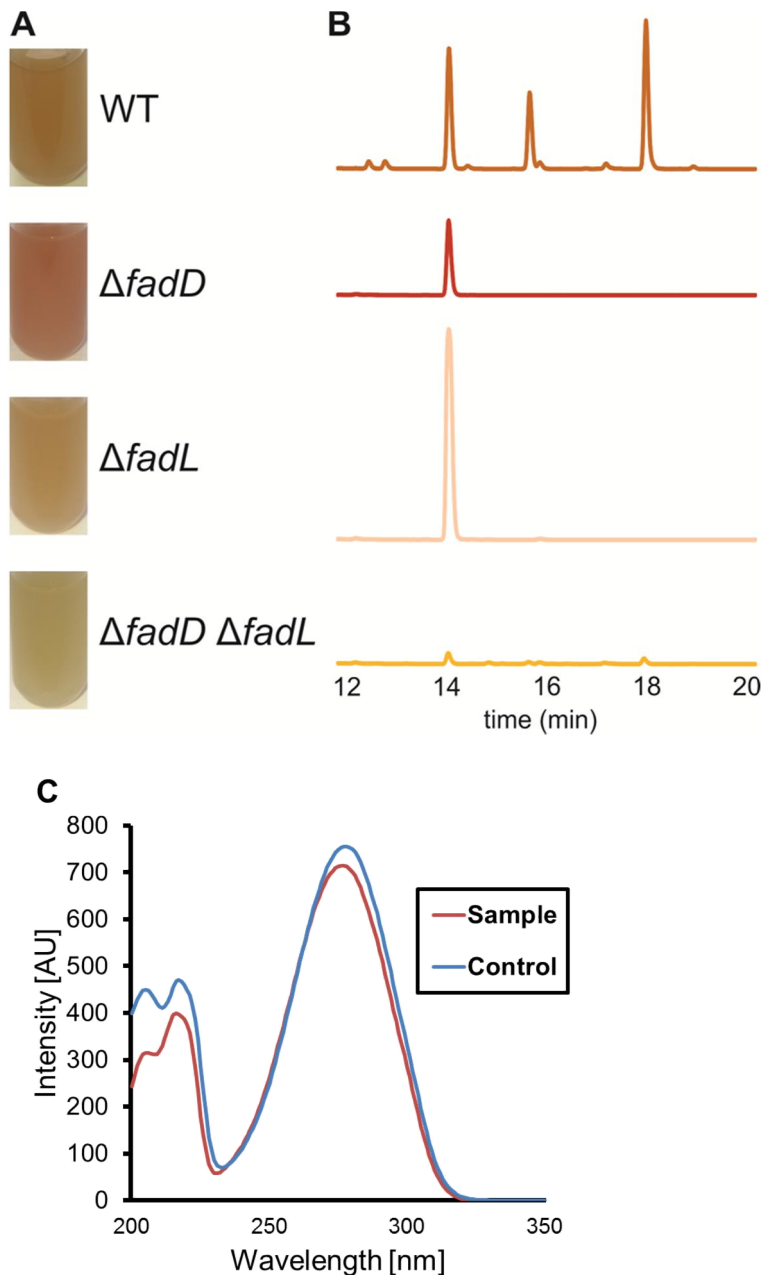


**Figure 3.2.2: Influence of FadD and FadL on pigmentation of *P. luminescens* DJC cultures** **A)** Pigmentation of cultures of *P. luminescens* DJC wild type (WT), *P. luminescens* DJC  $\Delta fadD$ , *P. luminescens* DJC  $\Delta fadL$  and *P. luminescens* DJC  $\Delta fadD \Delta fadL$ . **B)** Selected section of the HPLC UV-Vis (300 nm) chromatograms of the culture supernatant of *P. luminescens* DJC wild type (WT), *P. luminescens* DJC  $\Delta fadD$ , *P. luminescens* DJC  $\Delta fadL$  and *P. luminescens* DJC  $\Delta fadD \Delta fadL$ . In all mutants there are less and smaller peaks than in *P. luminescens* DJC wild type. Only at 14 min one distinct peak was prominent in this part of the chromatogram (300 nm). **C)** The peak at 14 min was identified as cinnamic acid by UV spectrum comparison. (Figure adapted from (Brehm et al. 2021))

As many secondary metabolites of *Photorhabdus* are virulence factors to kill the insect host a pathogenicity assay was performed to observe, whether the altered

production affects the pathogenicity of the mutants. Therefore, *G. mellonella* larvae were injected with the wild type and the mutants of *P. luminescens* DJC and *P. asymbiotica*. Within 72h all strains showed wild type-like pathogenicity and no decrease in pathogenicity was shown for *P. luminescens* DJC and *P. asymbiotica* mutants lacking *fadD* and/or *fadL* (Fig. 3.2.3).

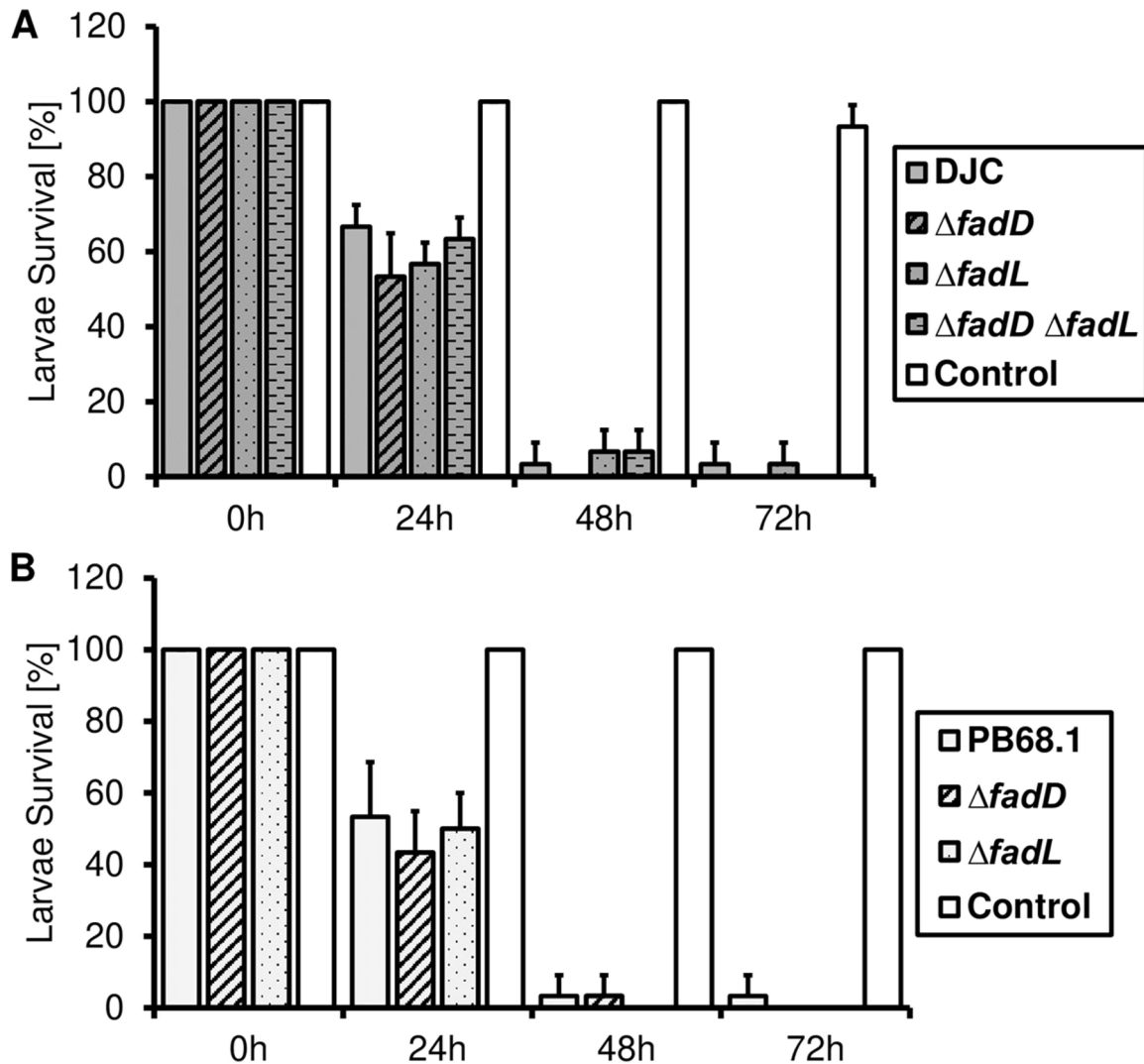


**Figure 3.2.3: Influence of FadD and FadL on pathogenicity of *Photorhabdus* against *G. mellonella*.** **A)** Within 48 h *Galleria mellonella* larvae are killed by *P. luminescens* DJC wild type. The *P. luminescens* DJC  $\Delta fadD$ , *P. luminescens* DJC  $\Delta fadL$  and *P. luminescens* DJC  $\Delta fadD \Delta fadL$  mutants show the same pathogenicity. **B)** Within 48 h *Galleria mellonella* larvae are killed by *P. asymbiotica* PB68.1 wild type. The *P. asymbiotica*  $\Delta fadD$  and *P. asymbiotica*  $\Delta fadL$  mutants show the same pathogenicity. The assay was repeated three times with 10 larvae per strain. (Figure from (Brehm et al. 2021))

### 3.2.3 *P. luminescens* $\Delta fadL$ and *P. asymbiotica* $\Delta fadL$ show decreased $P_{pcfA}$ activity

FadD and FadL are generally transporting and utilizing substances through the membrane that are hydrophobic, which is a characteristic that also applies for PPYD and DARs of *Photorhabdus*. As reported, import of the QS signaling molecules PPYD and DAR is reduced in *E. coli*  $\Delta fadD$  and *E. coli*  $\Delta fadL$ . To validate the observations of a fluorescence-based reporter systems was used in *Photorhabdus*. The intracellular response of PluR and PauR was analyzed in  $\Delta fadD$  and  $\Delta fadL$  mutants of *P. asymbiotica* strain PB68.1 and *P. luminescens* DJC. Therefore, the expression of the *mCherry* reporter gene was measured, which was under the control of the promoter affected by PluR and PauR  $P_{pcfA P.l.}$  or  $P_{pcfA P.a.}$ , respectively. The fluorescence signal analysis of  $P_{pcfA P.l.}$  showed decreased activity in *P. luminescens*  $\Delta fadL$  and *P. luminescens*  $\Delta fadD \Delta fadL$  but not in the *P. luminescens*  $\Delta fadD$  strain (**Fig. 3.2.4A**). In *P. asymbiotica* the activity of  $P_{pcfA P.a.}$  was decreased in both: slightly in the  $\Delta fadD$  and dramatically in the  $\Delta fadL$  mutant (**Fig. 3.2.4B**). To verify the signal measurement in the plate reader the samples were visualized under a fluorescence microscope. The mean fluorescence calculated from the images was significantly decreased in the *P. luminescens*  $\Delta fadL$  and *P. luminescens* double mutant (**Fig. 3.2.4C**). Addition of the corresponding QS signaling molecule did not affect the  $P_{pcfA}$  activity.

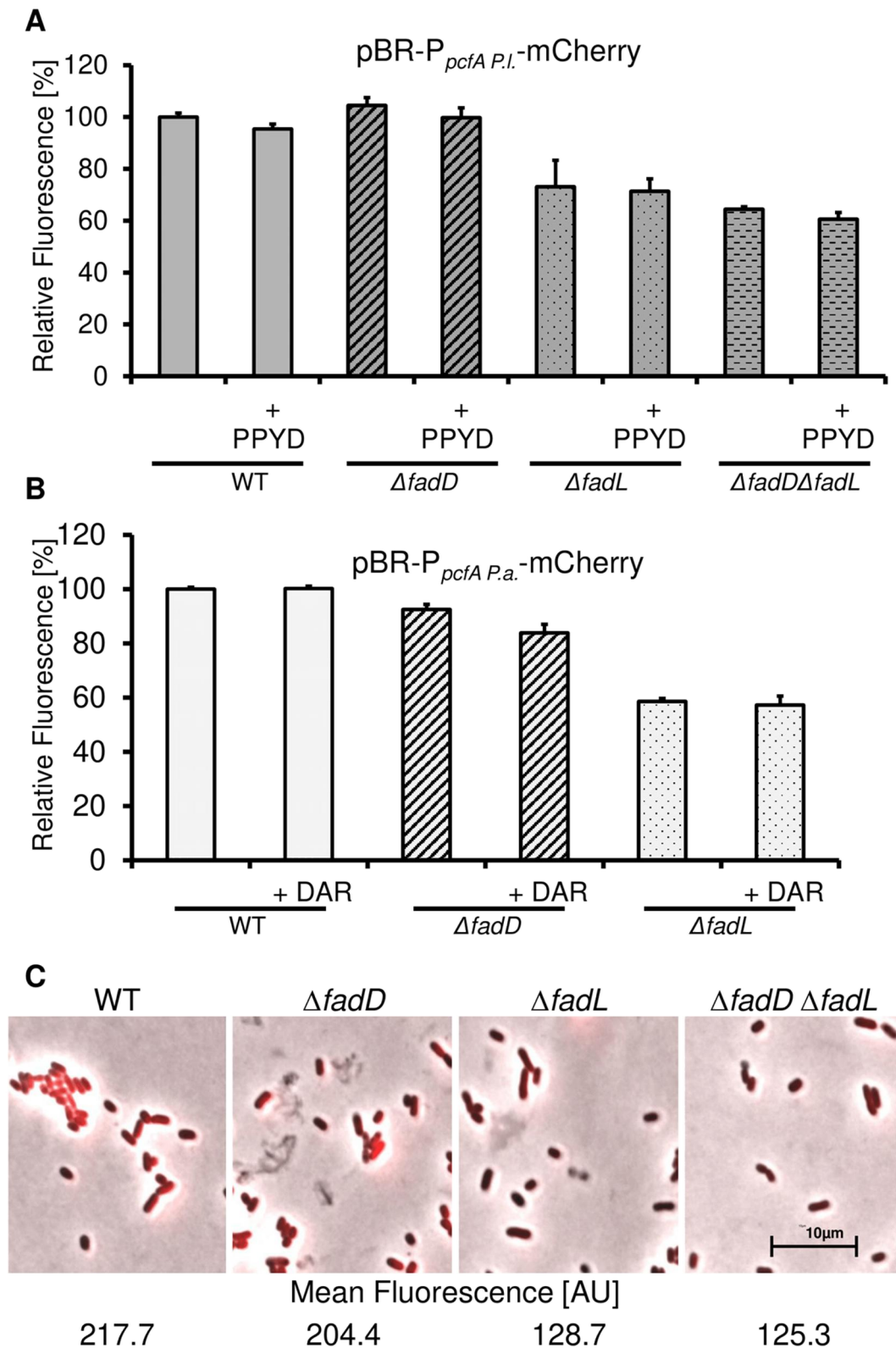


**Figure 3.2.4: Relative fluorescence intensity of the reporter assay in *P. luminescens* DJC strains. A)** *P. luminescens* DJC  $\Delta fadD$  shows wild type-like fluorescence signal intensity, whereas the signal in *P. luminescens* DJC  $\Delta fadL$  and *P. luminescens* DJC  $\Delta fadD \Delta fadL$  was dramatically decreased. **B)** *P. asymbiotica*  $\Delta fadD$  shows slightly decreased fluorescence signal intensity, whereas the signal in *P. asymbiotica*  $\Delta fadL$  was dramatically decreased. Additional supplementation of the corresponding QS signaling molecule did not change the signal intensity. The signal intensity of the wild type was set to 1. **C)** Fluorescence microscopy images and the

calculated mean fluorescence of *P. luminescens* DJC wild type, *P. luminescens* DJC  $\Delta fadD$ , *P. luminescens* DJC  $\Delta fadL$  and *P. luminescens* DJC  $\Delta fadD \Delta fadL$ . Figure from (Brehm et al. 2021).

### 3.2.4 PPYD import is facilitated by FadL in *P. luminescens*

As signal response of PluR is related to the amount of PPYD signaling molecules present in the cultures of *P. luminescens* DJC wild type, *P. luminescens* DJC  $\Delta fadL$ , *P. luminescens* DJC  $\Delta fadD$  and *P. luminescens* DJC  $\Delta fadL \Delta fadD$  strains, an LC-MS analysis was performed to verify the intracellular (ic.) as well as the extracellular (ec.) amount of PPYD. This was only performed for PPYD in *P. luminescens* as a viable knockout mutant of *P. luminescens* DJC  $\Delta fadL \Delta fadD$  was not achieved.

The peak of the hydrophobic PPYD appeared at around 17 min in the LC-MS chromatogram (**Fig. 3.2.5AB**). The extracts showed differences in the PPYD content between *P. luminescens* wild type and the knockout mutants, especially when comparing the distribution between intracellular PPYD and extracellular PPYD content within each strain (**Fig. 3.2.5C**). The intracellular PPYD amount was 2-fold higher in the *P. luminescens* wild type as well as in *P. luminescens* DJC  $\Delta fadD$  compared to the extracellular amount. The opposite occurred in *P. luminescens* DJC  $\Delta fadD$  and *P. luminescens* DJC  $\Delta fadL \Delta fadD$  mutants, where PPYD was accumulated 8 to 9-fold in the extracellular fraction compared to the intracellular fraction (Fig. 7C). In particular the comparison of the overall amounts of PPYD (ec. + ic.) illustrates the influence of FadD and FadL in the transport and production of PPYD in *P. luminescens* (Fig. D). The overall amount in *P. luminescens* DJC  $\Delta fadD$  is only slightly decreased compared to the wild type. The opposite was shown in *P. luminescens* DJC  $\Delta fadL$ , where the overall PPYD was 2.6-fold higher. The culture of the double knockout strain contained only about 31% of overall PPYD compared to the wild type.

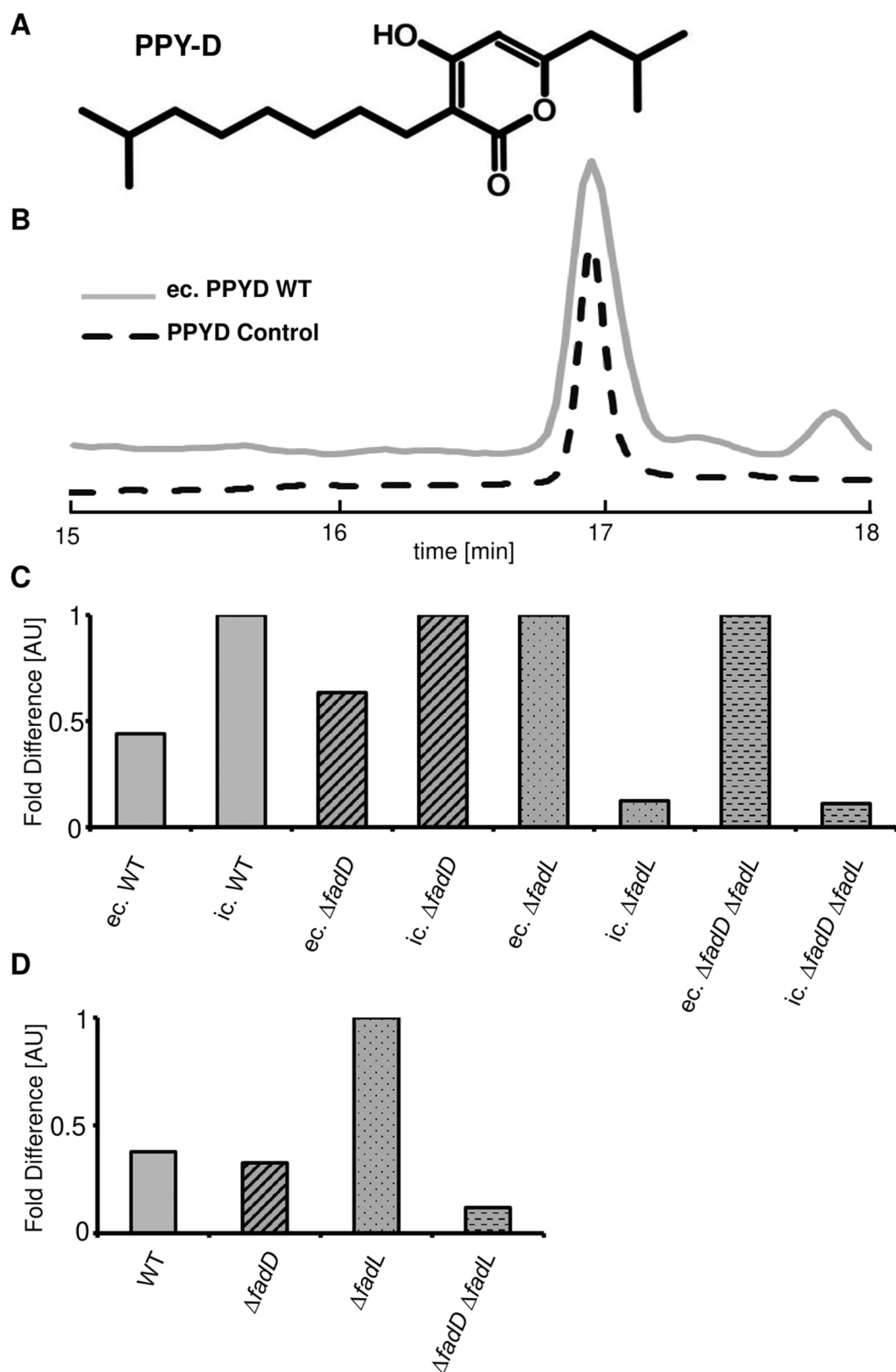


**Figure 3.2.5: Influence of FadD and FadL on PPYD content in *P. luminescens* strains** **A**) Structure of PPY-D **B**) LC-MS chromatogram (295 M/z, positive mode) extracellular (ec.) extract of *P. luminescens* wild type (grey). LC-MS chromatogram (295 M/z, positive mode) of pure PPYD (striped) **C**) Fold difference in signal intensity (AU) of PPYD between extracellular extract (ec.) and intracellular extract (ic.) from *P. luminescens* wild type,  $\Delta fadD$ ,  $\Delta fadL$  and  $\Delta fadL \Delta fadD$ . The AU of the higher amount of PPYD was set to 1. **D**) The relative overall amount of extracellular and intracellular

PPYD in *P. luminescens* wild type, *P. luminescens* DJC  $\Delta fadD$ , *P. luminescens* DJC  $\Delta fadL$  and *P. luminescens* DJC  $\Delta fadL \Delta fadD$  compared to each other. The PPYD amount in the  $\Delta fadL$  mutant was set to 1. (Figure from (Brehm et al. 2021))

### 3.2.5 Deletion of *fadL* and *fadD* reduces relative activity of $P_{plu0258}$ in *P. luminescens*

Due to the results of the import of QS signaling molecules by the fatty acid transport related proteins FadL and FadD, the influence of the fluorescence signal intensity of reporter strains lacking *fadL* and *fadD* was investigated. Therefore, the reporter system was additionally set up in *P. luminescens* DJC  $\Delta fadL$  pBR  $P_{plu0258}$ -mCherry and *P. luminescens* DJC  $\Delta fadD$  pBR  $P_{plu0258}$ -mCherry. The fluorescence signal intensity was dramatically decreased by about 50% in *P. luminescens* DJC  $\Delta fadD$  pBR  $P_{plu0258}$ -mCherry and even down to about 20% in *P. luminescens* DJC  $\Delta fadL$  pBR  $P_{plu0258}$ -mCherry compared to the signal intensity in the *P. luminescens* DJC wild type reporter strain (Fig 3.2.6).

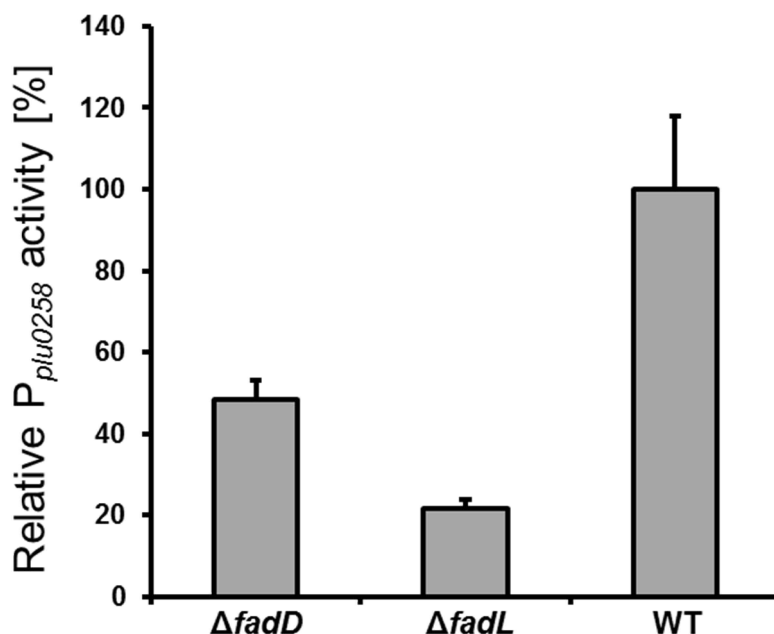


Figure 3.2.6: Relative activity of  $P_{plu0258}$  in the reporter strains *P. luminescens* DJC pBR- $P_{plu0258}$ -mCherry, *P. luminescens* DJC  $\Delta fadD$  pBR- $P_{plu0258}$ -mCherry and *P. luminescens* DJC  $\Delta fadL$  pBR- $P_{plu0258}$ -mCherry. All reporter strains were supplemented with 1% (v/v) of “fraction 1”, containing the signaling molecules of PikR1 / PikR2. *P. luminescens* DJC  $\Delta fadD$  pBR- $P_{plu0258}$ -mCherry showed about 50%

of the signal intensity and *P. luminescens* DJC  $\Delta fadL$  pBR- $P_{plu0258}$ -mCherry only about 20% of the fluorescence signal intensity of the *P. luminescens* DJC wild type reporter strain

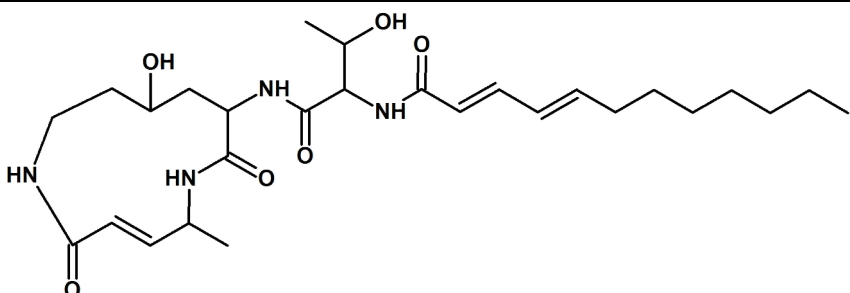
These results show that the import of the QS signaling molecules PPYD in *P. luminescens* DJC and DAR in *P. asymbiotica* is facilitated by FadL. Furthermore, FadD and FadL have an influence on the production and diversity of secondary metabolites in *P. luminescens* DJC, but not on the pathogenicity. Especially with the importance for the import of the quorum sensing molecules and the inter-kingdom signaling molecules FadD and FadL might be potential drug targets to interact with the bacterial communication.

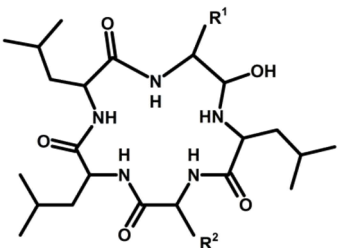
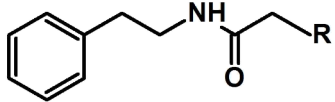
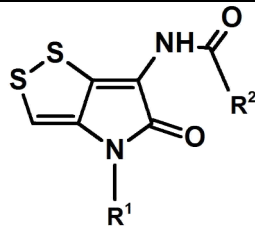
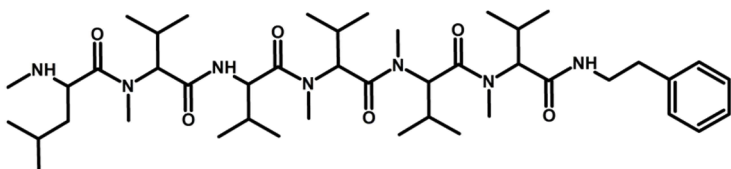
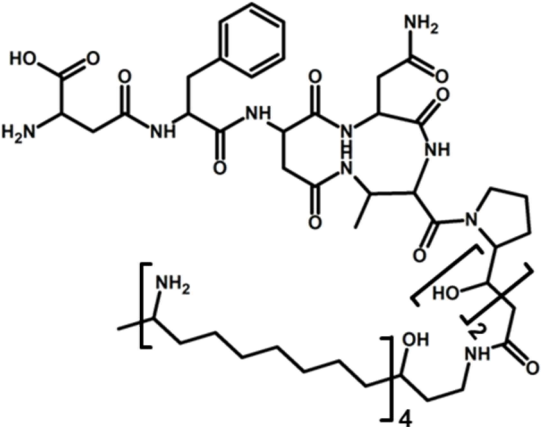
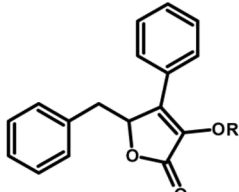
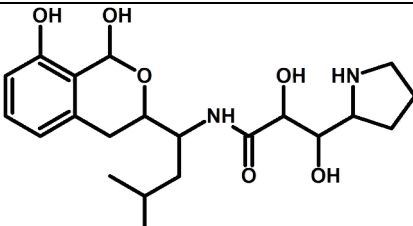
### 3.3 Identification of cytotoxic secondary metabolites from *Xenorhabdus* and *Photorhabdus*

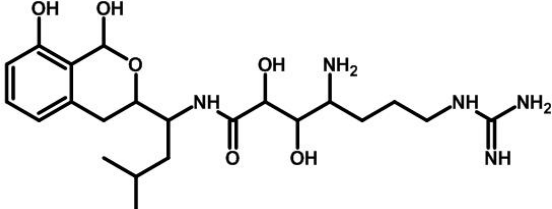
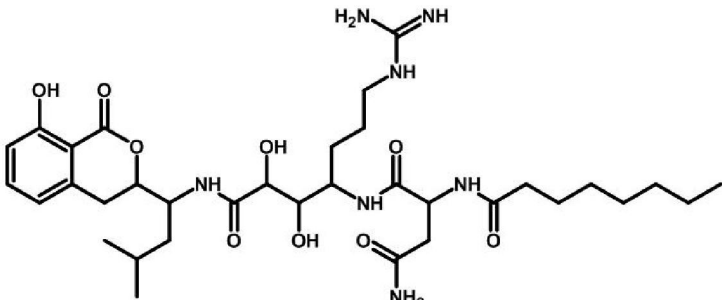
When invading and sensing the insect host *Xenorhabdus* spec. and *Photorhabdus* spec. quickly need to respond with virulence factors to kill the insect. Therefore, the entomopathogens harbor a high number of biosynthesis gene clusters encoding proteins involved in secondary metabolite production. These secondary metabolites from *Xenorhabdus* spec. and *Photorhabdus* spec. harbor still high potential for several characteristics that have not been discovered so far. As antibiotic activities and antifungal activities are explored for most identified secondary metabolites from *Xenorhabdus* and *Photorhabdus*, this work concentrated on metabolites with putative cytotoxic effects. These substances might extend the variety of substances for the development of drugs.

To investigate the cytotoxic effect of chosen secondary metabolites from these entomopathogens we used several  $\Delta hfg$  strains and wild type strains of *P. luminescens*, *X. doucetiae*, *X. szentirmaii* and *X. nematophila* with an arabinose inducible promoter upstream of a specific biosynthesis gene cluster were used (Tab. 2.3).

**Table 3.3.1: Secondary metabolites from *Photorhabdus* and *Xenorhabdus* investigated for cytotoxic activity.** In this table all secondary metabolites are listed, that were overproduced and analyzed for cytotoxic effects against cell lines.

Structure	Secondary metabolite
	Glidobactin (Schellenberg et al. 2007)

	<p>GameXpeptides (Nollmann et al. 2015)</p>
	<p>Phenethylamides (Bode 2009)</p>
	<p>Xenorhabdin (Bode 2009)</p>
	<p>Rhabdopeptide (Reimer et al. 2013)</p>
	<p>Fabclavine (Fuchs et al. 2014)</p>
	<p>Xenofuranone (Brachmann et al. 2006)</p>
	<p>Xenocoumacin 2 (Park et al. 2009)</p>

 <p>The structure of Xenocoumacin 1 features a coumarin core with two hydroxyl groups at positions 6 and 7. It is substituted at position 3 with a 2-isopropylbutyl chain. This chain is further substituted with a side chain containing a primary amide, a dihydroxyethyl group, a primary amine, and a terminal guanidino group.</p>	<p>Xenocoumacin 1 (Park et al. 2009)</p>
 <p>The structure of Prexencoumacin 1 features a coumarin core with a hydroxyl group at position 6 and a carbonyl group at position 2. It is substituted at position 3 with a 2-isopropylbutyl chain. This chain is further substituted with a side chain containing a primary amide, a dihydroxyethyl group, a guanidino group, a secondary amide, a primary amide, and a terminal heptyl chain.</p>	<p>Prexencoumacin 1 (Park et al. 2009)</p>

### 3.3.1 Cytotoxic effects of cell free culture supernatants of *Xenorhabdus* and *Photorhabdus* wild type cultures

To get a first overview whether *Xenorhabdus* and *Photorhabdus* strains are producing cytotoxic substances during cultivation in CASO at 30°C, 200 µl of the cell free culture supernatants (CFCS) of cultures of the wild type strains of *P. luminescens*, *X. doucetiae* and *X. szentirmaii* were added to HeLa and NIH3T3 cell cultures. With this a cell viability assay with HeLa and NIH3T3 cells was performed to identify, whether these strains produce cytotoxic substances under laboratory conditions. Images were taken after 24 h. Cell free culture supernatants (CFCSs) of cultures of *X. doucetiae* DSM17909 and *X. szentirmaii* showed strong cytotoxic effects on NIH3T3 cells. CFCSs of the cultures of the *E. coli* DH5alpha and *P. luminescens* did not show any cytotoxic effect on NIH3T3 cells (**Fig 3.3.1A**). When HeLa cell cultures were treated with the same CFCSs only for the CFCS of a culture of *X. doucetiae* was observed to have cytotoxic effects (**Fig 3.3.1B**). This proved that these *Xenorhabdus* spec. produce cytotoxic substances that are produced by the wild type under laboratory conditions.

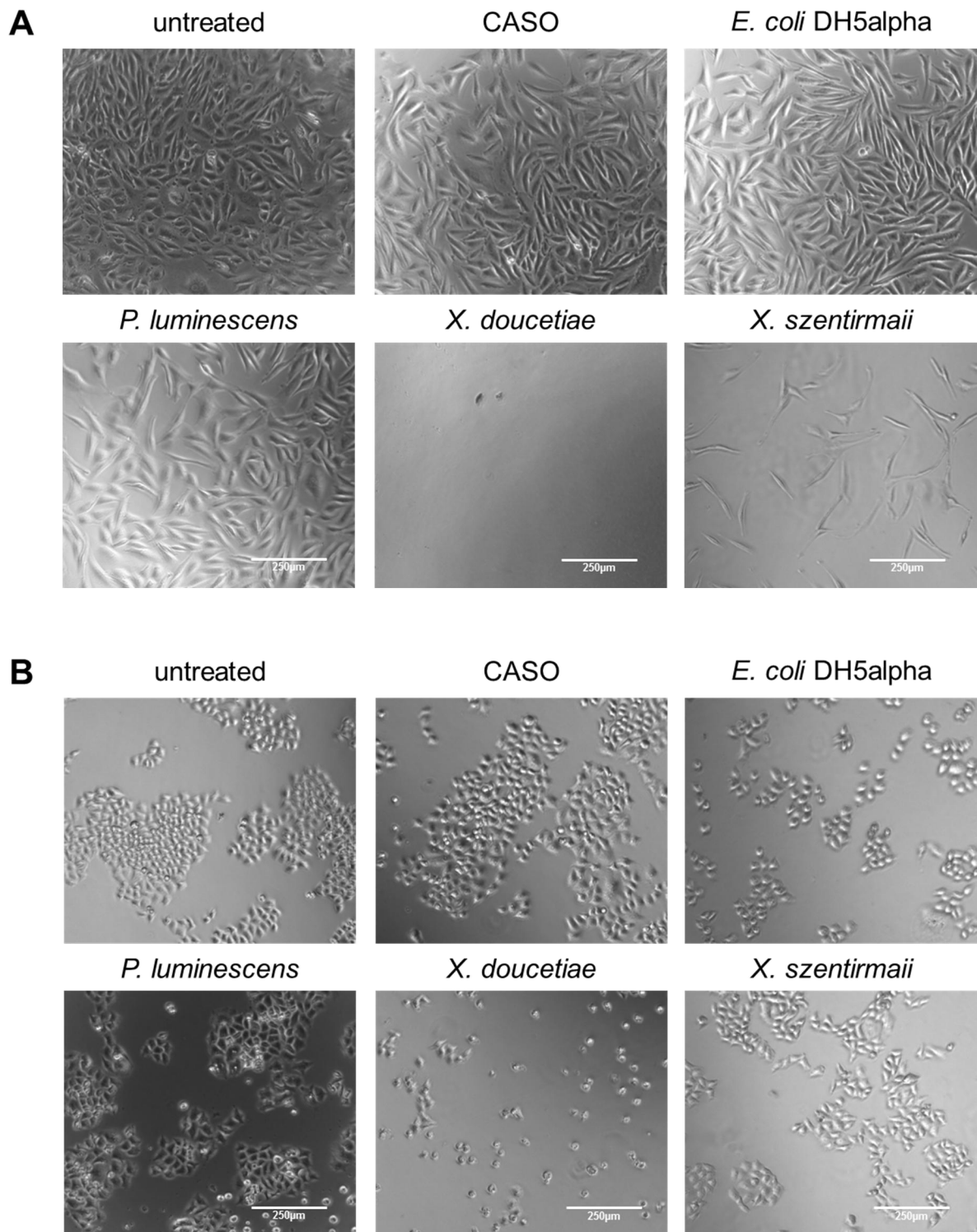
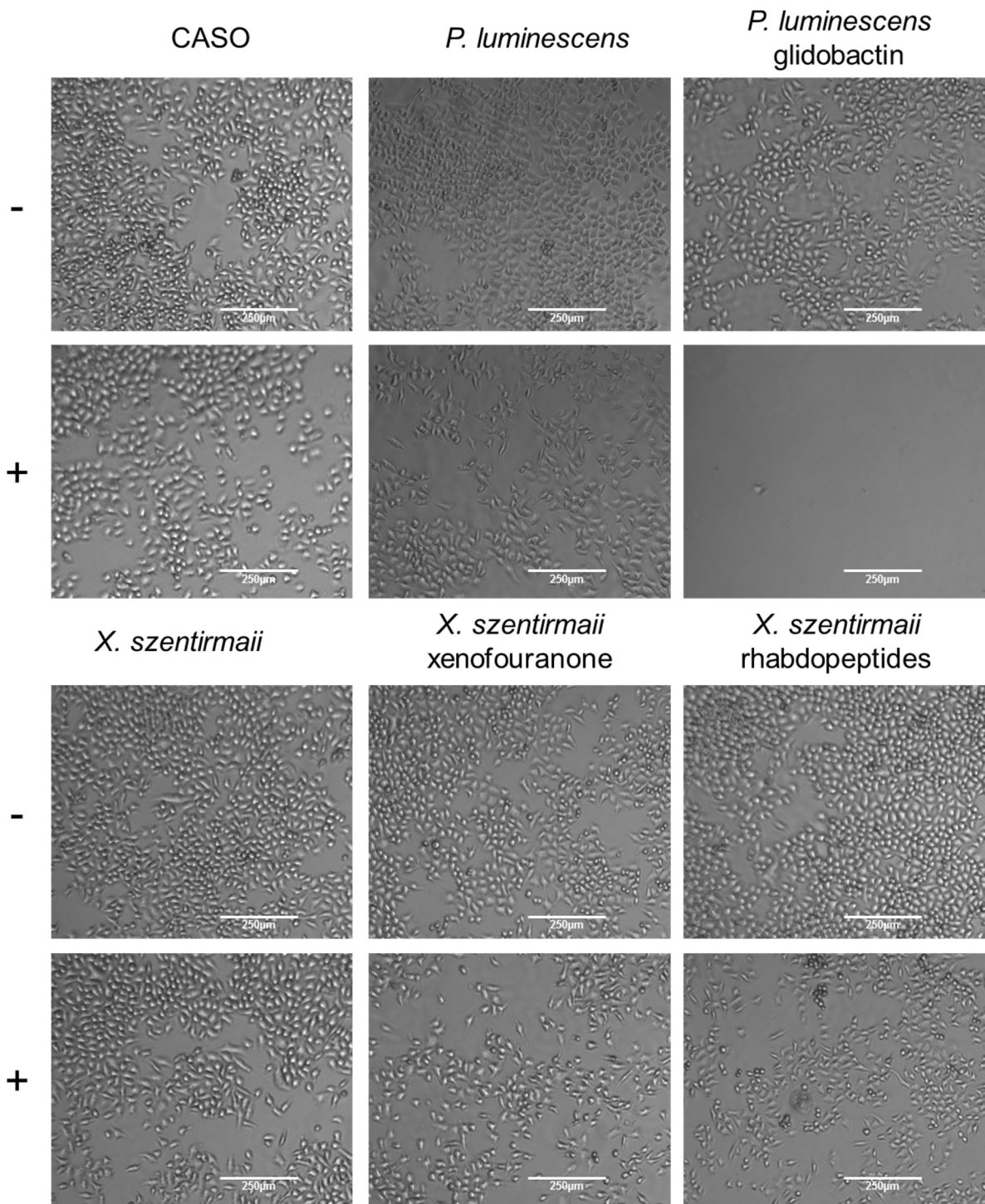


**Figure 3.3.1: HeLa and NIH3T3 cells after treatment with cell free culture supernatant (CFCS) of CASO, *E. coli* DH5alpha, *P. luminescens*, *X. doucetiae* and *X szentirmaii*.** **A)** NIH3T3 cells treated with CFCS of cultures of *E. coli* DH5alpha, *P. luminescens*, *X. doucetiae* and *X szentirmaii*. As negative control one culture was left untreated and another was treated with CASO handled as the CFCSs. Two cell cultures treated with CFCS of the cultures of *X. doucetiae* and *X. szentirmaii* showed a strong cytotoxic effect, which was stronger with the CFCS of the culture of *X. doucetiae*. The other cell cultures remained vital. **B)** HeLa cells treated with CFCS of cultures of *E. coli* DH5alpha, *P. luminescens*, *X. doucetiae* and

*X. szentirmaii*. As negative control one culture was left untreated and another was treated with CASO handled as the CFCSs. Two cell cultures treated with CFCS of the culture of *X. doucetiae* showed a cytotoxic effect. The other cell cultures remained vital.

### **3.3.2 Secondary metabolites from *Xenorhabdus* and *Photorhabdus* show cytotoxic activity**

As glidobactin, which is produced by *P. luminescens* and can be overproduced in the strain *P. luminescens* DJC  $\Delta$ hfq pCEP-*plu1881*, is known to have cytotoxic characteristics (Theodore et al. 2012), was used as a positive control of a cytotoxic effect. Synthesis was activated by inducing the biosynthesis gene cluster of the corresponding secondary metabolite in constructed *Xenorhabdus* and *Photorhabdus* strains by the addition of arabinose. Before addition of the cell free culture supernatant the sample was sterile filtrated. As control a similarly treated CASO control was used, which shows no changes in viability after 24h with or without arabinose. The same was observed for the cells treated with CFCS of *P. luminescens* wild type (WT), *X. szentirmaii* WT, *X. doucetiae* DSM17909, *X. doucetiae* DSM17909  $\Delta$ hfq pBAD *gxpsA* (GameXPepitides), *X. szentirmaii*  $\Delta$ hfq pCEP-KM-*xfxA* (xenofuranone), *X. szentirmaii*  $\Delta$ hfq pCEP-KM-*fcIC* (fabclavine) and *X. szentirmaii*  $\Delta$ hfq pCEP-KM-3397 (rhabdopeptides). Cells treated with the CFCS (with and without arabinose) of *X. doucetiae* WT were dead within 24h. Cells treated with the CFCS of a *P. luminescens* DJC  $\Delta$ hfq pCEP-*plu1881* (glidobactin) culture only showed a strong cytotoxic effect, when treated with CFCS in which the biosynthesis gene cluster of glidobactin was induced with arabinose. The same is shown for the cells treated with CFCS of the culture of *X. doucetiae* DSM17909  $\Delta$ hfq pBAD *xcnA* (xenocoumacin). Less but still visible cytotoxic effects were shown by HeLa cells treated with CFCSs of the cultures of *X. doucetiae* DSM17909  $\Delta$ hfq pBAD *xrdA* (xenorhabdin) and *X. doucetiae* DSM17909  $\Delta$ hfq pBAD decarboxylase (phenethylamides) (**Fig. 3.3.2**).



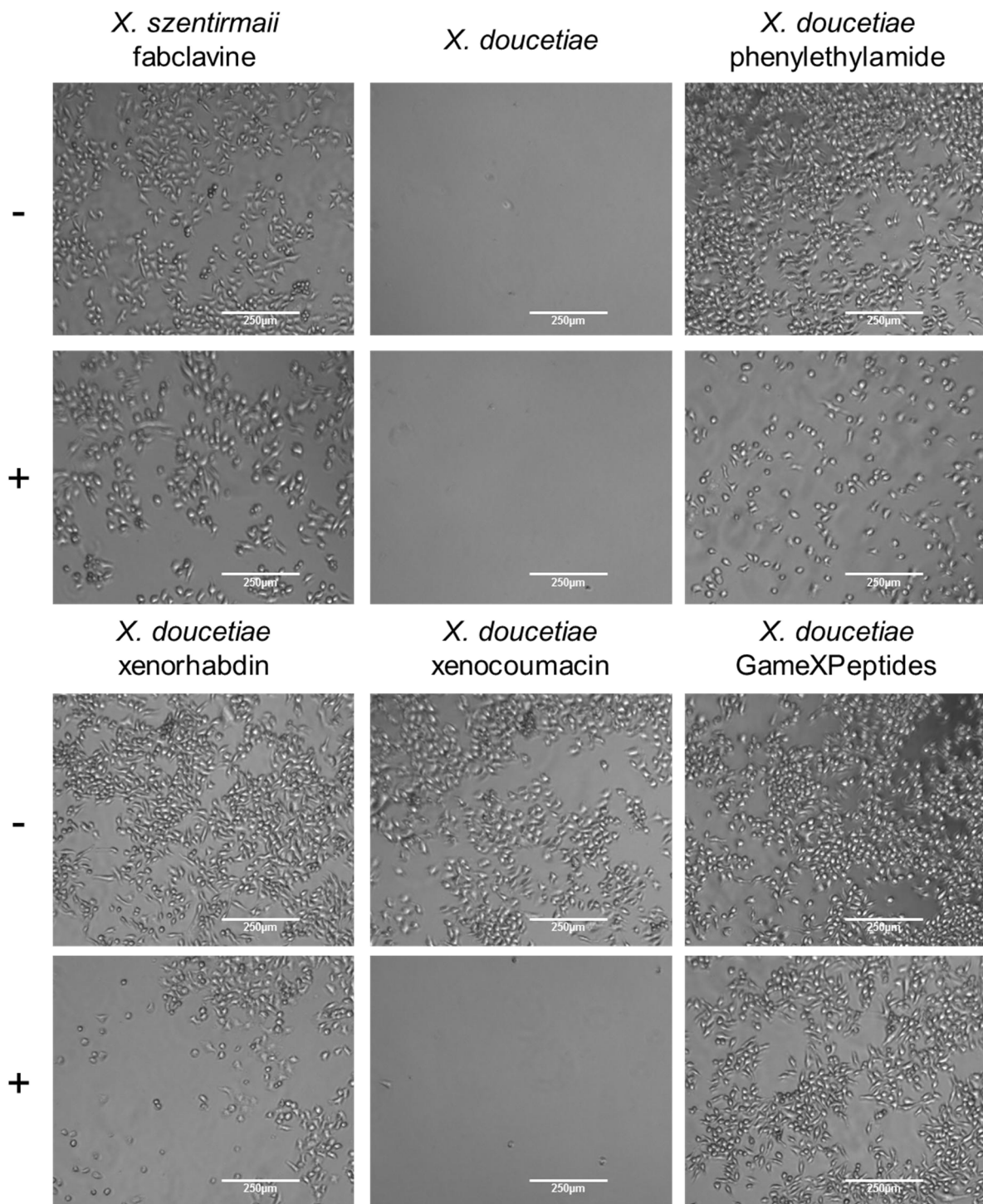
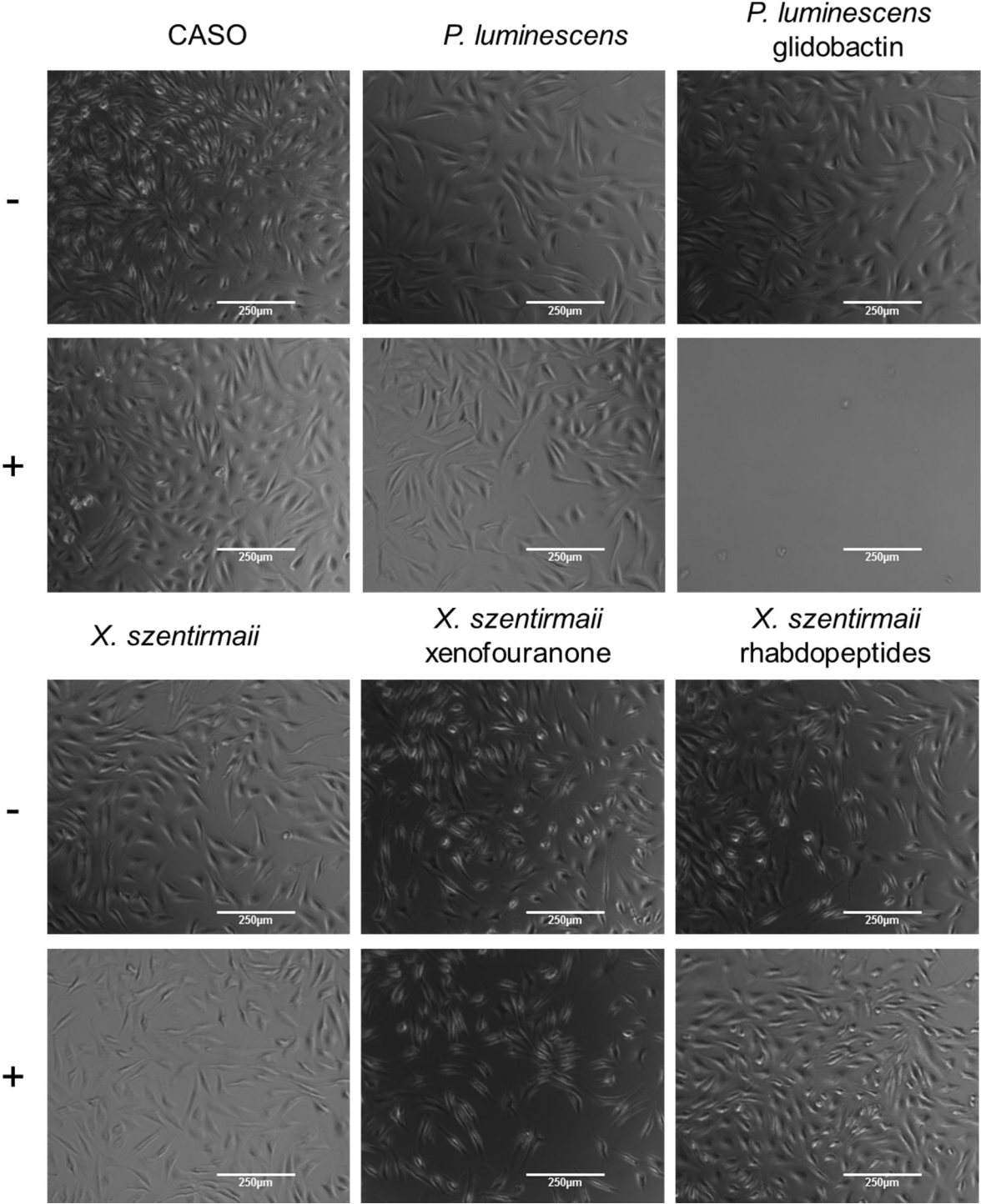


**Figure 3.3.2: HeLa cells treated with cell free culture supernatants (CFCS) of *Photorhabdus* and *Xenorhabdus* cultures.** The upper part of each row shows cells treated with CFCS without arabinose (-), whereas the lower part shows images of cells treated with CFCS of cultures with arabinose (+). Arabinose was added to the cultures from the beginning to induce the gene expression of the biosynthesis gene cluster of certain secondary metabolites. Images of HeLa cells after 24h after the treatment with cell free culture supernatant of *P. luminescens*, *X. doucetiae*, *X. szentirmaii* and several  $\Delta hfq$  strains with an arabinose inducible promoter in front of the corresponding biosynthesis gene cluster of certain secondary metabolites. As control a similarly treated CASO control was used, which shows no changes in

viability after 24h with or without arabinose. The same was observed for the cells treated with CFCS of *P. luminescens* wild type (WT), *X. szentirmaii* WT, *X. doucetiae* DSM17909, *X. doucetiae* DSM17909  $\Delta hfq$  pBAD *gxpsA* (GameXPeptides), *X. szentirmaii*  $\Delta hfq$  pCEP-KM-*xfA* (xenofuranone), *X. szentirmaii*  $\Delta hfq$  pCEP-KM-*fcIC* (fabclavine) and *X. szentirmaii*  $\Delta hfq$  pCEP-KM-3397 (rhabdopeptides). Cells treated with the CFCS (with and without arabinose) of *X. doucetiae* WT were dead within 24h. Cells treated with the CFCS of a *P. luminescens* DJC  $\Delta hfq$  pCEP-*plu1881* (glidobactin) culture only showed a strong cytotoxic effect, when treated with CFCS in which the biosynthesis gene cluster of glidobactin was induced with arabinose. The same is shown for the cells treated with CFCS of the culture of *X. doucetiae* DSM17909  $\Delta hfq$  pBAD *xcnA* (xenocoumacin). Less but still visible cytotoxic effects were shown by HeLa cells treated with CFCSs of the cultures of *X. doucetiae* DSM17909  $\Delta hfq$  pBAD *xrdA* (xenorhabdin) and *X. doucetiae* DSM17909  $\Delta hfq$  pBAD decarboxylase (phenethylamides).

The treatment with the same CFCSs was performed with NIH3T3 cells. As control a similarly treated CASO control was used, which shows no changes in viability after 24h with or without arabinose. The same was observed for the cells treated with CFCS of *P. luminescens* wild type (WT), *X. szentirmaii* WT, *X. doucetiae* DSM17909, *X. doucetiae* DSM17909  $\Delta hfq$  pBAD *gxpsA* (GameXPeptides), *X. szentirmaii*  $\Delta hfq$  pCEP-KM-*xfA* (xenofuranone) and *X. szentirmaii*  $\Delta hfq$  pCEP-KM-3397 (rhabdopeptides). Cells treated with the CFCS (with and without arabinose) of *X. doucetiae* WT were dead within 24h. Cells treated with the CFCS of a *P. luminescens* DJC  $\Delta hfq$  pCEP-*plu1881* (glidobactin) culture only showed a strong cytotoxic effect, when treated with CFCS in which the biosynthesis gene cluster of glidobactin was induced with arabinose. The same was shown for the cells treated with CFCS of the cultures of *X. doucetiae* DSM17909  $\Delta hfq$  pBAD *xcnA* (xenocoumacin) and *X. doucetiae* DSM17909  $\Delta hfq$  pBAD *xrdA* (xenorhabdin). Less but still visible cytotoxic effects were shown by HeLa cells treated with CFCSs of the cultures of *X. szentirmaii*  $\Delta hfq$  pCEP-KM-*fcIC* (fabclavine) and *X. doucetiae* DSM17909  $\Delta hfq$  pBAD decarboxylase (phenethylamides) (**Fig. 3.3.3**). The CFCS of the culture of *X. szentirmaii*  $\Delta hfq$  pCEP-KM-*fcIC* (fabclavine) showed also a cytotoxic effect when

added to NIH3T3 cells but not as strong as the other CFCSs. Overall, the cytotoxic effects of the CFCS seemed stronger on NIH3T3 cells than on HeLa cells.



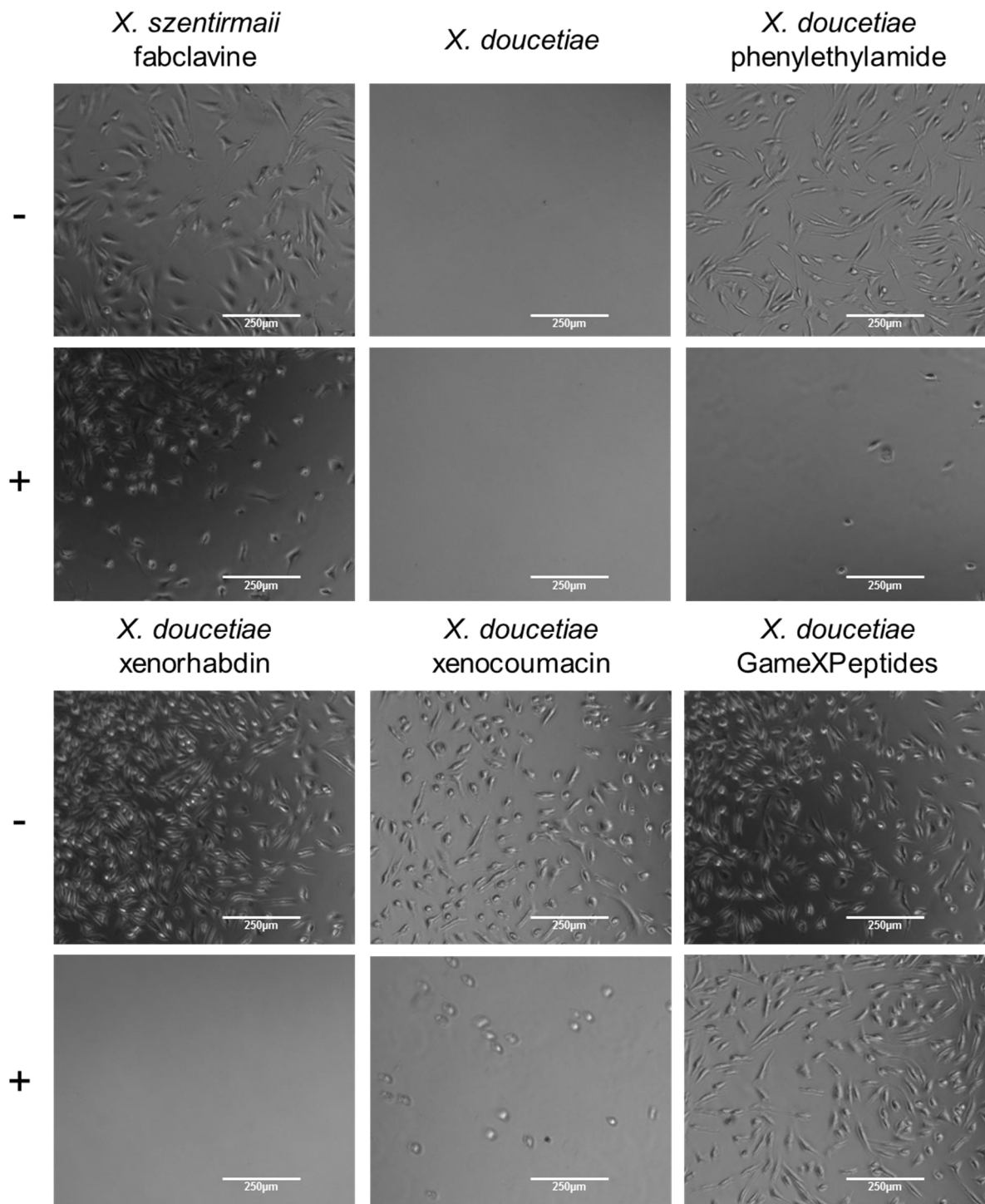


**Figure 3.3.3: NIH3T3 cells treated with cell free culture supernatants (CFCS) of *Photorhabdus* and *Xenorhabdus* cultures.** The upper part of each row shows cells treated with CFCS without arabinose (-), whereas the lower part shows images of cells treated with CFCS of cultures with arabinose (+). Arabinose was added to the cultures from the beginning to induce the gene expression of the biosynthesis gene cluster of certain secondary metabolites. Images of NIH3T3 cells after 24 h after the treatment with cell free culture supernatant of *P. luminescens*, *X. doucetiae*, *X. szentirmaii* and several  $\Delta hfq$  strains with an arabinose inducible promoter in front of the corresponding biosynthesis gene cluster of certain secondary metabolites. As control a similarly treated CASO control was used, which shows no changes in

viability after 24h with or without arabinose. The same was observed for the cells treated with CFCS of *P. luminescens* wild type (WT), *X. szentirmaii* WT, *X. doucetiae* DSM17909, *X. doucetiae* DSM17909  $\Delta hfq$  pBAD *gxpsA* (GameXPptides), *X. szentirmaii*  $\Delta hfq$  pCEP-KM-*xfsa* (xenofuranone) and *X. szentirmaii*  $\Delta hfq$  pCEP-KM-3397 (rhabdopeptides). Cells treated with the CFCS (with and without arabinose) of *X. doucetiae* WT were dead within 24h. Cells treated with the CFCS of a *P. luminescens* DJC  $\Delta hfq$  pCEP-*plu1881* (glidobactin) culture only showed a strong cytotoxic effect, when treated with CFCS in which the biosynthesis gene cluster of glidobactin was induced with arabinose. The same is shown for the cells treated with CFCS of the culture of *X. doucetiae* DSM17909  $\Delta hfq$  pBAD *xcnA* (xenocoumacin). Less but still visible cytotoxic effects were shown by NIH3T3 cells treated with CFCSs of the cultures of *X. doucetiae* DSM17909  $\Delta hfq$  pBAD *xrdA* (xenorhabdin) and *X. doucetiae* DSM17909  $\Delta hfq$  pBAD decarboxylase (phenethylamides). The CFCS of the culture of *X. szentirmaii*  $\Delta hfq$  pCEP-KM-*fcIC* (fabclavine) showed also a cytotoxic effect but not as strong as the other cytotoxic CFCSs.

### 3.3.3 Xenorhabdin induces apoptosis in HeLa cells

The results of HeLa and NIH3T3 cells treated with CFCS of cultures from containing only one class of secondary metabolites showed several secondary metabolites with cytotoxic effects. CFCSs containing xenocoumacin and xenorhabdin occurred to have the strongest cytotoxic effects on HeLa and NIH3T3 cells. Therefore, a time lapse microscopy was performed with the CFCSs containing these secondary metabolites. HeLa cells treated with CASO as control. During the time period of 24 h images were taken. Cells treated with the CASO control did not show any morphological changes and showed normal growth behavior. HeLa cells treated with CFCS containing xenorhabdin showed apoptotic behavior and within 12 h membrane blebbing was visible. Most of the cells showed membrane blebbing and the formation of apoptotic bodies during the observed time period. (**Fig. 3.3.4**)

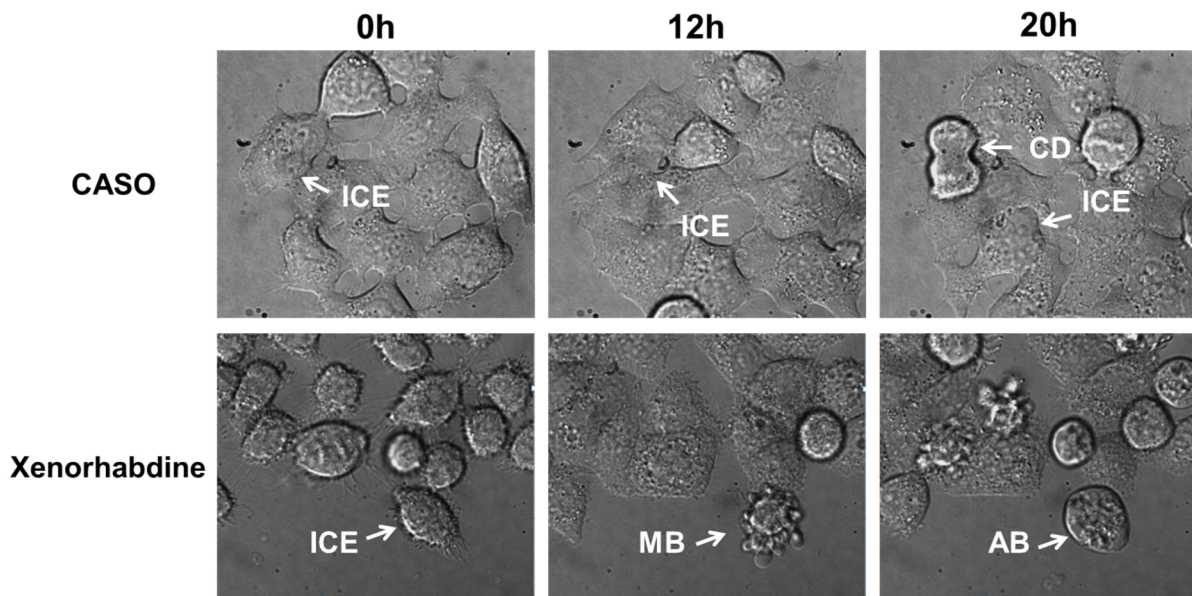
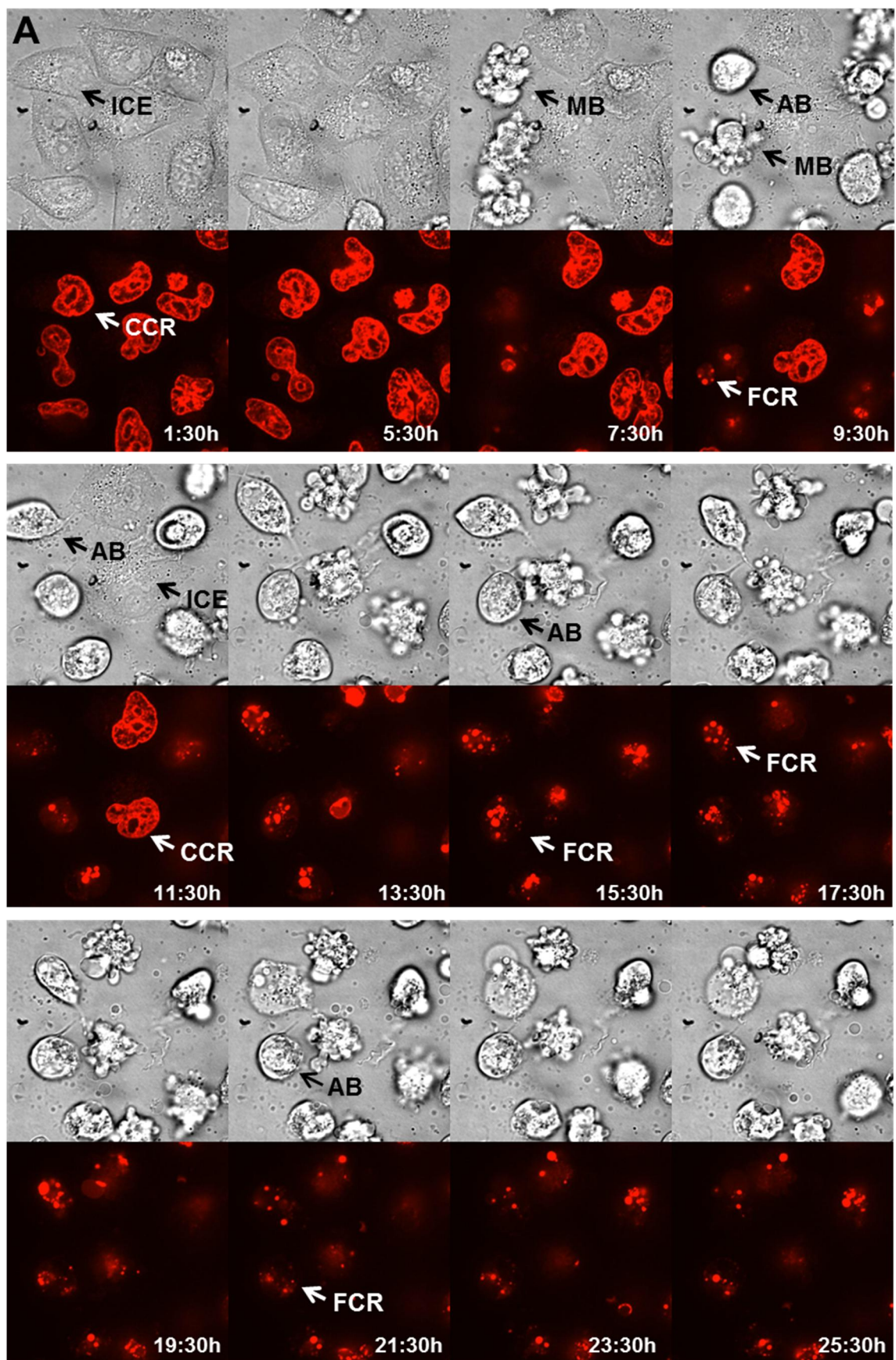


**Figure 3.3.4: Morphological changes of HeLa cells treated with CFCS containing xenorhabdin and a CASO control.** In the cells treated with the CASO control no morphological changes are visible. In the lower panel images of cells treated with CFCS containing xenorhabdin are visualized, which show membrane blebbing after about 12 h and the formation of apoptotic bodies within 20 h. Within the observed time period not all cell were undergoing apoptosis. AB: apoptotic body, MB: Membrane blebbing, ICE: intact cell, CD: cell division. 40x magnification

### 3.3.4 Xenocoumacin induces apoptosis in HCT116 cells

For further analysis of the lapse of the morphological changes induced by the treatment with 100 $\mu$ l CFCS of *X. nematophila* ATCC 19061  $\Delta$ *hfq* pBAD *xcnA* culture containing about 1 $\mu$ M of xenocoumacin 2, SiR-DNA was used to stain the chromatin. For this investigation HCT116 colon cancer cells were used, and a fluorescence time lapse microscopy was performed. During the first 5 h after the addition of the cell free cultures supernatant no change in the morphology of the cell was visible and the cells were intact. Here the chromatin was shown in the fluorescence channel as condensed chromatin (CCR). The first membrane blebbing (MB) occurred after about 5:30 h. The chromatin started to get fractionated and was not visible as CCR in the fluorescence channel anymore. Within the following 8 h all visualized cells were undergoing the membrane blebbing process. 13.5 h after the treatment of the cells no intact cell was visible. The membrane blebbing was followed by the formation of

apoptotic bodies (AB). In the fluorescence channel the fractionated chromatin (FC) was shown as red dots within these apoptotic bodies. After 25:30 h in most of the cells the apoptosis was completed, and the chromatin was fractionated and apoptotic bodies were visible (**Fig. 3.3.5**).



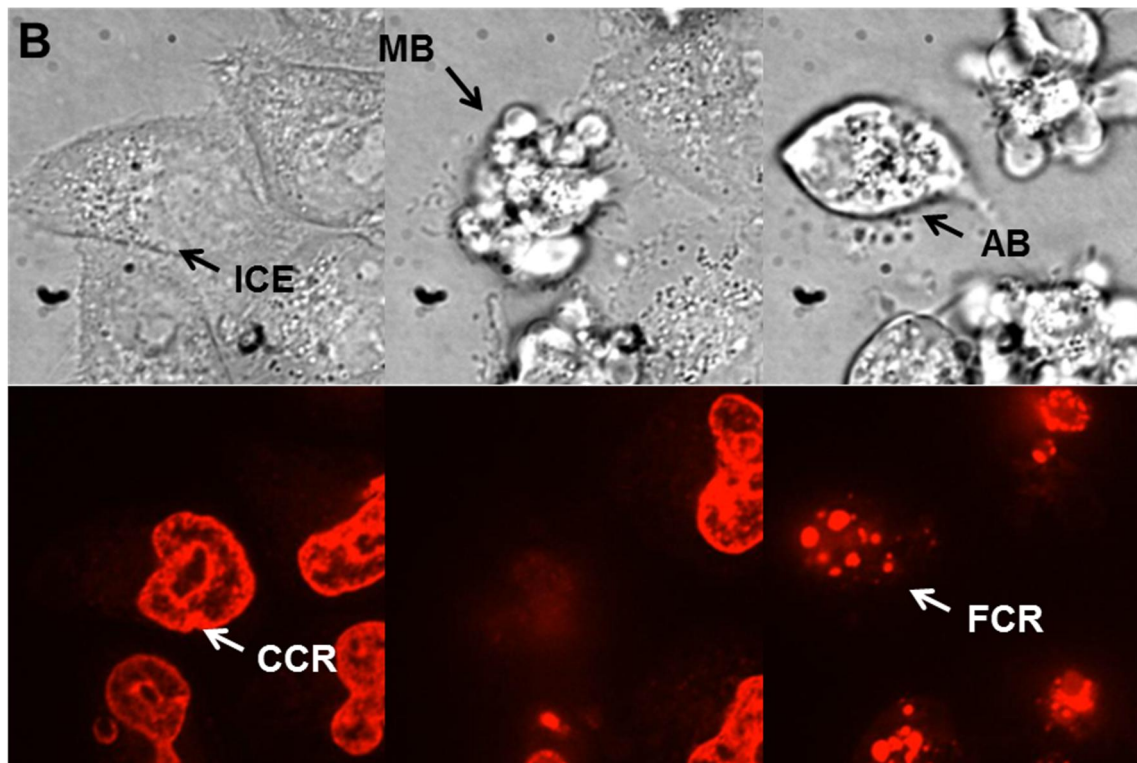


**Figure 6.3.5: Morphological changes of HCT116 colon cancer cells during the treating of cell free *X. nematophila*  $\Delta hfq$  pBAD *xcnA* culture supernatant containing xenocoumacin** **A)** Screenshots were taken every 2 h after the first morphological changes were visible. A time-laps microscopy showing HCT116 cells undergoing apoptosis induced by the addition of cell free culture supernatant containing xenocoumacin (about 1  $\mu\text{M}$ ). The first cells show membrane blebbing after about 5.5 h. Apoptotic bodies are seen after 9:30 h. After 13:30h no intact HCT116 cell is visible anymore. **B)** Enlarged images of HCT116 cells undergoing apoptosis. 1:30 h after the addition of xenocoumacin the cell is still intact, and the chromatin is condensed. 6h later the cell membrane shows membrane blebbing and 9:30 h after the addition of xenocoumacin and apoptotic body is formed. In shades of grey in the upper part are the phase contrast microscopy images. In red / black in the lower part are the luminescence microscopy images. ICE: intact cell, MB. Membrane blebbing, AB: apoptotic body, CCR: condensed chromatin, FCR: fractionated chromatin. 40x magnification (A). Images were acquired in collaboration with Anna Lena Weber & Hartmann Harz, LMU München.

### 3.3.5 Xenocoumacin 2 is a cytotoxic bacterial secondary metabolite

In the CFCS of the *X. nematophila*  $\Delta hfq$  pBAD *xcnA* culture that was used for the time lapse microscopy over 24h are also the intermediates of xenocoumacin 2 present, which are prexenicoumacin 1 and xenocoumacin 1. To outline whether one of these intermediates or just xenocoumacin 2 is responsible for the cytotoxic affects a viability assay was performed with strains of *X. nematophila* producing only of

these compounds. Upon the induction of the biosynthesis gene cluster of xenocoumacin by arabinose *X. nematophila* ATCC 19061 $\Delta$ *hfq* pBAD *xcnA* produces xenocoumacin 2, *X. nematophila* ATCC 19061 $\Delta$ *hfq*  $\Delta$ *xcnMN* pBAD *xcnA* produces xenocoumacin 1 and *X. nematophila* ATCC 19061  $\Delta$ *hfq*  $\Delta$ *xcnG* pBAD *xcnA* produces prexenocoumacin 1. The CFCSs of these cultures were applied to NIH3T3 cells and observed for cytotoxic effects. Images were taken after 6.5h, 24h and 48h after the addition of 100 $\mu$ l of the CFCSs. Cell cultures supplemented with CFCSs containing CASO, preXcn1 and Xcn1 did not show a significant cytotoxic effect within 24h, whereas the cell cultures treated with CFCS containing Xcn2 showed after 6.5h first impressions of cytotoxic effects which were very strong within 24h. After 48h no live cell was observed (Fig. 6.3.6).

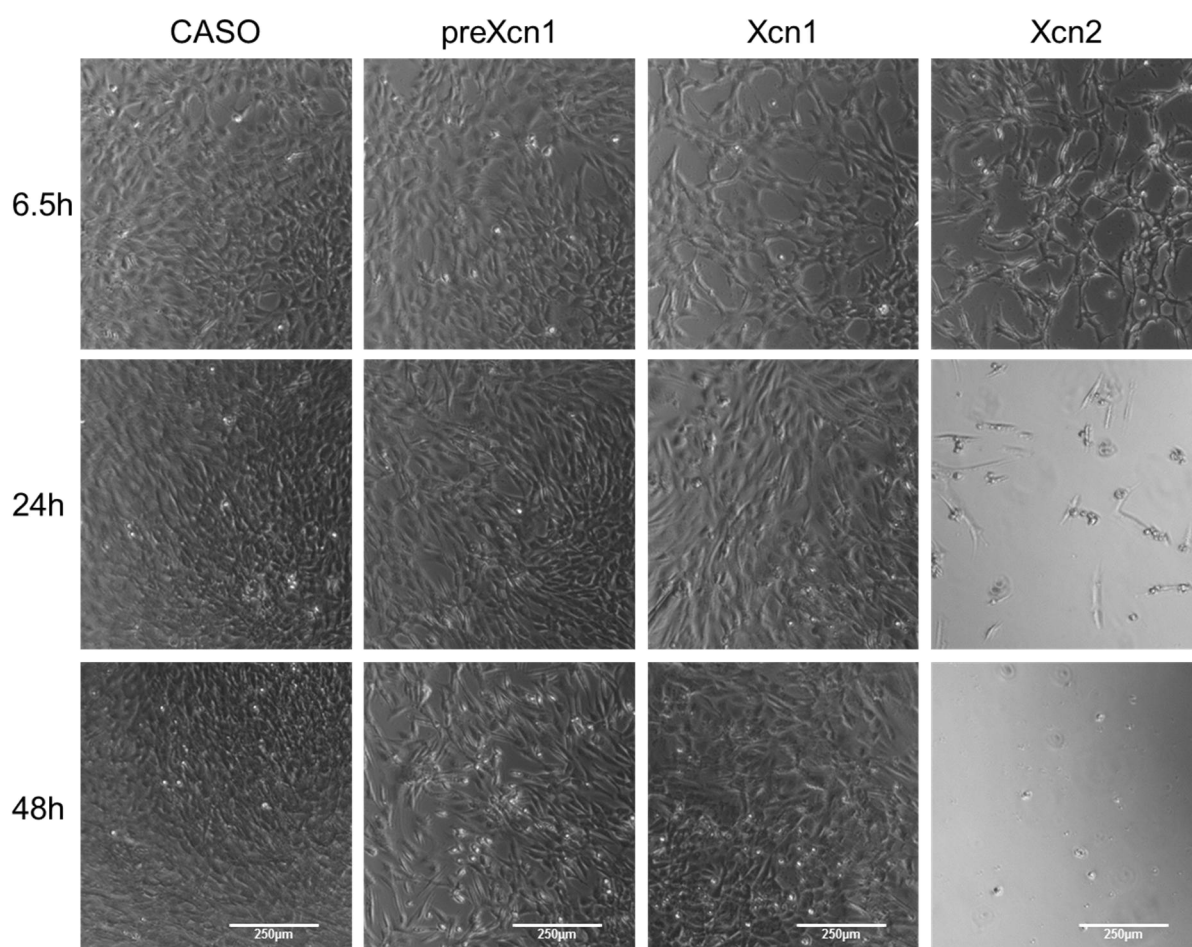


**Figure 6.3.6: Cell viability of NIH3T3 after treatment of cells with CFCSs of *Xenorhabdus* cultures producing precenocoumacin1 (preXcn1),**

**xenocoumacin1 (Xcn1) and xenocoumacin2 (Xcn2).** Images were taken after 6.5 h, 24 h and 48 h after the addition of 100 µl of the CFCSs. Cell cultures supplemented with CFCSs containing CASO, preXcn1 and Xcn1 did not show a significant cytotoxic effect, whereas the cell cultures treated with CFCS containing Xcn2 showed after 6.5 h first impressions of cytotoxic effects which were very strong within 24 h. After 48 h no live cell was observed.

These results show the cytotoxic effect of secondary metabolites produced by *Xenorhabdus* and *Photorhabdus* spec. Glidobactin, xenorhabdin and especially xenocoumacin 2 have strong and in the case of fabclavine and phenethylamides moderate cytotoxic effects against HeLa, NIH3T3 and HCT116 cells. Further it was shown that apoptosis is induced in HeLa cells when treated with xenorhabdin and in HCT116 colon cancer cells when substituted with xenocoumacin. Hence, these three molecules were newly described as cytotoxic active and have potential for further use in the development of drugs for cancer therapy.

## 4 Discussion

The pathogenic part of the entomopathogenic bacteria of *Xenorhabdus* spec. and *Photorhabdus* spec. is still an uncharted field of the lifecycle. This work could close some of these knowledge gaps and reveal in particular that two molecules from the insect larvae *G. mellonella*, stearic acid and palmitic acid, are sensed via inter-kingdom signaling by the PAS4-LuxR solos PikR1 / PikR2 in *P. luminescens*. The import of these fatty acids as well as the import of QS signaling molecules PPYD and DARs in *P. luminescens* and *P. asymbiotica* is facilitated by FadL. Furthermore, this work reveals the cytotoxic characteristics of several secondary metabolites from the entomopathogenic *Xenorhabdus* bacteria.

### 4.1 Inter-kingdom signaling via the PAS4-LuxR solos PikR1 / PikR2 by sensing of fatty acids from *G. mellonella*

Sensing the host is an essential step in the beginning of the pathogenic part of the lifecycle of *Photorhabdus* and *Xenorhabdus*. Only very few bacterial inter-kingdom signaling systems are known and none of them includes a PAS4-LuxR-type receptor (Tobias et al. 2020). *P. luminescens* harbors a vast amount of PAS4-LuxR solos (Brameyer et al. 2014), with yet unknown function. Here, it was demonstrated for the first time that PikR1 / PikR2 are involved in inter-kingdom signaling as the PAS4-LuxR solos by sensing the fatty acids stearic acid and palmitic acid originating from *G. mellonella*.

It was demonstrated that deletion of *pikR1* / *pikR2* resulted in decreased pathogenicity against *G. mellonella* larvae (Manske 2011), which indicated that these PAS4-LuxR solos sense a signal originating from *G. mellonella*. This missing regulation of the genes encoding toxins (**Supplementary Tab. S 3.1.2**) in *P. luminescens*  $\Delta$ *PikR1* / *PikR2* could explain the reduced pathogenicity against *G. mellonella*. Therefore, the PAS4-LuxR solos in *Photorhabdus* could be used as drug

targets for future development of novel antimicrobial drugs. The HPLC fractions of *G. mellonella* larvae homogenate, which showed high fluorescence signal intensity, were highly hydrophobic indicating the non-polar characteristics of the ligand. The insect larvae of *G. mellonella* contain an exceptional high fat proportion (60%) (Rumpold und Schlüter 2013; Sánchez-Muros et al. 2014; Statistisches Bundesamt 2020). The composition and content of fatty acids and proteins varies between insect larvae. *G. mellonella* has, compared to several other insect larvae, a high content of fatty acids. Especially palmitic acid (59.7g/kg) and palmitoleic acid (3.95 g/kg) are abounding. Stearic acid (4.09 g/kg), oleic acid (79.0 g/kg), linoleic acid (17.6 g/kg) and linolenic acid (2.91 g/kg) are also present in high amounts (Finke 2015; Rumpold und Schlüter 2013). This goes along with the regulation of several metabolic related genes by PikR1 / PikR2. Recently a growing group of bacteria is identified to use fatty acids as signaling molecules, which regulate a wide range of cellular functions such as biofilm formation and virulence factors (Davis 2020). Several *Burkholderia* species are using *cis*-2-dodecenoic acid as quorum sensing signaling molecule (Ryan et al. 2009; Deng et al. 2010). Interestingly several fatty acids have also been shown to act as cross-kingdom signaling molecules as *C. albicans* was found to respond to fatty acids originating from prokaryotes such as *cis*-2-dodecenoic acid from *Burkholderia cenocepacia* or *trans*-2-decenoic acid from *Streptococcus mutans* (Boon et al. 2008; Vílchez et al. 2010). Furthermore, unsaturated fatty acids were shown to be high-affinity ligands of the C-terminal PAS domain from the human hypoxia-inducible transcription factor 3 $\alpha$  (Fala et al. 2015).

With these high proportions of fatty acid in *G. mellonella* it could be assumed that PikR1 / PikR2 specifically sense these insect larvae. It also shows the wide distribution of fatty acids as signaling molecules and opens new perspectives for the development of inhibitors of these receptors.

In the reporter assay basal fluorescence signal intensity was observed also in absence of the signaling molecule. This could be caused by parallel activation of  $P_{plu0258}$  by other regulators. Plu0258 also was found in the comparative proteomic analysis also be differently expressed in the  $\Delta plu0918-plu0925$  mutant compared to the wild type. In a similar reporter assay with *P. luminescens*  $\Delta plu0918-plu0925$  mutant low fluorescence signal intensity was detected, which was increased upon larvae homogenate supplementation (Rothmeier 2010). This shows that  $P_{plu0258}$  might be regulated by other regulators as well, but is highly activated only upon presence of PikR1 / PikR2 and the signaling molecule. This would also explain the reduced, but not abundant, pathogenicity of *P. luminescens*  $\Delta pikR1-pikR2$  against *G. mellonella* larvae.

Furthermore, *P. luminescens* harbors 35 PAS4-LuxR solos, which is the highest number among Gram-negative bacteria so far known (Brameyer et al. 2014). This goes along with a broad range of hosts. The PAS4-LuxR solos putatively response specifically to several classes of hosts. It would be economically gainful for the bacterial community to express not all genes for inter-kingdom signaling in every cell, but distribute it over the whole population as a “public good” to sense the specific host. This kind of cooperation is known for the production toxins, siderophores, metabolites and enzymes (Smith und Schuster 2019; Becker et al. 2018). Fluorescence microscopy images of the reporter strain showed different activity of  $P_{plu0258}$  among the cells in the same culture of the reporter strains. In presence of stearic acid or palmitic acid the overall fluorescence intensity was high, but the distribution of signal intensity was heterogeneous. This might be resulting from loss of the reporter plasmid in some cells. But it also could be explained by heterogeneously expressed genes encoding the PAS4-LuxR solos among the bacterial population. This spatial organization is known for many bacteria (Cremer et al. 2019) and especially in microbial biofilm communities (Tolker-Nielsen und Molin

2000). Furthermore, several studies have shown extensive heterogeneity within pathogenic bacterial populations with virulence factors only be produced by subsets of the population (Davis 2020). This heterogeneity might be expanded from “public goods” to “public services” such as expression of genes encoding the different PAS4-LuxR solos for specific host sensing.

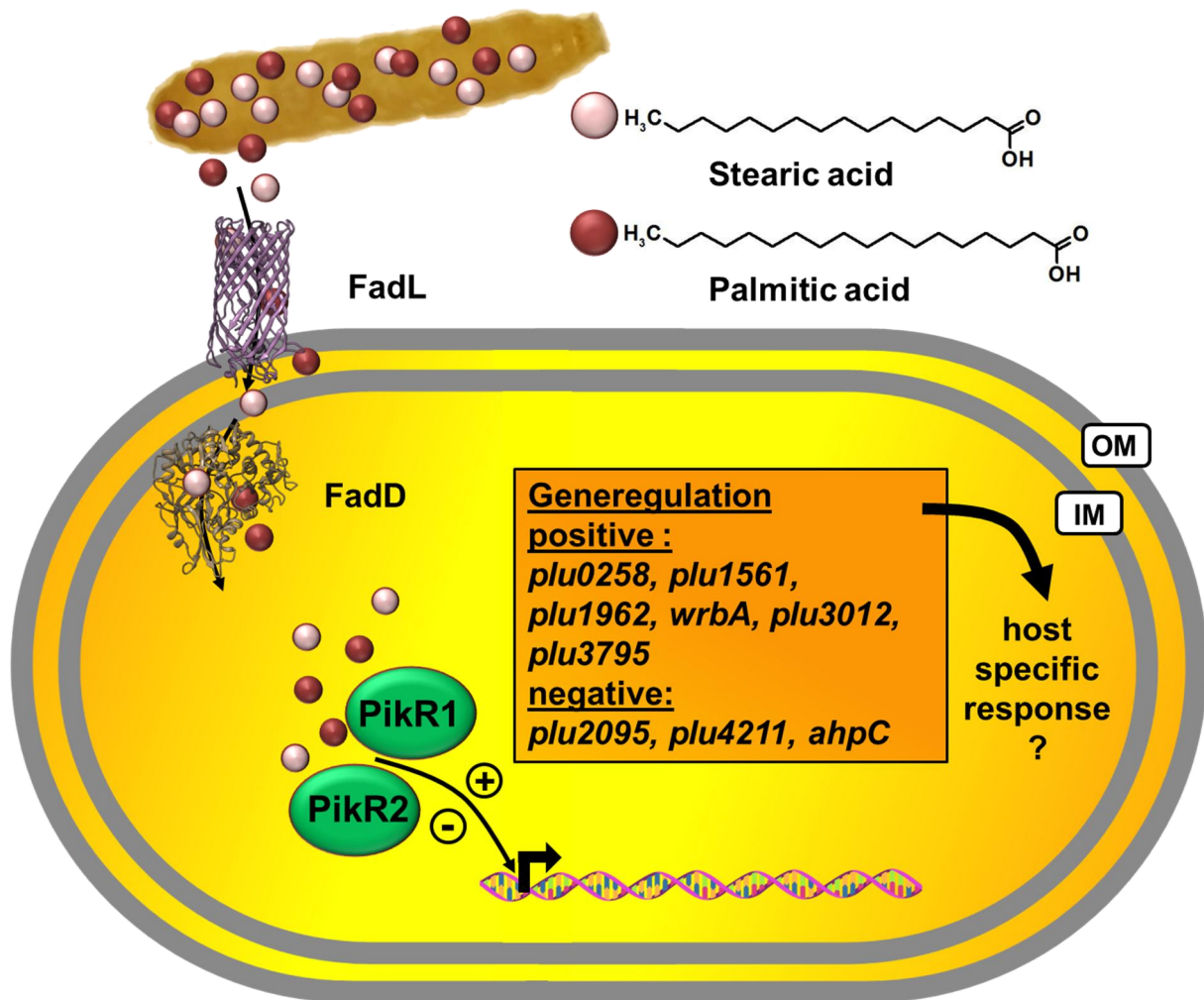


**Figure 4.1.1: Inter-kingdom signaling by the PAS4-LuxR solo(s) PikR1 / PikR2 in *P. luminescens*.** *G. mellonella* larvae contain among others stearic acid and palmitic acid, which is sensed by PikR1 / PikR2. The transport of the fatty acids into the cell seems to be facilitated by FadL and FadD. When the fatty acids bind to PikR1 / PikR2 they are able to upregulate several genes such as *plu0258*, *plu1561* and *plu1962* or downregulate *plu2095*, *plu4211* and *ahpC*, which might be a host specific response.

The sensing and recognition of stearic acid and palmitic acid from the insect host by the PAS4-LuxR solos PikR1 / PikR2 is important for the switch from symbiotic to pathogenic lifestyle. As pathogen the production of secondary metabolites plays a

major role for entomopathogens to kill the insect, to repel competitors and to digest the insect cadaver.

These findings can be beneficial for the research on inhibitors of the inter-kingdom signaling between pathogenic bacteria and the eukaryotic host. PAS4-LuxR-type receptors are wide spread among symbionts and pathogens (ffrench-Constant et al. 2003; ffrench-Constant 2017) and also present in human pathogens such as the closely related human pathogen *P. asymbiotica* (Fischer-Le Saux et al. 1999), which harbors 17 PAS4-LuxR solos (Brameyer et al. 2014). Another human pathogen is known to communicate via PAS4-LuxR-type receptor is *Vibrio cholerae* (Papenfort et al. 2017). This demonstrates the importance of PAS4-LuxR-type receptors for the communication of human pathogens.

The understanding of the inter-kingdom signaling by *Photorhabdus* via PikR1 / PikR2 and the identification of the signaling molecules might contribute to the innovation of novel antimicrobial drugs that reduce pathogenicity. PAS4-LuxR-type receptors might be a new class of targets for inhibitors of host sensing and QS. As PAS4-LuxR-type receptors are not only present in *Photorhabdus* species but also in other human pathogens, such as *Vibrio cholera*, there is high potential for the development of PAS4-LuxR-type inhibitors.

## **4.2 Transport of QS signaling molecules in *Photorhabdus* species**

Other targets for inhibitors of bacterial communication are FadD and FadL. During the pathogenic part of the lifecycle group behavior within the population is coordinated via QS. For the adaptation of the newly recognized change of the host quorum sensing requires the transport of the QS signaling molecules. The import and export mechanisms of hydrophobic signaling molecules like the QS signaling molecules acyl HSLs are poorly revealed so far. For the QS signaling molecules of *Photorhabdus*, PPYD and DARs, FadL has been demonstrated to be involved in the

import of those molecules. Furthermore, the potential role of both FadD and FadL in importing the signaling molecules PPYD and CHDs/DARs in *Photorhabdus* species was demonstrated heterologously in *E. coli* (Brameyer 2015a). These aspects show the importance of FadD and especially FadL in the communication of bacteria and demonstrate the potential as drug targets for substances inhibiting the communication of bacteria.

Structure comparison of predicted structures of FadL homologs of *E.coli*, *P. luminescens* DJC, *P. asymbiotica* and *S. meliloti* and were shown to share the characteristic  $\beta$ -barrel structure of FadL channels (van den Berg 2005). The hydrophobic tunnel that is formed by the  $\beta$ -barrel structure in FadL homologs enhances hydrophobic substrates to diffuse through the polar lipopolysaccharide (LPS) layer into the periplasm. This diffusion-based transport of hydrophobic substances from outside of the cell into the lipid bilayer was demonstrated for FadL homologs of *E. coli* and *P. aeruginosa*. The pores formed by FadL allow hydrophobic structures to pass through the outer membrane by avoiding the aqueous phase (Hearn et al. 2009). Fatty acids are utilized by the IM-associated fatty acyl-CoA synthetase FadD, important for the activation of imported LCFAs through the IM (Pech-Canul et al. 2011). In *P. luminescens* and *P. asymbiotica* two homologs of FadD (PluDJC\_11395, PluDJC\_18030 and Pb6\_01559, Pb6\_04001) were identified, but protein sequence analysis indicated that only one FadD homolog in each strain seemed to play a role the transport of the QS signaling molecules of *Photorhabdus*. A comparison between the two FadD homologs (FadD1 and FadD2) of *P. aeruginosa* (Kang et al. 2010) did only show around 51% identity and did not reveal differences in similarity, when comparing both protein sequences of the FadD homologs from *Photorhabdus* with the protein sequences from *P. aeruginosa*. These FadD homologs from *P. aeruginosa* show differences in the favourability to utilize different length of fatty acids (Kang et al. 2010). As protein sequence comparison did not

show correlation to the FadD homologs from *Photorhabdus*, no connection to chain length favourability of FadD homologs from *Photorhabdus* could be made. Moreover, protein sequence analysis of FadL and FadD homologs of *P. luminescens* and *P. asymbiotica* showed high protein sequence identity with FadD and FadL from *E. coli*, but not with the homologs of *S. meliloti*, which has a conserved extracellular loop 5, important for the specificity of long-chain acyl-HSLs transport (Krol und Becker 2014). As this loop 5 is not conserved in FadL homologs of *Photorhabdus* spec. AHLs might not be the major substrate besides LCFAs. The comparisons of the predicted structures show that FadD and FadL proteins of different species share the similar structures. This indicates the possibility to transfer inhibitory substances from known FadD or FadL-like drug targets to the inhibition of the import of QS signaling molecules by blocking FadD or FadL in bacteria. FATP2 is a protein involved in transport of exogenous fatty acids in human (Black et al. 2016). Examples of inhibitors of the human fatty acid transport protein 2 are CB2 ((5E)-5-[(3-bromo-4-hydroxy-5-methoxyphenyl)methylene]-3-(3-chlorophenyl)-2-thioxothiazolidin-4-one) and CB5 (grassofermata) (Sandoval et al. 2010; Saini et al. 2015).

A fluorescence-based reporter assay confirmed that PluR and PauR show less response to PPYD and DARs, respectively, which shows the major role of FadL in the import of PPYD from the extracellular matrix into the cell.

Moreover, a dramatic change in the ratio between intracellular (ic.) and extracellular (ec.) concentration of PPYD in *P. luminescens* DJC, by comparison of levels in the wild type to the levels in *P. luminescens* DJC  $\Delta$ *fadL* and in *P. luminescens* DJC  $\Delta$ *fadL*  $\Delta$ *fadD*. This was also shown for  $\Delta$ *fadL* mutants of *S. meliloti*, where AHLs accumulated in culture supernatant (Krol und Becker 2014). This demonstrates the importance of FadL for the import, but not the export of the QS signaling molecule PPYD in *P. luminescens*.

It was shown that an anti-FadL antibody was inhibiting the transport of fatty acids in *E. coli* (Black 1990). This shows the possibility to inhibit substance transport by FadL. Due to the slightly different structure of FadL in *Photobacterium* it might be possible to inhibit these transport function more selectively for specific bacteria.

As neither FadD nor FadL seem to facilitate the export of PPYD other ABC transporters or / and efflux pumps might support the export of the QS signaling molecule of *P. luminescens*. Several of these are present in the genome of *P. luminescens* (Duchaud et al. 2003; Zamora-Lagos et al. 2018). The QS signaling molecule of *P. aeruginosa*, N-(3-oxododecanoyl) homoserine lactone, is actively exported by an efflux pump (Pearson et al. 1999).

Moreover, in *P. luminescens* DJC  $\Delta fadL \Delta fadD$  the overall levels of PPYD (ic. + ec.) were considerably reduced, whereas the extracellular PPYD levels in the culture supernatant of *P. luminescens* DJC  $\Delta fadL$  were multiple times increased compared to the other *P. luminescens* mutants and the wild type. The accumulation in the extracellular supernatant could be explained by a missing negative feedback loop, since the intracellular levels are decreased, when compared to the wild type. While many QS systems create a positive feedback loop (Fuqua und Winans 1994; Stauff und Bassler 2011; Meyer et al. 2012), this was not observed for *P. luminescens* (Brachmann et al. 2013). Thus, synthesis is enhanced by low intracellular levels of PPYD, which leads to extracellular enrichment when import is reduced.

In contrast, FadD only plays a minor role for the transport of PPYD in *P. luminescens* DJC. As the response of PPYD by PluR and transport into the cell seems not to be dependent on FadD, the utilization and the transmission through the IM seems not to be relevant. An example for a LuxR receptor localized as a monomer at the inner membrane is TraR. Only in presence of the corresponding acyl-HSL TraR dimerizes and is released into the cytoplasmic compartment (Qin et al. 2000). QscR of *P. aeruginosa* is another example of a receptor that only achieves significant soluble

levels in presence of AHLs (Oinuma und Greenberg 2011). Therefore, it can be concluded that PluR is localized at the inner membrane and becomes active and soluble in the presence of PPYD, when imported by FadL into the periplasm. PluR might be amphipathic and membrane associated as supposed for LuxR of *V. fischeri* (Kolibachuk und Greenberg 1993), thus FadD is required to activate the signaling molecule with CoA for utilization within the cell.

*P. luminescens* DJC  $\Delta fadD$  showed nearly wild type-like PPYD levels and might not be important for the import of QS signaling molecules. But FadD utilizes long-chain fatty acids (Pech-Canul et al. 2011), which are then accessible for  $\beta$ -oxidation. The head to head condensation to form PPYD is catalyzed by the ketosynthase PpyS (Brachmann et al. 2013) and requires CoA bound thioesters or acyl carrier protein, depending from their origin (Kresovic et al. 2015). Therefore it can be assumed that a decreased amount of precursors from the  $\beta$ -oxidation for the biosynthesis leads to decreased overall levels of PPYD in *P. luminescens* DJC  $\Delta fadL$   $\Delta fadD$ . A similar behavior is suspected for DARs from *P. asymbiotica* as both biosynthesis pathways for photopyrones and dialkylresorcinols rely on the same precursor (Tobias et al. 2020).

Furthermore, phenotypic differences occurred between the *P. luminescens* DJC wild type and *P. luminescens* DJC  $\Delta fadL$ , *P. luminescens* DJC  $\Delta fadD$  and *P. luminescens* DJC  $\Delta fadD$   $\Delta fadL$ . Not only the transport and the synthesis of the QS signaling molecules were affected, but also patterns like pigmentation and the amount of cinnamic acid was impacted by the deletion of *fadL* and *fadD* in *P. luminescens* DJC. Secondary metabolite production was also altered in the *P. luminescens* DJC mutants. The reason might be that the mutants *P. luminescens* DJC  $\Delta fadD$ , *P. luminescens* DJC  $\Delta fadL$  and especially *P. luminescens* DJC  $\Delta fadD$   $\Delta fadL$  provide the cells with lower amount of accessible fatty acids for the  $\beta$ -oxidation cycle, since the transport of fatty acids through the OM is facilitated by FadL (Nunn et al. 1986) and the utilization

of fatty acids is supported by FadD (Pech-Canul et al. 2011). A STRING network analysis (Szklarczyk et al. 2019) of FadD and FadL of *P. luminescens* DJC revealed tight connections to proteins of the  $\beta$ -oxidation cycle for the degradation of long chain fatty acids. The acyl-CoA dehydrogenase FadE and the fatty acid oxidation complex subunit FadB (Jimenez-Diaz et al. 2017) are some of the proteins with close relation. In the  $\beta$ -oxidation cycle long-chain fatty acids are degraded and released as shorter acyl-CoA and especially acetyl-CoA (Jimenez-Diaz et al. 2017), which could be building blocks for secondary metabolites like anthraquinones in *Photorhabdus* (Brachmann et al. 2007). A precursor in the synthesis of stilbene produced by *Photorhabdus* (Park et al. 2017) is cinnamic acid, but the biosynthesis also requires malonyl-CoA, and isovaleryl-CoA (Bode 2009). These small compounds might originate from degraded fatty acids. In case malonyl-CoA and / or isovaleryl-CoA are missing or are only present in small amounts the synthesis would slow down or stop and cinnamic acid is accumulated. In *P. luminescens* DJC  $\Delta fadD$  and *P. luminescens* DJC  $\Delta fadL$  the overall production of secondary metabolites might be reduced as a result of less fatty acid transport and therefore less accessible building blocks. Secondary metabolites and especially stilbene is required for nematode development and for infective juvenile recovery (Waterfield et al. 2009; Park et al. 2017; Tobias et al. 2017). Cinnamic acid is a precursor in the stilbene biosynthesis (Park et al. 2017) and the high amount of cinnamic acid might be a result of the upregulation of the production of stilbenes. Missing fatty acids due to decreased transport in *P. luminescens* DJC *fadD* and *P. luminescens* DJC *fadL* mutants could simulate the bacteria a depleted insect cadaver and triggers the signals for reassembly with the nematode and its development.

Even though, pathogenicity against *G. mellonella* larvae by strains of *P. luminescens* and *P. asymbiotica* lacking *fadD* and / or *fadL* was not reduced, the development of FadD and FadL inhibitors could decrease the ability of the bacteria to re-associate

with the nematodes and might reduce the production of secondary metabolites, essential for the nematode development. This could help by interfering with the distribution of the human pathogen *P. asymbiotica*, when the re-association with the symbiont is inhibited.

This work shows the importance of FadD and FadL for the QS and its influence on the production of secondary metabolites in the pathogenic part of the lifecycle of *Photorhabdus*. Therefore, FadD and FadL are putative drug targets for the future development of drugs interacting with the import of fatty acids and interfering with the bacterial Qs system. Furthermore, FadL and FadD have impact on the import of the inter-kingdom signaling molecules sensed by PikR1 / PikR2. An inhibitor of FadL would also decrease host sensing and would be beneficial for the speed of an infection.

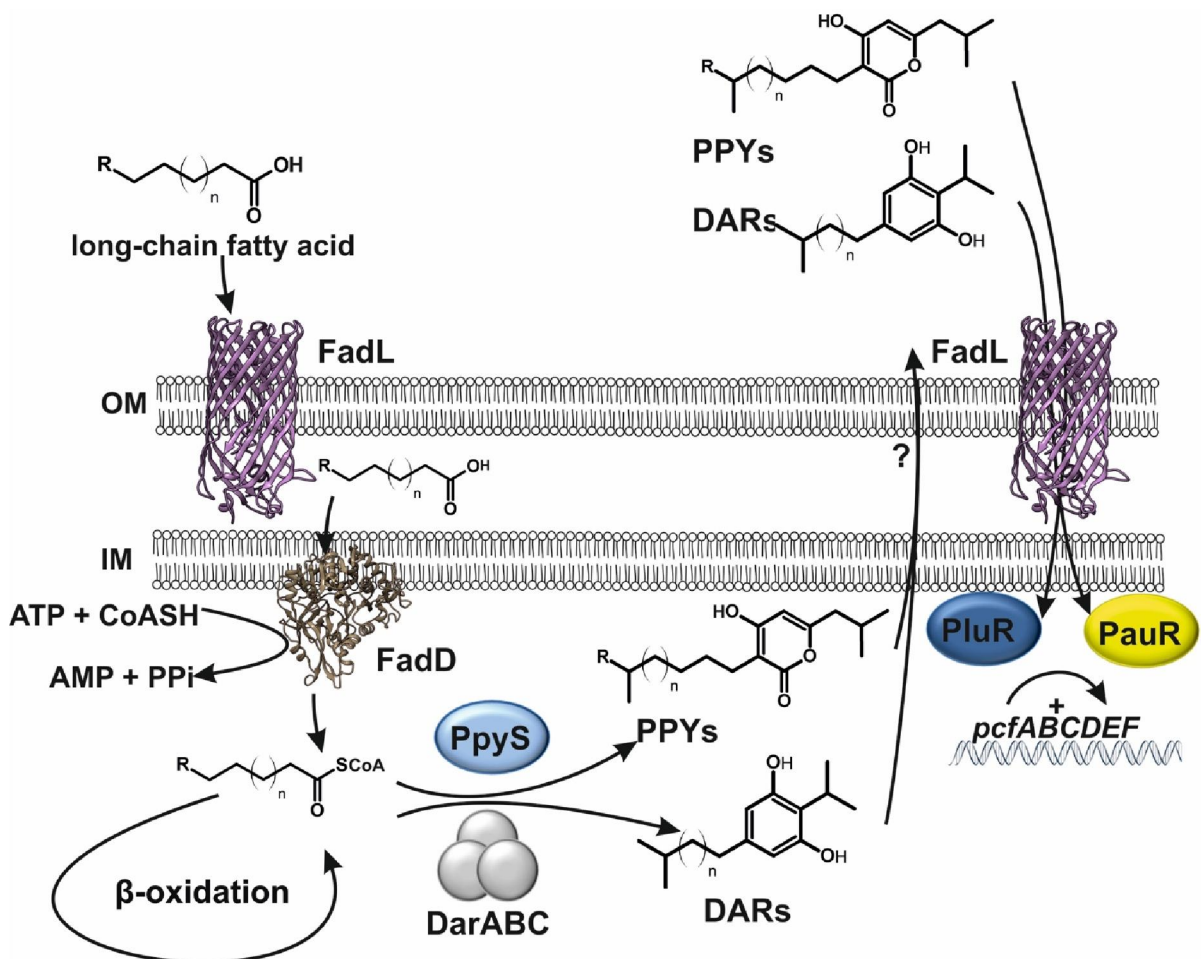


Figure 4.2.1: Transport and synthesis of QS signaling molecules in *Photorhabdus spec.* This model represents our current findings of the transport

mechanism for PPYs and /DARs in *Photorhabdus* species. Long-chain fatty acids are imported by FadL (purple) and activated by FadD (brown). We hypothesize that PpyS (light blue) and DarABC (grey) require precursors from  $\beta$ -oxidation of the CoA fatty acids to synthesize the corresponding signaling molecule. The export of the QS signaling molecules is not supported by FadL, whereas the import of extracellular QS signaling molecules through the outer membrane (OM) is facilitated by FadL. In presence of these quorum sensing molecules PluR (dark blue) and PauR (yellow) then regulate the expression of the *pcfABCDEF* operon. (Figure adapted from (Brehm et al. 2021))

### **4.3 Secondary metabolites xenocoumacin 2 and xenorhabdin from *Xenorhabdus* induce apoptosis**

The development of drugs for cancer therapy requires substances with cytotoxic characteristics to treat tumor cells. In the pathogenic part of the lifecycle *Xenorhabdus* and *Photorhabdus* produce a broad range of secondary metabolites. For three secondary metabolites phenethylamides, xenorhabdin and xenocoumacin 2, we expanded the properties to being additionally cytotoxic and therefore potential candidates for the use in cancer therapy research.

Cultures of NIH3T3 and HeLa cells were substituted cell free culture supernatant (CFCS) of several *Xenorhabdus* and *Photorhabdus* strains producing a broad range or specifically one class of secondary metabolites. The CFCSs of *X. doucetiae* and *X. szentirmaii* cultures showed strong cytotoxic effects indicating a production and export of cytotoxic secondary metabolites under laboratory conditions.

To investigate which substance in particular harmed the cells, further viability assays were performed with CFCSs of strains producing only one class of secondary metabolites. Cytotoxic effects were shown for CFCSs containing glidobactin A, xenocoumacin, xenorhabdin, fabclavine and phenethylamides.

For glidobactin A strong cytotoxic effects was observed. As glidobactin A is known to inhibit proteasome activity (Clerc et al. 2011; Dudnik et al. 2013), which leads to rapid and dramatic change in the levels of intracellular peptides and leading to cell death

(Gelman et al. 2013). Therefore, CFCS containing glidobactin A was used as positive control for cytotoxic activity.

Fabclavines only showed slight cytotoxic effects in NIH3T3 cell cultures, whereas these effects were stronger when treated with CFCS containing phenethylamides (Bode 2009). The moderate cytotoxic effects of fabclavine might be a result of the large size of the molecule and the resulting low uptake into the cell. The effect on NIH3T3 cells was stronger than on HeLa cells. This was observed throughout all viability assays. As the doubling time of HeLa cells (40-48h) is higher than the doubling time of NIH3T3 cells (about 20h) (DSMZ). With higher growth rate the sensitivity of cell lines towards stress appears to be higher (Assanga 2013). The strongest cytotoxic effects were observed when cells were treated with CFCSs containing xenorhabdin and xenocoumacin. This was a novel characteristic of these substances.

For cancer treatment it is preferable that the compound used as drug induces apoptosis rather than necrosis (Fesik 2005). During apoptosis the cells show membrane blebbing (Coleman et al. 2001), formation of apoptotic bodies (Akers et al. 2013) condensation of chromatin (Oberhammer et al. 1994) and the fragmentation of DNA (Zhang und Xu 2000). In this thesis it was demonstrate that xenocoumacin 2 and xenorhabdin induce apoptosis in HCT116 and HeLa cells. Membrane blebbing (Coleman et al. 2001), the first visible sight of apoptosis, was observed for both cell cultures treated with CFCS containing xenorhabdin and xenocoumacin. Cell cultures containing xenocoumacin showed them earlier than the ones with xenorhabdin showing a higher potency of xenocoumacin. The following formation of apoptotic bodies was observed for both cultures (Akers et al. 2013). The HCT116 cells cultures treated with xenocoumacin showed condensation of chromatin and DNA fragmentation and DNA fragmentation within apoptotic bodies.

Therefore, xenocoumacin and xenorhabdin are two novel secondary metabolites, which could be used for the cancer treatment research. For further application the mechanism of action inducing the apoptosis should be determined.

As these secondary metabolites do not share structural similarity with glidobactin A another mode of action in the cell is predicted (**Fig 4.3.1C**). Xenorhabdin persists a dithiopyrrolone structure (Qin et al. 2013), which is highly identical with the structure of thiolutin (**Fig. 4.3.1A**). Thiolutin inhibits the RNA polymerase by preventing the incorporation of uridine in *Saccharomyces cerevisiae* (Jimenez et al. 1973). This indicates that xenorhabdin also acts as an RNA-polymerase inhibitor (**Fig 4.3.1C**).

CFCS containing xenocoumacin might also contain the intermediates of the biosynthesis prexenocoumacin 1 and xenocoumacin 1. Only for xenocoumacin 2 a cytotoxic effect was verified.

Xenocoumacin 2 has a larger structure than xenorhabdin, but shares similarities with the cytotoxic substance isocoumarin 185322 (Hampl et al. 2011). Isocoumarin 185322 contains an 8-hydroxyisocoumarin structure, which is substituted with the heterocycle pyridine (Kawano et al. 2007) (**Fig 4.3.1**). Also xenocoumacin 1, prexenocoumacin 1 and xenocoumacin 2 have this structure included. Only xenocoumacin 2 has the heterocycle pyrrolidine incorporated at the opposite end (**Fig. 4.3.1B**). Cells treated with isocoumarin 185322 showed rapid decrease in tubulin assembly and lead to apoptosis of human multiple myeloma cell (Kawano et al. 2007). Thus, it is assumed that xenocoumacin 2 also inhibits microtubule polymerization (**Fig 4.3.1C**). The same mechanism is proposed for phenethylamides as the structure is similar to a part of the structure of the inhibitor of microtubule assembly arenastatin A (Koiso et al. 1996; Morita et al. 1997).

With the consolidated apoptotic mechanism a new approach of cancer treatment via antibody–drug conjugates with high specificity in drug delivery is possible. This was shown for the trastuzumab-emtansin antibody–drug conjugate, which is highly

specific to HER-2 receptors occurring in breast cancer cells (Niculescu-Duvaz 2010) and other compounds (Xu et al. 2019). For the conjugation of a large spectrum of compounds to an antibody the ethynylphosphonamidate-linker was found to be excellent (Kasper et al. 2019), therefore xenocoumacin 2 and xenorhabdin might be suitable candidates for antibody–drug conjugates.

This thesis discovered several secondary metabolites produced in the pathogenic part of the lifecycle of the entomopathogen *Xenorhabdus* that are cytotoxic against human cell lines and have high potential for further development in the field of cancer treatment, as they induce apoptosis, which is beneficial for drug candidates for this application.

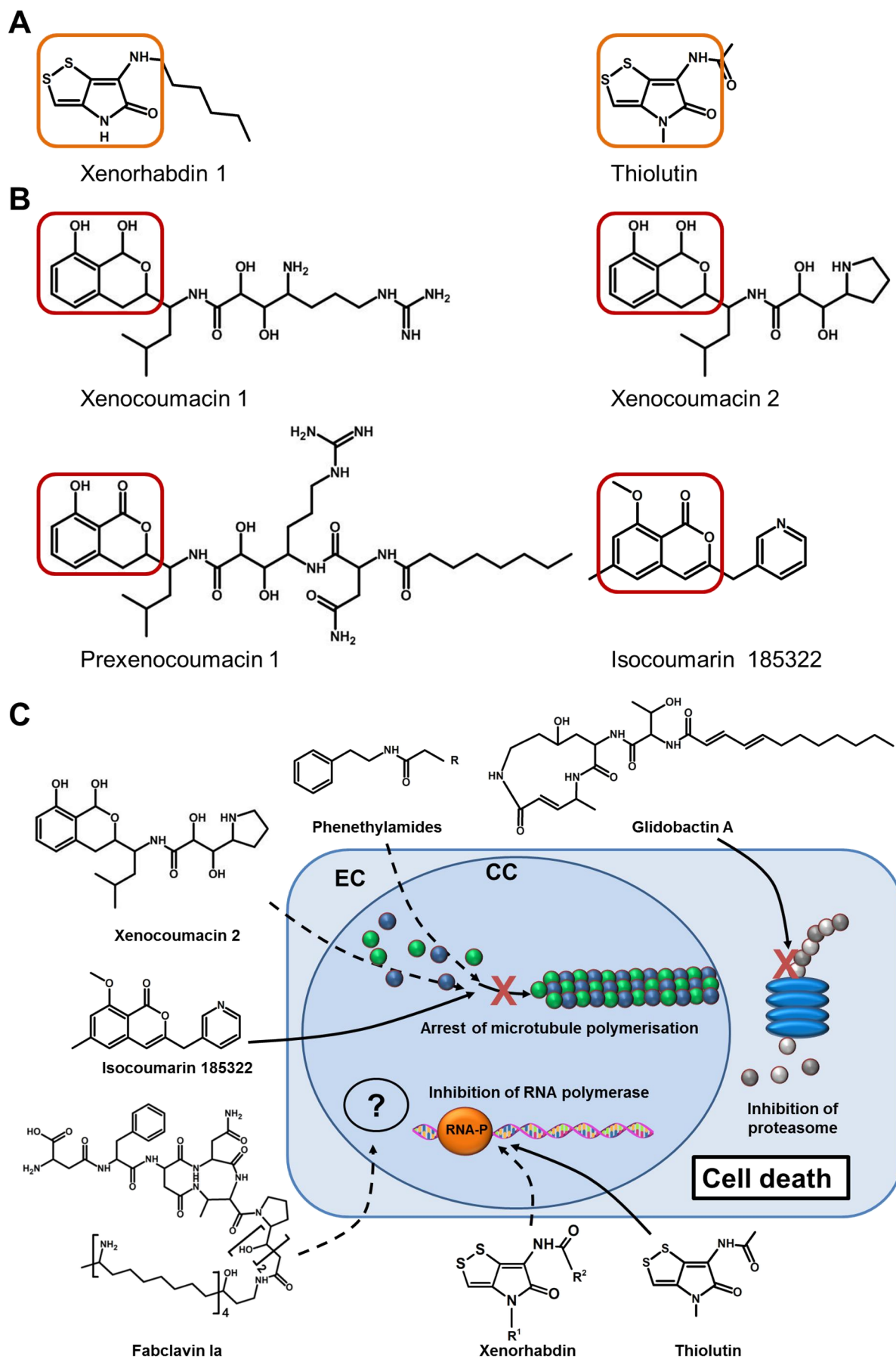


**Figure 4.3.1: Structure comparison of xenorhabdin, thiolutin, prexenocoumacin 1, xenocoumacin 1, xenocoumacin 2 and isocoumarin 185322 and their proposed**

**mode of action in eukaryotic cells. A)** The structures of xenorhabdin 1 and thiolutin have high structural similarity. The dithiopyrrolone structure (orange) is present in both molecules. **B)** The structures of prexenocoumacin 1, xenocoumacin 1, xenocoumacin 2 and isocoumarin 185322 share a similar structure of the 8-hydroxyisocoumarin (red). Isocoumarin 185322 and xenocoumacin 2 also share a heterocycle containing a nitrogen atom (pyridine and pyrrolidine, respectively) on the same end of the molecule, whereas prexenocoumacin 1 and xenocoumacin 1 have substitutes with higher nitrogen content (arginine) and no heterocycle. **C)** Isocoumarin 185322 inhibits the polymerization of the microtubule (Kawano et al. 2007). Therefore  $\alpha$ -tubulin (green) and  $\beta$ -tubulin (dark blue) are not added to the microtubule. Xenocoumacin 2 (Park et al. 2009) and phenethylamides (Bode et al. 2017) are supposed to have the same inhibitory effect. Glidobactin A is known to inhibit the proteasome (blue) (Clerc et al. 2011). Thiolutin is an inhibitor of the RNA polymerase (orange) (O'Neill et al. 2000), which is also assumed for the structural similar xenorhabdin 1. Fabclavine also has cytotoxic activity against eukaryotic cells but the mechanism or target is not known. Striped arrows describe the proposed mechanism; black arrows show the known mechanism. CC: cell core, EC: eukaryotic cell, Phenethylamide "R": Ph, Et or iPr, Xenorhabdin (I-V) R<sup>1</sup>: H, H, H, Me, Me; R<sup>2</sup>: *n*-pentyl, 4-methylpentyl, *n*-heptyl, *n*-heptyl, 4-methylpentyl.

## 4.4 Conclusion

This work reveals several aspects of the pathogenic part of the lifecycle of the entomopathogens *Xenorhabdus* and especially *Photorhabdus* useful for the future development of drug candidates. As entering the insect host *P. luminescens* is required to sense the specific host. The PAS4-LuxR solo(s) PikR1 / PikR2 are indicated as inter-kingdom signaling receptors and sense stearic acid and palmitic acid from *G. mellonella*. PikR1 / PikR2 activate the promoters of several genes as shown for  $P_{plu0258}$ ,  $P_{plu1561}$  and  $P_{plu1962}$ , when binding the fatty acids from the insect larvae (**Fig 4.4.1A**). As pathogenicity is reduced in strains lacking PikR1 / PikR2, PAS4-LuxR solos could be novel and specific targets for antibiotics not killing the bacteria but inhibiting or reducing pathogenicity. This would also decrease the chance of development of resistance mechanisms against these antimicrobial drugs. Furthermore, it was demonstrated that FadL and FadD have impact in the transport of these inter-kingdom signaling molecules. FadL also facilitates the transport of the QS signaling molecules PPYD in *P. luminescens* DJC and DARs in *P. asymbiotica*, whereas both, FadD and FadL, have influence on the secondary metabolite production in *P. luminescens* DJC (**Fig 4.4.1B**). This might add FadL and FadD as well as the receptors PauR and PluR as new target proteins in the future research for inhibiting bacterial communication and interaction with the secondary metabolite production. When sensing the host and switching to a pathogenic lifestyle the secondary metabolites such as xenorhabdin and xenocoumacin 2 are produced that have cytotoxic effects against eukaryotic cells by inducing apoptosis. Both, xenorhabdin and xenocoumacin 2 were found to be highly potent and induce apoptosis. The mechanism is not clarified yet, but might be caused by inhibition of the RNA polymerase and the inhibition of microtubule assembly, respectively, which leads to mitotic arrest (**Fig 4.4.1C**). These findings will add xenocoumacin 2 and

xenorhabdin as new substances to the portfolio of promising cytotoxic compounds in the field of cancer treatment research.



and DARs is facilitated by FadL. Long-chain fatty acids are transported through the outer membrane by FadL (violet) and utilized by FadD (light brown) for further usage in the  $\beta$ -oxidation. Precursors for the synthesis of DARs and PPYD might originate from the  $\beta$ -oxidation cycle. The QS signaling molecules are then transmitted into the extracellular matrix but FadD or FadL seem not to play role in the export. When imported via FadL the LuxR receptors PauR (yellow) and PluR (blue) bind DARs and PPYD, respectively and are then able to activate expression of the *pcfABCDEF* operon. Red arrows indicate potential drug targets for interruption of the inter-kingdom signaling of *P. luminescens*. **B)** The insect larvae *G. mellonella* is recognized by PikR1 / PikR2 by sensing the long chain fatty acids stearic acid (pink) and palmitic acid (red). The sensing of these was shown to be decreased in the absence of FadD and / or FadL as these play a major role in long-chain fatty acid transport. As PikR1 / PikR2 bind the fatty acid the PAS4-LuxR solos regulate expression of several genes such as plu0258. Red arrows indicate potential drug targets for interruption of the quorum sensing system of *P. luminescens*. **C)** The biosynthesis gene cluster of xenocoumacin in *Xenorhabdus* contains 14 genes and two know intermediates prexenocoumacin 1 (preXcn1) (orange) and xenocoumacin 1 (Xcn1) (brown) are produced as well as xenocoumacin 2 (Xcn2) (light red). These secondary metabolites are excreted out of the cell. Prexenocoumacin 1 and xenocoumacin 1 have no cytotoxic effect on eukaryotic cell, whereas xenocoumacin 2 has a strong cytotoxic effect against several eukaryotic cells and induces apoptosis probably by inhibiting microtubule polymerization. Xenorhabdin (Xrd) inhibits the RNA-polymerase (RNA-P) (orange). Therefore, these substances have high potential to be candidates for future drugs research for cancer treatment.

OM outer membrane, IM: inner membrane, preXcn1: prexenocoumacin 1, Xcn1: xenocoumacin 1, Xcn2: xenocoumacin 2, Xrd: xenorhabdin, RNA-P: RNA-polymerase, Xenorhabdin (I-V) R<sup>1</sup>: H, H, H, Me, Me; R<sup>2</sup>: *n*-pentyl, 4-methylpentyl, *n*-heptyl, *n*-heptyl, 4-methylpentyl

## 5 Outlook

The pathogenic part of the lifecycle of *Photorhabdus* and *Xenorhabdus* still poses a challenging field of research, to provide more information for the development of drugs such as antibiotics.

For better understanding of the PAS4-LuxR solos binding kinetics of PikR1 and PikR2 to the corresponding promoters could be performed with both proteins individually and in combination with and without the fatty acids. This might reveal whether the binding affinity is enhanced with one or the other ligand and which receptor preferably binds which fatty acid. This could also answer whether the receptors prefer to form heterodimers.

In comparison with the six amino acid motif of AHL-binding LuxR receptors three conserved amino acids were different. To verify whether these amino acids are responsible for ligand binding a single amino acid exchange could be performed. By analysis via SPR spectroscopy and with the fluorescence reporter assay the importance of these amino acids for binding would be revealed. Another SPR analysis could be performed PikR1 and PikR2 if the different amino acids in the motif were exchanged. In case these amino acids are important for binding either stearic acid or palmitic acid this would be detected by showing different binding kinetics in the SPR analysis.

Another approach for clarification of the amino acids of the binding pocket and the overall structure of these PAS4-LuxR solos might be the crystallization of PikR1 and PikR2 in presence of the bound ligand. Therefore, the purification of the proteins must be improved to increase the amount of protein purified after overproduction by further buffer and overproduction improvement. Overproduction could be improved by

supplementing the overproduction culture with the ligand as shown for QscR (Liu et al. 2010).

A major open question remains the function of the other PAS4-LuxR solos in *P. luminescens*, which are putatively other potential drug target proteins. As PikR1 / PikR2 are shown to sense eukaryotic signaling molecules this might apply for all PAS4-LuxR solos in *P. luminescens*. In thermal unfolding experiments via nanoDSF the PAS4-LuxR solo Plu0919 showed thermal stabilization in presence of nematode homogenate. This indicated that Plu0919 senses a ligand from the *Heterorhabditis* nematode (Franziska Hildebrandt 2018). Moreover, *P. luminescens* interacts with plant roots (Regaiolo et al. 2020), which might secrete a signal sensed by another PAS4-LuxR solo of *P. luminescens*.

These are possible sources of signals sensed by PAS4-LuxR solos to uncover more of the inter-kingdom communication of *Photorhabdus*. To identify the signaling molecules a similar approach as described in this thesis could be performed. A reporter system would be developed by analysis of the regulated genes by the corresponding PAS4-LuxR receptor. Extracts of the homogenate of plant root and nematodes could be fractionated via HPLC to reduce the number molecules in each fraction until the signaling molecule is separated.

Furthermore, a fluorescence-based reporter assay could determine whether cooperative behavior is the case for the PAS4-LuxR solos in *P. luminescens*. A *P. luminescens* reporter strain could be generated with different genes encoding the fluorescent proteins under the control of promoters from different PAS4-LuxR solos. Another approach could be the labeling of PAS4-LuxR solos from different gene clusters with fluorescence tags. These labeled PAS4-LuxR solos could be detected via fluorescence microscopy. With this the population could be analyzed for heterogeneous production of PAS4-LuxR solos.

These are possible sources of signals sensed by PAS4-LuxR solos to uncover more of the inter-kingdom communication of *Photorhabdus*. To identify the signaling molecules a similar approach as described in this thesis could be performed. A reporter system would be developed by analysis of the regulated genes by the corresponding PAS4-LuxR receptor. Extracts of the homogenate of plant root and nematodes could be fractionated via HPLC to reduce the number molecules in each fraction until the signaling molecule is separated.

The transport of PPYD and DARs is facilitated by FadL and deletion mutants show decreased import of Qs signal molecules. Furthermore, the secondary metabolite production appeared to be altered in *P. luminescens* DJC *fadD* and *P. luminescens* DJC *fadL*. For investigation of the stilbene production and symbiosis activity a nematode bioassay (Eckstein et al. 2019) could be performed as well as an HPLC analysis of stilbene production in *P. luminescens* DJC *fadD* and *P. luminescens* DJC *fadL* mutants. This could reveal if FadD and FadL inhibition would also interact with the symbiosis of *Photorhabdus* with the nematodes.

Besides from the signaling molecule of PikR1 / PikR2 this work revealed the cytotoxic effect of some of the secondary metabolites produced by the entomopathogenic *Xenorhabdus* species, which have potential for further use in cancer treatment research. Xenocoumacin 2 and xenorhabdin were found to be potent apoptosis inducing secondary metabolites. In a follow up experiment the half maximal inhibitory concentration ( $IC_{50}$ ) of purified Xcn2 was determined via resazurin assay and determined an  $IC_{50}$  of 1-0.9 $\mu$ M after 96h of treatment (Anna Lena Weber 2020). In a similar assay the  $IC_{50}$  of purified xenorhabdin could be specified. Also the mechanism of apoptosis induction is proposed but not clarified yet. Caspases are crucial effector molecules in apoptosis (Olsson und Zhivotovsky 2011) and activation of intrinsic and/ or extrinsic caspases pathway is usually associated with current anticancer strategies

(Fulda und Debatin 2006). Therefore a calorimetric assay and a proteomic analysis via SDS Page and Western-blot could illustrate time-dependent caspase -3, -8 and -9 activation upon induction of SKOV-3 cells with xenorhabdin and xenocoumacin 2 (Rahman et al. 2016). For better implications of the secondary metabolites as putative drugs in cancer therapy the exact mechanisms for the apoptosis induction should be determined.

Mitotic arrest often results from inhibition of microtubule polymerization (Jordan und Wilson 2004), which is also suggested for xenocoumacin 2. The microtubule could be labeled via  $\beta$ -microtubule antibody and visualized with a second fluorescently labeled antibody, to verify the inhibition of microtubule polymerization by xenocoumacin 2. Furthermore inhibition of microtubule assembly holds cells in the mitotic phase (Mollinedo und Gajate 2003), which can be detected by flow cytometry (Lakshmanan und Batra 2013).

Xenorhabdin putatively inhibits the RNA-polymerase by interacting with the incorporation of RNA nucleosides as shown for the structurally cognate thiolutin (Jimenez et al. 1973; Tipper 1973). To detect the malfunction the activity of RNA polymerase could be detected with analysis of incorporation of uridine (Tipper 1973). Moreover *Photorhabdus* may still harbor yet unidentified molecules of synthesized by repressed genes (Kontnik et al. 2010; Reen et al. 2015) with vast opportunity in the health or agricultural sector (Regaiolo et al. 2020)

Overall, the complex lifecycle of the entomopathogens *Photorhabdus* and *Xenorhabdus* and the accompanying broad spectrum of secondary metabolites and signaling receptors harbor high potential for future research in the development of different novel drugs.

## 6 References

- Abu Samaan, Tala M.; Samec, Marek; Liskova, Alena; Kubatka, Peter; Büsselberg, Dietrich (2019): Paclitaxel's Mechanistic and Clinical Effects on Breast Cancer. In: *Biomolecules* 9 (12). DOI: 10.3390/biom9120789.
- Akers, Johnny C.; Gonda, David; Kim, Ryan; Carter, Bob S.; Chen, Clark C. (2013): Biogenesis of extracellular vesicles (EV): exosomes, microvesicles, retrovirus-like vesicles, and apoptotic bodies. In: *Journal of neuro-oncology*, S. 1–11. DOI: 10.1007/s11060-013-1084-8.
- Akhurst, R. J.; Boemare, N. E. (1988): A numerical taxonomic study of the genus *Xenorhabdus* (Enterobacteriaceae) and proposed elevation of the subspecies of *X. nematophilus* to species. In: *Journal of general microbiology* 134 (7), S. 1835–1845. DOI: 10.1099/00221287-134-7-1835.
- Altschul, Stephen F.; Gish, Warren; Miller, Webb; Myers, Eugene W.; Lipman, David J. (1990): Basic local alignment search tool. In: *Journal of molecular biology* 215 (3), S. 403–410. DOI: 10.1016/S0022-2836(05)80360-2.
- Anna Lena Weber (2020): Bacterial Secondary Metabolite Xenocoumacin 2 Induces Cell Death via the Apoptotic Pathway in Human Cancer Cell Lines. Master thesis. Ludwig-Maximilians-Universität München, Munich, LMU. Biozentrum.
- Arivudainambi, U. S.E. (2014): Cytotoxic and antibacterial activities of secondary metabolites from endophytic fungus *Pestalotiopsis virgatula* VN2. In: *CREAM* 4 (1), S. 107–115. DOI: 10.5943/cream/4/1/9.
- Ashok, M.; Turner, C.; Wilson, T. G. (1998): Insect juvenile hormone resistance gene homology with the bHLH-PAS family of transcriptional regulators. In: *Proceedings of the National Academy of Sciences of the United States of America* 95 (6), S. 2761–2766. DOI: 10.1073/pnas.95.6.2761.
- Assanga, Iloki (2013): Cell growth curves for different cell lines and their relationship with biological activities. In: *Int. J. Biotechnol. Mol. Biol. Res.* 4 (4), S. 60–70. DOI: 10.5897/IJBMBR2013.0154.
- Becker, Felix; Wienand, Karl; Lechner, Matthias; Frey, Erwin; Jung, Heinrich (2018): Interactions mediated by a public good transiently increase cooperativity in growing *Pseudomonas putida* metapopulations. In: *Scientific reports* 8 (1), S. 4093. DOI: 10.1038/s41598-018-22306-9.
- Black, P. N. (1988): The fadL gene product of *Escherichia coli* is an outer membrane protein required for uptake of long-chain fatty acids and involved in sensitivity to bacteriophage T2. In: *Journal of bacteriology* 170 (6), S. 2850–2854. DOI: 10.1128/jb.170.6.2850-2854.1988.

- Black, Paul N. (1990): Characterization of FadL-specific fatty acid binding in *Escherichia coli*. In: *Biochimica et Biophysica Acta (BBA) - Lipids and Lipid Metabolism* 1046 (1), S. 97–105. DOI: 10.1016/0005-2760(90)90099-j.
- Black, Paul N.; Ahowesso, Constance; Montefusco, David; Saini, Nipun; Dirusso, Concetta C. (2016): Fatty Acid Transport Proteins: Targeting FATP2 as a Gatekeeper Involved in the Transport of Exogenous Fatty Acids. In: *MedChemComm* 7 (4), S. 612–622. DOI: 10.1039/c6md00043f.
- Boddicker, Andrew M.; Mosier, Annika C. (2018): Genomic profiling of four cultivated *Candidatus Nitrotoga* spp. predicts broad metabolic potential and environmental distribution. In: *The ISME journal*, S. 2864–2882. DOI: 10.1038/s41396-018-0240-8.
- Bode, Edna; He, Yue; Vo, Tien Duy; Schultz, Roland; Kaiser, Marcel; Bode, Helge B. (2017): Biosynthesis and function of simple amides in *Xenorhabdus doucetiae*. In: *Environmental microbiology* 19 (11), S. 4564–4575. DOI: 10.1111/1462-2920.13919.
- Bode, Edna; Heinrich, Antje K.; Hirschmann, Merle; Abebew, Desalegne; Shi, Yan-Ni; Vo, Tien Duy et al. (2019): Promoter Activation in  $\Delta hfg$  Mutants as an Efficient Tool for Specialized Metabolite Production Enabling Direct Bioactivity Testing. In: *Angew. Chem.* 131 (52), S. 19133–19139. DOI: 10.1002/ange.201910563.
- Bode, Helge B. (2009): Entomopathogenic bacteria as a source of secondary metabolites. In: *Current opinion in chemical biology* 13 (2), S. 224–230. DOI: 10.1016/j.cbpa.2009.02.037.
- Boemare, N. E.; Akhurst, R. J.; Mourant, R. G. (1993): DNA Relatedness between *Xenorhabdus* spp. (Enterobacteriaceae), Symbiotic Bacteria of Entomopathogenic Nematodes, and a Proposal To Transfer *Xenorhabdus luminescens* to a New Genus, *Photorhabdus* gen. nov. In: *International journal of systematic bacteriology* 43 (2), S. 249–255. DOI: 10.1099/00207713-43-2-249.
- Bollag, D. M.; McQueney, P. A.; Zhu, J.; Hensens, O.; Koupal, L.; Liesch, J. et al. (1995): Epothilones, a new class of microtubule-stabilizing agents with a taxol-like mechanism of action. In: *Cancer research* 55 (11), S. 2325–2333.
- Boon, Calvin; Deng, Yinyue; Wang, Lian-Hui; He, Yawen; Xu, Jin-Ling; Fan, Yang et al. (2008): A novel DSF-like signal from *Burkholderia cenocepacia* interferes with *Candida albicans* morphological transition. In: *The ISME journal* 2 (1), S. 27–36. DOI: 10.1038/ismej.2007.76.
- Brachmann, Alexander O.; Brameyer, Sophie; Kresovic, Darko; Hitkova, Ivana; Kopp, Yannick; Manske, Christian et al. (2013): Pyrones as bacterial signaling molecules. In: *Nature chemical biology* 9 (9), S. 573–578. DOI: 10.1038/nchembio.1295.
- Brachmann, Alexander O.; Forst, Steven; Furgani, Ghazala M.; Fodor, Andras; Bode, Helge B. (2006): Xenofuranones A and B: phenylpyruvate dimers from *Xenorhabdus szentirmaii*. In: *Journal of natural products* 69 (12), S. 1830–1832. DOI: 10.1021/np060409n.

- Brachmann, Alexander O.; Joyce, Susan A.; Jenke-Kodama, Holger; Schwär, Gertrud; Clarke, David J.; Bode, Helge B. (2007): A type II polyketide synthase is responsible for anthraquinone biosynthesis in *Phototrhobdus luminescens*. In: *Chembiochem : a European journal of chemical biology* 8 (14), S. 1721–1728. DOI: 10.1002/cbic.200700300.
- Brameyer, Sophie (2015a): Cell-cell communication via LuxR solos in *Phototrhobdus* species. Ludwig-Maximilians-Universität München.
- Brameyer, Sophie; Bode, Helge B.; Heermann, Ralf (2015b): Languages and dialects: bacterial communication beyond homoserine lactones. In: *Trends in microbiology* 23 (9), S. 521–523. DOI: 10.1016/j.tim.2015.07.002.
- Brameyer, Sophie; Kresovic, Darko; Bode, Helge B.; Heermann, Ralf (2014): LuxR solos in *Phototrhobdus* species. In: *Frontiers in cellular and infection microbiology* 4, S. 166. DOI: 10.3389/fcimb.2014.00166.
- Brameyer, Sophie; Kresovic, Darko; Bode, Helge B.; Heermann, Ralf (2015c): Dialkylresorcinols as bacterial signaling molecules. In: *Proceedings of the National Academy of Sciences of the United States of America* 112 (2), S. 572–577. DOI: 10.1073/pnas.1417685112.
- Brehm et al. (2021): FadL contributes to the facilitation of *Phototrhobdus*-specific hydrophobic signaling molecules across the cell envelope. submitted. BMC microbiology.
- Bundesministerium für Lebensmittel und Landwirtschaft (2020): Leitsätze für Speisefette und Speiseöle. [https://www.bmel.de/SharedDocs/Downloads/DE/\\_Ernaehrung/Lebensmittel-Kennzeichnung/LeitsaetzeSpeisefette.pdf;jsessionid=9C41BA7AC39545D7C5B1BA A0DD66DE5C.internet2841?\\_\\_blob=publicationFile&v=3](https://www.bmel.de/SharedDocs/Downloads/DE/_Ernaehrung/Lebensmittel-Kennzeichnung/LeitsaetzeSpeisefette.pdf;jsessionid=9C41BA7AC39545D7C5B1BA A0DD66DE5C.internet2841?__blob=publicationFile&v=3). Unter Mitarbeit von Bundesministerium für Lebensmittel und Landwirtschaft. Hg. v. BAnz AT 18.08.2020 B3, GMBI 2020 S. 530.
- Chalabaev, Sabina; Turlin, Evelyne; Bay, Sylvie; Ganneau, Christelle; Brito-Fravallo, Emma; Charles, Jean-François et al. (2008): Cinnamic acid, an autoinducer of its own biosynthesis, is processed via Hca enzymes in *Phototrhobdus luminescens*. In: *Applied and environmental microbiology* 74 (6), S. 1717–1725. DOI: 10.1128/AEM.02589-07.
- Chan, Ying Ying; Bian, Hao Sheng; Tan, Theresa May Chin; Mattmann, Margrith E.; Geske, Grant D.; Igarashi, Jun et al. (2007): Control of quorum sensing by a *Burkholderia pseudomallei* multidrug efflux pump. In: *Journal of bacteriology* 189 (11), S. 4320–4324. DOI: 10.1128/JB.00003-07.
- Charles, Jean-Philippe; Iwema, Thomas; Epa, V. Chandana; Takaki, Keiko; Rynes, Jan; Jindra, Marek (2011): Ligand-binding properties of a juvenile hormone receptor, Methoprene-tolerant. In: *Proceedings of the National Academy of Sciences of the United States of America* 108 (52), S. 21128–21133. DOI: 10.1073/pnas.1116123109.

- Chippendale, G. M. (1970): Development of Artificial Diets for Rearing the Angoumois Grain Moth<sup>12</sup>. In: *Journal of Economic Entomology* 63 (3), S. 844–848. DOI: 10.1093/jee/63.3.844.
- Choi, S. H.; Greenberg, E. P. (1991): The C-terminal region of the *Vibrio fischeri* LuxR protein contains an inducer-independent lux gene activating domain. In: *Proceedings of the National Academy of Sciences of the United States of America* 88 (24), S. 11115–11119.
- Cibi, R.; Nair, A. Jayakumaran (2016): Purification of Actinomycin D from *Streptomyces parvulus* Isolated from Mangrove Ecosystem of Kerala, India. In: *Int.J.Curr.Microbiol.App.Sci* 5 (7), S. 461–467. DOI: 10.20546/ijcmas.2016.507.049.
- Ciche, Todd A.; Blackburn, Michael; Carney, John R.; Ensign, Jerald C. (2003): Photobactin: a catechol siderophore produced by *Photorhabdus luminescens*, an entomopathogen mutually associated with *Heterorhabditis bacteriophora* NC1 nematodes. In: *Applied and environmental microbiology* 69 (8), S. 4706–4713. DOI: 10.1128/AEM.69.8.4706–4713.2003.
- Ciche, Todd A.; Ensign, Jerald C. (2003): For the insect pathogen *Photorhabdus luminescens*, which end of a nematode is out? In: *Applied and environmental microbiology* 69 (4), S. 1890–1897. DOI: 10.1128/aem.69.4.1890-1897.2003.
- Clerc, Jérôme; Li, Nan; Krahn, Daniel; Groll, Michael; Bachmann, André S.; Florea, Bogdan I. et al. (2011): The natural product hybrid of Syringolin A and Glidobactin A synergizes proteasome inhibition potency with subsite selectivity. In: *Chemical communications (Cambridge, England)* 47 (1), S. 385–387. DOI: 10.1039/c0cc02238a.
- Coleman, M. L.; Sahai, E. A.; Yeo, M.; Bosch, M.; Dewar, A.; Olson, M. F. (2001): Membrane blebbing during apoptosis results from caspase-mediated activation of ROCK I. In: *Nature cell biology* 3 (4), S. 339–345. DOI: 10.1038/35070009.
- Coutinho, Bruna G.; Mevers, Emily; Schaefer, Amy L.; Pelletier, Dale A.; Harwood, Caroline S.; Clardy, Jon; Greenberg, E. Peter (2018): A plant-responsive bacterial-signaling system senses an ethanalamine derivative. In: *Proceedings of the National Academy of Sciences of the United States of America* 115 (39), S. 9785–9790. DOI: 10.1073/pnas.1809611115.
- Crawford, Jason M.; Kontnik, Renee; Clardy, Jon (2010): Regulating Alternative Lifestyles in Entomopathogenic Bacteria. In: *Current Biology* 20 (1), S. 69–74. DOI: 10.1016/j.cub.2009.10.059.
- Cremer, J.; Melbinger, A.; Wienand, K.; Henriquez, T.; Jung, H.; Frey, E. (2019): Cooperation in Microbial Populations: Theory and Experimental Model Systems. In: *Journal of molecular biology* 431 (23), S. 4599–4644. DOI: 10.1016/j.jmb.2019.09.023.

- Crooks, Gavin E.; Hon, Gary; Chandonia, John-Marc; Brenner, Steven E. (2004): WebLogo: a sequence logo generator. In: *Genome research* 14 (6), S. 1188–1190. DOI: 10.1101/gr.849004.
- Davis, Kimberly M. (2020): For the Greater (Bacterial) Good: Heterogeneous Expression of Energetically Costly Virulence Factors. In: *Infection and immunity* 88 (7). DOI: 10.1128/IAI.00911-19.
- Deng, Yinyue; Wu, Ji'en; Eberl, Leo; Zhang, Lian-Hui (2010): Structural and functional characterization of diffusible signal factor family quorum-sensing signals produced by members of the *Burkholderia cepacia* complex. In: *Applied and environmental microbiology* 76 (14), S. 4675–4683. DOI: 10.1128/AEM.00480-10.
- Derzelle, Sylviane; Duchaud, Eric; Kunst, Frank; Danchin, Antoine; Bertin, Philippe (2002): Identification, characterization, and regulation of a cluster of genes involved in carbapenem biosynthesis in *Photobacterium luminescens*. In: *Applied and environmental microbiology* 68 (8), S. 3780–3789. DOI: 10.1128/AEM.68.8.3780-3789.2002.
- Di Yu-Wei; Li, Zhuo-Sheng; Xiong, Shu-Min; Huang, Ge; Luo, Yan-Fei; Huo, Tie-Ying et al. (2020): Paclitaxel induces apoptosis through the TAK1-JNK activation pathway. In: *FEBS open bio*. DOI: 10.1002/2211-5463.12917.
- Diamond, Spencer; Andeer, Peter F.; Li, Zhou; Crits-Christoph, Alexander; Burstein, David; Anantharaman, Karthik et al. (2019): Mediterranean grassland soil C-N compound turnover is dependent on rainfall and depth, and is mediated by genomically divergent microorganisms. In: *Nature microbiology*, S. 1356–1367. DOI: 10.1038/s41564-019-0449-y.
- Dirusso, Concetta C.; Black, Paul N. (2004): Bacterial long chain fatty acid transport: gateway to a fatty acid-responsive signaling system. In: *The Journal of biological chemistry* 279 (48), S. 49563–49566. DOI: 10.1074/jbc.R400026200.
- Dreyer, Jönike; Malan, Antoinette P.; Dicks, Leon M. T. (2018): Bacteria of the Genus *Xenorhabdus*, a Novel Source of Bioactive Compounds. In: *Frontiers in microbiology* 9, S. 3177. DOI: 10.3389/fmicb.2018.03177.
- DSMZ. Hg. v. DSMZ-German Collection of Microorganisms and Cell Cultures GmbH.
- Dubrovsky, Edward B. (2005): Hormonal cross talk in insect development. In: *Trends in endocrinology and metabolism: TEM* 16 (1), S. 6–11. DOI: 10.1016/j.tem.2004.11.003.
- Duchaud, Eric; Rusniok, Christophe; Frangeul, Lionel; Buchrieser, Carmen; Givaudan, Alain; Taourit, Séad et al. (2003): The genome sequence of the entomopathogenic bacterium *Photobacterium luminescens*. In: *Nature biotechnology* 21 (11), S. 1307–1313. DOI: 10.1038/nbt886.
- Dudnik, Alexey; Bigler, Laurent; Dudler, Robert (2013): Heterologous expression of a *Photobacterium luminescens* syrbactin-like gene cluster results in production of the

potent proteasome inhibitor glidobactin A. In: *Microbiological research* 168 (2), S. 73–76. DOI: 10.1016/j.micres.2012.09.006.

Eberhard, Anatol (1972): Inhibition and Activation of Bacterial Luciferase Synthesis. In: *Journal of bacteriology* 109 (3), S. 1101–1105.

Eckstein, Simone; Dominelli, Nazzareno; Brachmann, Andreas; Heermann, Ralf (2019): Phenotypic Heterogeneity of the Insect Pathogen *Photorhabdus luminescens*: Insights into the Fate of Secondary Cells. In: *Applied and environmental microbiology*. DOI: 10.1128/AEM.01910-19.

Eckstein, Simone; Heermann, Ralf (2019): Regulation of Phenotypic Switching and Heterogeneity in *Photorhabdus luminescens* Cell Populations. In: *Journal of molecular biology* 431 (23), S. 4559–4568. DOI: 10.1016/j.jmb.2019.04.015.

Elmore, Susan (2007): Apoptosis: a review of programmed cell death. In: *Toxicologic pathology* 35 (4), S. 495–516. DOI: 10.1080/01926230701320337.

Epothilone (2008). In: George P. Rédei (Hg.): *Encyclopedia of Genetics, Genomics, Proteomics and Informatics*. Dordrecht: Springer Netherlands, S. 625.

Fairman, James W.; Noinaj, Nicholas; Buchanan, Susan K. (2011): The structural biology of  $\beta$ -barrel membrane proteins: a summary of recent reports. In: *Current opinion in structural biology* 21 (4), S. 523–531. DOI: 10.1016/j.sbi.2011.05.005.

Fala, Angela M.; Oliveira, Juliana F.; Adamoski, Douglas; Aricetti, Juliana A.; Dias, Marilia M.; Dias, Marcio V. B. et al. (2015): Unsaturated fatty acids as high-affinity ligands of the C-terminal Per-ARNT-Sim domain from the Hypoxia-inducible factor 3 $\alpha$ . In: *Scientific reports* 5, S. 12698. DOI: 10.1038/srep12698.

Fesik, Stephen W. (2005): Promoting apoptosis as a strategy for cancer drug discovery. In: *Nature reviews. Cancer* 5 (11), S. 876–885. DOI: 10.1038/nrc1736.

French-Constant, Richard; Waterfield, Nicholas; Daborn, Phillip; Joyce, Susan; Bennett, Helen; Au, Candy et al. (2003): *Photorhabdus*: towards a functional genomic analysis of a symbiont and pathogen. In: *FEMS microbiology reviews* 26 (5), S. 433–456. DOI: 10.1111/j.1574-6976.2003.tb00625.x.

French-Constant, Richard H. (2017): *The Molecular Biology of Photorhabdus Bacteria*. Cham: Springer International Publishing (402).

Finke, Mark D. (2015): Complete nutrient content of four species of commercially available feeder insects fed enhanced diets during growth. In: *Zoo biology* 34 (6), S. 554–564. DOI: 10.1002/zoo.21246.

Finn, Robert D.; Mistry, Jaina; Schuster-Böckler, Benjamin; Griffiths-Jones, Sam; Hollich, Volker; Lassmann, Timo et al. (2006): Pfam: clans, web tools and services. In: *Nucleic acids research* 34 (Database issue), D247-51. DOI: 10.1093/nar/gkj149.

Fischer-Le Saux, M.; Viallard, V.; Brunel, B.; Normand, P.; Boemare, N. E. (1999): Polyphasic classification of the genus *Photorhabdus* and proposal of new taxa: *P. luminescens* subsp. *luminescens* subsp. nov., *P. luminescens* subsp. *akhurstii* subsp.

nov., *P. luminescens* subsp. *laumondii* subsp. nov., *P. temperata* sp. nov., *P. temperata* subsp. *temperata* subsp. nov. and *P. asymbiotica* sp. nov. In: *International journal of systematic bacteriology* 49 Pt 4, S. 1645–1656. DOI: 10.1099/00207713-49-4-1645.

Flavier, A. B.; Clough, S. J.; Schell, M. A.; Denny, T. P. (1997): Identification of 3-hydroxypalmitic acid methyl ester as a novel autoregulator controlling virulence in *Ralstonia solanacearum*. In: *Molecular microbiology* 26 (2), S. 251–259. DOI: 10.1046/j.1365-2958.1997.5661945.x.

Fleming, Alexander (1929): On the Antibacterial Action of Cultures of a *Penicillium*, with Special Reference to their Use in the Isolation of *B. influenzae*. In: *British journal of experimental pathology* 10 (3), S. 226–236.

Forst, S.; Clarke, D. (2002): Bacteria-nematode symbiosis. In: R. Gaugler (Hg.): *Entomopathogenic nematology*. Wallingford: CABI, S. 57–77.

Forst, S.; Dowds, B.; Boemare, N.; Stackebrandt, E. (1997): *Xenorhabdus* and *Photorhabdus* spp.: bugs that kill bugs. In: *Annu. Rev. Microbiol.* 51, S. 47–72. DOI: 10.1146/annurev.micro.51.1.47.

Franziska Hildebrandt (2018): The PAS4-LuxR solo Plu0919 of *P. luminescens* senses a *H. bacteriophora* nematode specific ligand. Masterarbeit. Ludwig-Maximilians-Universität München, Munich, LMU. Mikrobiologie.

Fuchs, Sebastian W.; Grundmann, Florian; Kurz, Michael; Kaiser, Marcel; Bode, Helge B. (2014): Fabclavines: bioactive peptide-polyketide-polyamino hybrids from *Xenorhabdus*. In: *ChemBiochem : a European journal of chemical biology* 15 (4), S. 512–516. DOI: 10.1002/cbic.201300802.

Fulda, S.; Debatin, K-M (2006): Extrinsic versus intrinsic apoptosis pathways in anticancer chemotherapy. In: *Oncogene* 25 (34), S. 4798–4811. DOI: 10.1038/sj.onc.1209608.

Fuqua, W. C.; Winans, S. C. (1994): A LuxR-LuxI type regulatory system activates *Agrobacterium* Ti plasmid conjugal transfer in the presence of a plant tumor metabolite. In: *Journal of bacteriology* 176 (10), S. 2796–2806. DOI: 10.1128/jb.176.10.2796-2806.1994.

Gaugler, R. (Hg.) (2002): *Entomopathogenic nematology*. Wallingford: CABI.

Gelman, Julia S.; Sironi, Juan; Berezniuk, Iryna; Dasgupta, Sayani; Castro, Leandro M.; Gozzo, Fabio C. et al. (2013): Alterations of the intracellular peptidome in response to the proteasome inhibitor bortezomib. In: *PLoS ONE*, e53263. DOI: 10.1371/journal.pone.0053263.

Gerrard, John G.; Joyce, Susan A.; Clarke, David J.; French-Constant, Richard H.; Nimmo, Graeme R.; Looke, David F. M. et al. (2006): Nematode symbiont for *Photorhabdus asymbiotica*. In: *Emerging infectious diseases* 12 (10), S. 1562–1564. DOI: 10.3201/eid1210.060464.

- Gerrard, John G.; McNevin, Samantha; Alfredson, David; Forgan-Smith, Ross; Fraser, Neil (2003a): *Photorhabdus* species: bioluminescent bacteria as emerging human pathogens? In: *Emerging infectious diseases* 9 (2), S. 251–254. DOI: 10.3201/eid0902.020222.
- Gerrard, John G.; Vohra, Renu; Nimmo, Graeme R. (2003b): Identification of *Photorhabdus asymbiotica* in cases of human infection. In: *Communicable diseases intelligence quarterly report* 27 (4), S. 540–541.
- Gey et al. (1952): Tissue culture studies of the proliferative capacity of cervical carcinoma and normal epithelium. In: *Cancer research* 12 (12(1)), S. 264–265.
- Gilson, L.; Kuo, A.; Dunlap, P. V. (1995): AinS and a new family of autoinducer synthesis proteins. In: *Journal of bacteriology* 177 (23), S. 6946–6951. DOI: 10.1128/jb.177.23.6946-6951.1995.
- Goodrich-Blair, Heidi; Clarke, David J. (2007): Mutualism and pathogenesis in *Xenorhabdus* and *Photorhabdus*: two roads to the same destination. In: *Molecular microbiology* 64 (2), S. 260–268. DOI: 10.1111/j.1365-2958.2007.05671.x.
- Grandori, R.; Khalifah, P.; Boice, J. A.; Fairman, R.; Giovanielli, K.; Carey, J. (1998): Biochemical characterization of WrbA, founding member of a new family of multimeric flavodoxin-like proteins. In: *The Journal of biological chemistry* 273 (33), S. 20960–20966. DOI: 10.1074/jbc.273.33.20960.
- Guzman, L. M.; Belin, D.; Carson, M. J.; Beckwith, J. (1995): Tight regulation, modulation, and high-level expression by vectors containing the arabinose PBAD promoter. In: *Journal of bacteriology* 177 (14), S. 4121–4130. DOI: 10.1128/jb.177.14.4121-4130.1995.
- HAMPL, Veronika; Wetzels, Isolde; Bracher, Franz; Krauss, Jürgen (2011): New substituted isocoumarins and Dihydroisocoumarins and their cytotoxic activities. In: *Scientia pharmaceutica*, S. 21–30. DOI: 10.3797/scipharm.1011-10.
- Handa, Noriko; Terada, Takaho; Doi-Katayama, Yukiko; Hirota, Hiroshi; Tame, Jeremy R. H.; Park, Sam-Yong et al. (2005): Crystal structure of a novel polyisoprenoid-binding protein from *Thermus thermophilus* HB8. In: *Protein science : a publication of the Protein Society*, S. 1004–1010. DOI: 10.1110/ps.041183305.
- Hanzelka, B. L.; Greenberg, E. P. (1995): Evidence that the N-terminal region of the *Vibrio fischeri* LuxR protein constitutes an autoinducer-binding domain. In: *Journal of bacteriology* 177 (3), S. 815–817.
- Harding, Clare R.; Schroeder, Gunnar N.; Collins, James W.; Frankel, Gad (2013): Use of *Galleria mellonella* as a model organism to study *Legionella pneumophila* infection. In: *Journal of visualized experiments : JoVE* (81), e50964. DOI: 10.3791/50964.
- Hawver, Lisa A.; Jung, Sarah A.; Ng, Wai-Leung (2016): Specificity and complexity in bacterial quorum-sensing systems. In: *FEMS microbiology reviews* 40 (5), S. 738–752. DOI: 10.1093/femsre/fuw014.

Hearn, Elizabeth M.; Patel, Dimki R.; Lepore, Bryan W.; Indic, Mridhu; van den Berg, Bert (2009): Transmembrane passage of hydrophobic compounds through a protein channel wall. In: *Nature* 458 (7236), S. 367–370. DOI: 10.1038/nature07678.

Heermann, Ralf; Fuchs, Thilo M. (2008): Comparative analysis of the *Photorhabdus luminescens* and the *Yersinia enterocolitica* genomes: uncovering candidate genes involved in insect pathogenicity. In: *BMC Genomics* 9, S. 40. DOI: 10.1186/1471-2164-9-40.

Hefti, Marco H.; François, Kees-Jan; Vries, Sacco C. de; Dixon, Ray; Vervoort, Jacques (2004): The PAS fold. A redefinition of the PAS domain based upon structural prediction. In: *European journal of biochemistry* 271 (6), S. 1198–1208. DOI: 10.1111/j.1432-1033.2004.04023.x.

Henry, Jonathan T.; Crosson, Sean (2011): Ligand-Binding PAS Domains in a Genomic, Cellular, and Structural Context. In: *Annu. Rev. Microbiol.* 65 (1), S. 261–286. DOI: 10.1146/annurev-micro-121809-151631.

Hoffman, E. C.; Reyes, H.; Chu, F. F.; Sander, F.; Conley, L. H.; Brooks, B. A.; Hankinson, O. (1991): Cloning of a factor required for activity of the Ah (dioxin) receptor. In: *Science (New York, N.Y.)* 252 (5008), S. 954–958. DOI: 10.1126/science.1852076.

Höfle, Gerhard; Bedorf, Norbert; Steinmetz, Heinrich; Schomburg, Dietmar; Gerth, Klaus; Reichenbach, Hans (1996): Epothilon A und B – neuartige, 16gliedrige Makrolide mit cytotoxischer Wirkung: Isolierung, Struktur im Kristall und Konformation in Lösung. In: *Angew. Chem.* 108 (13-14), S. 1671–1673. DOI: 10.1002/ange.19961081342.

Hou, Jian; Sun, E.; Zhang, Zhen-Hai; Wang, Jing; Yang, Lei; Cui, Li et al. (2017): Improved oral absorption and anti-lung cancer activity of paclitaxel-loaded mixed micelles. In: *Drug delivery* 24 (1), S. 261–269. DOI: 10.1080/10717544.2016.1245370.

Hu, K. (2000): Antibiotic production in relation to bacterial growth and nematode development in *Photorhabdus–Heterorhabditis* infected *Galleria mellonella* larvae. In: *FEMS microbiology letters* 189 (2), S. 219–223. DOI: 10.1016/S0378-1097(00)00288-3.

Hu, Kaiji; Li, Jianxiong; Li, Bin; Webster, John M.; Chen, Genhui (2006): A novel antimicrobial epoxide isolated from larval *Galleria mellonella* infected by the nematode symbiont, *Photorhabdus luminescens* (Enterobacteriaceae). In: *Bioorganic & medicinal chemistry* 14 (13), S. 4677–4681. DOI: 10.1016/j.bmc.2006.01.025.

Hughes, David T.; Sperandio, Vanessa (2008): Inter-kingdom signalling: communication between bacteria and their hosts. In: *Nature reviews. Microbiology* 6 (2), S. 111–120. DOI: 10.1038/nrmicro1836.

Jensen, K. F. (1993): The *Escherichia coli* K-12 "wild types" W3110 and MG1655 have an rph frameshift mutation that leads to pyrimidine starvation due to low pyrE

expression levels. In: *Journal of bacteriology* 175 (11), S. 3401–3407. DOI: 10.1128/jb.175.11.3401-3407.1993.

Ji, Quanjiang; Chen, Peter J.; Qin, Guangrong; Deng, Xin; Hao, Ziyang; Wawrzak, Zdzislaw et al. (2016): Structure and mechanism of the essential two-component signal-transduction system WalkR in *Staphylococcus aureus*. In: *Nature communications* 7, S. 11000. DOI: 10.1038/ncomms11000.

Jimenez, A.; Tipper, D. J.; Davies, J. (1973): Mode of Action of Thiolutin, an Inhibitor of Macromolecular Synthesis in *Saccharomyces cerevisiae*. In: *Antimicrobial Agents and Chemotherapy* 3 (6), S. 729–738. DOI: 10.1128/aac.3.6.729.

Jimenez-Diaz, L.; Caballero, A.; Segura, A. (2017): Pathways for the Degradation of Fatty Acids in Bacteria. In: Fernando Rojo (Hg.): *Aerobic Utilization of Hydrocarbons, Oils and Lipids*. Cham: Springer International Publishing, S. 1–23.

Jordan, Mary Ann; Wilson, Leslie (2004): Microtubules as a target for anticancer drugs. In: *Nature reviews. Cancer* 4 (4), S. 253–265. DOI: 10.1038/nrc1317.

Joyce, Susan A.; Brachmann, Alexander O.; Glazer, Itamar; Lango, Lea; Schwär, Gertrud; Clarke, David J.; Bode, Helge B. (2008): Bacterial biosynthesis of a multipotent stilbene. In: *Angewandte Chemie (International ed. in English)* 47 (10), S. 1942–1945. DOI: 10.1002/anie.200705148.

Kai, Kenji; Ohnishi, Hideyuki; Shimatani, Mika; Ishikawa, Shiho; Mori, Yuka; Kiba, Akinori et al. (2015): Methyl 3-Hydroxymyristate, a Diffusible Signal Mediating phc Quorum Sensing in *Ralstonia solanacearum*. In: *Chembiochem : a European journal of chemical biology* 16 (16), S. 2309–2318. DOI: 10.1002/cbic.201500456.

Kamp, F.; Zakim, D.; Zhang, F.; Noy, N.; Hamilton, J. A. (1995): Fatty acid flip-flop in phospholipid bilayers is extremely fast. In: *Biochemistry* 34 (37), S. 11928–11937. DOI: 10.1021/bi00037a034.

Kang, Yun; Zarzycki-Siek, Jan; Walton, Chad B.; Norris, Michael H.; Hoang, Tung T. (2010): Multiple FadD acyl-CoA synthetases contribute to differential fatty acid degradation and virulence in *Pseudomonas aeruginosa*. In: *PLoS ONE* 5 (10), e13557. DOI: 10.1371/journal.pone.0013557.

Kasper, Marc-André; Stengl, Andreas; Ochtrop, Philipp; Gerlach, Marcus; Stoschek, Tina; Schumacher, Dominik et al. (2019): Ethynylphosphonamidates for the Rapid and Cysteine-Selective Generation of Efficacious Antibody–Drug Conjugates. In: *Angew. Chem.* 131 (34), S. 11757–11762. DOI: 10.1002/ange.201904193.

Kawano, Takeshi; Agata, Naoki; Kharbanda, Surender; Avigan, David; Kufe, Donald (2007): A novel isocoumarin derivative induces mitotic phase arrest and apoptosis of human multiple myeloma cells. In: *Cancer chemotherapy and pharmacology* 59 (3), S. 329–335. DOI: 10.1007/s00280-006-0274-x.

Kelley, Lawrence A.; Mezulis, Stefans; Yates, Christopher M.; Wass, Mark N.; Sternberg, Michael J. E. (2015): The Phyre2 web portal for protein modeling,

prediction and analysis. In: *Nature protocols* 10 (6), S. 845–858. DOI: 10.1038/nprot.2015.053.

Kerr, J. F.; Wyllie, A. H.; Currie, A. R. (1972): Apoptosis: a basic biological phenomenon with wide-ranging implications in tissue kinetics. In: *British journal of cancer* 26 (4), S. 239–257. DOI: 10.1038/bjc.1972.33.

Kimatu, Josphert Ngui (Hg.) (2018): *Advances in Plant Pathology*: InTech.

King, K. L.; Cidlowski, J. A. (1998): Cell cycle regulation and apoptosis. In: *Annual review of physiology* 60, S. 601–617. DOI: 10.1146/annurev.physiol.60.1.601.

Kiratisin, Pattarachai; Tucker, Kenneth D.; Passador, Luciano (2002): LasR, a transcriptional activator of *Pseudomonas aeruginosa* virulence genes, functions as a multimer. In: *Journal of bacteriology* 184 (17), S. 4912–4919. DOI: 10.1128/JB.184.17.4912-4919.2002.

Koiso, Yukiko; Morita, Koji; Kobayashi, Motomasa; Wang, Weiqi; Ohyabu, Naoki; Iwasaki, Shigeo (1996): Effects of arenastatin A and its synthetic analogs on microtubule assembly. In: *Chemico-Biological Interactions* 102 (3), S. 183–191. DOI: 10.1016/s0009-2797(96)03743-x.

Kolibachuk, D.; Greenberg, E. P. (1993): The *Vibrio fischeri* luminescence gene activator LuxR is a membrane-associated protein. In: *Journal of bacteriology* 175 (22), S. 7307–7312. DOI: 10.1128/jb.175.22.7307-7312.1993.

Kontnik, Renee; Crawford, Jason M.; Clardy, Jon (2010): Exploiting a global regulator for small molecule discovery in *Photobacterium luminescens*. In: *ACS chemical biology* 5 (7), S. 659–665. DOI: 10.1021/cb100117k.

Kouřimská, Lenka; Adámková, Anna (2016): Nutritional and sensory quality of edible insects. In: *NFS Journal* 4, S. 22–26. DOI: 10.1016/j.nfs.2016.07.001.

Kresovic, Darko; Schempp, Florence; Cheikh-Ali, Zakaria; Bode, Helge B. (2015): A novel and widespread class of ketosynthase is responsible for the head-to-head condensation of two acyl moieties in bacterial pyrone biosynthesis. In: *Beilstein journal of organic chemistry* 11, S. 1412–1417. DOI: 10.3762/bjoc.11.152.

Krin, Evelyne; Chakroun, Nesrine; Turlin, Evelyne; Givaudan, Alain; Gaboriau, François; Bonne, Isabelle et al. (2006): Pleiotropic role of quorum-sensing autoinducer 2 in *Photobacterium luminescens*. In: *Applied and environmental microbiology* 72 (10), S. 6439–6451. DOI: 10.1128/AEM.00398-06.

Krol, Elizaveta; Becker, Anke (2014): Rhizobial homologs of the fatty acid transporter FadL facilitate perception of long-chain acyl-homoserine lactone signals. In: *Proceedings of the National Academy of Sciences of the United States of America* 111 (29), S. 10702–10707. DOI: 10.1073/pnas.1404929111.

Kuzlik (2016): PAS4-LuxR-Solos zur "Inter-kingdom"-Kommunikation in *Photobacterium luminescens*. Saskia Kuzlik. Bachelorarbeit. Ludwig-Maximilians-Universität München, München. Mikrobiologie.

- Kwadha, Charles A.; Ong'amo, George O.; Ndegwa, Paul N.; Raina, Suresh K.; Fombong, Ayuka T. (2017): The Biology and Control of the Greater Wax Moth, *Galleria mellonella*. In: *Insects* 8 (2). DOI: 10.3390/insects8020061.
- Lady, Lovely (2021): Beekeepers: Beware of Wax Moths. Online verfügbar unter <https://owlcation.com/stem/Beekeepers-Beware-of-Wax-Moths>, zuletzt aktualisiert am 05.02.2021, zuletzt geprüft am 05.02.2021.
- Lakshmanan, Imayavaramban; Batra, Surinder K. (2013): Protocol for Apoptosis Assay by Flow Cytometry Using Annexin V Staining Method. In: *Bio-protocol* 3 (6).
- Lassak, Jürgen; Henche, Anna-Lena; Binnenkade, Lucas; Thormann, Kai M. (2010): ArcS, the cognate sensor kinase in an atypical Arc system of *Shewanella oneidensis* MR-1. In: *Applied and environmental microbiology* 76 (10), S. 3263–3274. DOI: 10.1128/AEM.00512-10.
- Lengyel, Katalin; Lang, Elke; Fodor, András; Szállás, Emilia; Schumann, Peter; Stackebrandt, Erko (2005): Description of four novel species of *Xenorhabdus*, family Enterobacteriaceae: *Xenorhabdus budapestensis* sp. nov., *Xenorhabdus ehlersii* sp. nov., *Xenorhabdus innexi* sp. nov., and *Xenorhabdus szentirmaii* sp. nov. In: *Systematic and applied microbiology* 28 (2), S. 115–122. DOI: 10.1016/j.syapm.2004.10.004.
- Liu, Hai-Bo; Kim, Jung Sun; Park, Sunghoon (2011): Development and comparison of whole-cell assay systems for quorum-sensing inhibitors based on TraR, LasR, and QscR. In: *Journal of biomolecular screening* 16 (9), S. 986–994. DOI: 10.1177/1087057111416656.
- Liu, Hai-Bo; Lee, Joon-Hee; Kim, Jung Sun; Park, Sunghoon (2010): Inhibitors of the *Pseudomonas aeruginosa* quorum-sensing regulator, QscR. In: *Biotechnology and bioengineering* 106 (1), S. 119–126. DOI: 10.1002/bit.22672.
- M. Mori et al. (1988): Structure of cCF10, a peptide sex pheromone which induces conjugative transfer of the *Streptococcus faecalis* tetracycline resistance plasmid, pCF10. In: *Journal of Biological Chemistry* 263 (28), S. 14574–14578.
- Machado, Ricardo A. R.; Wüthrich, Daniel; Kuhnert, Peter; Arce, Carla C. M.; Thönen, Lisa; Ruiz, Celia et al. (2018): Whole-genome-based revisit of *Photorhabdus phylogeny*: proposal for the elevation of most *Photorhabdus subspecies* to the species level and description of one novel species *Photorhabdus bodei* sp. nov., and one novel subspecies *Photorhabdus laumondii* subsp. *clarkei* subsp. nov. In: *International journal of systematic and evolutionary microbiology* 68 (8), S. 2664–2681. DOI: 10.1099/ijsem.0.002820.
- Magnuson, Roy; Solomon, Jonathan; Grossman, Alan D. (1994): Biochemical and genetic characterization of a competence pheromone from *B. subtilis*. In: *Cell* 77 (2), S. 207–216. DOI: 10.1016/0092-8674(94)90313-1.
- Maldonado, Antonio; Jiménez-Díaz, Rufino; Ruiz-Barba, José Luis (2004): Induction of Plantaricin Production in *Lactobacillus plantarum* NC8 after Coculture with Specific

Gram-Positive Bacteria Is Mediated by an Autoinduction Mechanism. In: *Journal of bacteriology* 186 (5), S. 1556–1564. DOI: 10.1128/JB.186.5.1556-1564.2004.

Maneesakorn, Patchareewan; An, Ruisheng; Daneshvar, Hannah; Taylor, Kara; Bai, Xiaodong; Adams, Byron J. et al. (2011): Phylogenetic and cophylogenetic relationships of entomopathogenic nematodes (*Heterorhabditis*: Rhabditida) and their symbiotic bacteria (*Photorhabdus*: Enterobacteriaceae). In: *Molecular phylogenetics and evolution* 59 (2), S. 271–280. DOI: 10.1016/j.ympev.2011.02.012.

Manske, Christian (2011): Endogene und exogene Signalwahrnehmung über die LuxR-Solos Plu4562 und Plu2018/Plu2019 bei *Photorhabdus luminescens*. Diploma thesis. Ludwig-Maximilians-Universität München, München. Biologie.

Marketon, Melanie M.; Gronquist, Matthew R.; Eberhard, Anatol; González, Juan E. (2002): Characterization of the *Sinorhizobium meliloti* sinR/sinI locus and the production of novel N-acyl homoserine lactones. In: *Journal of bacteriology* 184 (20), S. 5686–5695. DOI: 10.1128/JB.184.20.5686–5695.2002.

Martens, Eric C.; Heungens, Kurt; Goodrich-Blair, Heidi (2003): Early colonization events in the mutualistic association between *Steinernema carpocapsae* nematodes and *Xenorhabdus nematophila* bacteria. In: *Journal of bacteriology* 185 (10), S. 3147–3154. DOI: 10.1128/jb.185.10.3147-3154.2003.

McCann (2007): Pupa - Galleria mellonella. Unter Mitarbeit von Sean McCann. Hg. v. BugGuide. Online verfügbar unter <https://bugguide.net/node/view/103781>, zuletzt aktualisiert am 05.02.2021, zuletzt geprüft am 05.02.2021.

McInerney, B. V.; Taylor, W. C.; Lacey, M. J.; Akhurst, R. J.; Gregson, R. P. (1991): Biologically active metabolites from *Xenorhabdus* spp., Part 2. Benzopyran-1-one derivatives with gastroprotective activity. In: *Journal of natural products* 54 (3), S. 785–795. DOI: 10.1021/np50075a006.

Medina, Gerardo; Juárez, Katy; Valderrama, Brenda; Soberón-Chávez, Gloria (2003): Mechanism of *Pseudomonas aeruginosa* RhlR transcriptional regulation of the rhlAB promoter. In: *Journal of bacteriology* 185 (20), S. 5976–5983. DOI: 10.1128/JB.185.20.5976-5983.2003.

Merkel, O.; Wacht, N.; Sifft, E.; Melchardt, T.; Hamacher, F.; Kocher, T. et al. (2012): Actinomycin D induces p53-independent cell death and prolongs survival in high-risk chronic lymphocytic leukemia. In: *Leukemia* 26 (12), S. 2508–2516. DOI: 10.1038/leu.2012.147.

Meyer, Andrea; Megerle, Judith A.; Kuttler, Christina; Müller, Johannes; Aguilar, Claudio; Eberl, Leo et al. (2012): Dynamics of AHL mediated quorum sensing under flow and non-flow conditions. In: *Physical biology* 9 (2), S. 26007. DOI: 10.1088/1478-3975/9/2/026007.

Minogue, T. D. (2005): The cell density-dependent expression of stewartan exopolysaccharide in *Pantoea stewartii* ssp. *stewartii* is a function of EsaR-mediated

repression of the *rcaA* gene. In: *Mol. Microbiol.* 2005 (56), S. 189–203. Online verfügbar unter doi:10.1111/j.1365-2958.2005.04529.x.

Mlcek, Jiri; Rop, Otakar; Borkovcova, Marie; Bednarova, Martina (2014): A Comprehensive Look at the Possibilities of Edible Insects as Food in Europe – A Review. In: *Pol. J. Food Nutr. Sci.* 64 (3), S. 147–157. DOI: 10.2478/v10222-012-0099-8.

Möglich, Andreas; Ayers, Rebecca A.; Moffat, Keith (2009): Structure and signaling mechanism of Per-ARNT-Sim domains. In: *Structure (London, England : 1993)* 17 (10), S. 1282–1294. DOI: 10.1016/j.str.2009.08.011.

Mollinedo, F.; Gajate, C. (2003): Microtubules, microtubule-interfering agents and apoptosis. In: *Apoptosis : an international journal on programmed cell death* 8 (5), S. 413–450. DOI: 10.1023/a:1025513106330.

Molloy, Evelyn M.; Hertweck, Christian (2017): Antimicrobial discovery inspired by ecological interactions. In: *Current opinion in microbiology* 39, S. 121–127. DOI: 10.1016/j.mib.2017.09.006.

Morita, K.; Koiso, Y.; Hashimoto, Y.; Kobayashi, M.; Wang, W.; Ohyabu, N.; Iwasaki, S. (1997): Interaction of arenastatin A with porcine brain tubulin. In: *Biological & pharmaceutical bulletin* 20 (2), S. 171–174. DOI: 10.1248/bpb.20.171.

Mowlds, Peter; Barron, Aoife; Kavanagh, Kevin (2008): Physical stress primes the immune response of *Galleria mellonella* larvae to infection by *Candida albicans*. In: *Microbes and infection* 10 (6), S. 628–634. DOI: 10.1016/j.micinf.2008.02.011.

Mowlds, Peter; Kavanagh, Kevin (2008): Effect of pre-incubation temperature on susceptibility of *Galleria mellonella* larvae to infection by *Candida albicans*. In: *Mycopathologia* 165 (1), S. 5–12. DOI: 10.1007/s11046-007-9069-9.

Nambu, John R.; Lewis, Josephine O.; Wharton, Keith A.; Crews, Stephen T. (1991): The *Drosophila* single-minded gene encodes a helix-loop-helix protein that acts as a master regulator of CNS midline development. In: *Cell* 67 (6), S. 1157–1167. DOI: 10.1016/0092-8674(91)90292-7.

Nealson, K. H.; Hastings, J. W. (1979): Bacterial bioluminescence: its control and ecological significance. In: *Microbiological Reviews* 43 (4), S. 496–518.

Nealson, K. H.; Platt, T.; Hastings, J. W. (1970): Cellular control of the synthesis and activity of the bacterial luminescent system. In: *Journal of bacteriology* 104 (1), S. 313–322. DOI: 10.1128/jb.104.1.313-322.1970.

Newman, David J.; Cragg, Gordon M. (2020): Natural Products as Sources of New Drugs over the Nearly Four Decades from 01/1981 to 09/2019. In: *Journal of natural products* 83 (3), S. 770–803. DOI: 10.1021/acs.jnatprod.9b01285.

Niculescu-Duvaz, Ion (2010): Trastuzumab emtansine, an antibody-drug conjugate for the treatment of HER2+ metastatic breast cancer. In: *Current opinion in molecular therapeutics* 12 (3), S. 350–360.

Nollmann, Friederike I.; Dauth, Christina; Mulley, Geraldine; Kegler, Carsten; Kaiser, Marcel; Waterfield, Nick R.; Bode, Helge B. (2015): Insect-specific production of new GameXPeptides in *Photorhabdus luminescens* TTO1, widespread natural products in entomopathogenic bacteria. In: *Chembiochem : a European journal of chemical biology* 16 (2), S. 205–208. DOI: 10.1002/cbic.201402603.

Nunn, W. D.; Colburn, R. W.; Black, P. N. (1986): Transport of long-chain fatty acids in *Escherichia coli*. Evidence for role of fadL gene product as long-chain fatty acid receptor. In: *The Journal of biological chemistry* 261 (1), S. 167–171.

Oberhammer, F. A.; Hochegger, K.; Fröschl, G.; Tiefenbacher, R.; Pavelka, M. (1994): Chromatin condensation during apoptosis is accompanied by degradation of lamin A+B, without enhanced activation of cdc2 kinase. In: *The Journal of Cell Biology* 126 (4), S. 827–837. DOI: 10.1083/jcb.126.4.827.

Oinuma, Ken-Ichi; Greenberg, E. Peter (2011): Acyl-homoserine lactone binding to and stability of the orphan *Pseudomonas aeruginosa* quorum-sensing signal receptor QscR. In: *Journal of bacteriology* 193 (2), S. 421–428. DOI: 10.1128/JB.01041-10.

Oka, M.; Yaginuma, K.; Numata, K.; Konishi, M.; Oki, T.; Kawaguchi, H. (1988): Glidobactins A, B and C, new antitumor antibiotics. II. Structure elucidation. In: *The Journal of antibiotics* 41 (10), S. 1338–1350. DOI: 10.7164/antibiotics.41.1338.

Olsson, M.; Zhivotovsky, B. (2011): Caspases and cancer. In: *Cell death and differentiation* 18 (9), S. 1441–1449. DOI: 10.1038/cdd.2011.30.

O'Neill, Alexander; Oliva, Brunello; Storey, Christopher; Hoyle, Anthony; Fishwick, Colin; Chopra, Ian (2000): RNA Polymerase Inhibitors with Activity against Rifampin-Resistant Mutants of *Staphylococcus aureus*. In: *Antimicrob. Agents Chemother.* 44 (11), S. 3163–3166. DOI: 10.1128/aac.44.11.3163-3166.2000.

Orozco, Rousel A.; Molnár, István; Bode, Helge; Stock, S. Patricia (2016): Bioprospecting for secondary metabolites in the entomopathogenic bacterium *Photorhabdus luminescens* subsp. *sonorensis*. In: *Journal of Invertebrate Pathology* 141, S. 45–52. DOI: 10.1016/j.jip.2016.09.008.

Pacheco, Aline R.; Sperandio, Vanessa (2009): Inter-kingdom signaling: chemical language between bacteria and host. In: *Current opinion in microbiology* 12 (2), S. 192–198. DOI: 10.1016/j.mib.2009.01.006.

Pan, Zhi; Avila, Andrew; Gollahon, Lauren (2014): Paclitaxel induces apoptosis in breast cancer cells through different calcium--regulating mechanisms depending on external calcium conditions. In: *International journal of molecular sciences* 15 (2), S. 2672–2694. DOI: 10.3390/ijms15022672.

Papenfort, Kai; Silpe, Justin E.; Schramma, Kelsey R.; Cong, Jian-Ping; Seyedsayamdost, Mohammad R.; Bassler, Bonnie L. (2017): A *Vibrio cholerae* autoinducer-receptor pair that controls biofilm formation. In: *Nature chemical biology* 13 (5), S. 551–557. DOI: 10.1038/nchembio.2336.

- Park, Dongjin; Ciezki, Kristin; van der Hoeven, Ransome; Singh, Swati; Reimer, Daniela; Bode, Helge B.; Forst, Steven (2009): Genetic analysis of xenocoumacin antibiotic production in the mutualistic bacterium *Xenorhabdus nematophila*. In: *Molecular microbiology* 73 (5), S. 938–949. DOI: 10.1111/j.1365-2958.2009.06817.x.
- Park, Hyun Bong; Sampathkumar, Parthasarathy; Perez, Corey E.; Lee, Joon Ha; Tran, Jeannie; Bonanno, Jeffrey B. et al. (2017): Stilbene epoxidation and detoxification in a *Photorhabdus luminescens*-nematode symbiosis. In: *The Journal of biological chemistry*, S. 6680–6694. DOI: 10.1074/jbc.M116.762542.
- Patankar, Arati V.; González, Juan E. (2009): Orphan LuxR regulators of quorum sensing. In: *FEMS microbiology reviews* 33 (4), S. 739–756. DOI: 10.1111/j.1574-6976.2009.00163.x.
- Pearson, J. P.; van Delden, C.; Iglewski, B. H. (1999): Active efflux and diffusion are involved in transport of *Pseudomonas aeruginosa* cell-to-cell signals. In: *Journal of bacteriology* 181 (4), S. 1203–1210. DOI: 10.1128/JB.181.4.1203-1210.1999.
- Pech-Canul, Ángel; Nogales, Joaquina; Miranda-Molina, Alfonso; Álvarez, Laura; Geiger, Otto; Soto, María José; López-Lara, Isabel M. (2011): FadD is required for utilization of endogenous fatty acids released from membrane lipids. In: *Journal of bacteriology* 193 (22), S. 6295–6304. DOI: 10.1128/JB.05450-11.
- Peel, M. M.; Alfredson, D. A.; Gerrard, J. G.; Davis, J. M.; Robson, J. M.; McDougall, R. J. et al. (1999): Isolation, identification, and molecular characterization of strains of *Photorhabdus luminescens* from infected humans in Australia. In: *Journal of clinical microbiology* 37 (11), S. 3647–3653. DOI: 10.1128/JCM.37.11.3647-3653.1999.
- Pettersen, Eric F.; Goddard, Thomas D.; Huang, Conrad C.; Couch, Gregory S.; Greenblatt, Daniel M.; Meng, Elaine C.; Ferrin, Thomas E. (2004): UCSF Chimera--a visualization system for exploratory research and analysis. In: *Journal of computational chemistry* 25 (13), S. 1605–1612. DOI: 10.1002/jcc.20084.
- Procópio, Rudi Emerson de Lima; Silva, Ingrid Reis da; Martins, Mayra Kassawara; Azevedo, João Lúcio de; Araújo, Janete Magali de (2012): Antibiotics produced by *Streptomyces*. In: *The Brazilian journal of infectious diseases : an official publication of the Brazilian Society of Infectious Diseases* 16 (5), S. 466–471. DOI: 10.1016/j.bjid.2012.08.014.
- Qin, Y.; Luo, Z. Q.; Smyth, A. J.; Gao, P.; Beck von Bodman, S.; Farrand, S. K. (2000): Quorum-sensing signal binding results in dimerization of TraR and its release from membranes into the cytoplasm. In: *The EMBO Journal* 19 (19), S. 5212–5221. DOI: 10.1093/emboj/19.19.5212.
- Qin, Zhiwei; Huang, Sheng; Yu, Yi; Deng, Hai (2013): Dithiolopyrrolone natural products: isolation, synthesis and biosynthesis. In: *Marine drugs*, S. 3970–3997. DOI: 10.3390/md11103970.
- Rahman, Mashitoh Abd; Ramli, Faiqah; Karimian, Hamed; Dehghan, Firouzeh; Nordin, Noraziah; Ali, Hapipah Mohd et al. (2016): Artonin E Induces Apoptosis via

Mitochondrial Dysregulation in SKOV-3 Ovarian Cancer Cells. In: *PLoS ONE* 11 (3), e0151466. DOI: 10.1371/journal.pone.0151466.

Rajput, Akanksha; Kaur, Karambir; Kumar, Manoj (2016): SigMol: repertoire of quorum sensing signaling molecules in prokaryotes. In: *Nucleic acids research* 44 (D1), D634–9. DOI: 10.1093/nar/gkv1076.

Rajput, Ashwani; Dominguez San Martin, Ivan; Rose, Rebecca; Beko, Alexander; Levea, Charles; Sharratt, Elizabeth et al. (2008): Characterization of HCT116 human colon cancer cells in an orthotopic model. In: *The Journal of surgical research* 147 (2), S. 276–281. DOI: 10.1016/j.jss.2007.04.021.

Ramarao, Nalini; Nielsen-Leroux, Christina; Lereclus, Didier (2012): The insect *Galleria mellonella* as a powerful infection model to investigate bacterial pathogenesis. In: *Journal of visualized experiments : JoVE* (70), e4392. DOI: 10.3791/4392.

Reen, F. Jerry; Romano, Stefano; Dobson, Alan D. W.; O'Gara, Fergal (2015): The Sound of Silence: Activating Silent Biosynthetic Gene Clusters in Marine Microorganisms. In: *Marine drugs* 13 (8), S. 4754–4783. DOI: 10.3390/md13084754.

Regaiolo, Alice; Dominelli, Nazzareno; Andresen, Karsten; Heermann, Ralf (2020): The Biocontrol Agent and Insect Pathogen *Photorhabdus luminescens* Interacts with Plant Roots. In: *Applied and environmental microbiology* 86 (17). DOI: 10.1128/AEM.00891-20.

Reimer, Daniela; Cowles, Kimberly N.; Proschak, Anna; Nollmann, Friederike I.; Dowling, Andrea J.; Kaiser, Marcel et al. (2013): Rhabdopeptides as insect-specific virulence factors from entomopathogenic bacteria. In: *Chembiochem : a European journal of chemical biology* 14 (15), S. 1991–1997. DOI: 10.1002/cbic.201300205.

Reimer, Daniela; Pos, Klaas M.; Thines, Marco; Grün, Peter; Bode, Helge B. (2011): A natural prodrug activation mechanism in nonribosomal peptide synthesis. In: *Nature chemical biology* 7 (12), S. 888–890. DOI: 10.1038/nchembio.688.

Rembold, Heinz; Sehnal, František (1987): Juvenile hormones and their titer regulation in *Galleria mellonella*. In: *Insect Biochemistry* 17 (7), S. 997–1001. DOI: 10.1016/0020-1790(87)90109-0.

Rickman, Lisa; Saldanha, José W.; Hunt, Debbie M.; Hoar, Dominic N.; Colston, M. Joseph; Millar, Jonathan B. A.; Buxton, Roger S. (2004): A two-component signal transduction system with a PAS domain-containing sensor is required for virulence of *Mycobacterium tuberculosis* in mice. In: *Biochemical and biophysical research communications* 314 (1), S. 259–267. DOI: 10.1016/j.bbrc.2003.12.082.

Rothmeier, Eva (2010). Diploma thesis. Ludwig-Maximilians-Universität München, München. Biologie.

Rumpold, Birgit A.; Schlüter, Oliver K. (2013): Nutritional composition and safety aspects of edible insects. In: *Molecular nutrition & food research* 57 (5), S. 802–823. DOI: 10.1002/mnfr.201200735.

- Ryan, Robert P.; McCarthy, Yvonne; Watt, Steven A.; Niehaus, Karsten; Dow, J. Maxwell (2009): Intraspecies signaling involving the diffusible signal factor BDSF (cis-2-dodecenoic acid) influences virulence in *Burkholderia cenocepacia*. In: *Journal of bacteriology* 191 (15), S. 5013–5019. DOI: 10.1128/JB.00473-09.
- Saini, Nipun; Black, Paul N.; Montefusco, David; Dirusso, Concetta C. (2015): Fatty acid transport protein-2 inhibitor Grassofermata/CB5 protects cells against lipid accumulation and toxicity. In: *Biochemical and biophysical research communications* 465 (3), S. 534–541. DOI: 10.1016/j.bbrc.2015.08.055.
- Sánchez-Muros, María-José; Barroso, Fernando G.; Manzano-Agugliaro, Francisco (2014): Insect meal as renewable source of food for animal feeding: a review. In: *Journal of Cleaner Production* 65, S. 16–27. DOI: 10.1016/j.jclepro.2013.11.068.
- Sandoval, Angel; Chokshi, Aalap; Jesch, Elliot D.; Black, Paul N.; Dirusso, Concetta C. (2010): Identification and characterization of small compound inhibitors of human FATP2. In: *Biochemical pharmacology* 79 (7), S. 990–999. DOI: 10.1016/j.bcp.2009.11.008.
- Schatz, A.; Bugle, E.; Waksman, S. A. (1944): Streptomycin, a Substance Exhibiting Antibiotic Activity Against Gram-Positive and Gram-Negative Bacteria.\*. In: *Experimental Biology and Medicine* 55 (1), S. 66–69. DOI: 10.3181/00379727-55-14461.
- Schauder, S.; Shokat, K.; Surette, M. G.; Bassler, B. L. (2001): The LuxS family of bacterial autoinducers: biosynthesis of a novel quorum-sensing signal molecule. In: *Molecular microbiology* 41 (2), S. 463–476. DOI: 10.1046/j.1365-2958.2001.02532.x.
- Schellenberg, Barbara; Bigler, Laurent; Dudler, Robert (2007): Identification of genes involved in the biosynthesis of the cytotoxic compound glidobactin from a soil bacterium. In: *Environmental microbiology* 9 (7), S. 1640–1650. DOI: 10.1111/j.1462-2920.2007.01278.x.
- Schellenberger, Ute; Oral, Jarred; Rosen, Barbara A.; Wei, Jun-Zhi; Zhu, Genhai; Xie, Weiping et al. (2016): A selective insecticidal protein from *Pseudomonas* for controlling corn rootworms. In: *Science (New York, N.Y.)*, S. 634–637. DOI: 10.1126/science.aaf6056.
- Schimming, Olivia; Challinor, Victoria L.; Tobias, Nicholas J.; Adihou, Hélène; Grün, Peter; Pöschel, Laura et al. (2015): Structure, Biosynthesis, and Occurrence of Bacterial Pyrrolizidine Alkaloids. In: *Angew. Chem.* 127 (43), S. 12893–12896. DOI: 10.1002/ange.201504877.
- Schmidt, Ruth; Ulanova, Dana; Wick, Lukas Y.; Bode, Helge B.; Garbeva, Paolina (2019): Microbe-driven chemical ecology: past, present and future. In: *The ISME journal* 13 (11), S. 2656–2663. DOI: 10.1038/s41396-019-0469-x.
- Schuster, M.; Urbanowski, M. L.; Greenberg, E. P. (2004): Promoter specificity in *Pseudomonas aeruginosa* quorum sensing revealed by DNA binding of purified

LasR. In: *Proceedings of the National Academy of Sciences of the United States of America* 101 (45), S. 15833–15839. DOI: 10.1073/pnas.0407229101.

Sharon, Gil; Garg, Neha; Debelius, Justine; Knight, Rob; Dorrestein, Pieter C.; Mazmanian, Sarkis K. (2014): Specialized metabolites from the microbiome in health and disease. In: *Cell metabolism* 20 (5), S. 719–730. DOI: 10.1016/j.cmet.2014.10.016.

Shi, Yi-Ming; Bode, Helge B. (2018): Chemical language and warfare of bacterial natural products in bacteria-nematode-insect interactions. In: *Natural product reports* 35 (4), S. 309–335. DOI: 10.1039/c7np00054e.

Silver, Lynn L. (2011): Challenges of antibacterial discovery. In: *Clinical microbiology reviews* 24 (1), S. 71–109. DOI: 10.1128/CMR.00030-10.

Silver, Lynn L. (2016): Appropriate Targets for Antibacterial Drugs. In: *Cold Spring Harbor perspectives in medicine* 6 (12). DOI: 10.1101/cshperspect.a030239.

Smith, Parker; Schuster, Martin (2019): Public goods and cheating in microbes. In: *Current biology : CB* 29 (11), R442-R447. DOI: 10.1016/j.cub.2019.03.001.

Söding, Johannes; Biegert, Andreas; Lupas, Andrei N. (2005): The HHpred interactive server for protein homology detection and structure prediction. In: *Nucleic acids research* 33 (Web Server issue), W244-8. DOI: 10.1093/nar/gki408.

Sperandio, Vanessa (2010): SdiA sensing of acyl-homoserine lactones by enterohemorrhagic *E. coli* (EHEC) serotype O157:H7 in the bovine rumen. In: *Gut microbes* 1 (6), S. 432–435. DOI: 10.4161/gmic.1.6.14177.

Statistisches Bundesamt (2020): Todesursachen nach Krankheitsarten. [https://www.destatis.de/DE/Themen/Gesellschaft-Umwelt/Gesundheit/Todesursachen/\\_inhalt.html#sprg229156](https://www.destatis.de/DE/Themen/Gesellschaft-Umwelt/Gesundheit/Todesursachen/_inhalt.html#sprg229156). In: 2018.

Stauff, Devin L.; Bassler, Bonnie L. (2011): Quorum sensing in *Chromobacterium violaceum*: DNA recognition and gene regulation by the CviR receptor. In: *Journal of bacteriology* 193 (15), S. 3871–3878. DOI: 10.1128/JB.05125-11.

Subramoni, Sujatha; Venturi, Vittorio (2009): LuxR-family 'solos': bachelor sensors/regulators of signalling molecules. In: *Microbiology (Reading, England)* 155 (Pt 5), S. 1377–1385. DOI: 10.1099/mic.0.026849-0.

Surette, M. G.; Miller, M. B.; Bassler, B. L. (1999): Quorum sensing in *Escherichia coli*, *Salmonella typhimurium*, and *Vibrio harveyi*: a new family of genes responsible for autoinducer production. In: *Proceedings of the National Academy of Sciences of the United States of America* 96 (4), S. 1639–1644. DOI: 10.1073/pnas.96.4.1639.

Szklarczyk, Damian; Gable, Annika L.; Lyon, David; Junge, Alexander; Wyder, Stefan; Huerta-Cepas, Jaime et al. (2019): STRING v11: protein-protein association networks with increased coverage, supporting functional discovery in genome-wide experimental datasets. In: *Nucleic acids research* 47 (D1), D607-D613. DOI: 10.1093/nar/gky1131.

Tailliez, Patrick; Pagès, Sylvie; Ginibre, Nadège; Boemare, Noël (2006): New insight into diversity in the genus *Xenorhabdus*, including the description of ten novel species. In: *International journal of systematic and evolutionary microbiology* 56 (Pt 12), S. 2805–2818. DOI: 10.1099/ijs.0.64287-0.

Thanwisai, Aunchalee; Tandhavanant, Sarunporn; Saiprom, Natnaree; Waterfield, Nick R.; Ke Long, Phan; Bode, Helge B. et al. (2012): Diversity of *Xenorhabdus* and *Photorhabdus* spp. and their Symbiotic Entomopathogenic Nematodes from Thailand. In: *PLoS ONE* 7 (9). DOI: 10.1371/journal.pone.0043835.

Theodore, Christine M.; King, Jarrod B.; You, Jianlan; Cichewicz, Robert H. (2012): Production of cytotoxic glidobactins/luminmycins by *Photorhabdus asymbiotica* in liquid media and live crickets. In: *Journal of natural products* 75 (11), S. 2007–2011. DOI: 10.1021/np300623x.

Theuretzbacher, Ursula; Outtersson, Kevin; Engel, Aleks; Karlén, Anders (2020): The global preclinical antibacterial pipeline. In: *Nature reviews. Microbiology* 18 (5), S. 275–285. DOI: 10.1038/s41579-019-0288-0.

Thoma, Sabrina; Schobert, Max (2009): An improved *Escherichia coli* donor strain for diparental mating. In: *FEMS microbiology letters* 294 (2), S. 127–132. DOI: 10.1111/j.1574-6968.2009.01556.x.

THOMAS, G. M.; POINAR, G. O. (1979): *Xenorhabdus* gen. nov., a Genus of Entomopathogenic, Nematophilic Bacteria of the Family Enterobacteriaceae. In: *International journal of systematic bacteriology* 29 (4), S. 352–360. DOI: 10.1099/00207713-29-4-352.

Tipper, D. J. (1973): Inhibition of yeast ribonucleic acid polymerases by thiolutin. In: *Journal of bacteriology* 116 (1), S. 245–256. DOI: 10.1128/JB.116.1.245-256.1973.

Tobias, Nicholas J.; Brehm, Jannis; Kresovic, Darko; Brameyer, Sophie; Bode, Helge B.; Heermann, Ralf (2020): New Vocabulary for Bacterial Communication. In: *ChemBiochem : a European journal of chemical biology* 21 (6), S. 759–768. DOI: 10.1002/cbic.201900580.

Tobias, Nicholas J.; Heinrich, Antje K.; Eresmann, Helena; Wright, Patrick R.; Neubacher, Nick; Backofen, Rolf; Bode, Helge B. (2017): *Photorhabdus*-nematode symbiosis is dependent on hfq-mediated regulation of secondary metabolites. In: *Environmental microbiology* 19 (1), S. 119–129. DOI: 10.1111/1462-2920.13502.

Tobias, Nicholas J.; Mishra, Bagdevi; Gupta, Deepak K.; Sharma, Rahul; Thines, Marco; Stinear, Timothy P.; Bode, Helge B. (2016): Genome comparisons provide insights into the role of secondary metabolites in the pathogenic phase of the *Photorhabdus* life cycle. In: *BMC Genomics* 17, S. 537. DOI: 10.1186/s12864-016-2862-4.

TODARO, G. J.; GREEN, H. (1963): Quantitative studies of the growth of mouse embryo cells in culture and their development into established lines. In: *The Journal of Cell Biology* 17, S. 299–313. DOI: 10.1083/jcb.17.2.299.

- Tolker-Nielsen; Molin (2000): Spatial Organization of Microbial Biofilm Communities. In: *Microbial ecology* 40 (2), S. 75–84. DOI: 10.1007/s002480000057.
- UMEZAWA, H. (1958): Kanamycin: its discovery. In: *Annals of the New York Academy of Sciences* 76 (2), S. 20–26. DOI: 10.1111/j.1749-6632.1958.tb54688.x.
- van den Berg, Bert (2005): The FadL family: unusual transporters for unusual substrates. In: *Current opinion in structural biology* 15 (4), S. 401–407. DOI: 10.1016/j.sbi.2005.06.003.
- van den Berg, Bert; Black, Paul N.; Clemons, William M.; Rapoport, Tom A. (2004): Crystal structure of the long-chain fatty acid transporter FadL. In: *Science (New York, N.Y.)* 304 (5676), S. 1506–1509. DOI: 10.1126/science.1097524.
- Vannini, A. (2002): The crystal structure of the quorum sensing protein TraR bound to its autoinducer and target DNA. In: *The EMBO Journal* 21 (17), S. 4393–4401. DOI: 10.1093/emboj/cdf459.
- Ventola, C. Lee (2015): The Antibiotic Resistance Crisis: Part 1: Causes and Threats. In: *Pharmacy and Therapeutics* 40 (4), S. 277–283.
- Vigneux, Fabienne; Zumbihl, Robert; Jubelin, Grégory; Ribeiro, Carlos; Poncet, Joël; Baghdiguan, Stephen et al. (2007): The xaxAB genes encoding a new apoptotic toxin from the insect pathogen *Xenorhabdus nematophila* are present in plant and human pathogens. In: *The Journal of biological chemistry*, S. 9571–9580. DOI: 10.1074/jbc.M604301200.
- Vílchez, Ramiro; Lemme, André; Ballhausen, Britta; Thiel, Verena; Schulz, Stefan; Jansen, Rolf et al. (2010): *Streptococcus mutans* inhibits *Candida albicans* hyphal formation by the fatty acid signaling molecule trans-2-decenoic acid (SDSF). In: *Chembiochem : a European journal of chemical biology* 11 (11), S. 1552–1562. DOI: 10.1002/cbic.201000086.
- Vizcaino, Maria I.; Guo, Xun; Crawford, Jason M. (2014): Merging chemical ecology with bacterial genome mining for secondary metabolite discovery. In: *Journal of industrial microbiology & biotechnology* 41 (2), S. 285–299. DOI: 10.1007/s10295-013-1356-5.
- Wang; Gaugler (1998): Host and penetration site location by entomopathogenic nematodes against japanese beetle larvae. In: *Journal of Invertebrate Pathology* 72 (3), S. 313–318. DOI: 10.1006/jjipa.1998.4805.
- Waterfield, Nick R.; Ciche, Todd; Clarke, David (2009): *Photorhabdus* and a host of hosts. In: *Annu. Rev. Microbiol.* 63, S. 557–574. DOI: 10.1146/annurev.micro.091208.073507.
- Waters, Christopher M.; Bassler, Bonnie L. (2005): Quorum sensing: cell-to-cell communication in bacteria. In: *Annual review of cell and developmental biology* 21, S. 319–346. DOI: 10.1146/annurev.cellbio.21.012704.131001.

- Wesche, Frank; He, Yue; Bode, Helge B. (2017): Solid-phase enrichment and analysis of electrophilic natural products. In: *Beilstein journal of organic chemistry* 13, S. 405–409. DOI: 10.3762/bjoc.13.43.
- Whitehead, N. A.; Barnard, A. M.; Slater, H.; Simpson, N. J.; Salmond, G. P. (2001): Quorum-sensing in Gram-negative bacteria. In: *FEMS microbiology reviews* 25 (4), S. 365–404. DOI: 10.1111/j.1574-6976.2001.tb00583.x.
- Wu, Hai; Li, Minjun; Guo, Haojie; Zhou, Huan; Li, Bing; Xu, Qin et al. (2019): Crystal structure of the *Vibrio cholerae* VqmA-ligand-DNA complex provides insight into ligand-binding mechanisms relevant for drug design. In: *The Journal of biological chemistry* 294 (8), S. 2580–2592. DOI: 10.1074/jbc.RA118.006082.
- Xu, Zhuyu; Guo, Dandan; Jiang, Zhongliang; Tong, Rongsheng; Jiang, Peidu; Bai, Lan et al. (2019): Novel HER2-Targeting Antibody-Drug Conjugates of Trastuzumab Beyond T-DM1 in Breast Cancer: Trastuzumab Deruxtecan(DS-8201a) and (Vic-)Trastuzumab Duocarmazine (SYD985). In: *European journal of medicinal chemistry* 183, S. 111682. DOI: 10.1016/j.ejmech.2019.111682.
- Zamora-Lagos, Maria-Antonia; Eckstein, Simone; Langer, Angela; Gazanis, Athanasios; Pfeiffer, Friedhelm; Habermann, Bianca; Heermann, Ralf (2018): Phenotypic and genomic comparison of *Photorhabdus luminescens* subsp. *laumondii* TT01 and a widely used rifampicin-resistant *Photorhabdus luminescens* laboratory strain. In: *BMC Genomics* 19. DOI: 10.1186/s12864-018-5121-z.
- Zhang, J. H.; Xu, M. (2000): DNA fragmentation in apoptosis. In: *Cell research* 10 (3), S. 205–211. DOI: 10.1038/sj.cr.7290049.
- Zhang, Rong-guang; Pappas, Katherine M.; Pappas, Terina; Brace, Jennifer L.; Miller, Paula C.; Oulmassov, Tim et al. (2002): Structure of a bacterial quorum-sensing transcription factor complexed with pheromone and DNA. In: *Nature* 417 (6892), S. 971–974. DOI: 10.1038/nature00833.
- Zhou, Xuan; Zhang, Nan; Xia, Liming; Li, Qing; Shao, Jiahui; Shen, Qirong; Zhang, Ruifu (2018): ResDE Two-Component Regulatory System Mediates Oxygen Limitation-Induced Biofilm Formation by *Bacillus amyloliquefaciens* SQR9. In: *Applied and environmental microbiology* 84 (8). DOI: 10.1128/AEM.02744-17.

## Supplements

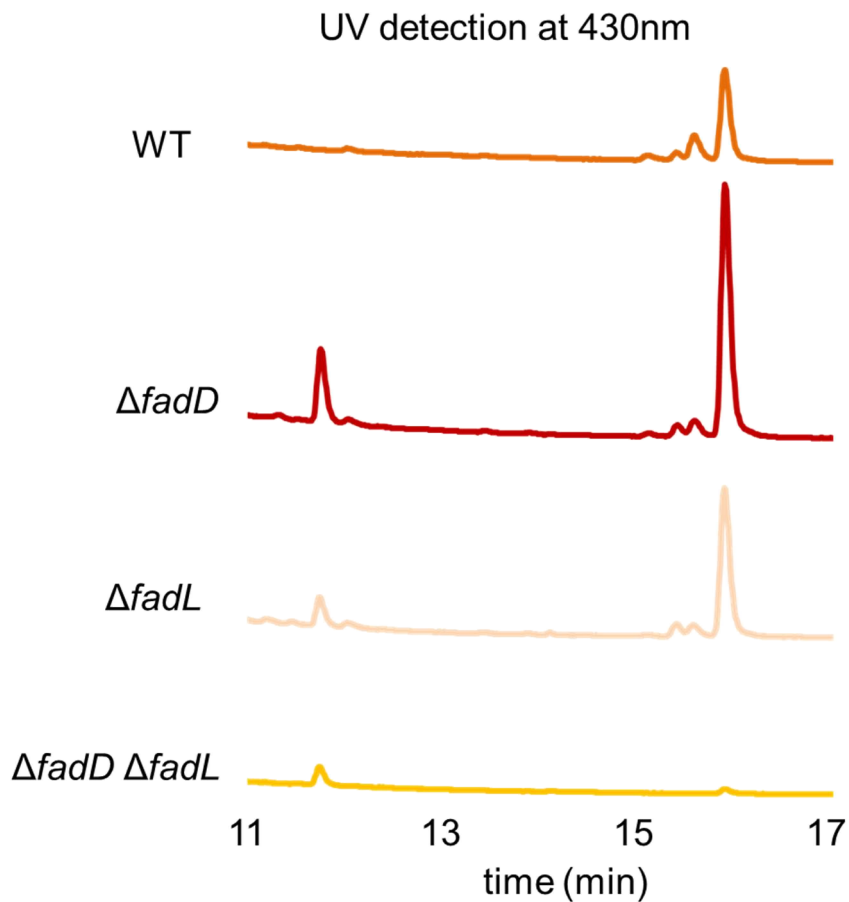
### Supplementary tables:

**Table S 3.1.2: Proteins with differences in comparative proteomic analysis between *P. luminescens* TT01 wild type and *P. luminescens* TT01  $\Delta pikR1-pikR2$ .** In the upper part are shown the proteins with changed patterns in the production between *P. luminescens* TT01 wild type and *P. luminescens* TT01  $\Delta pikR1-pikR2$  in presence of larvae and nematode homogenate, whereas the lower part presents the proteins, which were absent in *P. luminescens* TT01  $\Delta pikR1-pikR2$  without larvae or nematode homogenate. Proteins identified as virulence factors are shown in blue. Stress response related proteins are shown in red. Proteins related to metabolism are shown in yellow and proteins with a so far unknown function are shown in black. Similarities to other genes and functions were determined by a BLAST analysis (Altschul et al. 1990). The table was edited from results from a comparative proteomic analysis (Rothmeier 2010).

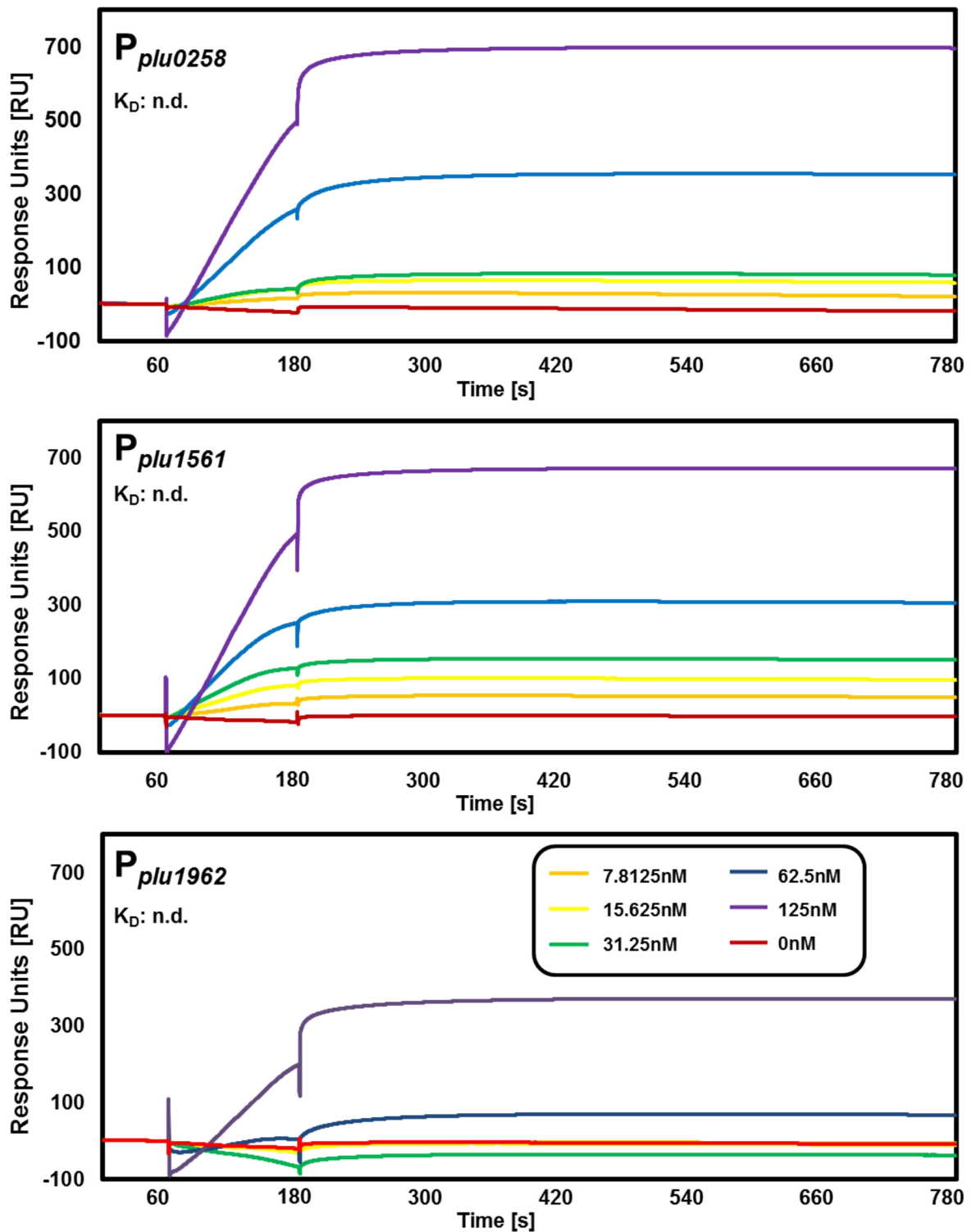
Protein	Fold change	Growth phase	Similarity / Function
<b>In presence of larvae and nematode homogenate</b>			
<b>Plu0258</b>	-3,0	stationary	similarity to cornworm toxin from <i>Pseudomonas chlororaphis</i> (Schellenberger et al. 2016)
<b>Plu1962</b>	only in WT	exponential	XaxA toxin subunit A
<b>Plu4211</b>	only in mutant	stationary	Hcp family type VI secretion system effector ( <i>Photorhabdus luminescens</i> )
<b>WrbA (plu1964)</b>	only in WT	stationary	NAD(P)H quinone oxidoreductase ( <i>Photorhabdus luminescens</i> ) (Grandori et al. 1998)
<b>Plu2095</b>	+3,0	stationary	Ycel family protein ( <i>Thermus thermophiles</i> ) (Handa et al. 2005)
<b>AhpC (Plu3907)</b>	+6,6	exponential	peroxiredoxin C ( <i>Photorhabdus luminescens</i> )
<b>Plu3795</b>	-2,7	stationary	hypothetical protein
<b>Plu3012</b>	-3,5	stationary	phage associated protein
<b>Without larvae and nematode homogenate</b>			
<b>Plu1561</b>	only in WT	stationary	hypothetical protein
<b>Plu4566</b>	only in WT	stationary	amidinotransferase ( <i>Chloroflexi bacterium</i> ) (Diamond et al. 2019) and N-Dimethylarginine dimethylaminohydrolase <i>Candidatus Nitrotoga</i> sp. LAW (Boddicker und Mosier 2018)

IscS (Plu3283)	only in WT	exponential	IscS subfamily cysteine desulfurase ( <i>Photorhabdus luminescens</i> )
----------------	------------	-------------	---

### Supplementary figures:



**Supplementary Fig. S 3.1.1: HPLC UV/Vis analysis of *P. luminescens* culture supernatant at a wavelength of 430nm.** Selected section of the HPLC UV-Vis (430nm) chromatograms of the culture supernatant of *P. luminescens* DJC wild type (WT), *P. luminescens* DJC  $\Delta fadD$ , *P. luminescens* DJC  $\Delta fadL$  and *P. luminescens* DJC  $\Delta fadD \Delta fadL$ . In all mutants was a peak detected after around 11.5 min that is absent in the chromatogram of *P. luminescens* DJC wild type. The peak at around 16 min is almost absent in *P. luminescens* DJC  $\Delta fadD \Delta fadL$ , but was more prominent in *P. luminescens* DJC  $\Delta fadD$  and *P. luminescens* DJC  $\Delta fadL$  than in *P. luminescens* DJC wild type.



**Supplementary Figure S 3.1.2: SPR binding kinetics of PikR2 and P<sub>plu0258</sub>, P<sub>plu1561</sub> and P<sub>plu1962</sub> after the addition of 200 mM stearic acid.** The three promoters P<sub>plu0258</sub>, P<sub>plu1561</sub> and P<sub>plu1962</sub> were immobilized to a SA sensor chip. Binding affinity kinetics of different concentrations (7.8125nM (orange)), 15.625nM (yellow), 31.25nM (green), 62.5nM (blue), 125nM (violet) and 0nM (red)) of PikR2 were measured with 120 seconds of contact time followed by 600 seconds of dissociation. PikR2 showed binding with all surface bound promoters. Stable binding to P<sub>plu1962</sub> was measured at

concentrations of 62.5nM and higher, whereas stable binding occurred with P<sub>plu0258</sub> and P<sub>plu1561</sub> in all tested concentrations of PikR2. Due to very slow dissociation and bulk effects the kd values were outside measurable limits, therefore the K<sub>D</sub> values were not determined.

## **Acknowledgement**

First of all, I want to express my sincere gratitude to Prof. Dr. Ralf Heermann for giving me the opportunity to work in his group and study the very interesting but also challenging pathogenic part of the lifecycle of *Photorhabdus* and *Xenorhabdus*. I would like to thank him for great support, guidance and advice throughout the six shared years. Especially, his staff management and handling of personal issues was outstanding in the department, such as the early and full disclosure about the relocation from Munich to Mainz. In particular after my skiing accident he supported me without any pressure and gave me all the time I needed for recovery. Furthermore, he supported my interest in instrumental analytics by giving me the opportunity to learn several new techniques such as the fabulous SPR.

I am very thankful to my thesis committee, especially to Prof. Dr. Heinrich Jung for being the second examiner of my thesis.

A refreshing part during the days at the LMU was the coffee break with FunFacts and gossip in friendly atmosphere with all members of the groups from Prof. Dr. Kirsten Jung, Prof. Dr. Heinrich Jung. The Christmas party, Wiesn and the staff outings were always nice events, which supported the group bonding.

With the members of our group, Atha, Alice, Simone and Nazza we always had a fun time in our lab with great music from Sabine☺ and later with the disturbing singing from Armin in Mainz.

Many thanks go to the office gang Angi, Hannah, Nicola and (later) Miri who made the start at the LMU really easy for me and made the office time really enjoyable.

Most fun, also after working hours, I had with Simone, Ralph and Lutti. It was really nice to have met you and to become friends. I hope we will keep in contact as we did over the last two years and will have many more drinks in the Fend and Fox. (after Corona)

Furthermore, I want to thank Meike and Petra from the IBWF in Kaiserslautern for analysis of many samples via HPLC as well as Jeannette, who supported me by handling all of the cell culture experiment and viability assays.

In Mainz we realized even more what an outstanding secretary we had in Munich, who always knew where to find things or who to call. Thank you very much Grazyna.

I really want to thank our technical assistance in Munich, Tatjana, Ingrid and Korinna, who made work in the lab easy by providing technical knowledge as well as all kind of technical services and made sure that all chemical were always available. The same assistance was gratefully given by Kirsten in Mainz, who hopefully enjoyed our long talks about SPR, as much as I did☺.

Of course I want to thank my best friend Max for (sometimes) answering my calls after work and making my bike ride home less exhausting. Klasse!

Especially, I want to thank my parents who supported me from the beginning of my PhD in all kind of ways. My awareness and interest in science began in my childhood during many cycling tours and adventurous trips through the nature.

Finally, I want to thank my wife Ines, who always supported me during the time in Munich and also made the long distance marriage during the time in Mainz less tiring. In particular, when coming home after long and exhausting days in the lab she enjoyed the meals that I cooked in the evening. I am looking forward to the next decades with her at my side.

# Curriculum vitae

## Personal Data

Name: Jannis Cornelius Brehm  
Date of Birth: 23.01.1990  
Place of Birth: Hamburg, Germany  
Nationality: German

## Education

05/19- 12/20      Johannes Gutenberg-Universität Mainz (Germany)  
  
PhD student at the Institute of Molecular Physiology,  
Microbiology and Wine research  
  
Prof. Dr. Ralf Heermann  
  
Topic: Investigation and analysis of bacterial communication of  
*Photorhabdus* species.

04/15 – 05/19      Ludwig-Maximilians-Universität, Munich (Germany)  
  
PhD student at the Department Biology I, Microbiology  
  
PD Dr. Ralf Heermann  
  
Topic: Investigation and analysis of bacterial communication of  
*Photorhabdus* species.

12/14              License to practice pharmacy

11/13 – 04/14      Albert-Ludwigs-Universität Freiburg (Germany)  
  
Diploma thesis at the Department of pharmaceutical Biology and  
Biotechnology  
  
Prof. Dr. Andreas Bechthold  
  
Topic: Investigation on the production and transport of the  
bacterial secondary metabolite Rishirilide

10/09 - 10/13      Albert-Ludwigs-Universität Freiburg (Germany)  
Study of Pharmacy

08/07- 06/09      Sophie-Barat Schule, Hamburg (Germany)  
Abitur (1.9)

### **Work experience**

05/14 - 11/14      Leibniz Apotheke, Berlin (Germany)  
Trainee pharmacist as part of the practical year

11/13 – 04/14      Albert-Ludwigs-Universität Freiburg (Germany)  
Research assistant at the institute for Pharmaceutical Biology  
Supervisor: Prof. Dr. Bechthold

09/10                CSL Behring, Marburg (Germany)  
Internship, Department of Quality Control

07/09 – 09/09      Steinfeld und Partner Grundbauingenieure, Hamburg (Germany)  
Laboratory of Sediment analysis

### **Conferences**

03/19                VAAM Conference, Mainz (Germany)  
**Oral presentation :** Inter-kingdom signaling by *Photorhabdus luminescens* - sensing eukaryotic hosts by PAS4-LuxR receptors

10/19                RLP Symposium, Kaiserslautern  
**Oral presentation:** Rhabdo-Tags Cytotoxic secondary metabolites from *Xenorhabdus* and *Photorhabdus*

- 09/18 Mechanisms of Gene Regulation, Tutzing (Germany)  
**Oral presentation:** Host sensing by *Photorhabdus luminescens* – PAS4-LuxR solos as inter-kingdom-signaling receptors
- 09/18 VAAM Meeting, Marburg (Germany)  
**Poster presentation**
- 04/18 VAAM Conference, Wolfsburg (Germany)  
**Poster presentation**
- 10/17 6th ASM Conference on Cell–Cell Communication in Bacteria, Athens (USA)  
**Oral presentation:** “Bugging bugs” - quorum sensing and inter-kingdom-signaling by entomopathogenic bacteria
- 03/17 VAAM Conference, Würzburg (Germany)  
**Poster presentation**
- 03/16 VAAM Conference, Jena (Germany)  
**Poster presentation**
- 10/15 EMBO Conference, Heidelberg (Germany)  
**Poster presentation**

## Publications

New Vocabulary for Bacterial Communication

Tobias NJ, **Brehm J**, Kresovic D, Brameyer S, Bode HB, Heermann R

Chembiochem. 2019 Nov 11. doi: 10.1002/cbic.201900580

Deciphering the rules underlying xenogeneic silencing and counter-silencing of Lsr2-like proteins using CgpS of *Corynebacterium glutamicum* as a model

Wiechert J<sup>1</sup>, Filipchuk A<sup>1</sup>, Hünnefeld M<sup>1</sup>, Gätgens C<sup>1</sup>, **Brehm J**<sup>2</sup>, Heermann R<sup>2</sup>, Frunzke J<sup>3</sup>

mBio. 2020 Feb 4;11(1):e02273-19. doi: 10.1128/mBio.02273-19

Two novel XRE-like transcriptional regulators control phenotypic heterogeneity in *Photorhabdus luminescens* cell populations

Eckstein S<sup>1,2</sup>, **Brehm. J**<sup>1</sup>, Seidel M<sup>2</sup>, Lechtenfeld M<sup>1</sup>, Heermann R<sup>1</sup>

BMC microbiology, 2021 (accepted)

FadL and FadD contribute to the facilitation of *Photorhabdus*-specific hydrophobic signalling molecules across the cell envelope

**Brehm J**<sup>1</sup>, Brameyer S<sup>2</sup>, Brachmann A<sup>3</sup>, Heermann R<sup>1</sup>

BMC microbiology, 2021 (submitted)

Identification of Gip as a novel phage-encoded gyrase inhibitor protein featuring a 1 broad activity profile 2 3 Running title: CGP3-encoded Gip inhibits DNA gyrase 4 5

Kever L<sup>1</sup>, Hünnefeld M<sup>1</sup>, **Brehm J**<sup>2</sup>, Heermann R<sup>2</sup>, Frunzke J<sup>1</sup>

Molecular Microbiology, 2021 (submitted)